

SERI/TR-252-3108
UC Category: 262
DE89000822

Direct-Contact Condensers for Open-Cycle OTEC Applications

Model Validation with Fresh Water Experiments for Structured Packings

D. Bharathan
B. K. Parsons
J. A. Althof

October 1988

Prepared under Task No. OE713101

Solar Energy Research Institute

A Division of Midwest Research Institute

1617 Cole Boulevard
Golden, Colorado 80401-3393

Prepared for the
U.S. Department of Energy
Contract No. DE-AC02-83CH10093


PREFACE

This report describes the status of our direct-contact condenser model validation effort performed under the FY 1986 task entitled "Heat and Mass Transfer Model." This task is a subset of an overall objective to develop a detailed, analytical computer model for various open-cycle ocean thermal energy conversion (OC-OTEC) components. This report describes a complete set of process equations and an integration method for a one-dimensional, steady-state model of cocurrent and countercurrent condensers. Extensive sets of comparisons between experimental data and model predictions for structured packing in fresh water are provided. The report also summarizes results obtained in previous years that are pertinent to the model validation effort.

The Pascal modeling code was developed and debugged on an IBM-AT computer using the Turbo Pascal™ compiler. We have also run the code on available IBM personal computers. The condenser model represents the state of the art in direct-contact heat exchange for condensation for OC-OTEC applications. This is expected to provide a basis for optimizing OC-OTEC plant configurations.

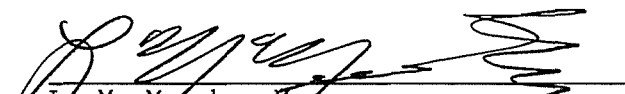
This model is an excellent tool for use in data reduction for the planned research activities with seawater at the Natural Energy Laboratory of Hawaii, for design and system evaluations for OC-OTEC, and for other low-temperature energy technologies.

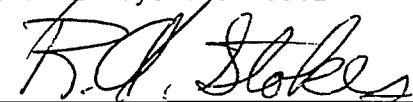
We would like to thank Andrew Trenka, Oceans Program leader, for his leadership and Terry Penney and David Johnson for their encouragement. The efforts of Ben Shelpuk, principal engineer, are also appreciated. Gratitude is expressed to Gene Winkler, Munters Corporation, and to Neil Yeoman, Koch Engineering Company, Inc., for providing valuable information on their companies' products. Critical reviews provided by Kenneth Bell, Oklahoma State University, Stillwater; Anthony Mills, University of California at Los Angeles; and G. B. Wallis, Dartmouth College, guided us in accomplishing our goals in this task.


Desikan Bharathan, Senior Engineer

Approved for

SOLAR ENERGY RESEARCH INSTITUTE


L. M. Murphy, Manager
Thermal Systems Research Branch


Robert A. Stokes, Acting Director
Solar Heat Research Division

SUMMARY

Objective

To develop analytical methods for evaluating the design and performance of advanced, high-performance heat exchangers that are reliable and cost-effective for use in the open-cycle ocean thermal energy conversion (OC-OTEC) process.

Discussion

This report describes the progress made on validating a one-dimensional, steady-state analytical computer model of direct-contact condenser using structured packings based on extensive sets of fresh water experiments. The condenser model represents the state of the art in direct-contact heat exchange for condensation for OC-OTEC applications. This is expected to provide a basis for optimizing OC-OTEC plant configurations. Using the model, we examined two condenser geometries, a cocurrent and a countercurrent configuration.

We developed a computer model for evaluating direct-contact condenser geometries and optimum flow parameters for OC-OTEC applications. Use of this model, however, was limited to structured packings. This report provides detailed validation results for important condenser parameters for cocurrent and countercurrent flows. With modifications this model can be used for other industrial applications as well.

The model establishes the viability of packed-column geometries for use in OC-OTEC systems and illustrates the variations of condenser performance as geometric and flow parameters are altered.

Conclusions

We developed a one-dimensional, steady-state model that captures the heat, mass, and momentum processes in steam-water, direct-contact applications in the presence of noncondensable gases for both cocurrent and countercurrent condensers. The model also incorporates the mass transfer of dissolved gases in the coolant. Portable Turbo-Pascal™ computer codes for cocurrent and countercurrent condensers were developed. These codes were exercised over a wide range of geometrical and condenser flow geometries to predict performances of tested condenser geometries. The predictions were compared with the experimental data to quantify deviations.

Based on the comparisons and uncertainty overlap between the experimental data and predictions, the model is shown to predict critical condenser performance parameters with an uncertainty acceptable for general engineering design and performance evaluations.

TABLE OF CONTENTS

	<u>Page</u>
Nomenclature.....	xiii
1.0 Introduction.....	1
1.1 Objective and Goal.....	4
1.2 Approach.....	5
1.3 Scope and Limitation.....	7
1.4 Background.....	8
1.5 Report Organization.....	11
2.0 Model Description.....	13
2.1 Cocurrent Condenser.....	13
2.1.1 Interface Temperature.....	13
2.1.2 Transfer Fluxes.....	15
2.1.3 Process Equations.....	15
2.1.4 Equilibrium Calculations.....	18
2.2 Countercurrent Condenser.....	18
2.2.1 Differences in Countercurrent Operation.....	18
2.2.2 Process Equations.....	18
2.2.3 Equilibrium Calculations.....	20
2.3 Structured Packings.....	20
2.3.1 Geometry Definitions.....	20
2.3.2 Transfer Correlations.....	22
2.4 Integration Scheme.....	28
3.0 Experimental Details.....	31
3.1 Facility.....	31
3.2 Instrumentation.....	31
3.3 Condenser Test Models	34
3.4 Test Procedure.....	37
4.0 Model Validation.....	39
4.1 Cocurrent Condenser.....	40
4.1.1 AX Packing.....	41
4.1.2 Plasdek 19060 Packing.....	42
4.1.3 4X Packing.....	43
4.1.4 Free Jets.....	44
4.1.5 Summary of Cocurrent Condenser Findings.....	47
4.2 Countercurrent Condenser.....	48
4.2.1 AX Packing.....	48
4.2.2 Plasdek 19060 Packing.....	51
4.2.3 3X Packing.....	51
4.2.4 Plasdek 27060 Packing.....	53
4.2.5 Summary of Countercurrent Condenser Findings.....	53
4.3 Summary.....	56

TABLE OF CONTENTS (Concluded)

5.0 Numerical Results and Parametric Studies.....	57
5.1 Cocurrent Condenser.....	57
5.1.1 Condensation Process.....	57
5.1.2 Influence of Packing Geometry.....	61
5.1.3 Influence of Flow Parameters.....	64
5.2 Countercurrent Condenser.....	72
5.2.1 Condensation Process.....	72
5.2.2 Influence of Packing Geometry.....	78
5.2.3 Influence of Flow Parameters.....	81
6.0 Conclusions and Recommendations.....	85
6.1 Conclusions.....	85
6.2 Recommendations.....	87
7.0 References	90
Nomenclature for Appendices.....	93
Appendix A Experimental Facility and Instrumentation.....	95
Appendix B Measurement Uncertainties and Their Propagation.....	112
Appendix C Relative Ranking of Tested Contact Devices.....	122
Appendix D Data Tables for Experiments Using Structured Packings.....	132
Appendix E Data Tables for Countercurrent Condenser Geometries Other Than Structured Packing.....	163
Appendix F Computer Program Listings.....	189
Appendix G Equilibrium Calculations.....	246
Appendix H Water, Steam, and Air Properties.....	250
Selected Distribution List.....	255

LIST OF FIGURES

	<u>Page</u>
1-1 Schematic of an open-cycle ocean thermal energy conversion system.....	1
1-2 Diagram of desalinated water production scheme using direct contact condenser.....	2
1-3 Schematic of barometric direct-contact condenser subsystem indicating steam and noncondensable gas mixture flow through cocurrent and countercurrent sections using structured packings....	3
1-4 Relative performance comparison of a few tested countercurrent condenser configurations.....	6
2-1 Representation of temperature distribution in coolant, gas, and interface during condensation: condensing steam flux and noncondensable mass flux.....	14
2-2 A slice of a cocurrent direct-contact condenser indicating the modeling variables for one-dimensional flow.....	16
2-3 A slice of a countercurrent direct-contact condenser indicating the modeling variables for one-dimensional flow.....	19
2-4 Structured sheet packing.....	21
2-5 Structured packing geometry definition.....	21
2-6 Liquid film flow on an inclined structured packing geometry.....	23
3-1 Heat- and mass-transfer laboratory flow loop schematic.....	32
3-2 Schematic of cocurrent condenser test article arrangement.....	35
3-3 Schematic of countercurrent condenser test article arrangement.....	35
4-1 Comparison of condensed steam for AX packing in cocurrent flow.....	41
4-2 Comparison of pressure loss for AX packing in cocurrent flow.....	42
4-3 Comparison of condensed steam for 19060 packing in cocurrent flow.....	43
4-4 Comparison of pressure loss for 19060 packing in cocurrent flow....	44
4-5 Comparison of condensed steam for 4X packing in cocurrent flow.....	45
4-6 Comparison of pressure loss for 4X packing in cocurrent flow.....	45
4-7 Free-falling jets in cocurrent configuration.....	46

LIST OF FIGURES (Continued)

	<u>Page</u>
4-8 Comparison of measured condensed steam for a cocurrent condenser with and without 19060 packing.....	46
4-9 Comparison of measured pressure loss for a cocurrent condenser with and without 19060 packing.....	47
4-10 Flooding limits for countercurrent condensers using the correlation of Wallis (1969).....	50
4-11 Comparison of condensed steam predictions with data for type AX packing in countercurrent flow.....	50
4-12 Comparison of pressure loss for AX packing in countercurrent flow.....	51
4-13 Pressure loss comparison for 19060 packing in countercurrent flow.....	52
4-14 Comparison of condensed steam for 3X packing in countercurrent flow.....	52
4-15 Comparison of pressure loss for 3X packing in countercurrent flow.....	53
4-16 Comparison of condensed steam for 27060 packing in countercurrent flow.....	54
4-17 Comparison of pressure loss for 27060 packing in countercurrent flow.....	54
5-1 Variations of temperatures within the condenser versus downstream distance in cocurrent flow.....	58
5-2 Variations of pressure loss, interfacial steam flux, and inert content in steam within the condenser versus downstream distance in cocurrent flow.....	59
5-3 Process path in cocurrent condensation.....	60
5-4 Influence of effective area fraction on cocurrent condenser performance	62
5-5 Influence of packing size on cocurrent condenser performance.....	63
5-6 Influence of packing height-to-base ratio on cocurrent condenser performance.....	64
5-7 Influence of channel inclination on cocurrent condenser performance.....	65

LIST OF FIGURES (Continued)

	<u>Page</u>
5-8 Influence gas loading on cocurrent condenser performance.....	66
5-9 Influence of Jakob number varied via water flow rate on cocurrent condenser performance at $G = 0.6 \text{ kg/m}^2 \text{ s}$	69
5-10 Influence of Jakob number varied via water flow rate on cocurrent condenser performance at $G = 0.4 \text{ kg/m}^2 \text{ s}$	70
5-11 Cocurrent condenser operating diagram.....	71
5-12 Influence of Jakob number varied via inlet steam temperature on cocurrent condenser performance at $G = 0.6 \text{ kg/m}^2 \text{ s}$	73
5-13 Influence of Jakob number varied via inlet steam temperature on cocurrent condenser performance at $G = 0.4 \text{ kg/m}^2 \text{ s}$	74
5-14 Variations of temperatures within the condenser versus downstream distance in countercurrent flow.....	75
5-15 Variations of pressure loss, interfacial steam flux, and inert content in steam within condenser versus downstream distance in countercurrent flow.....	76
5-16 Steam and inert gas mixture process path in countercurrent flow....	77
5-17 Influence of effective area fraction on countercurrent condenser performance.....	78
5-18 Influence of packing size on countercurrent condenser performance..	79
5-19 Influence of packing height-to-base ratio on countercurrent condenser performance.....	80
5-20 Influence of channel inclination on countercurrent condenser performance.....	81
5-21 Influence of gas loading on countercurrent condenser performance...	82
5-22 Influence of Jakob number varied via water flow on countercurrent condenser performance.....	83
A-1 Heat- and mass-transfer laboratory test chamber: condenser, left; evaporator, right.....	96
A-2 Vacuum test chamber with end caps rolled back.....	98
A-3 Water piping and an end view of the test chamber.....	98

LIST OF FIGURES (Concluded)

	<u>Page</u>
A-4 Schematic of laboratory piping.....	99
A-5 Temperature measurement system.....	102
A-6 Typical water temperature measurement RTD installation.....	105
A-7 Summary curve of 20 step-linearized solutions for probe temperature calculations.....	106
A-8 Wet-bulb steam temperature measurement probe.....	109
B-1 Comparison of measured and calculated steam outlet temperature for cocurrent packing 19060.....	115
C-1 Countercurrent condenser.....	124
C-2 Spiral screen, condenser configuration 1.....	126
C-3 Baffle plate, disc donut, condenser configurations 2 through 4.....	126
C-4 Spiral rubber mat, condenser configuration 5.....	126
C-5 Munters packing, condenser configurations 6 and 7.....	126
C-6 Condenser configuration 8 with random packing.....	128
C-7 Performance of countercurrent disc-donut baffle condensers.....	129
C-8 Relative performance comparisons of countercurrent condenser configurations.....	130

LIST OF TABLES

	<u>Page</u>
2-1 Comparison of Correlation Data Base with Experimental Condenser Entrance Conditions.....	26
2-2 Correlations for SERI Direct-Contact Condenser Model.....	29
3-1 SERI Direct-Contact Laboratory Capabilities.....	33
3-2 Summary of Uncertainties in Primary Measurements.....	33
3-3 Estimated Uncertainties in Derived Quantities for Packing 19060....	34
3-4 Geometry Comparisons of the Tested Packings.....	36
3-5 Tested Range for Cocurrent Condensers.....	38
3-6 Tested Range for Countercurrent Condensers.....	38
4-1 Cocurrent Condenser Comparison Summary.....	48
4-2 Countercurrent Condenser Comparison Summary.....	55
5-1 Condenser Parameters.....	57
6-1 Comparison of the Influence of Rate Deaeration on a Two-Stage Condenser.....	88
A-1 SERI Low-Temperature Heat- and Mass-Transfer Laboratory Capabilities.....	97
A-2 Heat- and Mass-Transfer Laboratory Hardware Model Numbers and Specifications.....	97
A-3 Platinum-Resistance--Temperature-Detector Specifications.....	102
A-4 Typical Calibration Data for RTD.....	103
A-5 Summary of Uncertainties in Primary Measurements.....	110
B-1 Countercurrent Derived Parameter Uncertainty Estimates 19060 Packing.....	117
B-2 Primary Uncertainties.....	118
B-3 Uncertainties in Countercurrent Condenser Experimental Results.....	119
B-4 Uncertainties in Cocurrent Condenser Experimental Results.....	120
B-5 Cocurrent Derived Parameter Uncertainty Estimates 19060 Packing....	121

LIST OF TABLES (Concluded)

	<u>Page</u>
C-1 Summary of Countercurrent Condenser Configurations.....	125
D-1 Cocurrent Condenser Data for AX Packing.....	132
D-2 Cocurrent Condenser Data for 19060 Packing.....	134
D-3 Cocurrent Condenser Data for 4X Packing.....	136
D-4 Cocurrent Condenser Data for Falling Jets.....	138
D-5 Countercurrent Condenser Data for AX Packing.....	140
D-6 Countercurrent Condenser Data for 19060 Packing.....	143
D-7 Countercurrent Condenser Data for 3X Packing.....	149
D-8 Countercurrent Condenser Data for 27060 Packing.....	152
E-1 Countercurrent Condenser Data for Configuration 1 with Spiral Metal Screen.....	164
E-2 Countercurrent Condenser Data for Configuration 2 with Three Pairs of Baffles.....	167
E-3 Countercurrent Condenser Data for Configuration 3 with Two Pairs of Baffles.....	169
E-4 Countercurrent Condenser Data for Configuration 4 with One Pair of Baffles.....	171
E-5 Countercurrent Condenser Data for Configuration 5 with Spiral Matted Screen.....	172
E-6 Countercurrent Condenser Data for Configuration 8 with Random Packing.....	177
F-1 Cross Reference of Computer Program Variables.....	238

NOMENCLATURE[‡]

A	condenser cross-sectional area (m^2)
A	lumped pressure loss coefficient (Eq. 2-34)
Ack _f	Ackermann friction correction factor
Ack _h	Ackermann heat-transfer correction factor
a _f	effective area fraction
a _p	available surface area per unit volume (1/m)
B	packing base dimension (m)
C	pressure loss coefficient in packing (Eq. 2-34)
C _{Loss}	contact loss in area
C _o	dimensionless steam flux
C _p	specific heat (kJ/kg K)
D _L	diffusivity of inert gas in water (m^2/s)
d	diameter (m)
Fr	liquid Froude number (Eq. 2-33)
f	friction factor
G	gas loading of steam-inert mixture on planform condenser area ($\text{kg}/\text{m}^2 \text{ s}$)
g	gravitational acceleration (m/s^2)
He	Henry's Law constant for dissolved inerts (Pa)
h	heat-transfer coefficient [used with subscripts L or G] ($\text{kW}/\text{m}^2 \text{ K}$)
h	height of packing cross section (m)
h _{fg}	latent heat of condensation (kJ/kg)
Ja	Jakob number (Eq. 4-1)
j	superficial velocity (m/s)
k	mass-transfer coefficient ($\text{kg}/\text{m}^2 \text{ s}$)
L	liquid loading based on planform condenser area ($\text{kg}/\text{m}^2 \text{ s}$)
Le	Lewis number (Eq. 2-14)
ℓ	packing stack length (m)
M	molecular weight
ṁ	mass flow rate (kg/s)

[‡]Because of the large number of variables appearing in this report, some symbols are used to represent more than one variable. However, care was taken to use them in widely differing contexts to minimize possible misinterpretation and confusion. In addition, a separate nomenclature appears after Section 7.0 for the symbols used in the appendices.

NOMENCLATURE (Continued)

Nu	Nusselt number
n	Manning roughness coefficient
P	static pressure (Pa)
p	pressure (Pa)
pp	partial pressure (Pa)
Δp	pressure drop (Pa)
Pr	Prandtl number
Q	condenser heat load (kW)
q	heat transferred per unit mass flow per unit length (K/m) (Eqs. 2-12, 2-13)
q	gas dynamic pressure (Eq. 2-34)
R	universal gas constant (kJ/kg K)
Re	Reynolds number
S	slant height of packing cross section (m)
S'	distance over which liquid renewal occurs (m)
Sc	Schmidt number
Sh	Sherwood number
T	temperature ($^{\circ}\text{C}$, K)
t	packing sheet thickness (m)
U_{Geff}	effective gas velocity (m/s)
U_{Leff}	effective liquid film velocity (m/s)
u	gas velocity (m/s)
V	condenser vent fraction
w	interfacial mass transfer flux ($\text{kg/m}^2 \text{ s}$)
X	inert gas mass fraction
y	inert gas mole fraction
z	coordinate along the condenser
<u>Greek</u>	
α	modified flow surface inclination from horizontal (deg)
Γ	liquid film flow per unit surface area in unit length of packing (kg/m s)
Δ	changes in property
ϵ	void fraction of the packing
ϵ_w	condenser water effectiveness
δ	liquid film thickness (m)

NOMENCLATURE (Concluded)

θ	packing channel inclination from horizontal (deg)
μ	dynamic viscosity (kg/m s)
ρ	density (kg/m ³)
τ	shear stress (Pa)

Subscripts and Superscripts

b	bulk
c	condensed
eq	equilibrium, equivalent
ex,x	exhaust
f	liquid
G,g	gas or steam and inert gas mixture
i	inert
int	interface
L	liquid
max	maximum
o,out	outlet, outside column
S	based on slant height S
s	steam
sat	saturation
w	water
wet	wetted conditions
*	equilibrium

1.0 INTRODUCTION

This report summarizes extensive work carried out at the Solar Energy Research Institute (SERI) in developing direct-contact condensers for use in the Claude-cycle ocean thermal energy conversion systems. The primary focus of the effort was to develop a numerical model of the condenser and to determine how well this model predicts the behavior observed in the parallel experimental program using structured packings as the gas-liquid contacting device. We also provide detailed descriptions on the study's background, previous work in this field, the numerical model, the experimental facility and instrumentation, and the uncertainties in primary and derived parameters. Full sets of measurements made at SERI and their corresponding predictions yielded by the model accompany this report.

Figure 1-1 shows a schematic of an open-cycle (Claude-cycle) ocean thermal energy conversion (OC-OTEC) power system. Warm seawater (about 25°C) enters the evaporator section of a vacuum chamber. Pressure in the evaporator is maintained sufficiently low to produce steam. This is done by operating below the vapor pressure at the incoming surface water temperature. Water droplets carried by the wet steam are removed in a mist eliminator. The steam expands through a turbine between the evaporator and the condenser section of the chamber. Cold seawater (about 5°C), pumped from a depth of about 1000 m, is used as the heat sink in the condenser. The turbine is mechanically linked to a generator that yields net power after providing the power required to pump the warm and cold water streams and to remove noncondensable gases released in the vacuum chamber.

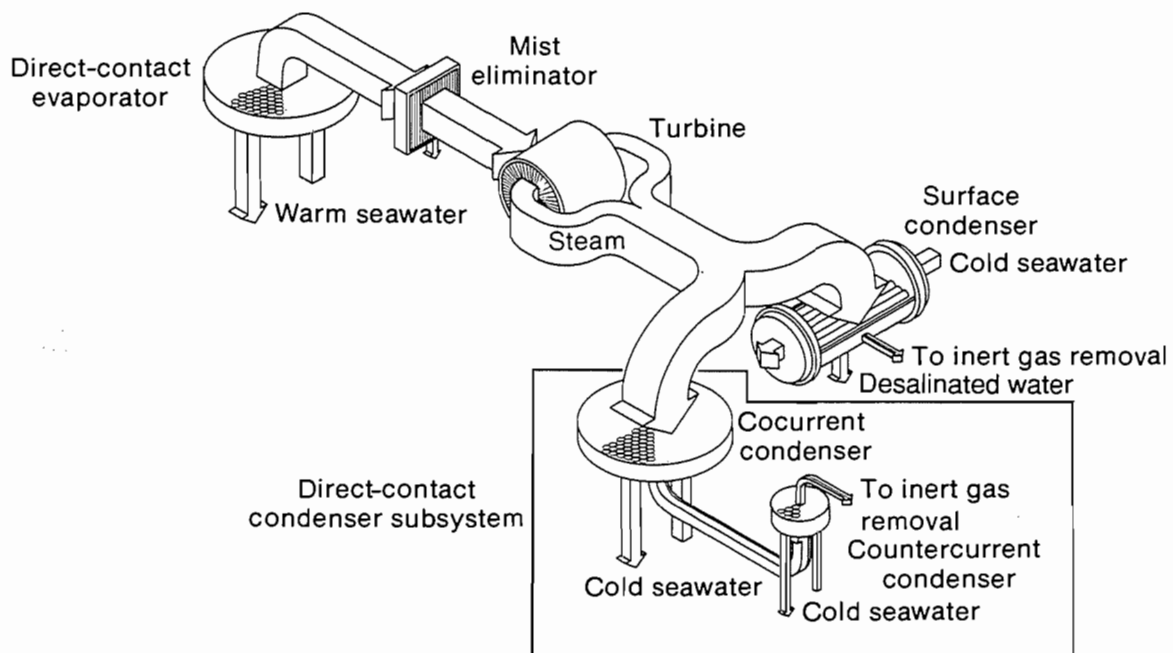


Figure 1-1. Schematic of an open-cycle ocean thermal energy conversion system

Dissolved gases in warm and cold water may come out of solution in the evaporator and condenser. Unless removed, these gases will accumulate in the condenser section of the vessel, blanketing the condensing surfaces and decreasing the condensation efficiency. Additional pumping power, therefore, must be expended to remove these gases and to maintain suitable operating pressure in the condenser. The condenser can be direct contact, surface, or a combination of both. A surface condenser can yield desalinated water as a by-product.

An alternative method for desalinated water production from the open cycle uses a direct-contact desalinated water condenser in a pump-around loop together with a desalinated water/seawater heat exchanger. A schematic of the use of a direct-contact condenser for desalinated water production is shown in Figure 1-2. In this method, the circulating, warmed desalinated water discharge from the condenser is cooled in a heat exchanger using the cold seawater. The attractiveness for this approach arises from the ability of the direct-contact condenser to handle low-density steam efficiently without a large pressure loss within a compact volume. However, it requires using a water/water heat exchanger and a desalinated water circulating pump. Preliminary estimates show that this type of a system may be less expensive compared with a large volume surface condenser. However, the relative cost-effectiveness of the surface condenser or a direct-contact condenser system for desalinated water production from an OTEC plant requires further study.

This report focuses on the boxed area in Figure 1-1, enclosing the direct-contact condenser subsystem. This condenser system, because of its barometric placement and system integration constraints, consists of two stages to keep

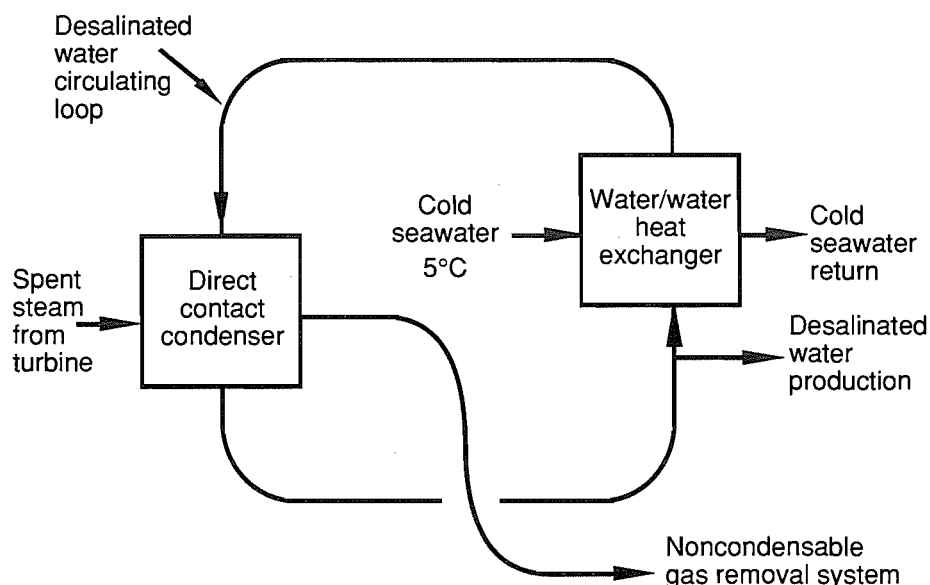


Figure 1-2. Diagram of desalinated water production scheme using direct-contact condenser

plant volume and water pumping power low. Figure 1-3 illustrates the steam flow through the stages. In the first stage, the steam and noncondensable gas mixture flows downward in a cocurrent mode along with the seawater. About 70% to 80% of the incoming steam is condensed here. The remaining steam then flows into a countercurrent condenser against the downward cooling water flow. This stage condenses most of the remaining steam and thereby concentrates the noncondensable gases to the maximum extent possible. The outgoing uncondensed steam and noncondensable gases are then removed by an exhaust vacuum pumping system.

Typically, in an open-cycle plant, the steam flow to be condensed ranges from 10 to 20 kg/s per MW_e gross output at temperatures from 9° to 13°C with the higher flow rate corresponding to the higher temperature (Parsons, Bharathan, and Althof 1987). Because of the progressive condensation of steam, the mass fraction of noncondensable gases in the steam can vary from 0.5% up to 40% within the condenser.

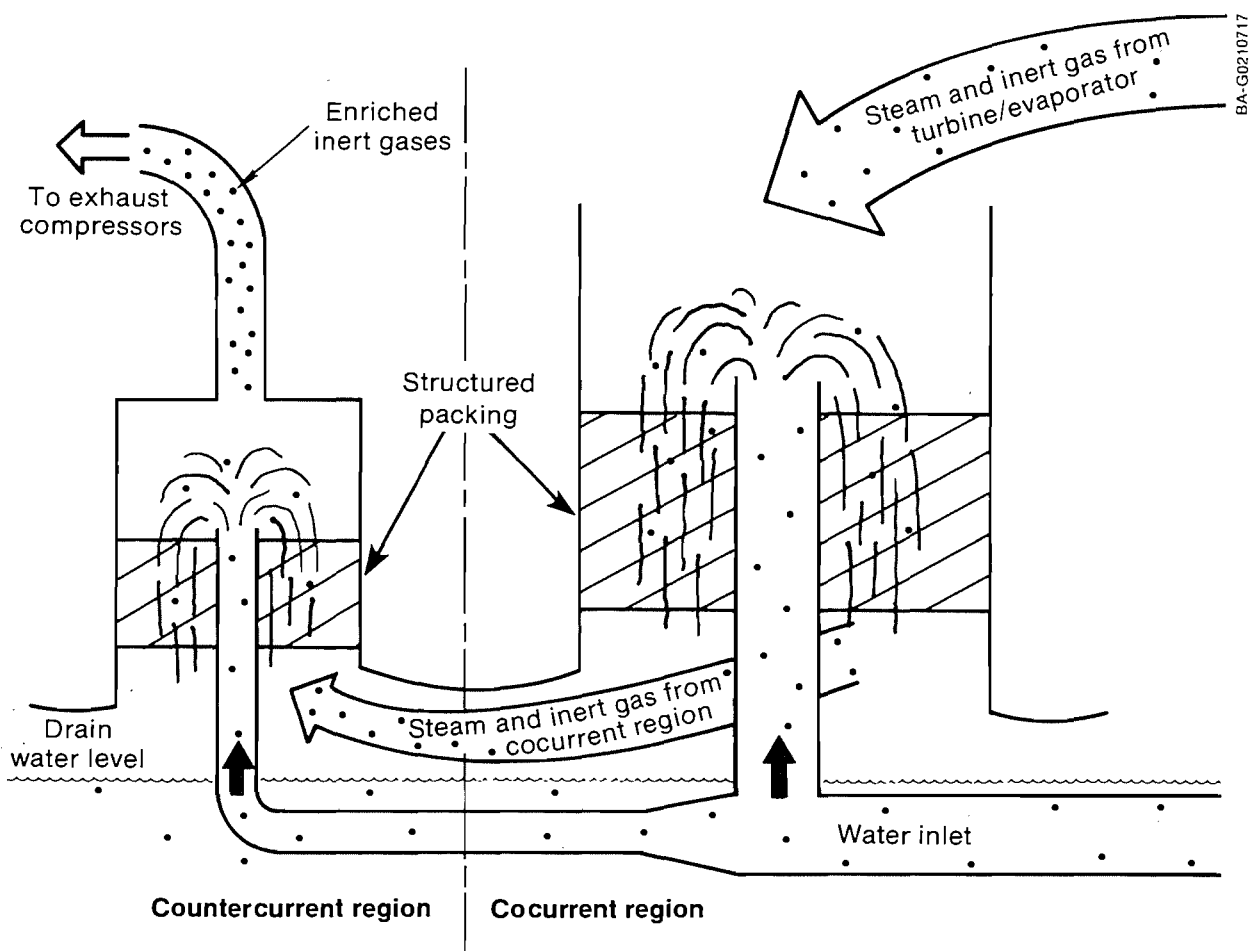


Figure 1-3. Schematic of barometric direct-contact condenser subsystem indicating steam and noncondensable gas mixture flow through cocurrent and countercurrent sections using structured packings

Because the temperature difference between the warm and cold water used in OTEC is small, the condenser must handle large quantities of cold seawater on the order of 2-4 m³/s per MW_e of gross power (Parsons, Bharathan, and Althof 1987). We estimate the overall water pumping head losses to be about 5 m in the cold-water hydraulic loop, which consists of the intake pipe (extending to a depth of about 1 km below sea level), the distribution manifold, the discharge pipe, and perhaps a predeaerating system. Nominally, a free-fall of 2 m is available for the seawater in the condenser. Each meter of additional head loss in the condenser can reduce the available power up to 6%.

In addition to removing spent steam, the condenser must efficiently remove noncondensable gases. These gases accumulate at the condenser because they desorb from the resource waters and because atmospheric air leaks into the vacuum system. Thus, the condenser performance is closely coupled to that of the noncondensable-gas removal (NCGR) system. The gas mixture exhausted through the NCGR system consumes a parasitic power of typically 10% to 15% of the gross power (Parsons, Bharathan, and Althof 1987).

The noncondensable gas removal system and the condenser performances are closely interrelated. The capacity of the NCGR system will dictate the back pressure and, thus, the condenser operating pressure. On the other hand, the effectiveness of the condenser in reducing the partial pressure of steam in the exhaust gas mixture and its gas-side pressure loss will affect the capacity of the removal system. Although it is difficult to separate the condenser and the noncondensable gas removal system requirements, from a system point of view, the key condenser design parameters are

- Low liquid-side pressure loss
- Low vapor-side pressure loss
- High condenser effectiveness
- Minimal degradation caused by the presence of noncondensable gases
- Simple liquid inlet and exit manifolds
- Simple gas exhaust manifold designs to concentrate the noncondensable gases
- Small volume
- Immunity to plant motion for floating platforms or to tides for shore-based plants
- Low cost of fabrication
- Low susceptibility to corrosion and biofouling
- Uniform liquid and gas loadings.

1.1 Objective and Goal

The objective of this study is to develop an engineering data base and to validate analytical methods to design and evaluate the performance of advanced, high-performance heat exchangers that are reliable and cost-effective for use in an OC-OTEC process.

The specific goal is to establish quantitatively the extent to which the developed numerical condenser model captures the observed behavior in the

experiments over an extensive set of data that covers a large portion of the expected condenser operating range for an OC-OTEC system.

1.2 Approach

Our approach in the engineering development of direct-contact condensers included the following steps:

1. Investigate experimentally a variety of likely condenser configurations such as commonly used gas-liquid contacting devices to establish their relative performance.
2. Evaluate and choose a device according to its performance as a condenser, its ease of integration into an OTEC system, and its commercial availability in terms of its geometry, material choices for seawater use, and cost.
3. Develop a numerical model for the chosen condenser configurations that captures the physical phenomena occurring within the condenser, with the goal of predicting key condenser performance parameters.
4. Establish the validity of the model by comparing the predictions with experimental observations for a variety of contactor geometries for the chosen device.
5. Generate parametric results to provide guidance in selecting suitable geometries as well as flow conditions for potential OTEC design options.

Experimental work carried out at SERI was aimed at addressing research issues on heat exchangers for the open cycle. For investigating evaporation and condensation at low pressures, an experimental facility using fresh water was commissioned in 1979 (see Section 3.0 and Appendix A). This facility allows us to quickly and efficiently investigate various heat exchanger configurations under controlled test conditions and to avoid unwanted external influences related to field-site operation. This well instrumented facility yields minimal uncertainties in the derived heat-exchanger performance parameters as well (see Appendix B). The fresh water results from this facility provide a firm technical basis for selecting prototype test articles for seawater testing. By properly accounting for seawater's varied physical properties, we anticipate being able to transfer fresh water results to seawater. This assumption will be tested using seawater at the experimental facility described in the following paragraph.

We investigated a variety of evaporator configurations in the early 1980s using this facility (Bharathan and Penney 1984). Screening the configuration with fresh water in this facility resulted in the selection of the spout evaporator as the preferred geometry for seawater tests. Ongoing experiments with seawater at the U.S. Department of Energy's (DOE) Seacoast Test Facility (STF) at the Natural Energy Laboratory of Hawaii substantially confirm the earlier findings obtained using fresh water.

We tested various direct-contact condenser configurations at this facility, including contactors using random and structured packings. Their performance was evaluated relative to their efficiency in cooling water usage and in handling the noncondensable gases present in steam. Typical test results for a countercurrent condenser are shown in Figure 1-4. The plot shows the water

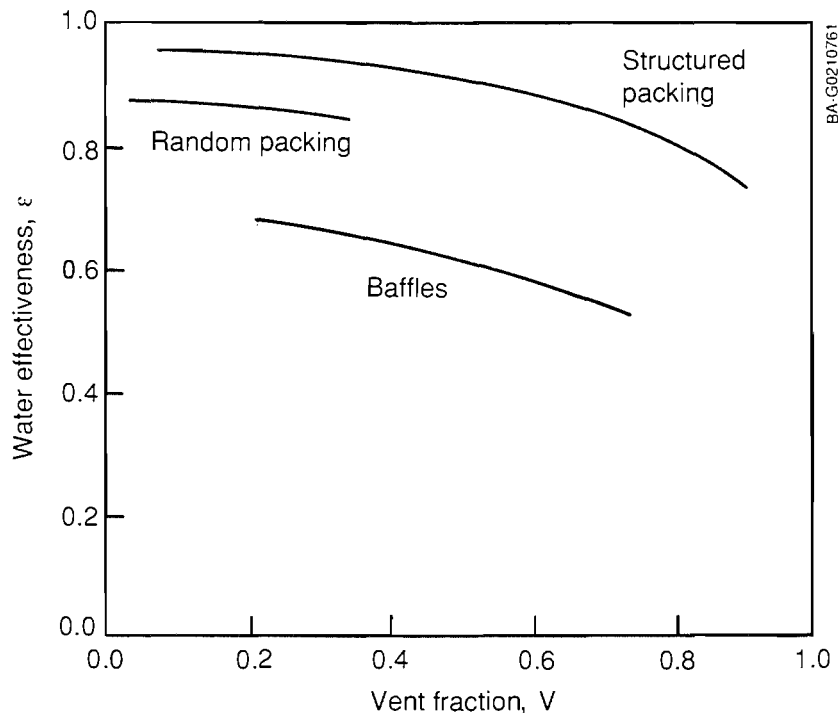


Figure 1-4. Relative performance comparison of a few tested countercurrent condenser configurations

effectiveness ϵ against a vent fraction V . The effectiveness represents the cooling water temperature rise as a fraction of the available temperature-driving potential. The vent fraction represents the ratio of volumetric exhaust flow for an ideal condenser to that of an actual condenser. From these definitions, we can see that for a good condenser configuration we should aim to achieve high values for both the effectiveness and the vent fraction. Typical test results for three condenser configurations, namely, baffles, randomly packed media, and structured packings, are shown in Figure 1-4. Among these and all other tested configurations, we found that the structured packings yielded the highest effectiveness and vent fraction at similar test conditions. These results indicate that for a direct-contact condenser, the structured packings yield the best performance among all tested configurations. A more detailed description of these test results and the evaluation of relative ranking of tested configurations are provided in Appendix C.

Based on these early experimental results, we narrowed our choice of gas-liquid contact media to structured packings. With the structured packing as the preferred configuration for the direct-contact condensers, we expanded the scope of our study to further experimentation, modeling, and validation efforts confined to this type of packing as summarized in this report.

The results from the fresh water facility provide the basis for selecting test articles and operating conditions for the planned seawater tests at the STF. We were encouraged in using such a basis because our ongoing seawater experiments successfully substantiate the fresh water investigations on evaporation conducted earlier at this facility. The utility of the SERI fresh water facility in efficiently and cost-effectively screening configurations

and in conducting detailed investigations of low-temperature heat and mass transfer phenomena cannot be overemphasized.

1.3 Scope and Limitation

Despite an ambitious scope, practical considerations limited our experimental investigations to five basic configurations: falling jets, spirally screened passages, disc-donut baffles, and random and structured packings. Results of our studies with jets were reported earlier by Bharathan et al. (1982). All other results are included in this report. Tabular data for structured packing are provided in Appendix D; data for other configurations are in Appendix E. Because of earlier experiments, we quickly narrowed our choice of a contacting device to structured packings. The ready commercial availability of these packings, commonly used in cooling towers and distillation and absorption applications in chemical engineering, also provided a substantial reason for choosing them. These packings are available in a wide variety of geometries and materials, so specific needs for an OTEC condenser can be readily met.

Based on the choice of structured packing as the appropriate contacting device, we chose to model the condensation process occurring within these for both cocurrent and countercurrent configurations. Presently, we model cocurrent and countercurrent condenser modules as separate entities; in other words, they are not interconnected. The computer algorithms to capture the physical process are written in the Turbo-Pascal™ language (version 3.0).

Suitable process transfer correlations for performance predictions for these geometries were not available in the open literature until the recent works of Bravo, Rocha, and Fair (1985 and 1986) at the University of Texas in Austin. We used transfer correlations provided by Bravo. Based on available experimental data, we made suitable modifications to the liquid-side transfer correlations for turbulent liquid films on inclined surfaces. An effective surface area fraction was introduced that represents the ratio of the packing's active surface to the total available geometric area. Although the surface area and heat-transfer coefficient are treated separately for the sake of modeling, such a separation is difficult to make based on the available experimental data; therefore, these quantities should be viewed as the product of the available area and the appropriate transfer coefficient rather than as individual quantities.

In this report, we supply extensive sets of comparisons of the analytical results with available fresh water experimental data. Currently, only experimental data on inlet and outlet conditions for condensers of a specified geometry and length are available. Thus, these comparisons indicate the overall correctness of the model.

Uncertainty overlaps between the predictions and the data indicate that the predictions agree with the data within generally acceptable engineering

*Turbo-Pascal™ is the trade name of a programming language by Borland International, Inc., Scotts Valley, Calif. We chose this language for its efficient error-tracking capability, ease of use, and compilation and execution speeds on personal computers.

uncertainties for performance predictions of heat exchangers. Thus, the validated model provides firm technical basis for design, optimization, and performance predictions of direct-contact condensers using structured packings.

We also conducted detailed parametric studies of the validated model (Section 5.0). These parameters were generally categorized as geometric and flow parameters. For some of these, we identified clear-cut, optimum choices based on predicted results. To select others, evaluations based on system optimization are required to yield the "best" cost or performance for an overall plant.

1.4 Background

In direct-contact condensation, a subcooled liquid stream enters a chamber holding the vapor to be condensed. The resistances to heat transfer consist in a series of a gas phase, an interfacial, and a liquid phase. In the absence of noncondensable impurity gases in the vapor, the gas-phase and interfacial resistances are small compared with the liquid-phase resistance. The heat-transfer mechanism can be described in two parts: as the molecular crossover mass transfer from the vapor to the interface and as the accompanying transfer of heat to the bulk liquid from the interface at an intermediate temperature. The overall transfer rate is governed by the molecular transport within the liquid and the differential rate of molecular crossing at the interface. For water at OTEC temperatures, the resistance to heat transfer at the interface is extremely small compared with the resistance on the liquid side (Maa 1967). For simple liquid geometry, such as films or uniform droplets, we can readily predict the heat-transfer resistance. Thus, the rate of condensation for simple geometries can be evaluated when the resistance resides primarily on the liquid side.

Seawater contains dissolved gases of which mostly nitrogen and oxygen will be released in the vacuum chamber of an OC-OTEC plant. These gases affect plant performance by raising the condenser pressure, degrading the performance of the condenser, and requiring compression power for their removal.

Analyzing direct-contact condensation is complicated because these noncondensable gases are present in the condensing vapor. Since the coolant acts as a sink, the gases are drawn to the exposed liquid interface by the condensing steam. Accumulating gases adjacent to the interface blanket the condensing surfaces. Therefore, the vapor must diffuse through the gaseous barrier before condensing, causing the gas-side resistance to increase significantly. To maintain satisfactory condensation efficiency, the accumulating gases must be continuously removed and exhausted.

For combined heat and mass transfer, Colburn and Hougen (1934) proposed a method to account for liquid-side heat-transfer resistance and gas-side mass- and heat-transfer resistances. Their approach treats the vapor flow from a mixture of vapor and noncondensable gas as diffusion through a stagnant film. They adopted a trial and error method to determine an intermediate interface temperature. Ackermann (1937) later derived multiplicative factors for evaluating transfer rates to account for high vapor fluxes toward the interface.

Bras (1953) showed that the vapor does not remain at saturation as it flows through the condenser. Depending on the relative magnitude of vapor-side

heat- and mass-transfer rates, the vapor may become subcooled or superheated. At relatively low diffusional rates, subcooling may cause fog to form in the flowing vapor stream.

A vast amount of literature exists on condensation related to surface condensers. Subjects range from a fundamental investigation of accommodation coefficients (see, for example, Mills and Seban [1967]) to two-dimensional analytical modeling of vapor flow through a complex array of tube bundles (see Johnson, Vanderplaats, and Marlo [1980]). It is beyond the scope of this work to provide a detailed summary of the surface-condenser literature. A succinct summary of condensation heat-transfer may be found in Metre (1973), Webb and Wanniarachchi (1980), and Butterworth and Hewitt (1978). For OC-OTEC, Panchal and Bell (1984) provide a theoretical analysis of surface condensers.

Direct-contact condensation differs from surface condensation in that an impermeable surface separating the coolant and the condensate is absent. Modeling the direct-contact condenser is similar to modeling a surface condenser except for the difficulty in defining an appropriate geometry and available surface area for the vapor-liquid interface. Turbulence level, back-mixing and recirculation, and instabilities at the interface result in large uncertainties in estimated transfer coefficients and available interfacial area for condensation.

Literature in the area of direct-contact condensation is scant. No comprehensive treatments are available for direct-contact applications for designing and analyzing industrial and power systems, such as those available for surface condensers. Sideman and Moalem-Mason (1982) provide a brief review of the majority of earlier works on this subject. Since the vapor-liquid interface geometry plays a major role in direct-contact condensation, they categorize the earlier works according to the available interface, such as free-liquid interface (including jets, films, and drops), bubble columns, and other contacting devices (such as packed beds and baffle trays).

Well-defined interfaces are amenable to analytical modeling. When the liquid-side heat-transfer resistance is dominant relative to the gas-side resistances, analytical models for cylindrical jets (Kutateladze 1959), planar jets (Hasson, Luss, and Peck 1964), fan sprays (Hasson, Luss, and Peck 1964), droplets (Kulic, Rhodes, and Sullivan 1975), and falling films (Dukler 1960) are available. For more complicated geometries, such as in spray nozzles or packed columns where the interfacial area is complicated, little modeling effort is reported. However, many industrial vapor-liquid contacting devices use the more complex geometries because of their inherently higher contacting efficiency.

Four general classifications exist for direct-contact gas (or vapor) to liquid heat-transfer processes: simple gas cooling, gas cooling with vaporization, gas cooling with partial condensation, and gas cooling with total condensation. These processes are complex, and each of them is described by a separate set of relations. Direct-contact heat exchange has traditionally been accomplished in one of the following devices: baffle tray columns, spray chambers, packed columns, cross-flow tray columns, or pipeline contactors. Design methods for each of them were summarized by Fair (1961 and 1972). The most common techniques used in industrial applications are the liquid spray column and the baffle-plate column. Fair compared these devices and showed

that the typical performance given in number of transfer units (NTU) is only about 1, yielding 60%-70% condenser effectiveness. This value is so low because of back-mixing, and in baffle columns there is also a large gas-side pressure drop. This is a particular disadvantage for OTEC applications where minimizing parasitic power consumption is of prime importance.

In addition to liquid-spray and baffle-plate columns, packed columns have been used in applications that require a large rate of heat and mass transfer per unit volume. Until recently, the packings or inserts commonly used in the columns were randomly distributed and thus created a complex flow pattern with a relatively large pressure loss. In the past decade or so, however, new types of packings have been introduced in the United States. They, unlike the classical, randomly placed packing elements, are fitted in an ordered and structured manner in the column to carefully match its size and operation. These structured packings show excellent performance characteristics. In particular, they yield a relatively low ratio of pressure drop to heat- or mass-transfer coefficient per unit volume (Bravo, Rocha, and Fair 1985 and 1986).

Although the cost per unit volume of structured packings is higher than that of classical packings such as Berl saddles and Pall rings, their favorable efficiency and pressure drop characteristics make these packings preferable for many applications, especially when operating in a vacuum such as an OTEC condenser. These new packings also provide a means of continually redistributing the liquid flow, while supplying a relatively straightforward flow path for the vapor, which significantly reduces the pressure drop. These packings, made of plastic sheets, have been used for some time in cooling towers; but recent improvements in manufacturing have made these packings available in the form of gauze or wire-mesh sheets. These surfaces allow vapor-to-liquid contact on both sides and also provide for uniform liquid distribution due to capillary action, even at low liquid loadings. Structured gauze packings increase the residence time of the liquid, and available data show that the entire area of the packing is effective in mass transfer. These high-performance packings were developed in Europe, and, unfortunately, performance data are largely proprietary, although some design equations for gauze-structured packings were recently published by Bravo, Rocha, and Fair (1985) over a limited range of operating parameters.

SERI began a research program in 1983 to better understand the mode of operation of various packings for direct-contact heat and mass transfer and to provide experimental data for developing a predictive model. SERI experiments show that structured packing offers an attractive geometry for condenser applications.

Direct-contact condensers have potential for use in many process applications as well as in power plants. One of the main reasons for the limited use of direct-contact condensers is that engineers do not have reliable design and performance prediction methods. Condensers are difficult to analyze for the following reasons:

- Vapor loading and heat and mass flux decrease continuously as vapor condenses. The vapor's velocity in a direct-contact device varies appreciably with the distance traveled because of continuous condensation; hence, the average values of heat- or mass-transfer coefficients used for design are usually not accurate.

- The latent heat of condensation is high, causing a great ratio of liquid-to-vapor mass flux (not typical in mass transfer applications); and little experimental data are available for that range of liquid loadings.
- For use with seawater, noncondensable gases are present, and their effects on the gas mass-transfer rates are difficult to predict quantitatively.
- Finally, in many practical situations, the flow changes from turbulent to laminar, and such a transition is not well understood in general and is difficult to quantify under condensation conditions.

For these reasons, the widely used NTU design methodology will generally not suffice (Kreith and Bohn 1986; Sherwood, Pigford, and Wilke 1975) because the transfer coefficients are not uniform as this approach assumes. Hence, it is necessary to integrate the rate of transfer numerically along the path of the vapor.

The first attempts to model a direct-contact condenser of falling-film geometry for OC-OTEC applications are reported by Wassel et al. (1982). Their model treated the condensation process rigorously and included pressure and temperature recovery terms resulting from the condensation reducing the velocity of the vapor-gas mixture. They investigated the effect of spacing plates 20 to 60 mm apart in a cocurrent condenser. They also varied flow rates and temperatures over a limited range to establish the trends of condenser performance variations. Wassel illustrated that

- For steam-water condensation when air is present at low pressures, condensation tends to superheat the incoming steam.
- Decreases in steam velocity provide sizable temperature and pressure recoveries.
- Considerable differences exist among available transfer correlations. Choosing an appropriate correlation necessitates an accompanying experimental program.

In an article presenting design methods for gas-to-liquid direct-contact heat transfer, Fair (1961) noted that design information was based on proprietary art instead of solid engineering know-how. This situation was reconfirmed in the National Science Foundation (NSF)-sponsored workshop "Direct-Contact Heat Transfer," held at SERI (Kreith and Boehm 1988). Consequently, these direct-contact heat- and mass-transfer devices have not been widely used for heat exchange despite the fact that they are simple, potentially economical, and able to handle fluids that would otherwise cause excessive fouling, corrosion, or mechanical stresses in conventional equipment.

1.5 Report Organization

In this report, we introduce the problem, describe the numerical model, and summarize the experimental details. We then provide validation attempts and results of parametric studies. The first five appendices provide more detailed descriptions of the experimental facility and instrumentation, performance parameters, uncertainties in the reported experimental data, and a first-cut evaluation of various tested contacting devices and their tabulated data. The last three appendices list the computer program codes, discuss the

assumptions made in the equilibrium calculations used for assessing performance, and describe how we evaluated the physical properties of water and steam.

2.0 MODEL DESCRIPTION

This section describes the basic modeling equations for the coolant and vapor-gas mixture as it flows through the condenser. Appendix F provides the detailed numerical codes for integrating the process equations and other iteration schemes for the cocurrent and countercurrent condensers.

2.1 Cocurrent Condenser

For cocurrent condensation, we developed process equations for a one-dimensional, steady-state model. These equations follow the approach of Butterworth and Hewitt (1977), as Wassel et al. (1982) originally proposed for OTEC condensers, and assume the following:

- The two-phase flow is in the separated flow regime (when gas and liquid are separated by a well-defined continuous interface) with the steam and water flowing downward by gravity.
- The coolant and condensate are well mixed so their temperature and dissolved inert gas content are identical.
- The interfacial steam flux is governed by combined heat- and mass-transfer processes (in the liquid and vapor, respectively), as modeled by the Colburn-Hougen (1934) approach.
- Suitable corrections on all vapor-side transfer rates and friction to capture the effects of high interfacial fluxes are modeled using the appropriate Ackermann (1937) factors. Similar corrections for liquid-side transfer rates are negligible.
- Diffusion of steam through the inert gas and steam mixture is modeled using the stagnant film theory (Sherwood, Pigford, and Wilke 1975).
- Steam and inert gases are well mixed with an identical temperature, nominally denoted by T_s (i.e., $T_G = T_i = T_s$).
- The flux of inert gas desorbed from the coolant water stream is small compared with the condensing steam flux throughout the condenser, i.e., ($w_i \ll w_s$).
- Desorption of inert gas from the coolant is controlled by diffusion and does not disturb the free interface between the steam and the coolant.
- For structured packings, the effective transfer area for heat and mass is expressed as $a_f a_p$, where a_f is the effective area fraction, assumed to lie in a range $0 < a_f \leq 1$, and a_p is the total available surface area per unit volume.

2.1.1 Interface Temperature

Using the stagnant-film theory, the condensing steam flux w_s , as indicated in Figure 2-1, can be expressed as[†]

$$w_s = k_G \ln \left[\frac{1 - y_{s,int}}{1 - y_s} \right], \quad (2-1)$$

[†]The term w_s is considered positive when steam flows from the vapor to the liquid.

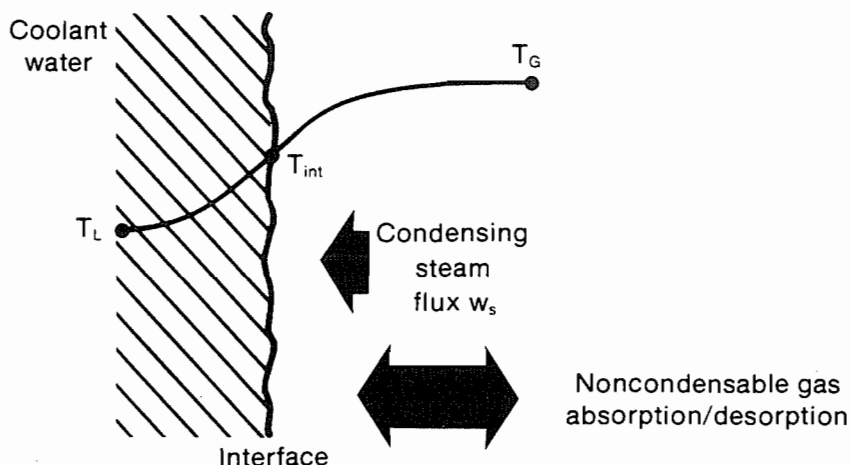


Figure 2-1. Representation of temperature distribution in coolant, gas, and interface during condensation: condensing steam flux and noncondensable mass flux

where

k_G = the vapor-side mass-transfer coefficient ($\text{kg}/\text{m}^2 \text{ s}$)

$y_s, y_{s,int}$ = the steam mole fractions in the bulk mixture and at the interface, respectively.

The heat flux to the coolant consists of two parts: sensible heat transferred from the gas mixture and latent heat caused by condensation. Using the Colburn-Hougen equation (1934), the interfacial steam flux and heat flux can be related to the interface temperature T_{int} as

$$h_L(T_{int} - T_L) = h_G(Ack_h)(T_G - T_{int}) + h_{fg}w_s, \quad (2-2)$$

where

h_L, h_G = the liquid-side and gas-side heat transfer coefficients, respectively, ($\text{kW}/\text{m}^2 \text{ K}$)

h_{fg} = the latent heat of condensation evaluated at the interface temperature (kJ/kg)

T_L, T_{int}, T_G = the liquid, interface, and gas temperatures, respectively.

The term Ack_h represents the Ackermann correction factor for heat transfer to account for high interfacial flux defined as

$$Ack_h = \frac{C_o}{1 - \exp(-C_o)}, \quad (2-3)$$

where

$$C_o = w_s C_{p_s} / h_G$$

and C_{p_s} = the specific heat capacity of the steam ($\text{kJ}/\text{kg K}$).

Equations 2-1, 2-2, and 2-3 allow us to iteratively evaluate the interface temperature T_{int} , provided we know the transfer coefficients h_L , h_G , and k_G .

2.1.2 Transfer Fluxes

Inert gas desorption from the coolant is primarily controlled by diffusion resistance in the liquid film. Inert gas flux from the coolant w_i is expressed as[†]

$$w_i = k_L(X^* - X) , \quad (2-4)$$

where

k_L = the liquid-side mass transfer coefficient ($\text{kg}/\text{m}^2 \text{ s}$)

X, X^* = the inert gas mass fraction in the bulk coolant and the equilibrium value at the partial pressure of inert gas in the bulk mixture, respectively.

The equilibrium value for the dissolved inert gas in the coolant is assumed to be governed by Henry's Law, such that

$$y^* = \frac{pp_i}{H_e} , \quad (2-5)$$

where

y^* = the inert gas mole fraction in equilibrium

pp_i = the partial pressure of inert gas in the bulk mixture (Pa)

H_e = Henry's Law constant, which may be a function of coolant temperature (Pa).

2.1.3 Process Equations

Process equations are derived from mass, momentum, and energy balances across a slice of the cocurrent condenser as shown in Figure 2-2.

2.1.3.1 Mass Balances

The following mass balances were used to develop process equations:

Steam flow:

$$\frac{d}{dz} (\dot{m}_s) = -w_s a_f a_p A \quad (2-6)$$

[†]Inert gas flux absorbed by the coolant is considered positive here.

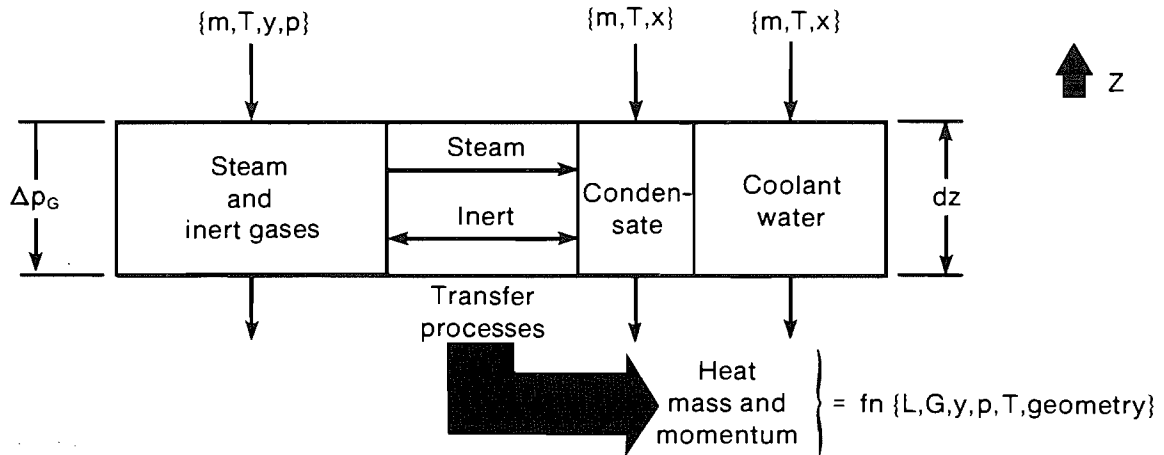


Figure 2-2. A slice of a cocurrent direct-contact condenser indicating the modeling variables for one-dimensional flow

Inert gas in steam and inert gas mixture:[‡]

$$\frac{d}{dz} (\dot{m}_{i,s}) = -w_{ia} a_p A \quad (2-7)$$

Coolant flow (condensate is added):

$$\frac{d}{dz} (\dot{m}_L) = - \frac{d}{dz} (\dot{m}_s) \quad (2-8)$$

Inert gas dissolved in the coolant:

$$\frac{d}{dz} (\dot{m}_{i,L}) = - \frac{d}{dz} (\dot{m}_{i,s}) . \quad (2-9)$$

2.1.3.2 Momentum and Energy Balances

Similarly, the following momentum and energy balances were used:

Condenser heat load:

$$\frac{dQ}{dz} = h_L (T_{int} - T_L) a_f a_p A \quad (2-10)$$

Water temperature:

$$\frac{dT_L}{dz} = \frac{1}{\dot{m}_L C_{pL}} \frac{dQ}{dz} . \quad (2-11)$$

Temperature and pressure of the steam and inert gas mixture are interrelated as follows:

$$\begin{bmatrix} 1 + \frac{u^2}{C_{pG} T} & -\frac{u^2}{p C_{pG}} \\ \frac{\rho u^2}{T} & 1 - \frac{u^2}{RT} \end{bmatrix} \begin{pmatrix} \frac{dT_G}{dz} \\ \frac{dp}{dz} \end{pmatrix} = \begin{pmatrix} \frac{q}{C_{pG}} - \frac{u}{\rho C_{pG}} (\rho u)' \\ -u(\rho u)' - \tau_{int} a_p \end{pmatrix} \quad (2-12 \text{ \& } 2-13)$$

[‡]Double subscripts in all of the following equations, i,s and i,L, refer to inert gas in steam and inert gas in liquid, respectively.

where

$$\begin{aligned} (\rho u)' &= \text{rate of change of gas loading, } \frac{dG}{dz} \text{ (kg/m}^3 \text{ s)} \\ q/C_{pG} &= \text{interfacial heat transfer per unit mass} \\ &\quad \text{flow rate, per unit length, divided by } C_{pG} \text{ (K/m)} \\ &= \frac{h_G(\text{Ack}_h)(T_G - T_{\text{int}}) \exp(-C_o) a_f a_p}{G C_{pG}}, \end{aligned}$$

and

$$\begin{aligned} \tau_{\text{int}} a_p &= \text{the frictional term expressed as} \\ &= \frac{1}{2} \rho_G (U_{\text{Geff}} \pm U_{\text{Leff}})^2 \\ &\quad f[(\text{Ack}_f) a_f a_p + (1 - a_f) a_p] \text{ (N/m}^3 \text{)}, \end{aligned}$$

where

$$\begin{aligned} u &= U_{\text{Geff}} = \text{effective gas velocity (m/s),} \\ U_{\text{Geff}} \pm U_{\text{Leff}} &= \text{gas relative velocity (m/s)} \\ f &= \text{friction factor} \\ \text{Ack}_f &= \text{Ackermann correction factor for high mass fluxes, expressed} \\ &\quad \text{as} \\ \text{Ack}_f &= (2w_s/Gf)/[1 - \exp(-2w_s/Gf)] \\ G &= \text{superficial gas loading (kg/s m}^2 \text{)}. \end{aligned}$$

Note that for the frictional term, the ineffective fraction of the available surface area $(1 - a_f)$ also contributes to pressure loss. The Ackermann correction is applied only where mass transfer occurs (i.e., over the fractional area $a_f a_p$, assuming all contribution to pressure loss occurs via interfacial shear). Other contributions to friction that may arise from form drag are assumed to be negligible.

Equations 2-6 through 2-13 can be integrated along the length of the condenser to arrive at variations of steam, inert, and coolant properties under steady-state conditions. Note that these equations allow us to evaluate the steam and inert gas mixture partial pressures and temperature independently. Steam is normally expected to enter the cocurrent condenser at saturated conditions. However, depending on the relative magnitudes of the vapor-side heat- and mass-transfer rates, the vapor may become supersaturated (forming fog) or superheated. For typical OC-OTEC operating conditions, the Lewis number

$$\text{Le} = \frac{\text{Pr}}{\text{Sc}}, \quad (2-14)$$

representing the ratio of mass to heat-transfer rates, generally ranges around 2. For $\text{Le} > 1$, the steam and inert gas mixture superheats as it goes through the condenser because of a dominating mass-transfer rate (Bras 1953; Sherwood, Pigford, and Wilke 1975).

2.1.4 Equilibrium Calculations[†]

To evaluate a maximum possible performance of a cocurrent condenser, we calculated an equilibrium outlet condition assuming the following:

- Steam and water exiting from the condenser are in equilibrium.
- Dissolved inert gas level in the exiting coolant is again in equilibrium at the partial pressure of inert gases in the exiting steam and inert gas mixture.
- Vapor pressure loss through the condenser is nonexistent.

These assumptions allow us to evaluate the equilibrium exit conditions iteratively and provide a measure to compare performance in an actual condenser with the maximum condenser performance achieved in an ideal condenser (see Appendix G).

2.2 Countercurrent Condenser

A slice of a countercurrent condenser is shown in Figure 2-3. All assumptions used for the cocurrent condenser also apply to the countercurrent condenser. We evaluated the steam-water interface temperature and steam and inert fluxes using the Colburn-Hougen approach described earlier.

2.2.1 Differences in Countercurrent Operation

Initial conditions in a countercurrent condenser are usually specified as flow properties for liquid at the top and for gas at the bottom. The integration scheme, however, requires that liquid and vapor properties be specified at one end of the condenser so the calculation can proceed through the full length of the unit from beginning to end. In this study, the integration proceeded from the bottom, requiring an initial guess of the coolant temperature, flow rate, and dissolved inert gas content exiting the condenser at the bottom. Calculations presented here reflect this reversal. These estimates are updated iteratively to match the calculated coolant inlet conditions at the top with the specified values (within an acceptable tolerance). Our experience indicates four to five iterations are necessary for coolant inlet temperatures to agree within $\pm 0.01^\circ\text{C}$.

2.2.2 Process Equations

The equations for countercurrent flow are essentially similar to the cocurrent flow except that the liquid flows in the negative z direction. Integration is carried out from the bottom of the condenser.

2.2.2.1 Mass Balances

The following mass balances were used to develop process equations for countercurrent flow.

[†]Note that these equilibrium calculations are not "rate-limited," and thus they project the outlet conditions should the heat and mass transfer rates or the condenser length be infinite.

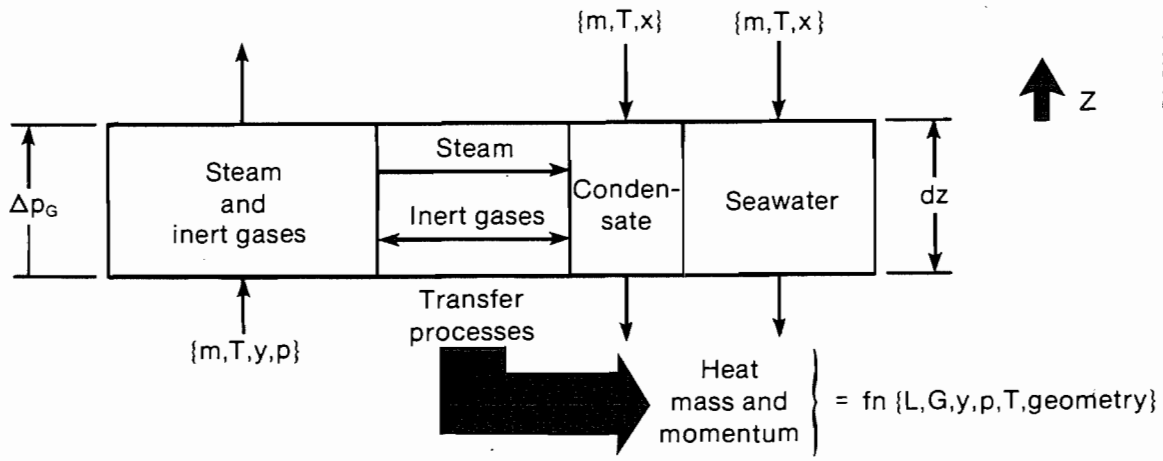


Figure 2-3. A slice of a countercurrent direct-contact condenser indicating the modeling variables for one-dimensional flow

Steam flow:

$$\frac{d}{dz} (\dot{m}_s) = -w_s a_f a_p A \quad (2-15)$$

Inert gas in steam and inert gas mixture:

$$\frac{d}{dz} (\dot{m}_{i,s}) = w_i a_f a_p A \quad (2-16)$$

Coolant flow (condensate is subtracted):

$$\frac{d}{dz} (\dot{m}_L) = \frac{d}{dz} (\dot{m}_s) \quad (2-17)$$

Inert gas dissolved in the coolant:

$$\frac{d}{dz} (\dot{m}_{i,L}) = \frac{d}{dz} (\dot{m}_{i,s}) \quad (2-18)$$

2.2.2.2 Momentum and Energy Balances

Similarly, the following momentum and energy balances were used:

Condenser heat load:

$$\frac{dQ}{dz} = h_L (T_{int} - T_L) a_f a_p A \quad (2-19)$$

Water temperature (decreases with z):

$$\frac{dT_L}{dz} = - \frac{1}{\dot{m}_L C_{PL}} \frac{dQ}{dz} \quad (2-20)$$

Derivatives of temperature and pressure of the steam-inert gas mixture are the same as given in Eqs. 2-12 and 2-13.

These equations allow us to integrate along the condenser's length if we estimate water temperature, flow rate, and dissolved inert gas content in the water at the outlet. Iterations are required to match the exact water flow conditions at the top of the condenser.

2.2.3 Equilibrium Calculations*

To evaluate the maximum performance of an ideal countercurrent condenser, we calculated the equilibrium assuming

- Water exiting the condenser is in equilibrium with the steam entering from the bottom.
- Dissolved inert gas in the water is also in equilibrium with the partial pressure of inert gases in the entering mixture at the bottom.
- The steam and inert gas mixture exiting from the top of the condenser is in equilibrium with the incoming water.
- The incoming water is deaerated to an extent corresponding to its equilibrium level with the steam and inert gas mixture at the top.

A detailed calculation procedure is provided in Appendix G.

2.3 Structured Packings

2.3.1 Geometry Definitions

The used structured packings are made of adjacent layers of corrugated sheets bound together. The sheets may be made of metallic or plastic solid sheets or gauze (wire mesh) sheets. Figure 2-4 shows a structured packing material tested in this study. The orientation of adjacent corrugated sheets is shown in Figure 2-5. The cross-section of the upflowing vapor channel alternates between triangle and diamond shapes.

The vapor flow channel is at an angle θ of 60 deg from the horizontal. This arrangement causes the vapor and liquid flowing between adjacent sheets to periodically redistribute within the bed. The base of the triangle is denoted by B, height by h, and slanted side by S.

Following Bravo, Rocha, and Fair (1985), an equivalent hydraulic diameter for the vapor flow d_{eq} can be defined as four times the flow area per unit perimeter:

$$d_{eq} = Bh \left(\frac{1}{B + 2S} + \frac{1}{2S} \right) \quad (2-21)$$

taken as the arithmetic mean of hydraulic diameters of triangular and diamond-shaped passages. The available surface area per unit volume of the packing, as approximated by Bravo, Rocha, and Fair, is $4/d_{eq}$ (1/m).

For packings made of solid sheets, the contact area (normally the glued or welded area between sheets) between adjacent sheets represents a loss in

*Note that these equilibrium calculations are not rate limited.

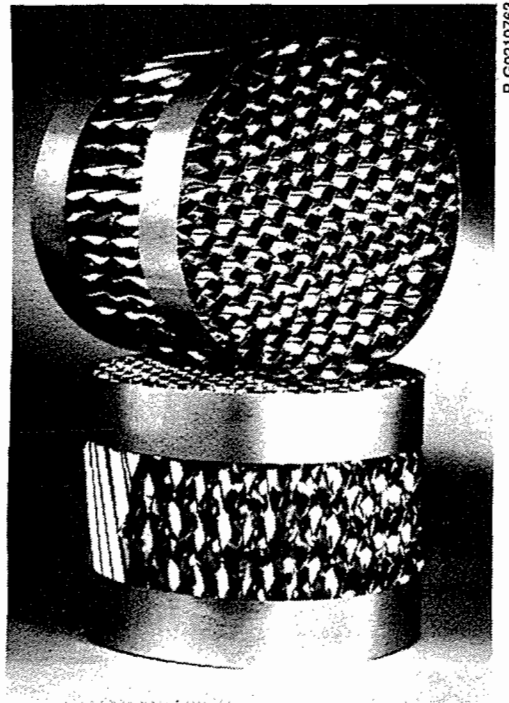


Figure 2-4. Structured sheet packing (Courtesy: Munters Corporation)

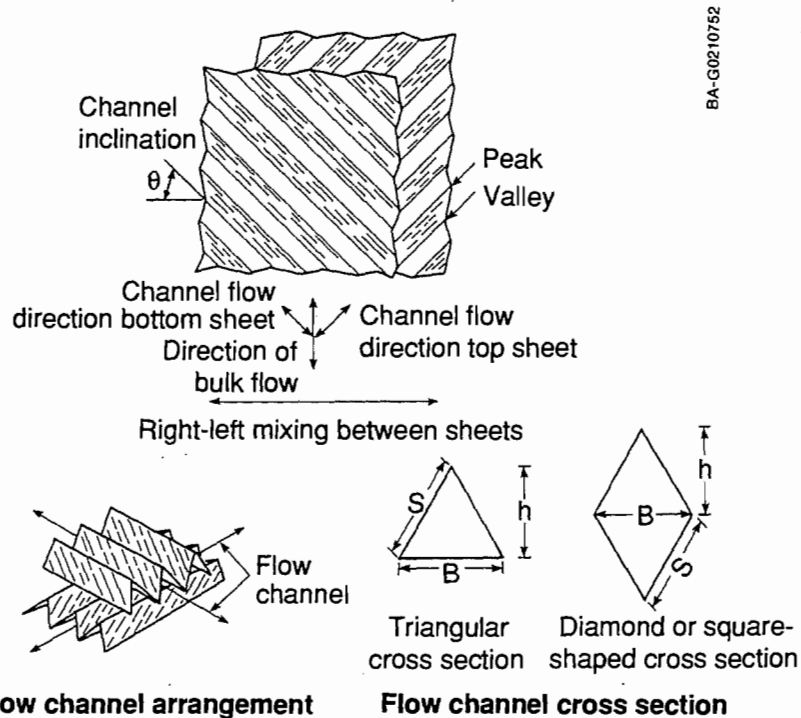


Figure 2-5. Structured packing geometry definition

available area. The thickness of the sheet causes a small but finite reduction in the available volume and void fraction.

Thus, the void fraction is estimated as

$$\epsilon = 1 - 4t/d_{eq} ,$$

where t is the sheet thickness (m).

If a contact loss is expressed as a percentage of total available area C_{Loss} , then we may use a better approximation for the available surface area per unit volume as

$$a_p = (1 - \frac{C_{Loss}}{100}) 4\epsilon/d_{eq} \quad (1/m) . \quad (2-22)$$

2.3.2 Transfer Correlations

The transfer correlations adopted in this study follow the approach of Bravo, Rocha, and Fair (1985). However, modifications were introduced in the liquid-side relations to accommodate high liquid loadings ($L \sim 30 \text{ kg/m}^2 \text{ s}$ versus 2.8 for Bravo).

2.3.2.1 Liquid-side Correlations

Mass Transfer. The liquid moves down by gravity as a film along the flow channel. For gauze-packing capillary action spreads the liquid into thin films (even at low liquid rates) to cover almost the entire available packing surface area. For packings made of solid sheets, however, only a fraction a_f ($0 < a_f < 1$) of the available packing area may be effective in the transfer process. The liquid flows as a film on a surface inclined vertically, as shown in Figure 2-6, as opposed to a vertical surface. Considering that the liquid flow on the inclined surface is equivalent to an "open-channel" flow, Manning's formula (see, for example, John and Haberman 1980) can be used to estimate the effective liquid-film thickness and velocity for water flow. For an inclined smooth surface, the water velocity can be expressed as

$$U_{Leff} = \frac{0.820}{n} \delta^{2/3} (\sin \alpha)^{1/2} \quad (m/s) , \quad (2-23)$$

where

α = modified inclination of the surface from horizontal

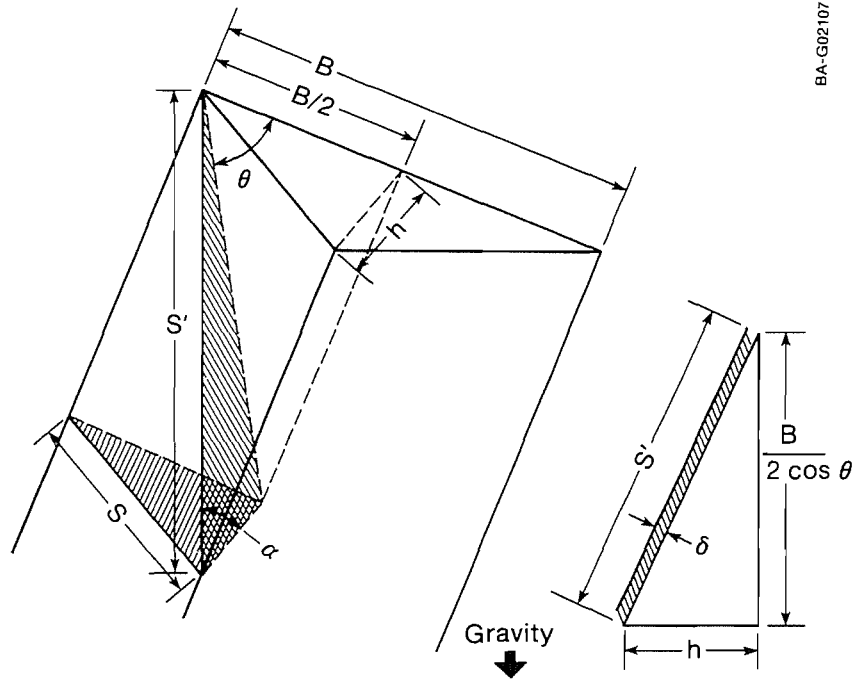
n = Manning roughness coefficient (= 0.010 for smooth surfaces),

δ = film thickness (m).

Using a value of 0.010 for n for smooth surfaces, we see that

$$\delta = \left[\frac{\Gamma}{82\rho_L(\sin \alpha)^{1/2}} \right]^{3/5} , \quad (2-24)$$

where Γ is the water flow per unit surface area in unit length of packing $\Gamma = \rho_L U_{Leff} \delta = L/a_f a_p$ (kg/m s). Here L is the superficial liquid loading ($\text{kg/m}^2 \text{ s}$).



BA-G0210718

Figure 2-6. Liquid film flow on an inclined structured packing geometry

Note that Eqs. 2-23 and 2-24 are in dimensional form, given here in metric units. These equations are valid only for turbulent water flow. Universal dimensionless correlations for turbulent flow on an inclined plane are not available in the literature for use with other liquids.

The typical distance over which liquid renewal occurs is the slanted side S modified by the inclination θ of the corrugation, or S' where

$$S' = \left[\left(\frac{B}{2 \cos \theta} \right)^2 + h^2 \right]^{1/2} \quad (2-25)$$

and

$$\sin \alpha = B / (2S' \cos \theta) . \quad (2-26)$$

The local liquid-side mass-transfer coefficient, based on the penetration theory of Higbie (1935) and as used by Bravo, Rocha, and Fair (1985), then can be expressed as

$$k_L = 2\rho_L (D_L U_{Leff} / \pi S')^{1/2} , \quad (2-27)$$

where

$$D_L = \text{air diffusivity in water (m}^2/\text{s)}$$

U_{Leff} = effective liquid film velocity (m/s)

S' = distance over which liquid renewal occurs (m)

k_L = liquid-side mass-transfer coefficient ($\text{kg}/\text{m}^2 \text{ s}$).

The expression in Eq. 2-27 differs from that of Bravo, Rocha, and Fair in that U_{Leff} is based on a turbulent water flow on an inclined plane rather than laminar flow on a vertical surface; and the renewal distance is S' , which is dependent on θ , as opposed to Bravo's shorter distance S , which is independent of θ .

These differences can be justified in that in all of Bravo's cases, ". . . the liquid-side resistance did not play a significant role in the overall mass transfer resistance," and, thus, the magnitude of the liquid-side resistance as formulated by Bravo possesses a larger degree of uncertainty.

Heat Transfer. The local liquid-side heat-transfer coefficient was evaluated using the Chilton-Colburn (1934) analogy:

$$\frac{h_L}{k_L C_{pL}} = \left(\frac{Sc_L}{Pr_L} \right)^{2/3}, \quad (2-28)$$

where

h_L = liquid-side heat-transfer coefficient ($\text{kW}/\text{m}^2 \text{ K}$)

k_L = liquid-side mass-transfer coefficient ($\text{kg}/\text{m}^2 \text{ s}$)

C_{pL} = specific heat of liquid ($\text{kJ}/\text{kg K}$)

Sc_L = liquid Schmidt number

Pr_L = liquid Prandtl number.

2.3.2.2 Gas-side Correlations

Mass Transfer. The local gas-side mass-transfer coefficient is based on extensive earlier investigations of wet-wall columns. Following Bravo, Rocha, and Fair (1985), the gas Sherwood number is expressed as

$$Sh_G = 0.0338(Re_G)^{4/5}(Sc_G)^{1/3}, \quad (2-29)$$

where

the Sherwood number, $Sh_G = k_G d_{eq} / \rho_G D_G$,

the gas Reynolds number, $Re_G = d_{eq} \rho_G (U_{Geff} \pm U_{Leff}) / \mu_G$, is based on a relative velocity, and

the gas Schmidt number, $Sc_G = \mu_G / \rho_G D_G$.

Here, k_G represents the gas-side mass-transfer coefficient ($\text{kg}/\text{m}^2 \text{ s}$), D_G is the gas diffusivity (m^2/s), and μ_G is the gas dynamic viscosity ($\text{kg}/\text{m s}$).

The effective gas velocity U_{Geff} is dependent on the superficial gas loading G ($\text{kg/m}^2 \text{ s}$), the void fraction of the packing ϵ , and the flow channel inclination θ , as

$$U_{Geff} = \frac{G}{\rho_G \epsilon \sin \theta} . \quad (2-30)$$

The valid range for Eq. 2-29, which Bravo, Rocha, and Fair verified for structured packings, is $220 < Re < 2000$ and $0.37 < Sc < 0.78$ (given in Table 2-1). Based on previous studies, Sherwood, Pigford, and Wilke (1975) claimed a valid range of $3000 < Re < 40,000$ and $0.5 < Sc < 3$. Thus, we expect this expression to be valid at a typical parameter range for an OTEC direct-contact condenser inlet of $800 < Re < 4000$ and $Sc \approx 0.44$ (shown in the lower part of Table 2-1).

Heat Transfer. The local gas-side heat-transfer coefficient is evaluated using the Chilton-Colburn (1934) analogy:

$$\frac{h_G}{k_G C_{pG}} = \left(\frac{Sc_G}{Pr_G} \right)^{2/3} , \quad (2-31)$$

where

h_G = gas-side heat-transfer coefficient ($\text{kW/m}^2 \text{ K}$)

C_{pG} = specific heat of gas (kJ/kg K)

Sc_G = gas Schmidt number

Pr_G = gas Prandtl number.

Gas Friction. The local gas friction is modeled based on the study of Bravo, Rocha, and Fair (1986) who compiled Δp measurements for long stacks of structured packing where six to ten individual layers were arranged so that successive layers are rotated by 90 deg in a horizontal plane. They express the pressure loss in such a stack under dry conditions Δp_0 , as

$$\Delta p_0 = (0.171 + 92.7/Re_S)(L/d_{eq})(\rho_G U_{Geff}^2) , \quad (2-32)$$

where Re_S is a gas Reynolds number based on length S as $\rho_G U_{Geff} S/\mu_G$, and L is the total packed length. For an irrigated packing, the increase due to liquid flow was accounted for as

$$\Delta p_{wet} = \Delta p_0 / (1 - C_3 Fr^{1/2})^5 , \quad (2-33)$$

where Fr is the liquid Froude number, U_{Leff}^2/gd_{eq} , and C_3 is a dimensionless constant with a value in the range of 3 to 7.5, depending upon the packing chosen.

Consider a single stack of packing. If we denote entrance and exit loss coefficients lumped together by A and the frictional coefficient within the packing in laminar flow by C/Re_S , then we may write the dry pressure loss for the single stack as

Table 2-1. Comparison of Correlation Data Base with Experimental Condenser Entrance Conditions

System	Pressure (mm Hg)	Packing Dia. (m)	Liquid Loading ² (kg/m ² s)	Vapor Loading ² (kg/m ² s)	Liquid Density ³ (kg/m ³)	Vapor Density ³ (kg/m ³)	Liquid Viscosity (kg/ms) (10 ⁻³)	Vapor Viscosity (kg/ms) (10 ⁻⁶)	Liquid Diff. (m ² /s) (10 ⁻⁹)	Vapor Diff. (m ² /s) (10 ⁻⁶)	Vapor Re (UL-ignored)	Vapor Sc	Vapor Sherwood Number	Remarks
o/p Xylenes	730	0.00723	0.41	0.41	765	3.100	0.23	8.8	6.0	4.05	426.8	0.701	3.82	Total Reflux
o/p Xylenes	730	0.00723	2.75	2.75	765	3.100	0.23	8.8	6.0	4.05	2862.5	0.701	17.49	Total Reflux
o/p Xylenes	300	0.00723	0.39	0.39	791	1.400	0.28	8.2	4.5	8.80	435.7	0.666	3.81	Total Reflux
o/p Xylenes	300	0.00723	2.57	2.57	791	1.400	0.28	8.2	4.5	8.80	2870.9	0.666	17.23	Total Reflux
o/p Xylenes	100	0.00723	0.29	0.29	819	0.480	0.38	7.6	3.0	43.10	349.5	0.367	2.62	Total Reflux
o/p Xylenes	100	0.00723	1.77	1.77	819	0.480	0.38	7.6	3.0	43.10	2133.3	0.367	11.15	Total Reflux
o/p Xylenes	16	0.00723	0.24	0.24	849	0.090	0.51	6.9	2.0	119.00	318.6	0.644	2.94	Total Reflux
o/p Xylenes	16	0.00723	0.96	0.96	849	0.090	0.51	6.9	2.0	119.00	1274.4	0.644	8.90	Total Reflux
EB/Styrene	100	0.00723	0.35	0.35	828	0.480	0.39	7.7	3.6	23.40	416.4	0.686	3.71	Total Reflux
EB/Styrene	100	0.00723	1.93	1.93	828	0.480	0.39	7.7	3.6	23.40	2296.0	0.686	14.56	Total Reflux
EB/Styrene	50	0.00723	0.26	0.26	842	0.260	0.47	7.4	2.8	43.00	321.8	0.662	2.99	Total Reflux
EB/Styrene	50	0.00723	1.47	1.47	842	0.260	0.47	7.4	2.8	43.00	1819.6	0.662	11.94	Total Reflux
Meth/Ethanol	760	0.00723	0.45	0.45	756	1.200	0.45	8.5	4.0	9.10	484.9	0.778	4.38	Total Reflux
Meth/Ethanol	760	0.00723	2.68	2.68	756	1.200	0.45	8.5	4.0	9.10	2888.1	0.778	18.24	Total Reflux
Glycols	10	0.00723	0.23	0.23	1010	0.080	2.80	9.6	5.0	420.00	219.5	0.762	2.30	Total Reflux
Glycols	10	0.00723	0.54	0.54	1010	0.030	2.80	9.6	5.0	420.00	515.3	0.762	4.56	Total Reflux
Steam-Air	12	0.0267	14.8	0.2	1000	0.012	1.15	8.6	2.4	1661.00	786.7	0.431	5.30	Entrance Conditions
Steam-Air	12	0.0267	59	0.8	1000	0.012	1.15	8.6	2.4	1661.00	3146.7	0.431	16.05	Entrance Conditions
Steam-Air	12	0.0355	14.8	0.2	1000	0.012	1.15	8.6	2.4	1661.00	1046.0	0.431	6.65	Entrance Conditions
Steam-Air	12	0.0355	59	0.8	1000	0.012	1.15	8.6	2.4	1661.00	4183.9	0.431	20.16	Entrance Conditions

Source: Bravo, Rocha, and Fair 1985

$$\Delta p/q = A + (C/Re_S)(\ell/d_{eq}) ,$$

where ℓ is a single stack length, and q is the dynamic pressure of the gas.

If an interstack loss coefficient, caused by entrance and exit effects and by rotations occurring in the region between two adjacent stacks, is denoted by B , then for a stack of n layers, the dry pressure loss is

$$(\Delta p/q) = A + (n - 1)B + (C/Re_S)(n\ell/d_{eq}) . \quad (2-34)$$

If A is of the order of B , we may approximate this expression as

$$(\Delta p/q) = nB + (C/Re_S)(n\ell/d_{eq}) . \quad (2-35)$$

Note that in Eq. 2-35, the first term is a constant dependent on the number of layers of packing but independent of the layer's length.

Expressing Eq. 2-32 in a similar form, we get

$$\Delta p_o/q = 2[0.171 + 92.7/Re_S](n\ell/d_{eq}) , \quad (2-36)$$

where the first term is multiplied by the layer length as well. There is an inconsistency in the Δp expression as provided by Bravo, Rocha, and Fair (1986). The inconsistency arises because the term that represents entrance and exit losses is multiplied by the layer length. However, as long as the same number of layers is used in other applications, Eq. 2-36 should yield pressure losses within $\pm 15\%$, as demonstrated by Bravo, Rocha, and Fair (1986).

For our condenser study experiments, we used a maximum of only two layers of packing. If we assume that in Bravo's studies, an eight-layer stack was used on the average, then the entrance and exit loss coefficients for our case should be $B = 0.342 \times 2/8 = 0.0855$. Thus an appropriate expression for the dry pressure loss for a two-stack condenser may be

$$\Delta p_o/q = 0.0855 + (185.4/Re_G)(L/d_{eq}) . \quad (2-37)$$

Although these arguments are speculative, our initial attempts to model Δp using Eq. 2-32 yielded predictions that were a factor of two higher than their corresponding measurements. For lack of justifiable data, we chose to model Δp as follows.

For the model predictions provided in this report we used an approximate expression for the "local friction" coefficient as

$$f = 0.171 + (92.7/Re_G) \quad (2-38)$$

in the Darcy-Weisbach equation as

$$\Delta p = f \frac{L}{d_{eq}} q . \quad (2-39)$$

Equations 2-38 and 2-39 yields a 50% smaller Δp for a two-stack layer than Eq. 2-32 for a multiple-stack layer.

The correction for increase in Δp due to liquid flow as in Eq. 2-33 yielded a negative frictional loss at high liquid loadings in the condenser (as opposed to lower liquid loadings investigated by Bravo, Rocha, and Fair [1986]). This correction for irrigated packings was not used in this study.

All correlation schemes are summarized in Table 2-2.

2.4 Integration Scheme

The process equations described in Section 2.2 were integrated using a fourth-order Runge-Kutta integration scheme. For cocurrent flow, integration proceeded along the superficial direction of steam and water flow. Because the conditions at the inlet to the condenser were known (an initial value problem), the procedure for integration was straightforward.

We assumed the packing was available at the entry into the condenser; no special treatment was made for the water distribution system and the accompanying liquid free-fall. We assumed the condenser packing was available until the end of the condenser length as well. Water free-fall into a drain pool was not modeled separately.

A description of the steps of the integration process follows.

- Evaluate the fundamental properties (namely, mixture density, viscosity, mutual diffusivity, and thermal conductivity) of the steam and inert gas mixture and the liquid-inert solution
- Based on the local flow rates at the beginning of the step, evaluate the effective liquid and gas mixture velocities
- Predict the local Nusselt and Sherwood numbers based on the chosen correlations using the local values of the liquid and gas Reynolds, Prandtl, and Schmidt numbers
- Evaluate an interfacial temperature, based on the local heat- and mass-transfer coefficients, using the Colburn-Hougen equation in an iterative manner that uses the ZEROIN subroutine outlined by Forsythe, Malcolm, and Moler (1977)
- Use the interface temperature to calculate a series of derivatives of the local state variables
- Based on the local derivatives, determine the state conditions at the end of the step.

For cocurrent flow, we integrated either to a specified condenser length or to a length at which the local steam saturation temperature is 0.02°C above the water temperature. For countercurrent flow, the inlet conditions specified for water and steam corresponded to the top and bottom of the condenser, respectively (a boundary-value problem). Thus, to match conditions at either end of the condenser, we implemented an iterative scheme. We chose to integrate the process equations from the bottom of the condenser. A set of state values for the water at the bottom were estimated. Integration proceeded to the top, up to the specified condenser length, in a manner similar to that used for cocurrent flow. We then compared the calculated water conditions at the top to the specified water inlet conditions (temperature, flow rate, and

Table 2-2. Correlations for SERI Direct-Contact Condenser Model
Liquid Side

Mass transfer (for water)

$$k_L = 2\rho_L [D_L U_{Leff}/(\pi S')]^{1/2} \quad (\text{kg/m}^2 \text{ s})$$

$$U_{L,eff}^\ddagger = \frac{0.820}{n} \delta^{2/3} (\sin \alpha)^{1/2} \quad (\text{m/s})$$

 With $n = 0.010$,

$$\delta^\ddagger = \left[\frac{\Gamma}{82\rho_L (\sin \alpha)^{1/2}} \right]^{3/5} \quad (\text{m})$$

$$S' = [(B/2 \cos \theta)^2 + h^2]^{1/2} \quad (\text{m})$$

$$\sin \alpha = B/(2S' \cos \theta)$$

$$\Gamma = L/a_f a_p \quad (\text{kg/m s})$$

Heat transfer

$$\left(\frac{h_L}{k_L C_{PL}} \right) = \left(\frac{Sc_L}{Pr_L} \right)^{2/3}$$

Gas Side

Mass transfer

$$Sh = 0.0338 Re^{0.8} Sc^{0.333}$$

$$\text{where } Re = \frac{\rho_G d_{eq}}{\mu_G} (U_{Geff} \pm U_{Leff})^\S$$

Heat transfer

$$\left(\frac{h_G}{k_G C_{PG}} \right) = \left(\frac{Sc_G}{Pr_G} \right)^{2/3}$$

Friction (Darcy-Weisbach formulation)

$$f = 0.171 + 92.7/Re_S$$

$$Re_S = ReS/d_{eq}$$

[‡]Dimensional equations using Mannings formula for open-channel flow given here for water in SI units. $n = 0.010$ for smooth surface.

[§]Use relative velocity, + for countercurrent flow, - for cocurrent.

dissolved level of inert gas in water). Based on the magnitude of these differences, we estimated new sets of bottom water conditions and repeated the integration. This procedure was repeated iteratively following a modified scheme similar to ZEROIN (Forsythe et al. 1977). Iterations were performed until the calculated and specified water temperatures at the top of the condenser differ to within $\pm 0.01^\circ\text{C}$. For typical countercurrent condenser operating conditions, we required a series of four iterations for convergence.

We found that an integration step size of 1 mm was suitable for most cases. Step sizes much less than 1 mm were tried but yielded the same results. However, at low levels of noncondensable gases and near the top of the countercurrent condenser, when the derivatives of steam mass flow or temperature and pressures are large, we reduced the step size to 0.25 mm.

At the end of the calculations, we printed summaries of condenser outlet conditions and stored them on diskettes for later use.

3.0 EXPERIMENTAL DETAILS

The experiments described in this report were performed in SERI's Low Temperature Heat- and Mass-Transfer Laboratory in Golden, Colo. The purpose of the laboratory is to investigate and improve methods of transferring heat and mass under small driving potentials that often exist when the sun is the energy source.

Although other processes could be investigated, the primary thrust was to examine direct-contact evaporators and condensers for OC-OTEC. The emphasis of the research in the lab was to simultaneously increase the transfer rates of the direct-contact heat exchangers and decrease the size and water flow requirements. These objectives are reflected in the design of the research facility.

3.1 Facility

A heat rate of up to 300 kW is transferred to the closed warm-water loop through a shell-and-tube heat exchanger. The exchanger receives heat from another closed loop fired by natural-gas boilers. The cold-water loop removes heat by routing the flow through vapor-compression chillers. Warm water flows through an evaporator in one end of the chamber, and cold water flows through a condenser at the other end, as shown in Figure 3-1. Heat and mass are exchanged by evaporation of the warm water and direct-contact condensation of the vapor in the cold water.

The pressure in the O-ring-sealed vacuum chamber is maintained by a three-stage compressor train consisting of a booster, a rotary-vane pump, and a liquid-ring vacuum pump. Inert gases, which affect heat- and mass-transfer rates, can be added to the steam through gas mass flow meters to examine the effect of vacuum leaks and desorbed gases that may evolve from natural seawater in OTEC systems. The concentration of these noncondensable gases in the vapor is measured at the vacuum exhaust or at other points in the test chamber with a gas mass spectrometer. A solenoid-operated butterfly valve in the line between the vacuum tank and the compressor train allows us to vary the venting rate and seal the tank under vacuum for leak tests and inactive periods. Table 3-1 summarizes the facility's capabilities.

3.2 Instrumentation

We monitor all temperatures using platinum resistance thermometers (Rosemount Model 785-01N-0900). We take steam temperature measurements with a wet-bulb arrangement to arrive at local saturation values. Water flow rates are measured using two 3-in. turbine flow meters (Flow Technology, Inc., Model FT-96C3000-LJC). We monitor the inert gas injection rate using a gas mass flow controller (Tylan Model FC262, 0 to 50 and 0 to 150 Standard L/min). The vacuum exhaust volumetric flow was fixed by the first stage rotary blower (Kinney, Model MB 2000) over an inlet pressure range of 10 to 1500 Pa. We measure pressures in the test cell using absolute pressure gauges (MKS Instruments, Model 222BHS-A-0-100). Differential pressures are measured using ΔP transducers (MKS Instruments, Model 221BD). Instruments were calibrated at SERI's in-house calibration facility or at the manufacturer's facilities.

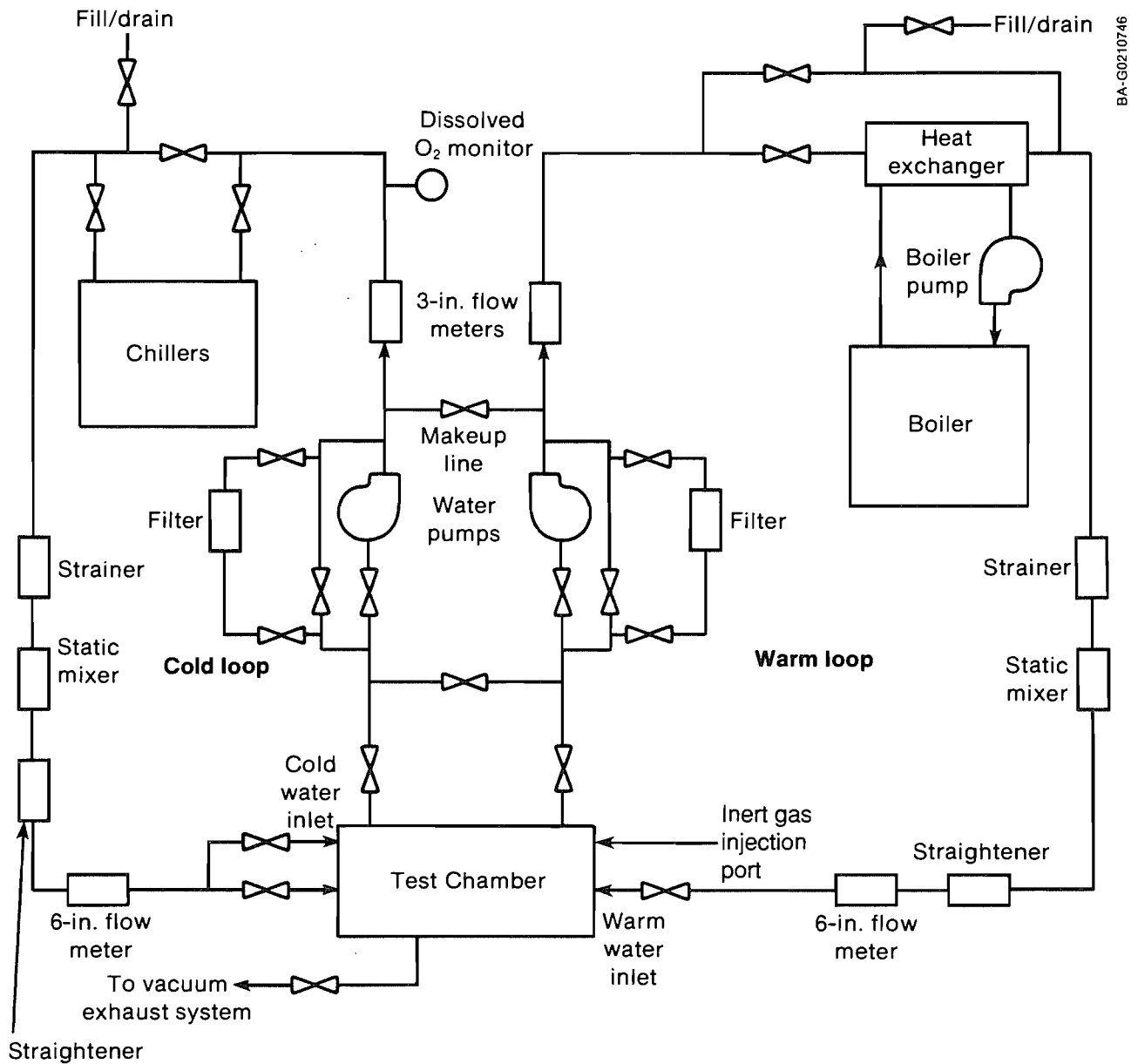


Figure 3-1. Heat- and mass-transfer laboratory flow loop schematic

We took extreme care to assure that the instruments were properly installed to avoid external influences in test results. Detailed sets of uncertainty analyses were conducted to identify error sources and minimize their influences. Table 3-2 summarizes the estimates of uncertainties in the primary measurements.

Further details on the facility, instrumentation, and uncertainty are also provided in Appendix A.

Uncertainties in the primary measurements affect the derived parameters such as the gas loading, Jakob number, inert gas inlet concentration, percentage of steam condensed, and pressure loss, as listed in data tables provided in Appendices D and E. We conducted detailed propagation analyses using the method of Kline and McClintock (1953). Table 3-3 summarizes the typical uncertainties in these derived quantities for a particular tested packing (19060).

Table 3-1. SERI Direct-Contact Laboratory Capabilities

Testing Condition	Warm-Water Loop	Cold-Water Loop
Heat input	0-300 kW	--
Heat rejection	--	0-300 kW
Temperature	3°-30°C	3°-30°C
Flow rate	50 kg/s	50 kg/s
Vacuum pressure	700 Pa	700 Pa
Leak rate	0.5 mg/s	0.5 mg/s
Vent capacity	0.57 m ³ /s	0.57 m ³ /s

Table 3-2. Summary of Uncertainties in Primary Measurements

Condenser Inlet Conditions

Steam temperature	±0.02°C
Total pressure	±0.5%
Inert gas flow	±2.0%
Water temperature	±0.01°C
Water flow rate	±1.0%

Condenser Outlet Conditions

Steam temperature	+0.02°C
Water temperature	±0.01°C
Pressure loss	±10 Pa or 10%

Exhaust Pump Conditions

Steam temperature (dry bulb)	20°-0°C
Total pressure	±0.5%
Volumetric flow	±3.0%

Table 3-3. Estimated Uncertainties in Derived Quantities for Packing 19060

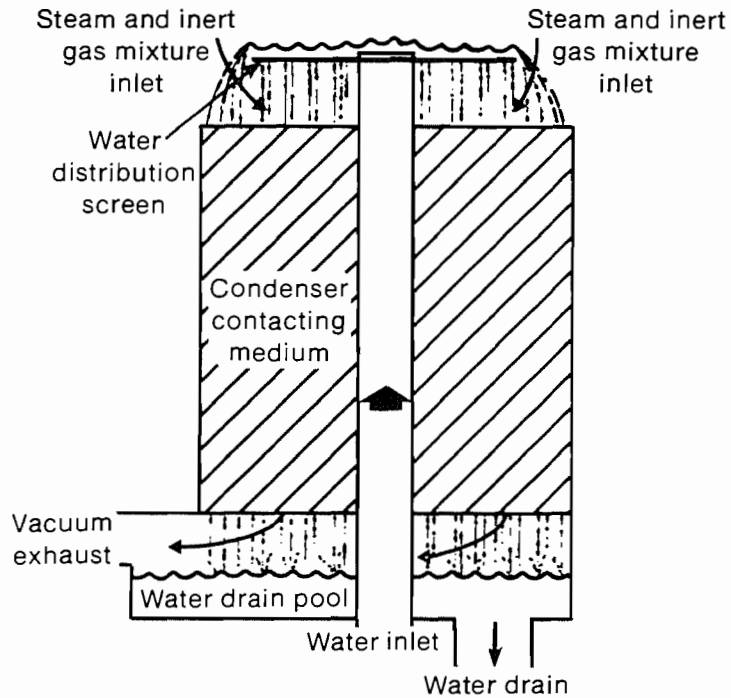
Derived Parameter	Cocurrent Condenser Error Range (%)	Countercurrent Condenser Error Range (%)
Gas loading	2.4-2.7	2.4-2.6
Jakob number	1.8-2.0	1.8-2.0
Inlet inert mass fraction	2.3-5.5	2.3-2.5
Outlet inert mass fraction	3.4-5.0	2.0-4.5
Effectiveness	0.17-0.75	0.19-0.70
Percentage condensed	1.7-5.0	1.7-2.0
Inlet pressure	0.12-0.14	0.12-0.20
Outlet pressure	0.38-0.93	0.40-0.94

3.3 Condenser Test Models

Figure 3-2 shows a schematic of the cocurrent condenser test set-up. The steam and inert-gas mixture enters the top of the condenser and flows downward. Cooling water flows onto a distributor on top and is allowed to flow freely onto a metallic screen. With the screen, water is distributed as evenly as practical over the contact medium. The warmed water from the condenser is collected in a drain pool. Noncondensable gases and uncondensed steam from the bottom of the condenser are routed to the vacuum exhaust pumps.

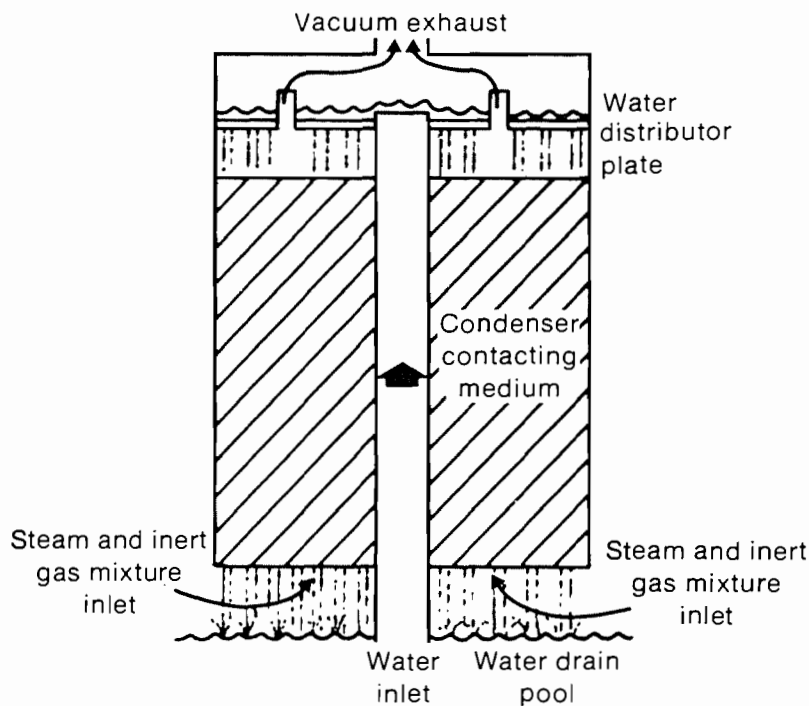
Figure 3-3 illustrates the test arrangement in countercurrent flow. The steam and inert-gas mixture enters the condenser from the bottom of a cylindrical enclosure. The water enters the condenser similarly to that for the cocurrent flow. A water distribution plate on top of the condenser allows uncondensed steam and inert gases to escape to the exhaust system.

We tested five different structured packings in either the cocurrent or countercurrent condenser configuration or both. Table 3-4 summarizes the relevant geometric characteristics of the tested packings. The AX packing was made of stainless steel wire mesh with 0.16-mm-diameter strands. This packing possesses the largest available surface area per volume of all tested packings ($250 \text{ m}^2/\text{m}^3$). The stack length for the AX packing was 0.18 m. All other packings were sheet-type packings. The articles 19060 and 27060 were made of 0.40-mm-thick polyethylene sheets and are commonly used as cooling tower fill. For these packings, we tested individual stacks of 0.61-m lengths. Packings 3X and 4X were made of 0.38-mm stainless steel sheet metal that was rippled and perforated with approximately 3-mm-diameter holes in a square pitch with a center-to-center spacing of 11 mm. The stack length for the 3X and 4X was 0.30 m. Two stacks rotated at 90 deg about a vertical axis were used to make up the required overall length.



BA-G0210747

Figure 3-2. Schematic of cocurrent condenser test article arrangement



BA-G0210748

Figure 3-3. Schematic of countercurrent condenser test article arrangement

Table 3-4. Geometry Comparisons of the Tested Packings

Packing Identifier	Base (mm) B	Height (mm) h	Sheet Thickness (mm) t	Inclination (deg) θ	Contact Loss (%) C_{Loss}	Surface Area per Volume (1/m) [†] a_p	Equivalent Diameter (mm) d_{eq}	Void Fraction (%) ϵ	Tested Packing Length (m)	Water Free-fall Length (m)
AX	26.0	13.0	0.32	60	0.0	250.0	14.6	91.2	0.36	1.08
19060 [§]	48.3	19.1	0.40	60	13.6	138.0	23.3	93.5	0.61	0.80
3X	50.8	25.4	0.38	60	0.0	133.0	28.5	94.7	0.61	0.80
27060 [§]	73.0	27.2	0.40	60	5.9	106.0	33.9	95.5	0.61	0.80
4X	94.0	47.0	0.38	60	0.0	73.7	52.7	97.1	0.61	1.08

[†]Quoted by manufacturers.

[§]Packings 19060 and 27060 are products of Munter's Corporation; packings AX, 3X, and 4X are products of Koch Engineering Company.

The packings used and the entire range of tested parameters for the cocurrent condenser are summarized in Table 3-5. A similar range for countercurrent flow is summarized in Table 3-6. A compilation of test data together with predictions for the structured packings is provided in Appendix D.

In addition to structured packings, other gas-liquid contactors were also tested in a countercurrent configuration. The results of these tests clearly showed the superiority of using structured packings as the gas-liquid contacting medium. Appendix C provides a summary of the relative comparisons of the tested media, and Appendix E tabulates the test data for devices other than structured packings when used in a countercurrent condenser.

3.4 Test Procedure

The test procedure for both cocurrent and countercurrent condensers was essentially the same. The test cell was evacuated to the lowest possible pressure with the vacuum butterfly valve fully open and all vacuum pumps running. We established warm and cold water flow rates and deaerated the water to approximately 20 ppb of dissolved oxygen. We turned on the chiller and boiler to select the desired thermal transfer rate. Atmospheric air at a selected airflow rate was introduced into the test cell as noncondensable gas. We adjusted the boiler and chiller controls to operate the condenser at a steady-state cold-water inlet temperature of nominally 5°C. The steam inlet temperature floated up or down to its steady-state level, depending on the condenser performance and the vacuum exhaust venting rate. A series of 10 measurements averaged over 15-minute intervals was taken at steady state.

At this point, we closed the vacuum butterfly valve slightly to increase the condenser pressure. We then corrected the heat inputs to the next steady-state operating condition and collected the next set of data. Gradually closing the valve forced the steam inlet temperature to increase and more steam to condense in the condenser. As we closed the butterfly valve, we typically collected a series of seven data points at the fixed water flow rate, heat rate, and noncondensable gas injection rate. For other series, the injected noncondensable gases, cooling water flow rate, or the heat rate may be varied.

Table 3-5. Tested Range for Cocurrent Condensers

Packing Identifier	Number of Points	T _{si} (°C)	T _{wi} (°C)	G (kg/m ² s)	Ja (---)	X _{ii} (%)	Remarks
AX	51	11.02 14.02	4.54 5.51	0.203 0.268	0.864 1.361	0.500 1.311	Single stack of 0.18 m length
19060	48	8.50 18.09	4.76 6.84	0.15 0.65	0.95 1.40	0.06 0.89	Single stack of 0.61 m length
4X	37	9.84 14.58	4.03 5.59	0.187 0.528	0.843 1.389	0.487 0.744	Two stacks of 0.30 m length each
Falling Jets	61	13.05 21.95	4.76 5.49	0.14 0.34	1.93 3.37	0.47 2.38	Water fall length of 0.8 m

Table 3-6. Tested Range for Countercurrent Condensers

Packing Identifier	Number of Points	T _{si} (°C)	T _{wi} (°C)	G (kg/m ² s)	Ja (---)	X _{ii} (%)	Remarks
AX	60	10.11 16.92	4.45 5.81	0.015 0.304	0.967 13.4	2.93 33.3	Two stacks of 0.18 m length each
19060	209	9.92 20.14	4.64 5.55	0.15 0.41	1.02 2.80	0.35 2.46	Single stack of 0.61 m length
3X	37	9.38 13.54	4.10 5.74	0.05 0.45	1.0 10.52	2.50 24.8	Two stacks of 0.30 m length each
27060	246	8.63 21.15	4.56 5.68	0.15 0.42	0.99 3.18	0.32 2.45	Single stack of 0.61 m length

4.0 MODEL VALIDATION

We developed the condenser model to provide guidance to a preferred design and to allow a designer to incorporate conservatism by overdesign to assure condenser performance. A common engineering practice to overcome prediction uncertainties is to include a margin of safety in the design. In general, uncertainties in predictive models decrease as the technology matures.

Current validation efforts for the direct-contact condenser attempt to establish that the model (1) captures the physical trends observed in the experiments over the entire range of test variables and geometries, (2) provides predictions that are comparable to the observations, and (3) possesses uncertainties of similar magnitude to those in the data.

The following approach is pursued in the remaining sections to validate the condenser model. For each tested packing, we generated a series of predictions at the condenser inlet conditions that corresponded to those of the experimental data. The predictions and experimental results are compared in graphs and tables.

We provide significant trends of performance measures with independent variables wherever they can be clearly illustrated. We illustrate the deviations between predictions and experiments with the independent parameters and explain their underlying causes. We characterize the performance measures for a particular geometry by the condensed steam (expressed as a percentage) and by its overall pressure loss. The deviations for the entire data set for a particular packing are quantified as an average and a standard deviation of the condensed steam (expressed as a percentage of the incoming steam) and the pressure loss. The independent variables in each set are the steam inlet saturation temperature T_{si} , the gas loading G , the Jakob number Ja , and the inert gas content in the incoming steam X_{ii} expressed as a mass percentage. Here, the Jakob number for the condenser is defined as

$$Ja = \dot{m}_{wi} C_{pw} (T_{si} - T_{wi}) / (\dot{m}_{si} h_{fg}) , \quad (4-1)$$

where \dot{m}_{wi} and \dot{m}_{si} represent the incoming water and steam mass flow rates (kg/s), respectively; T_{wi} and T_{si} represent the incoming water and steam saturation temperatures ($^{\circ}\text{C}$), respectively; C_{pw} is an average specific heat capacity of water (kJ/kg K); and h_{fg} is an average latent heat of condensation for steam (kJ/kg).

The scope of the comparisons focuses on illustrating the similar trends between the model and the experiments and quantifying the deviations. However, notable differences exist between the model and experiments with respect to their underlying assumptions and method of implementation, as discussed in the following paragraphs.

We used only fresh water in the experiments. The water was consistently deaerated to 20 ppb of dissolved oxygen for all of the tests. With steam condensation, deaeration from the coolant does not occur to the extent that it may occur in seawater.

In the experiments, we treated the condenser as a black box. Only measurements to characterize incoming and outgoing steam and water were made. We did not provide instrumentation to map out variations of process variables through the condenser. We simulated the presence of inert gas in steam by dispersing atmospheric air into the steam generated in the evaporator section of the test cell. The homogeneity of the mixture was verified using mass spectral traces at various locations.

Finite lengths of free-fall (distance between water distributor and the top of the packing) were required to distribute the water onto the condenser packing and to drain it from the packing. A pool of drained water settled in a pool below the condenser. These spaces on top and bottom of the packing, although devoid of packing, did allow a certain amount of condensation to take place. We did not attempt to isolate contributions from these spaces.

We tested the cocurrent jet condenser as a single-stage condenser in the experiments. The vacuum exhaust system could remove, at most, 14% of the uncondensed steam from this condenser (at a minimal noncondensable gas injection rate and steam flow). Although for OTEC applications a cocurrent section may condense 70% to 80% of the incoming steam. In some of these experiments, the cocurrent section condensed 80% to 98% of the incoming steam because there was no second-stage condenser, causing the data to be confined to large Jakob numbers.

The limitations of the numerical model are as follows. We assume the incoming steam contacts the water and begins condensing as soon as it enters the packing. The water distribution manifold and free water streams are not accounted for. We assume the packing extended to the height where the cooling water first contacts the steam. Draining streams of water from the bottom of the packing are not modeled.

The transfer correlations used in the numerical model possess uncertainties because of the nature of the empirical data upon which they were based. They apply to fully developed flows; whereas in short, efficient packings, there generally is not an adequate length for the flow to develop. Thus, they do underpredict the transfer rates where entrance effects persist.

The effective area over which transfer takes place is an interfacial area between the two phases and, in general, is difficult to define. After comparing the model with the data, we found that this area is comparable to the total geometric area of the packing. For generating comparable model results for the experimental data, we assumed that this area fraction a_f remains constant through the length of the condenser, although in practice this fraction may decrease continuously with decreased gas loading and increased steam condensation.

4.1 Cocurrent Condenser

We tested three different packings, namely, AX, 19060, and 4X and free-falling water jets in a cocurrent configuration.

4.1.1 AX Packing

The AX packing is made of stainless steel wire mesh (0.16 mm diameter). This gauze packing yields an effective transfer area equal to the total available area in mass transfer applications (Bravo, Rocha, and Fair 1985; and Meier 1979). This packing possesses the highest surface area per volume a_p of $250 \text{ m}^2/\text{m}^3$ and the lowest equivalent diameter of 14.6 mm of all the tested packings. For the tests, we introduced a short stack of 0.18-m length in a water free-fall of 1.08 m.

Figure 4-1 illustrates a comparison of condensed steam between the data and the predictions, plotted versus Jakob number. The data are for an inert level, X_{ii} of 0.55. The Jakob number varies from 0.87 to 1.4. For all the data, the gas loading is nominally $0.26 \text{ kg}/\text{m}^2 \text{ s}$.

At this inert gas concentration, we note that the condensed steam data increases with increasing Ja. The predictions show similar trends. For $Ja < 0.97$, the predictions match the data extremely well. For $0.97 < Ja < 1.1$, the data lie approximately 2% above the predictions. For even higher Ja, the data lie about 3% higher than the predictions. The cause for this deviation with increasing Ja is that the free-falling water jets contribute to an increase in condensation in the experiments. The model does not consider the free-fall contributions. Similar trends were observed at a higher inert gas concentration of 1.2% as well.

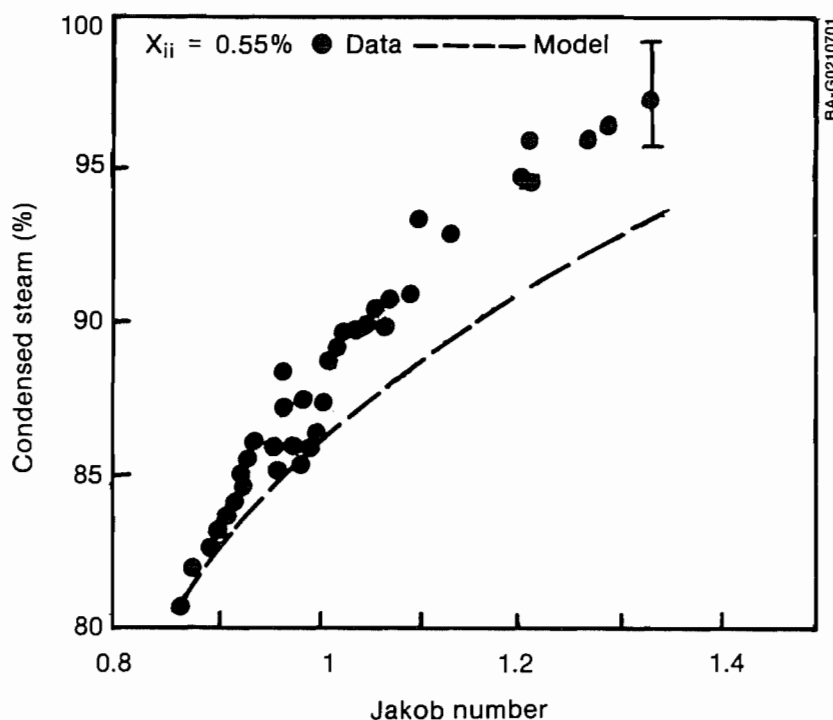


Figure 4-1. Comparison of condensed steam for AX packing in cocurrent flow

For the entire data set of 51 points, the model underpredicts condensed steam by less than 1.4% with a standard deviation of 1.5% of steam. The experimental data possess an uncertainty of $\pm 2\%$, as illustrated. In this and all the remaining figures illustrating the data, uncertainty estimates are indicated as vertical bars around a typical data point.

Figure 4-2 illustrates the comparison of pressure loss between data and predictions. The model predicts pressure losses with the same trend as the data, but about 5 Pa higher than the data. Measured pressure loss is estimated to possess an uncertainty of ± 10 Pa. Thus the predictions fall well within the uncertainty range of the data.

We tried to test this packing at higher gas loadings. In general, at $G > 0.3 \text{ kg/m}^2 \text{ s}$ the AX packing was observed to be overloaded, with dramatic increases in the measured pressure loss. Considering the low packing equivalent diameter, this limit is similar to a flooding limit in countercurrent flow (see Section 4.2.1) but somewhat higher in cocurrent applications. This particular gauze packing is unable to handle liquid loads higher than about $25 \text{ kg/m}^2 \text{ s}$ without the water bridging the gaps and causing significant resistance to the steam flow.

4.1.2 Plasdek 19060 Packing

This packing made of 0.4-mm-thick polyethylene sheets possesses a surface area per unit volume a_p of $138 \text{ m}^2/\text{m}^3$ and an equivalent diameter d_p of 23.3 mm. A single stack of 0.61-m length was introduced in the cocurrent configuration with a water free-fall height of 0.8 m.

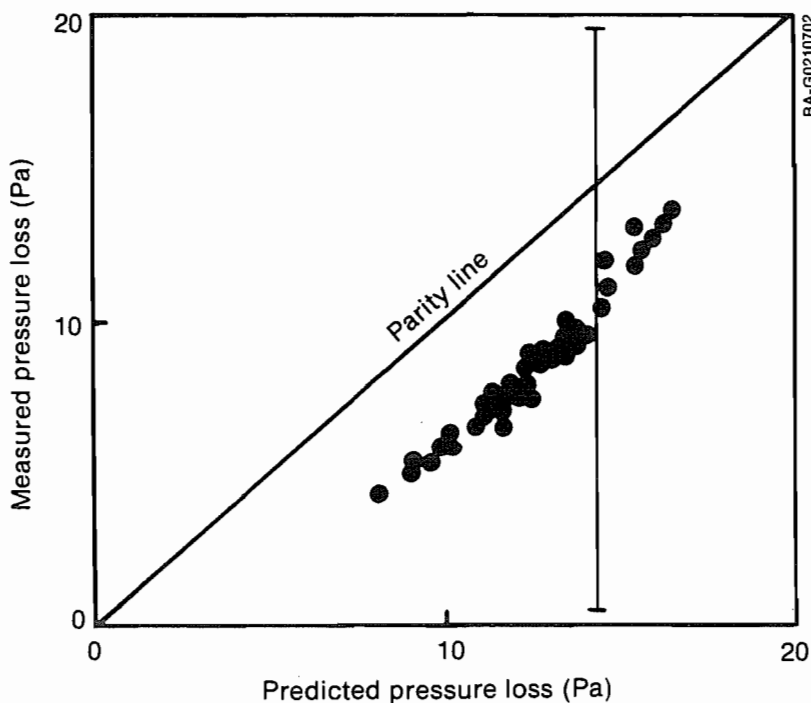


Figure 4-2. Comparison of pressure loss for AX packing in cocurrent flow

Figure 4-3 illustrates the comparison of condensed steam between the model and the data for a Jakob number range of 0.8 to 1.5. Six different data sets at varied levels of G and X_{ii} are included. To preserve clarity in the figure, only a faired line representing the predictions is shown in this figure. Detailed data set comparisons are provided in the tables in Appendix D. For $Ja < 1.2$ the predictions follow the data quite well, with a maximum deviation of less than 3% and well within the experimental uncertainty. For $Ja > 1.2$, the model overpredicts the data by as much as 4% at low G and X_{ii} levels.

Figure 4-4 compares pressure losses. Over the tested range, measured values are larger than the predictions by as much as 35 Pa. The model indicates a trend that is different from the data. Tests with this packing were conducted early in the program when we encountered some difficulty in the Δp measurement because water was clogging the pressure transducer connecting lines. This problem was later resolved by using larger diameter lines and maintaining a warmer constant temperature at the transducers.

The differing trend between the model and the data may be attributed to the measurement difficulties encountered for this set of data. Despite this discrepancy, considering the low mean value of the Δp data of around 50 Pa and the uncertainty in the data of ± 10 Pa, the comparison between the data and the model is reasonable.

4.1.3 4X Packing

The 4X packing we used was made with rippled and perforated stainless steel sheets. This packing possesses the highest equivalent diameter d_p of 52.7 mm and the lowest a_p of $74 \text{ m}^2/\text{m}^3$ of all packings tested. Two individual stacks of 0.3 m length were introduced in an overall condenser free-fall height of 1.1 m.

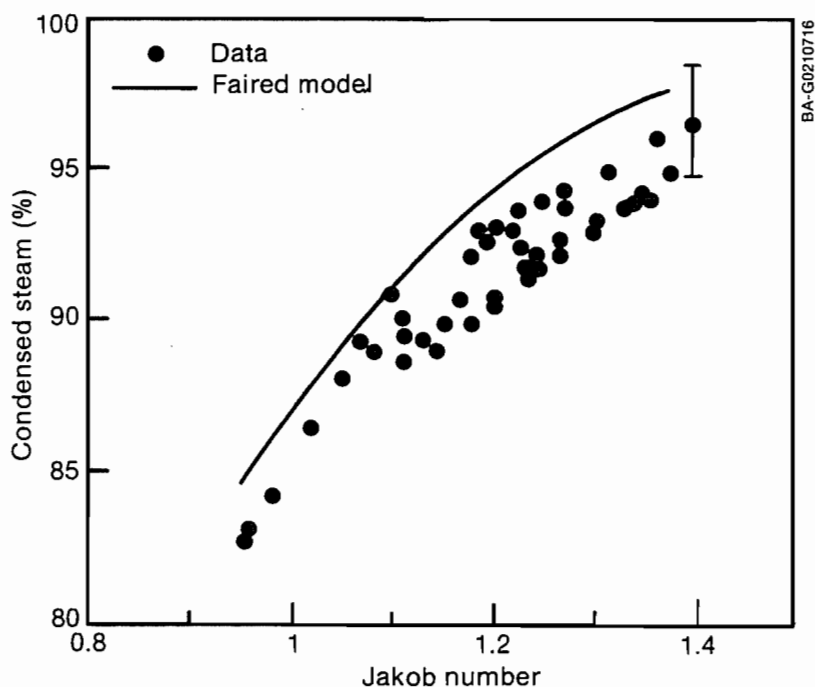


Figure 4-3. Comparison of condensed steam for 19060 packing in cocurrent flow

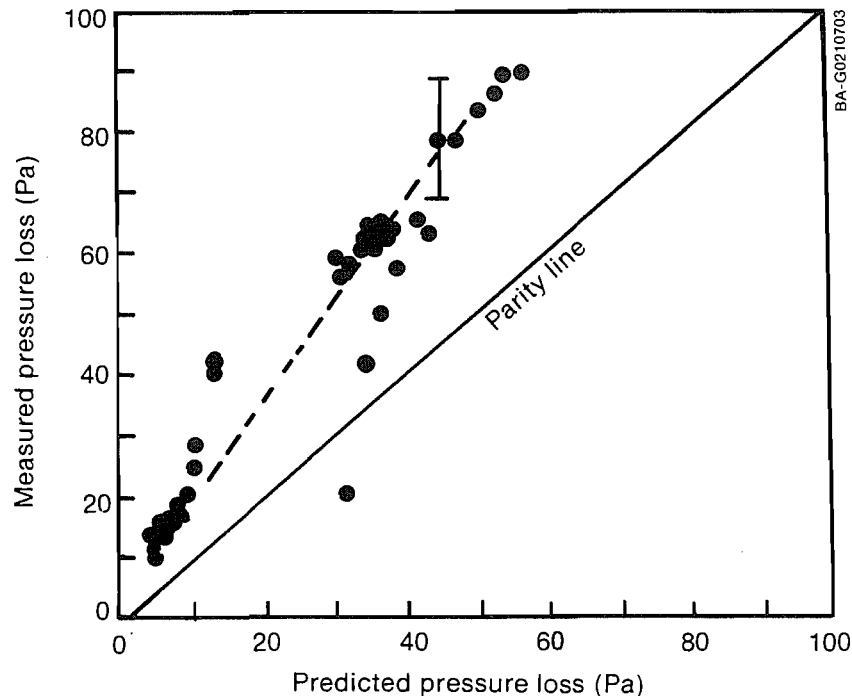


Figure 4-4. Comparison of pressure loss for 19060 packing in cocurrent flow

Because of its low a_p , this packing exhibited the largest influence of water free-fall. Predictions of condensed steam using the actual packing length of 0.61 m yielded about 9% lower values than did the experiments. Thus, we decided to include the contribution of the free-fall in the predictions by adopting the overall free-fall length of 1.1 m for the packing. Figure 4-5 illustrates the comparison of condensed steam at five levels of gas loading. Again, only a faired line through predictions is shown to preserve clarity. The predictions follow trends similar to the data. For $Ja < 1.5$, the predictions fall well within the experimental uncertainty. For $Ja > 1.5$, the model underpredicts the data by as much as 3%.

Figure 4-6 illustrates the comparison of pressure loss plotted versus Jakob number again at five levels of gas loading. The agreement between data and predictions is excellent and is well within the experimental uncertainty.

4.1.4 Free Jets

A series of tests were conducted with the packing removed from the cocurrent condenser. Water flowed onto the distributor plate (described in Section 3.3) and fell to the bottom pool 0.8 m below. This configuration (shown in Figure 4-7) was not backed by a second-stage condenser. We included the data obtained for this configuration to illustrate the improvement obtained with the packing. We did not try to model the jets here.

Figure 4-8 illustrates the experimental data taken with and without the presence of packing 19060 in the cocurrent configuration. The data for free-falling jets lie in a range of $1.8 < Ja < 3.4$. For an equivalent amount condensed, the introduction of the packing shifts the Jakob number range to less

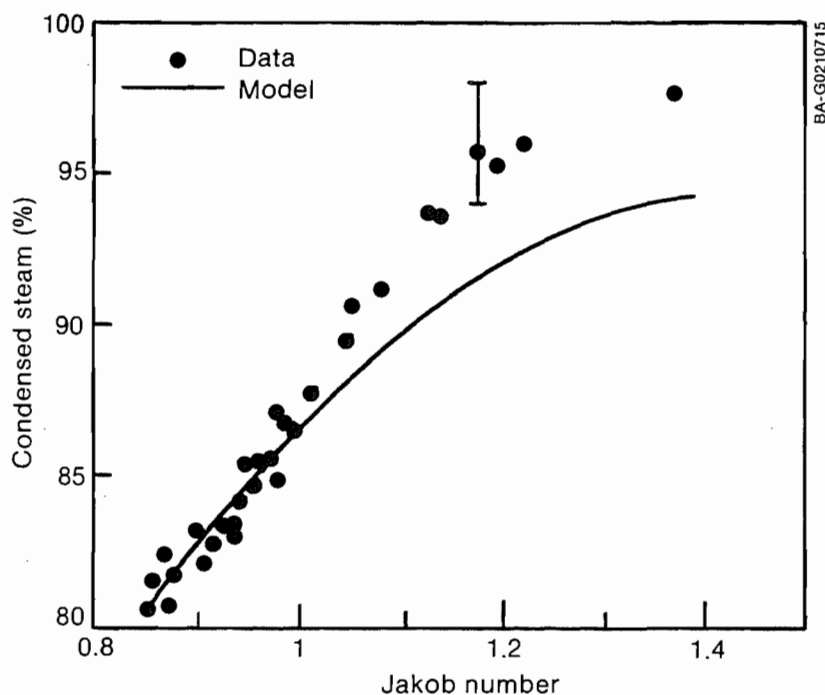


Figure 4-5. Comparison of condensed steam for 4X packing in cocurrent flow

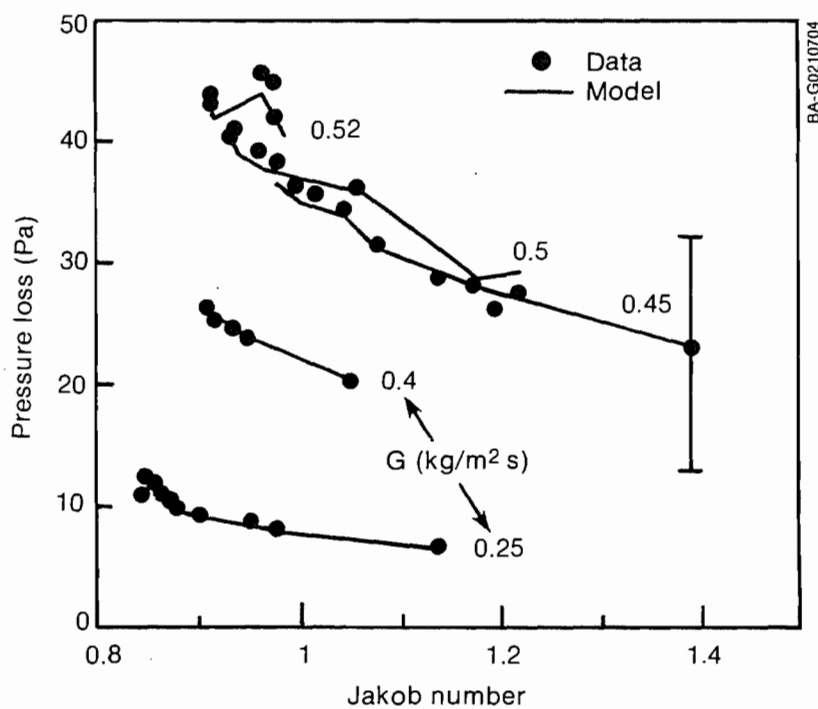


Figure 4-6. Comparison of pressure loss for 4X packing in cocurrent flow



Figure 4-7. Free-falling jets in cocurrent configuration

than 1.4. The free-jet data exhibit large sensitivity to both the gas loading and inert gas concentration (see data tables in Appendix D). This type of sensitivity is significantly reduced by using a packing as the contact medium.

These results also illustrate that the steam condenses mostly within the packing. The method of liquid distribution, as long as the distribution is reasonably uniform, is immaterial to the modeling approach as formulated.

Figure 4-9 illustrates the measured pressure losses with and without packing. Presence of packing results in higher pressure losses confined to much lower Jakob numbers. Of course, with a proper choice of packing, the increase in pressure loss can be minimized while the Jakob number can be reduced to a minimum possible to achieve equivalent performance from a cocurrent condenser.

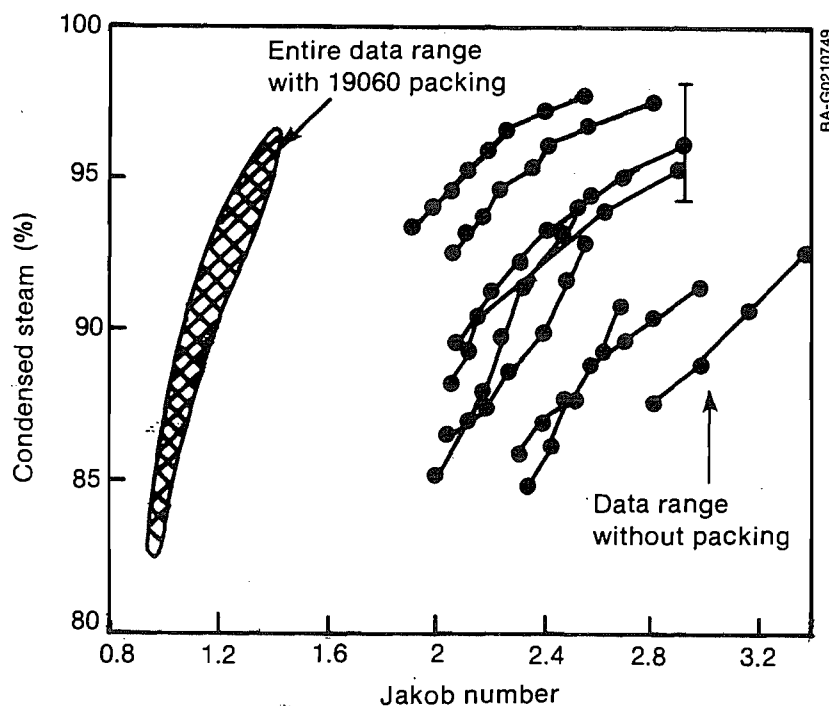


Figure 4-8. Comparison of measured condensed steam for a cocurrent condenser with and without 19060 packing

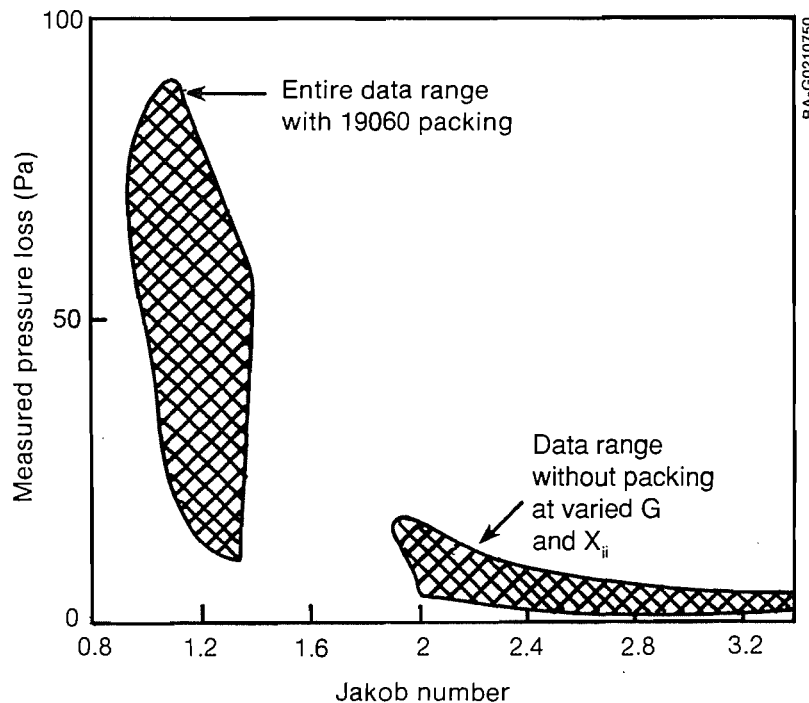


Figure 4-9. Comparison of measured pressure loss for a cocurrent condenser with and without 19060 packing

4.1.5 Summary of Cocurrent Condenser Findings

From the discussions of the data on cocurrent condensers presented in Section 4.1, the following findings result:

- Introducing a packing as a contact medium substantially reduces the water flow requirement as expressed by the Jakob number. The packing also causes higher condenser pressure losses. Selecting a condenser configuration requires a trade-off between the Jakob number and pressure loss to minimize both.
- We tested three structured packings with a wide range of surface areas per volume and presented their experimental data.
- The gauze packing with a low d_p limited an acceptable gas loading to less than $0.3 \text{ kg/m}^2 \text{ s}$ for OC-OTEC operating conditions.
- We tested the packing with the largest d_p of 52.7 mm at gas loadings of up to $0.52 \text{ kg/m}^2 \text{ s}$.
- The packing with the lowest a_p exhibited the largest influence of water free-fall. We obtained more accurate predictions for these experimental data using the total water free-fall length rather than the actual packing length.
- Table 4-1 summarizes the deviations between predictions and experiments. The average and standard deviations of the differences in condensed steam are less than 3%; these deviations are comparable to a measurement uncertainty of $\pm 2\%$.

Table 4-1. Cocurrent Condenser Comparison Summary

Packing Identifier	Number of Points	Deviation (Prediction-Experiment)			
		Condensed Steam (%)		Pressure Loss (Pa)	
		Average	Std. Deviation	Average	Std. Deviation
AX	51	-1.4	1.5	4.0	0.6
19060	48	2.8	2.4	-17.6	10.4
4X	37	-1.1	1.3	-0.1	1.2
Experimental Uncertainty	--	--	2.0	--	10.0

- The average and standard deviations of the differences in pressure loss are less than 3 Pa for AX and 4X packings. The data for 19060 exhibit larger differences of -18 Pa on the average and 11 Pa on standard deviation. The deviations for 19060 packing are well above those for the rest of the packings. As mentioned earlier, the experimental values of Δp for this packing are perhaps in question because of the waterlogged Δp transducer lines during some of the Δp measurements. However, in general the Δp differences in terms of their average and standard deviations are comparable to an estimated measurement uncertainty of ± 10 Pa.

4.2 Countercurrent Condenser

Four different structured packings, AX, 19060, 3X, and 27060, were tested in countercurrent flow.

4.2.1 AX Packing

For the tests, two short stacks of 0.18 m length were introduced in a water free-fall length of 0.8 m. This condenser was used as a second-stage condenser in a two-stage configuration. Because of this arrangement, we achieved a wide range of inlet parameters for the tests.

Flooding is a common limitation in countercurrent gas-liquid contactors. This packing, possessing the smallest equivalent diameter, was more prone to flooding at lower gas loading than others tested. Using d_p , we estimated the flooding limits using the correlations proposed by Wallis^p (1969) for circular tubes in turbulent flow as[†]

$$(j_g^*)^{1/2} + (j_f^*)^{1/2} = 0.7, \quad (4-2)$$

[†]Commonly available flooding correlations for random packings are not directly applicable to the regular geometry found in structured packings.

where

$$j_g^{*2} = \rho_g j_g^2 / \Delta \rho g d$$

$$j_f^{*2} = \rho_f j_f^2 / \Delta \rho g d$$

$j_{g,f}$ = superficial gas and liquid velocities (m/s)

$\rho_{g,f}$ = gas and liquid densities (kg/m³)

$$\Delta \rho = \rho_f - \rho_g$$

g = gravitational acceleration (m/s²)

d = tube diameter (m).

Figure 4-10 illustrates the flooding limits for steam and water flow at typical OTEC conditions for three different d_{eq} values. An acceptable liquid loading L is plotted versus the gas loading G . The limit of acceptable L decreases monotonically with increasing G . This limit increases with increasing tube diameter.

Also shown in this figure are two lines of constant Jakob number. These lines represent straight lines with L proportional to G . A countercurrent condenser may operate at $Ja \approx 1.2$; a cocurrent may operate at $Ja \approx 0.8$.

The intersection of the constant Ja line with the flooding limit represents acceptable maximum allowable gas and liquid loadings for a particular packing. This figure shows that for a 20-mm-diameter tube, an allowable limit gas loading of G is ≈ 0.32 kg/m² s.

The flow geometry in structured packings is different from that of circular tubes. We used this figure, however, to help select experimental conditions and estimate flooding envelopes.

The AX packing with an equivalent diameter d_p of 14.7 mm could not accept gas loadings over 0.25 kg/m² s without substantial increase in vapor pressure losses.

Figure 4-11 illustrates the comparison of condensed steam between predictions and measurements for $G < 0.25$ kg/m² s. The predictions lie close to the experimental data over the entire range. On the average, the difference is 0.9% with a standard deviation of 2%.

Figure 4-12 shows the comparison of pressure-loss predictions and the data. The comparison in this figure is not very good. The differences between predictions and measurements average 2 Pa but with a large standard deviation of 6 Pa. This standard deviation is comparable to the uncertainty in the Δp measurement of ± 10 Pa.

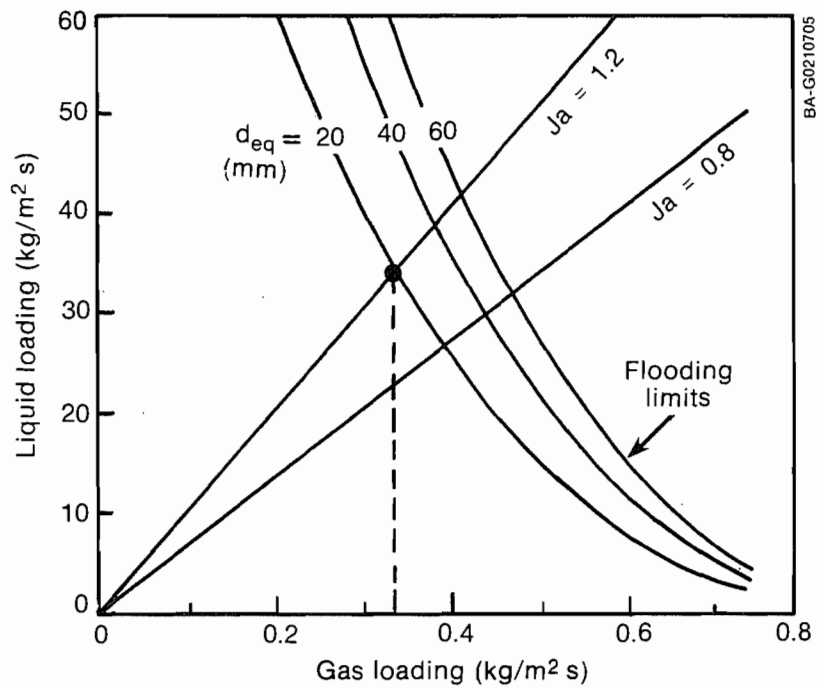


Figure 4-10. Flooding limits for countercurrent condensers using the correlation of Wallis (1969)

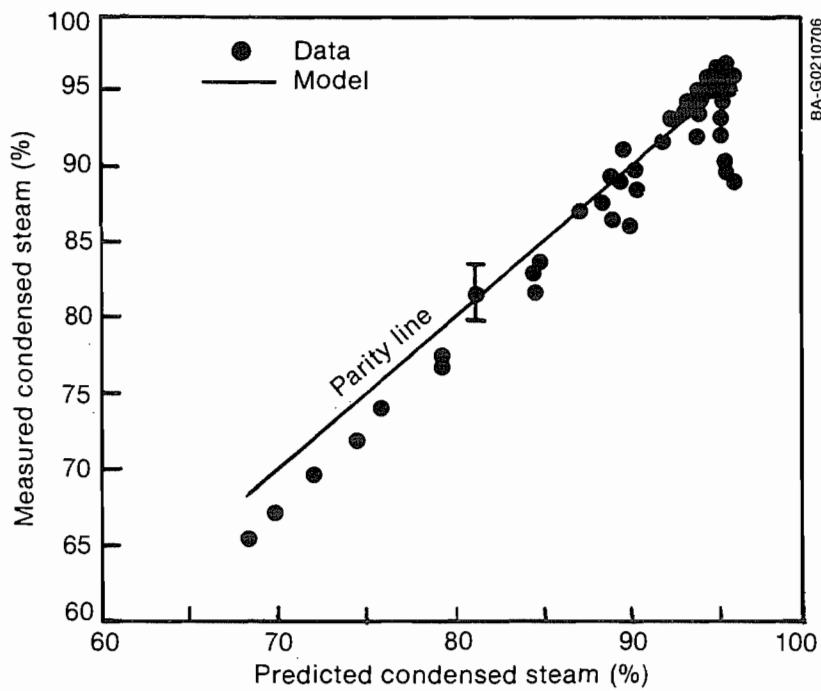


Figure 4-11. Comparison of condensed steam predictions with data for AX packing in countercurrent flow

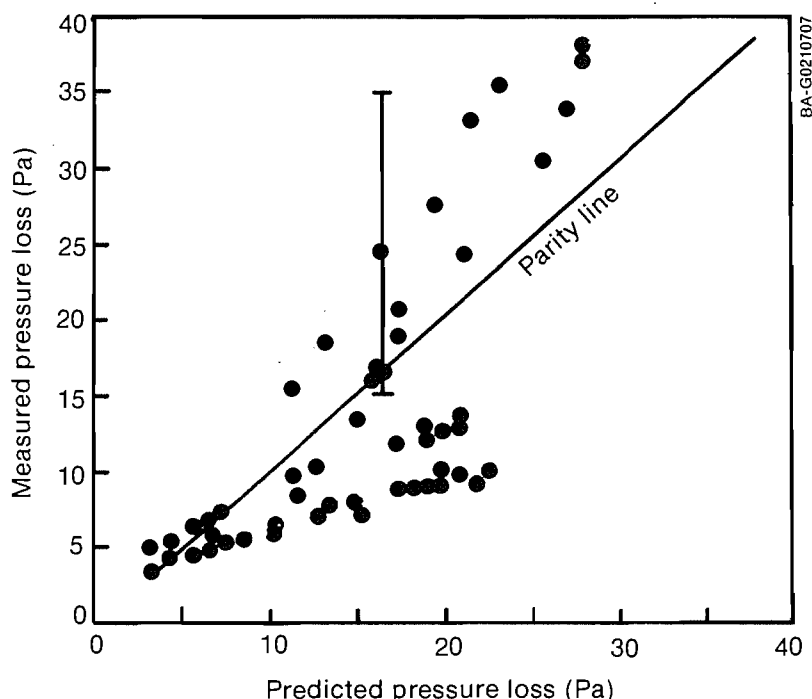


Figure 4-12. Comparison of pressure loss for AX packing in countercurrent flow

4.2.2 Plasdek 19060 Packing

A single stack length of 0.61 m was introduced in a water free-fall length of 0.8 m. For this packing, we compared an extensive set of 209 data points. The differences between predictions and measurements for the condensed steam yielded an average of 0.1% and a standard deviation of 0.8%.

For the pressure loss, comparison between experiments and predictions are shown in Figure 4-13. The predictions follow the measurements quite well. The differences yielded an average of 1 Pa with a standard deviation of 5 Pa.

4.2.3 3X Packing

The 3X packing used here is similar to the 4X described earlier, with a surface area a_p of $133 \text{ m}^2/\text{m}^3$ and a diameter d_p of 28.5 mm. Two stacks, each 0.30-m long, were placed in a water free-fall length of 0.8 m.

Because of its larger equivalent diameter, some condensation occurred in the free-falling water jets as it did with the 4X packing. Therefore, we did comparisons using two lengths, namely, the packing length of 0.61 m and a total free-fall length of 0.8 m.

Figure 4-14 shows the condensed steam comparison. Predictions for $l = 0.61 \text{ m}$ and $l = 0.8 \text{ m}$ are included. The experimental data generally fall within the two predictions. The differences between the predictions (at $l = 0.8 \text{ m}$) and the data yield an average of 1.1% with a standard deviation of 1.5%.

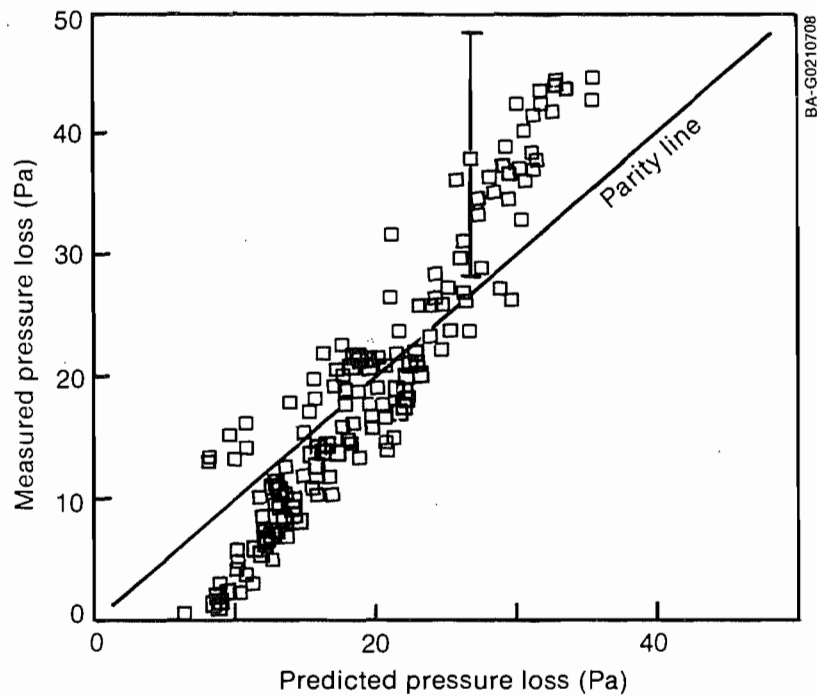


Figure 4-13. Pressure loss comparison for 19060 packing in countercurrent flow

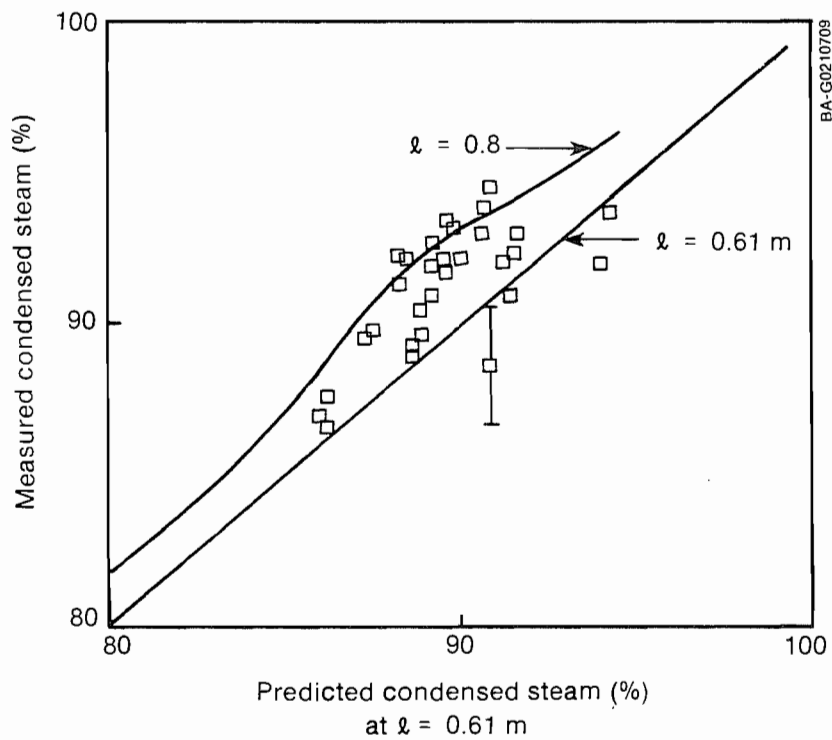


Figure 4-14. Comparison of condensed steam for 3X packing in countercurrent flow

Figure 4-15 shows the comparison of pressure loss with $\ell = 0.8$ m. The pressure loss is insensitive to length in the range of $\ell = 0.61$ to 0.8 m. The experimental data exhibit large scatter around the predictions. The differences between predictions and data yield an average 2 Pa, but with a large standard deviation of 12 Pa. The Δp measurements possess an uncertainty of ± 10 Pa.

4.2.4 Plasdek 27060 Packing

This packing possessed the highest equivalent diameter of the packings tested in countercurrent flow. A single stack length of 0.61 m was placed in a water free-fall length of 0.8 m.

Figure 4-16 shows the comparison of condensed steam between the data and predictions using the full water free-fall length of 0.8 m. The differences between predictions and data yield an average of -0.6% with a standard deviation of 0.7% , well within the experimental uncertainty of $\pm 2\%$.

Figure 4-17 shows the pressure loss comparison for this packing, demonstrating excellent comparison between data and predictions. The difference between predictions and data yields an average of 3.6 Pa with a standard deviation of 3.4 Pa, well within the Δp measurement uncertainty of ± 10 Pa.

4.2.5 Summary of Countercurrent Condenser Findings

Our investigation of using structured packing in a countercurrent condenser resulted in the following accomplishments and findings:

- We tested four different geometries for the packing with widely varied surface areas per unit volume.

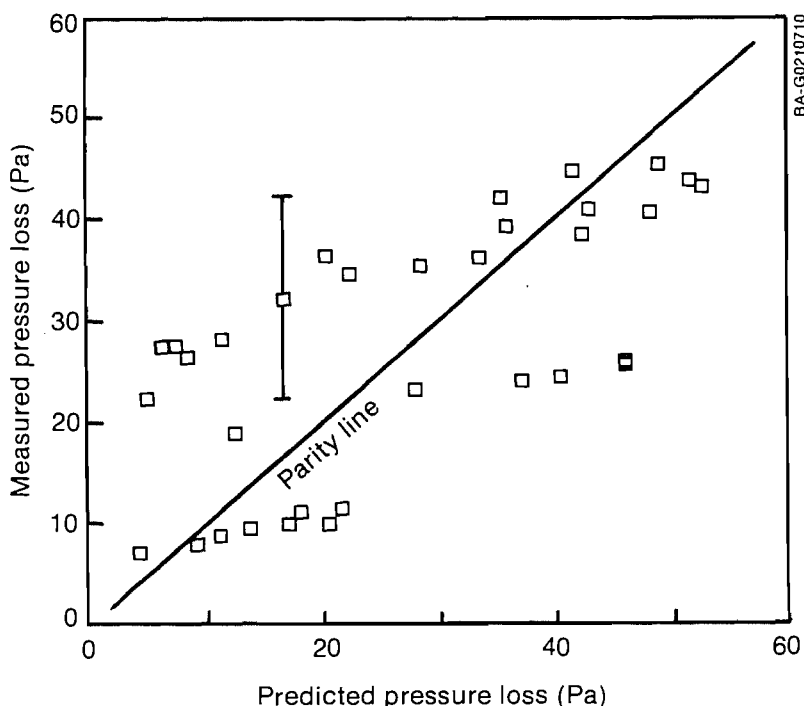


Figure 4-15. Comparison of pressure loss for 3X packing in countercurrent flow

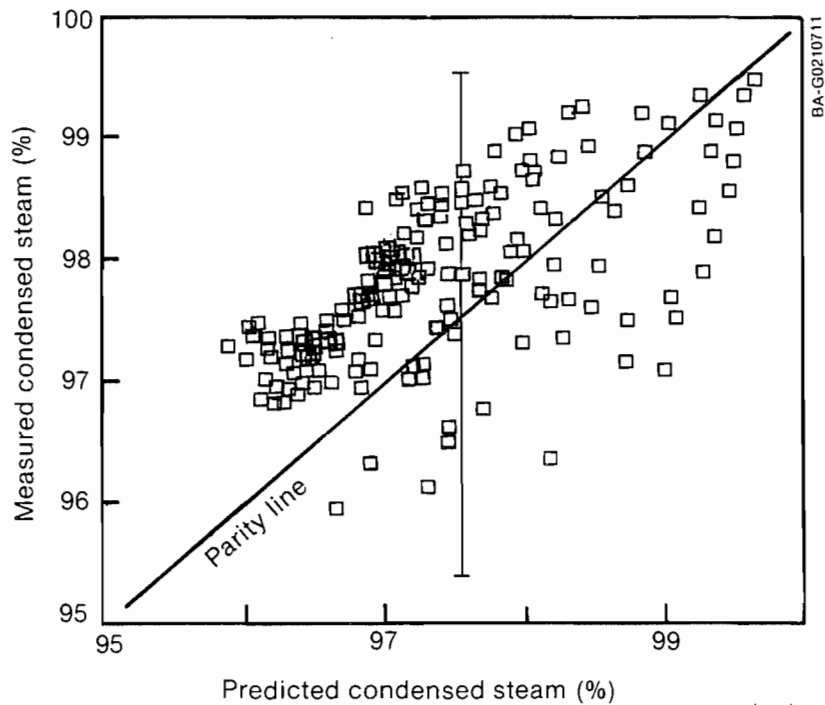


Figure 4-16. Comparison of condensed steam for 27060 packing in countercurrent flow

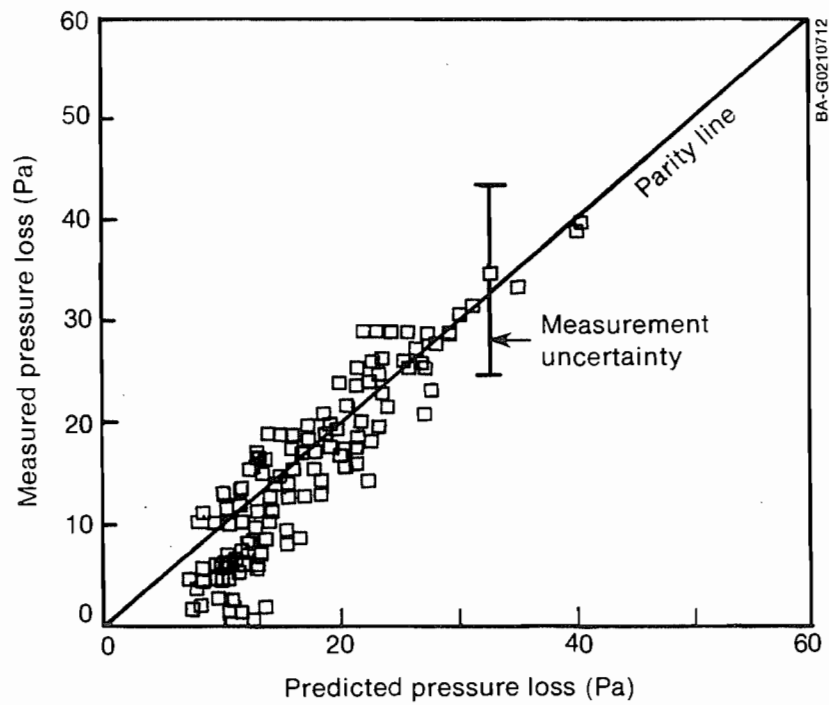


Figure 4-17. Comparison of pressure loss for 27060 packing in countercurrent flow

- The packing with the smallest d_p of 14.7 mm exhibited a flooding limit of acceptable gas loading of $0.25 \text{ kg/m}^2 \text{ s}$. We also observed a similar capacity limit in cocurrent flow for this packing.
- A maximum gas loading of up to $0.45 \text{ kg/m}^2 \text{ s}$ was included in the tests. None of the other tested packings showed a flooding capacity limit over the tested loadings.
- The packings with the largest diameter d_p exhibited the most influence of water free-fall; in other words, contributions to condensation in the water free-fall areas outside the packing could not be ignored in the predictions. A simple but heuristic method of accounting for this contribution is to treat the condenser as if the packing extended all through the water free-fall area. With this approach, we achieved excellent comparisons between the model and data.
- The model exhibited most of the trends observed in the experiments for all tested packings. Some discrepancies in the pressure loss comparisons are attributed to measurement difficulties.
- Table 4-2 summarizes comparisons between predictions and measurements. For the tested 548 data points, the condensed steam predicted by the model differs from the data by less than 1.2% on the average, with a standard deviation of less than 2%. This deviation is comparable to the experimental uncertainty of $\pm 2\%$ in the measurements.
- The model predictions of pressure loss differ from the data by less than 4 Pa on the average; the standard deviation of the differences is less than 6 Pa for three packings. For the tests with the 3X packing, considerably higher scatter in Δp measurements resulted in a standard deviation of the differences of 12.3 Pa. In general, the average and standard deviations of the Δp differences are comparable to the Δp measurement uncertainty of $\pm 10 \text{ Pa}$.

Table 4-2. Cocurrent Condenser Comparison Summary

Packing Identifier	Number of Points	Deviation (Prediction-Experiment)			
		Condensed Steam (%)		Pressure Loss (Pa)	
		Std.		Std.	
		Average	Deviation	Average	Deviation
AX	60	0.9	1.9	2.2	6.0
19060	209	0.1	0.8	1.0	5.1
3X	33	1.1	1.5	1.9	12.3
27060	246	-0.6	0.7	3.6	3.4
Experimental Uncertainty	--	--	2.0	--	10.0

4.3 Summary

The validation efforts described in this section show that (1) the model captures the physical trends observed in the experiments over the entire range of test variables, geometries, and condenser configuration; (2) the model provides predictions comparable to the observations; and (3) the deviations between predictions and measurements are of comparable magnitude to the uncertainty in the measurements. Given the experimental data and their accuracies, no further effort is called for to improve the analysis and verification.

Based on the entire sets of comparisons provided in this section, we find that the model provides predictions that differ from measurements well within acceptable limits for engineering design of direct-contact condensers. Hence, we conclude that this model is validated over the entire range of tested parameters reported here for both cocurrent and countercurrent condensers. These conclusions are based on fresh water results with injection of noncondensable gases into the steam. We anticipate extension of these results to seawater in the near future.

5.0 NUMERICAL RESULTS AND PARAMETRIC STUDIES

This section addresses the results of using the validated model over a wide range of geometric and flow parameters to show performance sensitivities and their potential effect on an overall OC-OTEC system. To illustrate the influence of key parameters on the condenser performance and to identify the best condenser configuration, we conducted two series of parametric studies for the cocurrent and countercurrent condensers. The parameters are broadly categorized as geometric and flow. Table 5-1 lists the parameters studied. The model carried out calculations until the steam saturation temperature approached the cooling water temperature within 0.02°C. The condenser performance was characterized by the following three parameters: percentage of incoming steam condensed, the vapor pressure loss (Pa), and the length of the required condenser. This section presents the results for both a cocurrent condenser and a countercurrent condenser.

5.1 Cocurrent Condenser

The cocurrent condenser, as the first stage of the condenser subsystem, will condense 70% to 90% of the incoming steam. To use the cooling water effectively, we need to limit the water flow into this condenser to yield a Jakob number of less than one. Also, since the steam saturation temperature and the water temperature approach each other in cocurrent flow, we need to keep the pressure loss from reducing the steam saturation temperature significantly within the condenser.

5.1.1 Condensation Process

Detailed cocurrent condenser numerical results are shown in Figures 5-1 through 5-3. We used a Jakob number of 0.8 for the simulations. Results are for area fraction a_f of one.

Figure 5-1 illustrates how the temperatures vary with condenser length. Water temperature increases monotonically from an inlet value of 5°C to the steam saturation temperature at a condenser length of 0.75 m. The steam and inert gas mixture comes in at a saturation temperature of 12°C. The saturation temperature of this gas mixture decreases continuously with length. The steam,

Table 5-1. Condenser Parameters

Geometric	Flow
Packing base B	Steam
Packing height h	Gas loading G
Channel inclination θ	Inlet gas temperature [†] T_{si}
Effective area fraction a_f	Inlet inert gas content X_{ii}
	Water [§]
	Jakob number, Ja

[†]Incoming steam was assumed to be saturated.

[§]For all the studies, water inlet temperature was assumed to be 5°C.

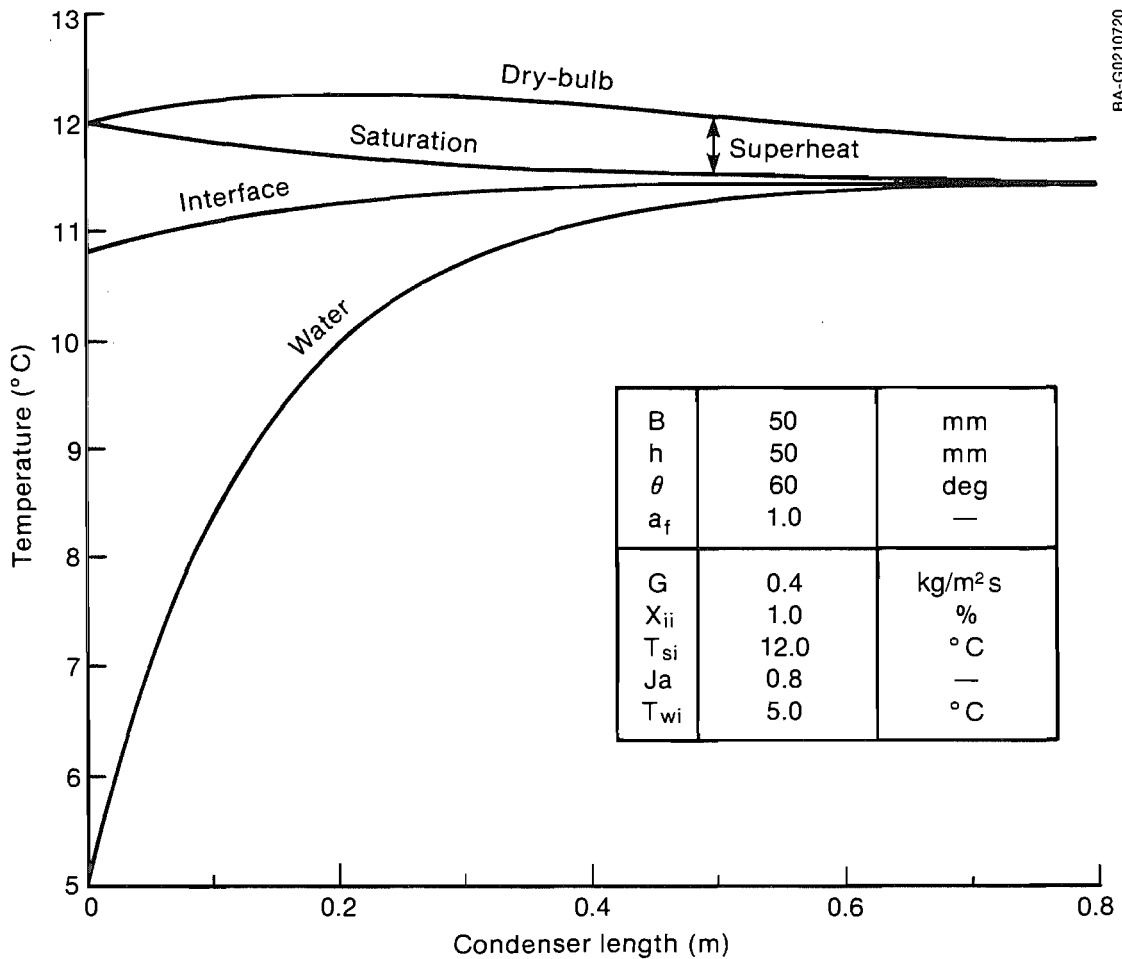
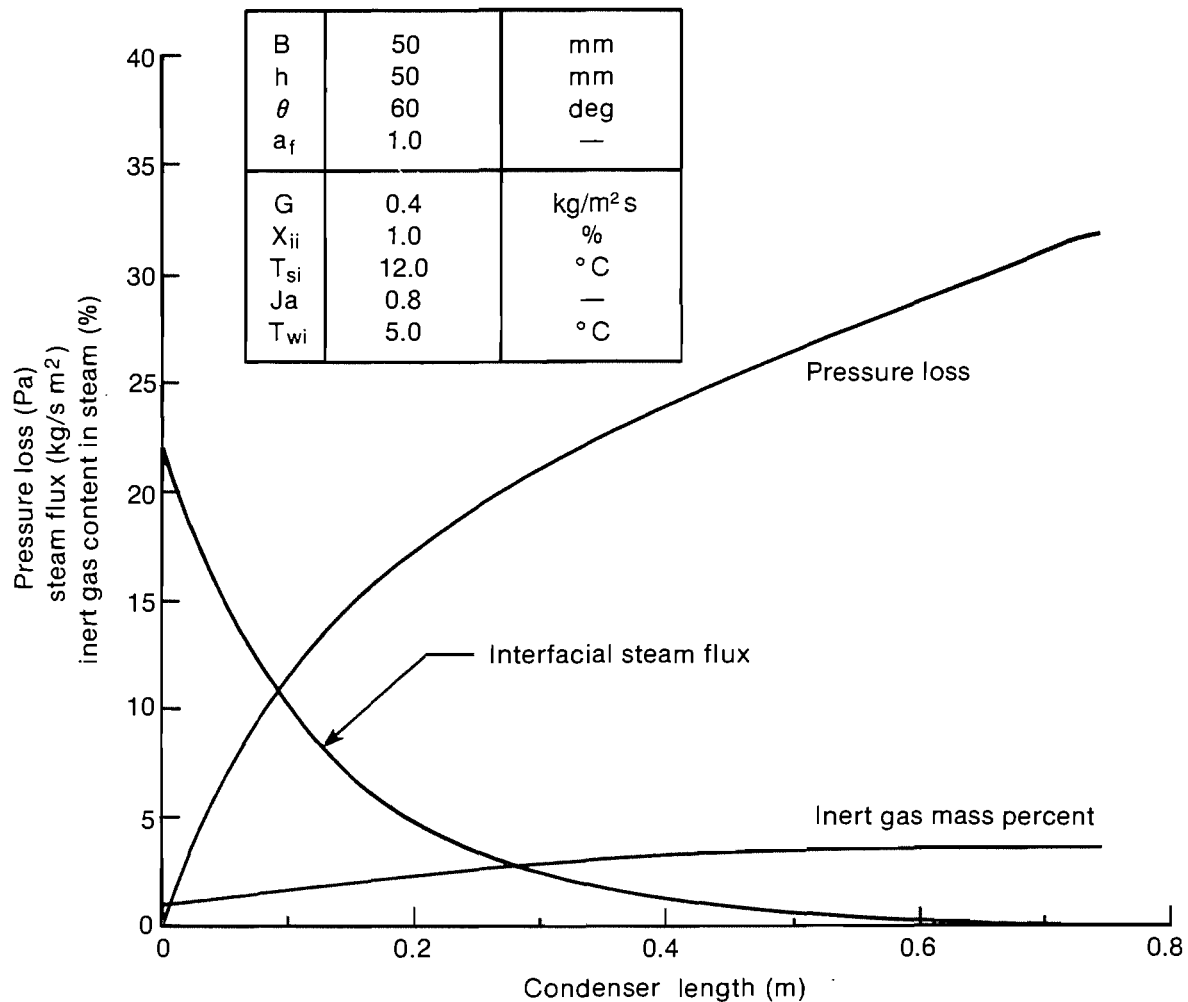


Figure 5-1. Variations of temperatures within the condenser versus downstream distance in cocurrent flow

however, superheats through the process, attaining approximately 0.5°C superheat at the condenser length of 0.75 m.

Also shown in this figure is the variation of the vapor-liquid interface temperature. At any length, the relative value of the interface temperature with respect to the water and saturation values indicates the relative magnitude of the liquid or the gas-side resistance to condensation. Generated with an inlet inert gas concentration of 1%, the interface temperature lies close to the saturation temperature at all lengths, indicating that the resistance is dominated by the liquid side. The condensation process was essentially complete at a length of 0.74 m. Approximately 74% of the incoming steam was condensed at this point.

Figure 5-2 shows the variations of the condensing steam flux w_s (kg/m² s), the static pressure loss Δp (Pa), and the inert gas mass percentage in the steam. The steam flux decreases monotonically with length, reaching negligible values at the end. The pressure loss increases with length. At 0.4 m, almost 70% of the overall pressure loss has occurred. Note that the calculation abruptly stops at a length of 0.74 m. If the steam were allowed



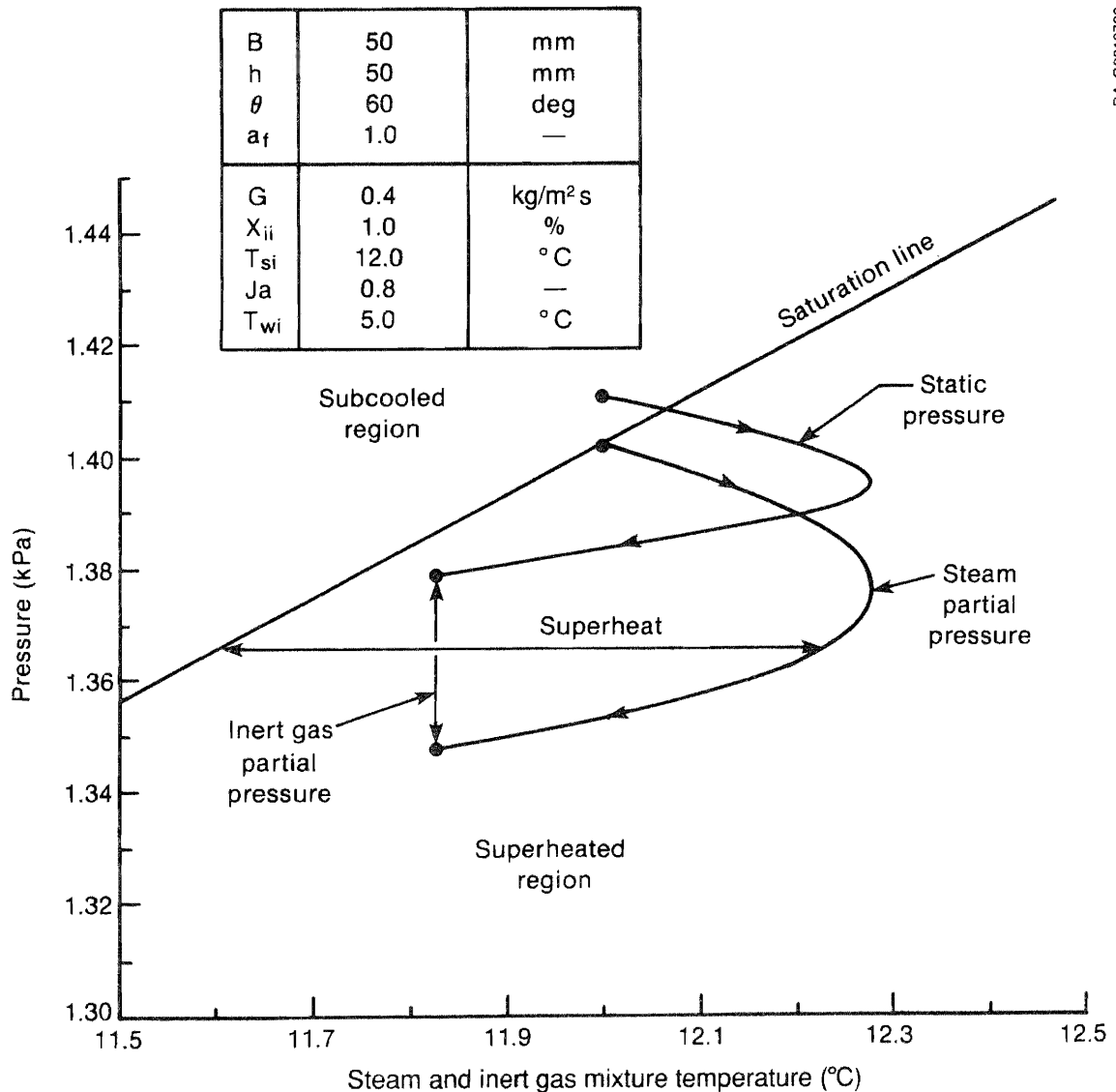
BA-G0210721

Figure 5-2. Variations of pressure loss, interfacial steam flux, and inert content in steam within the condenser versus downstream distance in cocurrent flow

to flow through this packing for longer lengths (about 36% of the steam remains uncondensed), the saturation pressure of the steam would continue to decrease due to friction and eventually drop below the saturation pressure of the water. At excessive condenser lengths this condition will result in the water reevaporating, which is contrary to the basic process of condensation. Reevaporation will occur only in the cocurrent condenser with excessive pressure loss, thus lowering the steam partial pressure to values below the water's saturation pressure. To avoid reevaporation, the cocurrent condenser length must be limited to values less than those required for thermal equilibrium between steam and water, accounting for all causes of pressure losses. Thus, pressure loss in the cocurrent flow plays a key role in the condensation process and hardware design.

Figure 5-2 also shows variations of inert-gas mass content of steam X_i , which increases monotonically from an inlet value of 1% to approximately 3%.

Figure 5-3 shows the process path of the steam and inert gas mixture in a pressure-versus-temperature diagram. The saturation line divides the steam into subcooled and superheated regions. The figure also shows how the static pressure of the mixture and partial pressure of steam varies along the process path (along the condenser length). Both of these pressures decrease continuously. The temperature of the mixture, however, increases initially and then decreases. The initial increase occurs partly from the decreasing gas mixture velocity caused by condensation and partly from frictional heating. The temperature eventually decreases as the heat transfers from the mixture to the water. The steam entering the condenser at saturation is driven into the superheated region as condensation proceeds in the condenser. For all conditions numerically simulated in this study, fog (vapor entering the subcooled region) never formed.



BA-G0210722

Figure 5-3. Process path in cocurrent condensation

5.1.2 Influence of Packing Geometry

Geometric parameters that influence condenser performance include effective area fraction, packing size, packing height, and channel inclination (Table 5-1). Among these geometric parameters, channel inclination θ and the effective area fraction a_f influenced condenser performance the most.

5.1.2.1 Effective Area Fraction

This fraction is the ratio of the active heat- and mass-transfer area to total available packing surface area. Although our experiments suggest that all of the area is active, under some circumstances only part of the area may be active in the transfer process.

A larger a_f causes the liquid to spread over a larger surface, thus decreasing liquid-film velocity and the corresponding heat-transfer coefficient. Although this aspect may be detrimental, increased a_f also provides more surface area for the steam to condense. In general, we find that larger a_f increases the overall condenser performance.

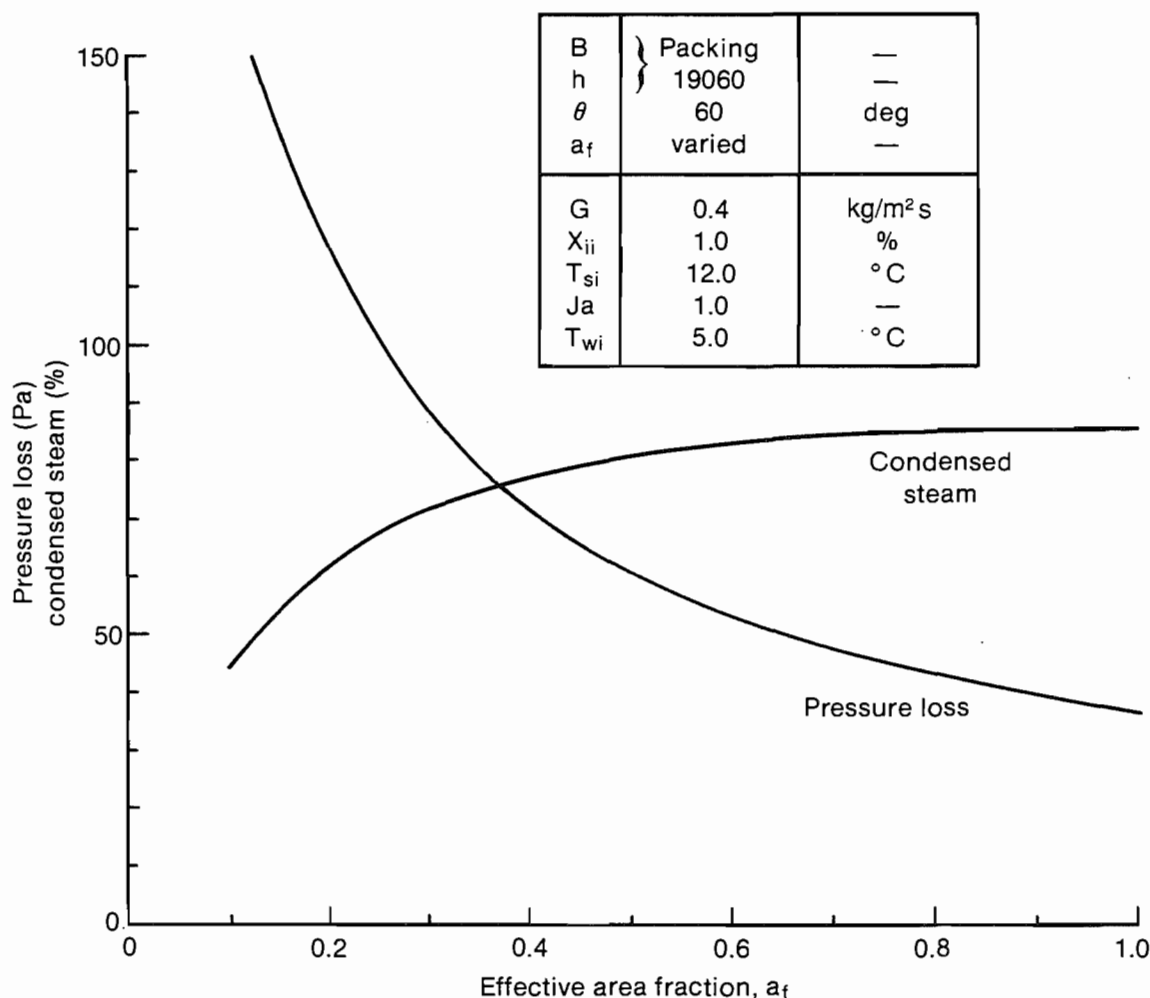
Figure 5-4 depicts the results of increasing the effective surface area fraction a_f from 0.1 to 1.0. For this series we used the packing geometry for packing 19060, and the condenser length was fixed at 0.8 m. With increasing a_f , the percentage of condensed steam increased smoothly from a value of about 45% at $a_f = 0.1$ to a maximum value of 86% at $a_f = 1$. The condenser pressure loss decreases continuously with increasing a_f , dramatically decreasing from nearly 150 Pa at $a_f = 0.15$ down to 35 Pa at $a_f = 1$. Because pressure loss in cocurrent flow reduces the condenser driving potential, a large value for a_f in cocurrent flow is beneficial. However, variation in a_f within the range of 0.6 to 1.0 does not alter the condenser performance significantly. Thus, a packing with an assured a_f in the neighborhood of 0.8 or more is desirable for cocurrent flow.

5.1.2.2 Packing Size (Base and height varied together)

We investigated the influence of packing size by varying the packing base from 10 to 120 mm and maintaining a height-to-base ratio of 0.35.

Figure 5-5 shows the influence of varying packing size ($a_f = 1$). The important features of this figure are that the condensed steam exhibits a maximum and the pressure loss a minimum at a packing base value of 45 mm. However, the maximum and minimum are shallow; a variation between 30 to 70 mm results in a less than 1% change in condensed steam and 4% change in the pressure loss. From this figure we also see that the required condenser length increases and the available surface area per unit volume decreases with increased packing size.

These findings suggest that at any cocurrent condenser inlet conditions, although an optimum packing size may be identified, condenser performance reductions of less than 5% may be expected when size deviates from an optimum by as much as 30%. Larger sizes will allow for higher acceptable gas loadings with minimal Δp .



BA-G0210723

Figure 5-4. Influence of effective area fraction on cocurrent condenser performance

5.1.2.3 Packing Height

The packing height of the experimentally tested articles ranged from 0.3 to 0.4 times their base dimension. To identify any significant influence of this height in relation to base, we conducted a study with the base set at 50 mm and varied the height from 0.1 to 1.2 times the base.

Figure 5-6 shows the results of this height variation. With increasing height-to-base (h/B) ratio, the condensed steam percentage increases, and the pressure loss decreases. The required condenser length is again found to increase, and the surface area per unit volume decreases. No clear-cut maximum or minimum was found over the range of h/B investigated. Thus the h/B ratio should be chosen based on a trade-off between the vapor pressure loss and the required condenser length. At an h/B ratio of 1, changes of $\pm 10\%$ in this ratio result in less than a 10% change in the condenser length and pressure loss. Hence, for the remaining set of cocurrent parametric studies presented in this section, the ratio of h/B was set to 1 (unless stated otherwise).

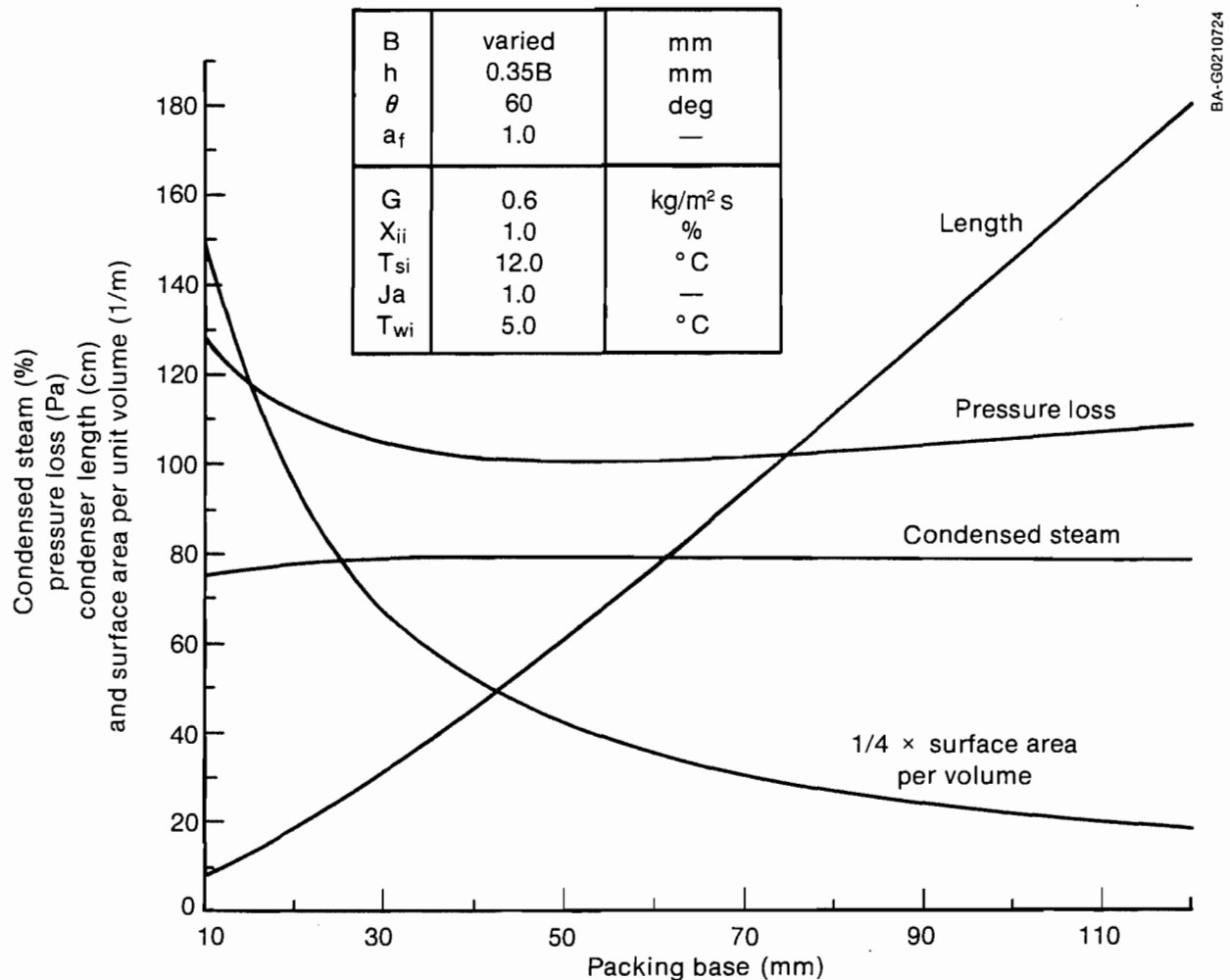
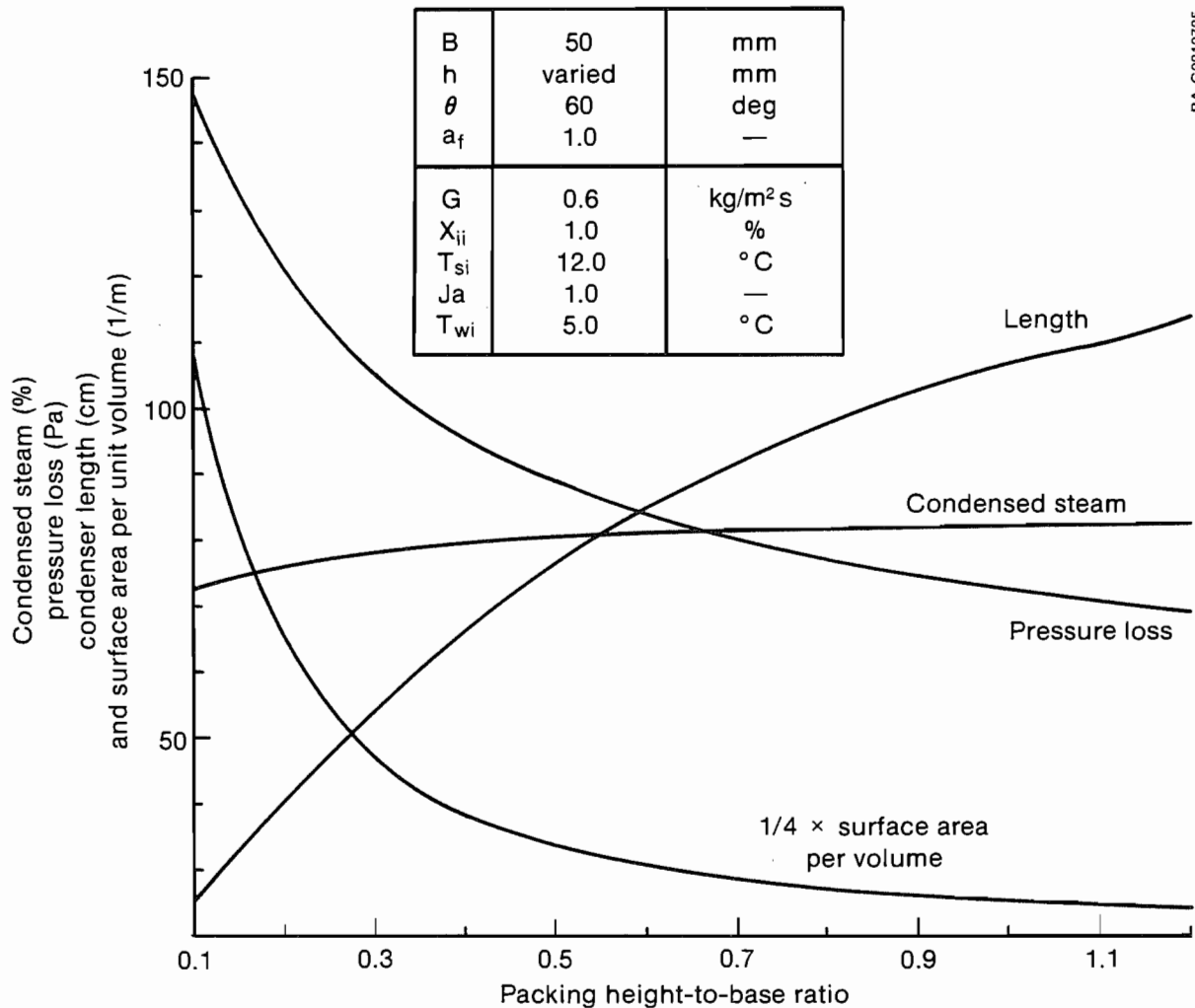


Figure 5-5. Influence of packing size on cocurrent condenser performance

5.1.2.4 Channel Inclination

The channel inclination θ from the horizontal for all the experimentally tested articles was 60 deg. Figure 5-7 shows the influence of this angle as it varies from 20 deg to 85 deg. Other packing parameters, namely, base and height, were fixed at 50 mm and 17.5 mm, respectively, resulting in a surface area per unit volume of 168 m²/m³. A clear-cut maximum in the condensed steam and a minimum in the pressure loss occur at $\theta = 60$ deg. The condenser length increased with increasing θ . At low values of θ , because of the accompanying large pressure losses, only short condenser lengths are needed. At $\theta > 60$ deg, the pressure loss and the required condenser length increase simultaneously.

Thus, for cocurrent condensers with this packing geometry, optimum performance occurs at a channel inclination angle of 60 deg. A deviation of ± 5 deg from this optimum, however, results in a less than 2% change in the condensed steam and a less than 5% change in the pressure loss.



BA-G0210725

Figure 5-6. Influence of packing height-to-base ratio on cocurrent condenser performance

5.1.3 Influence of Flow Parameters

Flow parameters that influence condenser performance include gas loading, inert gas content, Jakob number, and inlet gas temperature. To determine the effects of flow parameters on cocurrent condensation, we fixed the condenser packing geometry at a base and height = 50 mm, $\theta = 60$ deg, and $a_f = 1$.

5.1.3.1 Gas Loading

The condenser gas loading G is defined as the incoming steam and inert mixture flow rate per unit planform area of the condenser. The term "gas loading" is used in the conventional sense as found in chemical engineering literature. Figure 5-8 illustrates the influence of G on cocurrent condensers at three different inlet inert gas percentages X_{ji} (0.1%, 0.5%, and 1%) and at a water flow rate corresponding to a Jakob number of 0.8. Shown are variations of

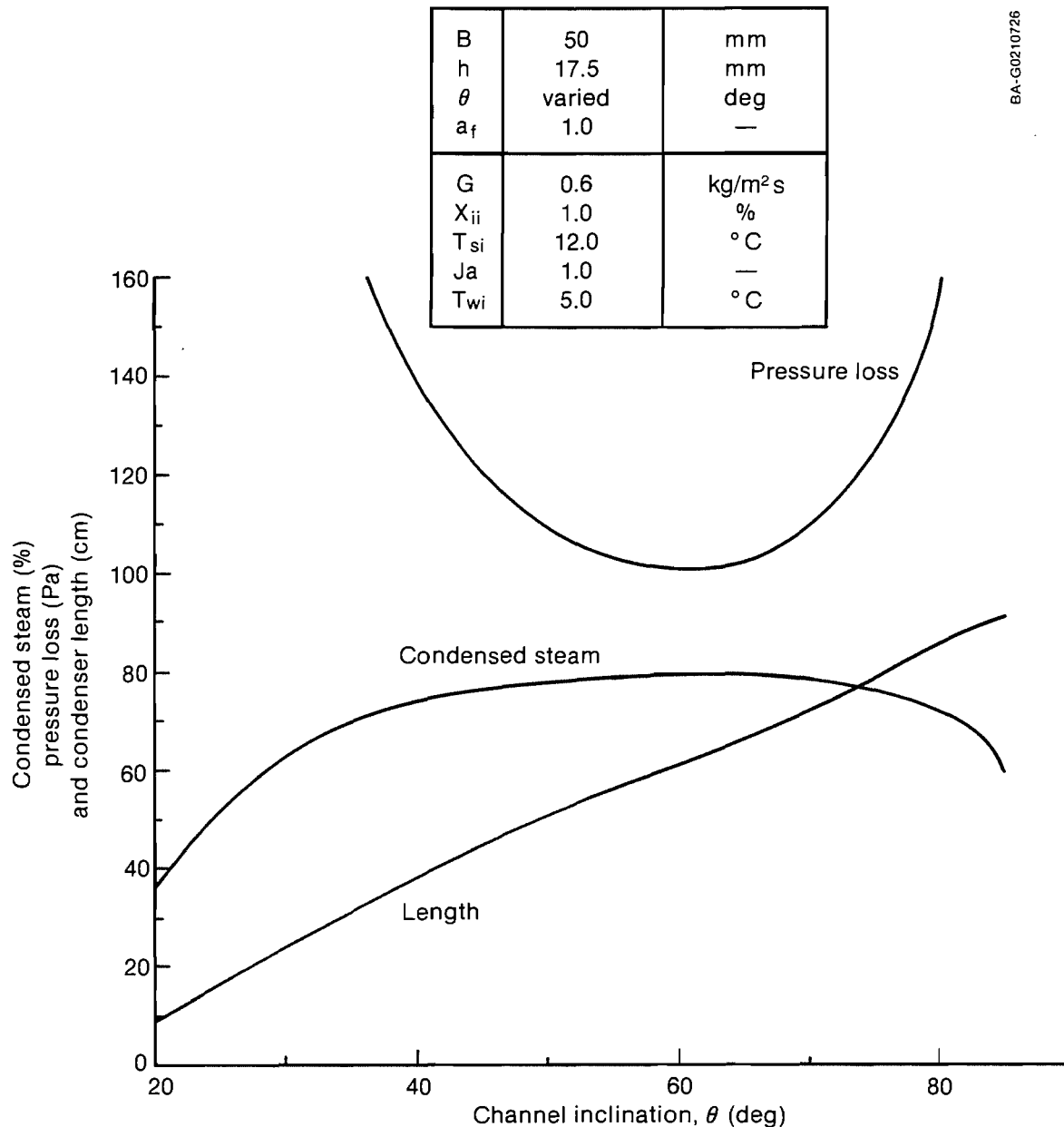


Figure 5-7. Influence of channel inclination on cocurrent condenser performance

condensed steam percentage, pressure loss, and required condenser length.[‡]The pressure loss increases nearly quadratically with increasing gas loading. Higher levels of inert gases result in higher pressure losses. The percentage of condensed steam decreases with increasing gas loading. Since the Jakob number is 0.8, the maximum possible value of 80% for condensed steam

[‡]The pressure loss and condenser length have been scaled by dividing by 2 to show salient features and preserve clarity in this figure.

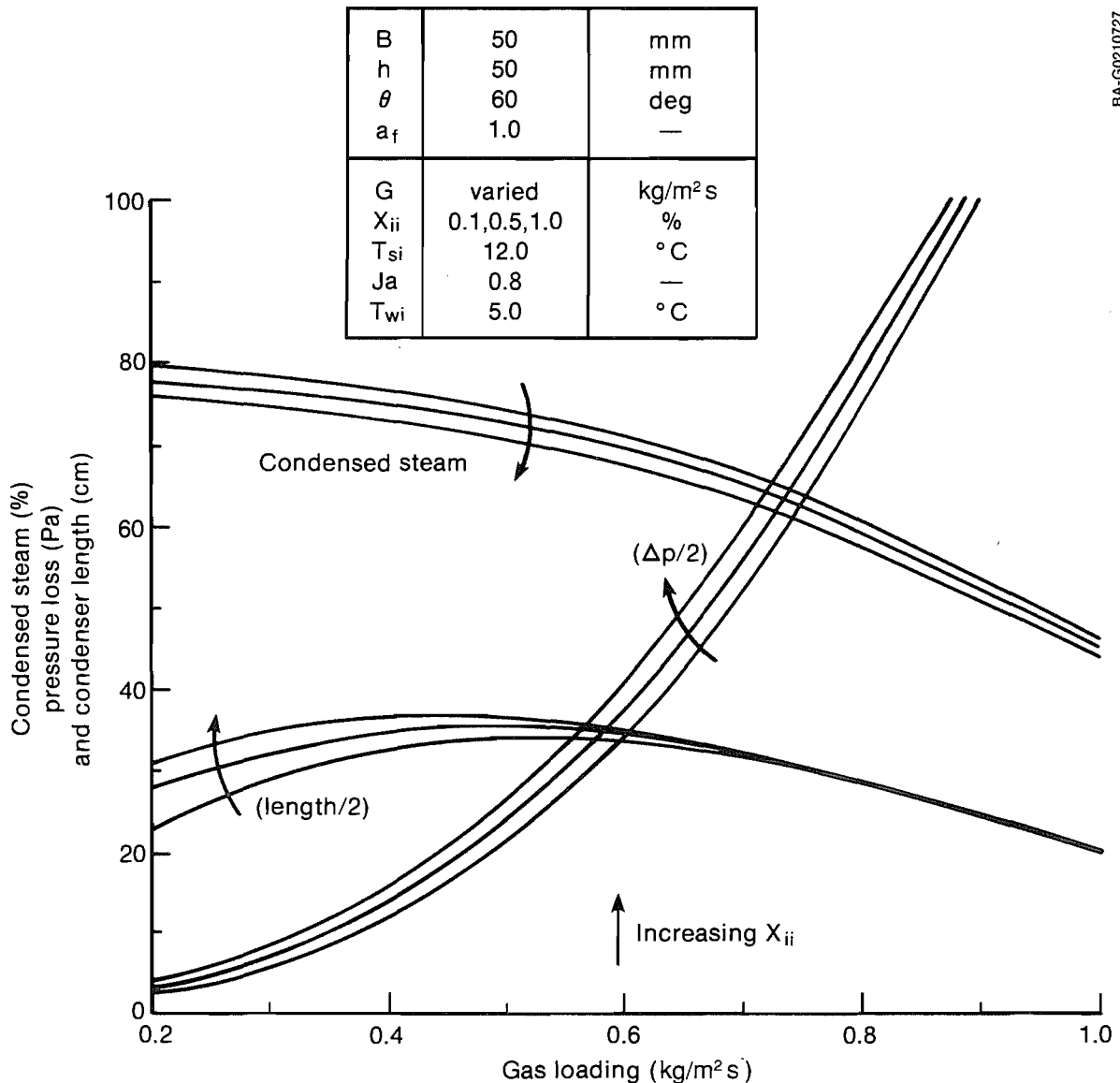


Figure 5-8. Influence gas loading on cocurrent condenser performance

is approached at low gas loadings. Increased levels of inert gas in the steam reduce the amount of steam condensed.

An important feature shown in this figure is the variation of required condenser length. The required length reaches a maximum at gas loadings that range from 0.4 to 0.6 kg/m² s and then decreases with increasing G. We reach the maximum at lower values of G as the inert gas content X_{ii} is increased. At gas loadings beyond the maximum length, the pressure loss incurred during the initial lengths decreases the steam saturation pressure enough to overcome the benefits of increasing the downstream length. As indicated earlier, lengths greater than those required would result in reevaporation and must be avoided.

5.1.3.2 Inert Gas Content

An inert gas content X_{ii} in the turbine exhaust steam on the order of 0.1% or less is typical of OTEC systems that can predeaerate incoming water (Parsons, Bharathan, and Althof 1985). The gas content X_{ii} may reach 0.5% in systems that do not predeaerate the water.[†] For the parametric studies, three specific values for X_{ii} were chosen: 0.1%, 0.5%, and 1.0%. The results of this study are included in Figure 5-8. The influences of increased X_{ii} over this range are to increase the condenser pressure loss by about 7% and to decrease the condensed steam by 5%. The required condenser length increases with increasing X_{ii} for gas loadings of up to 0.5 kg/m² s. At higher gas loadings, the influence of X_{ii} on required length is minimal.

Other results (not shown) to determine the optimum condenser geometry for cocurrent condensers with X_{ii} from 0.1% to 0.5% indicated that a base value from 20 to 30 mm yields the lowest pressure losses, with base = height and $a_f = 1$, at $Ja = 0.8$, and a gas loading of 0.6 kg/m² s. Decreasing the gas loading to 0.4 kg/m² s resulted in a larger base dimension from 40 to 50 mm.

5.1.3.3 Jakob Number

The Jakob number for the condenser is defined as

$$Ja = \dot{m}_{wi} C_{pw} (T_{si} - T_{wi}) / (\dot{m}_{si} h_{fg}) , \quad (5-1)$$

where

$\dot{m}_{wi}, \dot{m}_{si}$ = incoming water and steam mass flow rates (kg/s), respectively

T_{wi}, T_{si} = incoming water and steam saturation temperatures (°C), respectively

C_{pw} = average specific heat capacity of water (kJ/kg K)[§]

h_{fg} = average latent heat of condensation for steam (kJ/kg)[§].

A Jakob number of 1 represents the minimum water flow required to condense 100% of the incoming steam flow given certain inlet water and steam saturation inlet temperatures. Conversely, it can also represent a minimum required steam inlet saturation temperature to condense all the steam for a given water flow rate and its inlet temperature.

Note that two dimensionless parameters make up the Jakob number: $\dot{m}_{wi}/\dot{m}_{si}$, a ratio of cooling water to incoming steam flow rate, and $C_{pw}(T_{si} - T_{wi})/h_{fg}$, a ratio of the potential sensible heat capacity of the water to the latent heat of condensation. Thus, the Jakob number can be altered by varying either of these quantities.

[†]These values include an estimated atmospheric air leakage into the vacuum enclosure.

[§]For this study, $C_{pw} = 4.186$ kJ/kg K, and $h_{fg} = 2470$ kJ/kg.

For the following discussions, we define two other dimensionless quantities. The water effectiveness ϵ_w is expressed as

$$\epsilon_w = (T_{wo} - T_{wi}) / (T_{si} - T_{wi}) \quad , \quad (5-2)$$

which represents the ratio of actual water temperature rise to a maximum possible. An uncondensed steam percentage is defined as the percentage of steam that remains uncondensed in a particular condenser stage and, thus, must be handled by downstream equipment (a next-stage condenser or vacuum exhaust pumps). An ideal condenser subsystem with no pressure loss and no noncondensable gases present operates most effectively at $Ja = 1$. From the definitions, it follows that $\epsilon_w = 1$, and uncondensed steam = 0.

At Jakob numbers other than unity, ideal condenser operational limits are established as follows

- For $Ja > 1$, $\epsilon_w = 1/Ja$, and uncondensed steam % = 0
- For $Ja < 1$, $\epsilon_w = 1.0$, and uncondensed steam % = 100 (1 - Ja).

These criteria yield the asymptotes that bracket a condenser performance in Figures 5-9 through 5-13.

For a real condenser subsystem, the presence of noncondensable gases requires a finite amount of uncondensed steam to be purged from the system. Pressure losses through the condenser hardware cause reductions in the steam saturation temperature from an inlet value and thus limit the sensible ΔT that the cooling water can take up. This loss reduces the water effectiveness to values less than unity.

Because the cocurrent condenser represents the first stage of the condenser subsystem, only part of the incoming steam needs to be condensed here. Thus, for this condenser, operating at a local Jakob number of less than unity is possible and desirable if a water effectiveness close to unity should be approached for the overall condenser subsystem.

We varied the Jakob number from 0.4 to 1.2 by changing the water flow rate in the cocurrent condenser (Figure 5-9). For this figure, we fixed T_{si} and T_{wi} at 12° and 5°C, respectively, and assumed a gas loading G of 0.6 kg/m² s. Asymptotes for ϵ_w and uncondensed steam bracketing the condenser performance are also shown. Uncondensed steam decreases with increasing Ja , and is always higher than that given by the asymptote. The pressure loss through the condenser increases slightly with Ja in the range of 0.4 to 0.6, and then begins to decrease with further increases in Ja . The required condenser length increases with Ja up to a Ja of 1.0 because more of the steam is condensed at higher Ja . Water effectiveness increases with decreasing Ja , reaching an almost constant value of 0.85 for $Ja < 0.8$. Note that the predicted ϵ_w values are always lower than the corresponding ideal asymptotic limits. An upper limit on ϵ_w of 0.85 results primarily from the vapor pressure losses on the order of 85 Pa at the assumed gas loading of 0.6 kg/m² s.

Figure 5-10 illustrates the features of Figure 5-9 at a reduced gas loading value of 0.4 kg/m² s. Note that the condenser pressure losses were reduced by more than 50% from the previous figure to values of around 35 Pa. The reduced

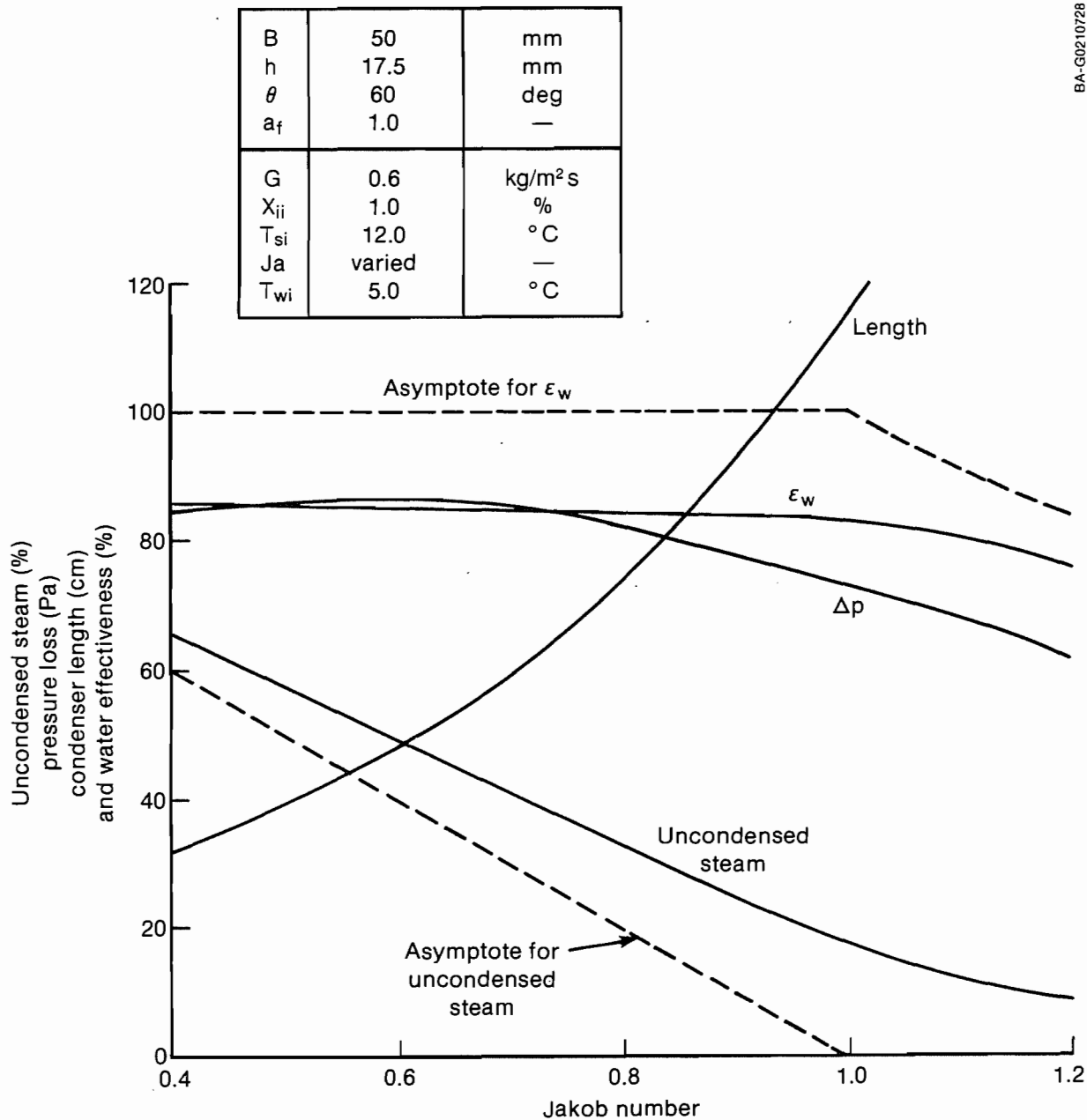


Figure 5-9. Influence of Jakob number varied via water flow rate on cocurrent condenser performance at $G = 0.6 \text{ kg/m}^2 \text{ s}$

pressure losses result in $\epsilon_w > 0.90$ for $Ja < 0.90$. Both ϵ_w and uncondensed steam are closer to their corresponding asymptotes at this lower gas loading of $0.4 \text{ kg/m}^2 \text{ s}$.

For Figures 5-9 and 5-10, the assumed packing geometry was close to optimum. Thus, for cocurrent flow, to achieve a water effectiveness of over 85%, the gas loading should be limited to less than $0.6 \text{ kg/m}^2 \text{ s}$ at an inert inlet concentration X_{ii} of 1%. Lowering the X_{ii} from 1.0% to 0.5% will allow either higher gas loadings at a fixed ϵ_w or higher ϵ_w at a fixed G .

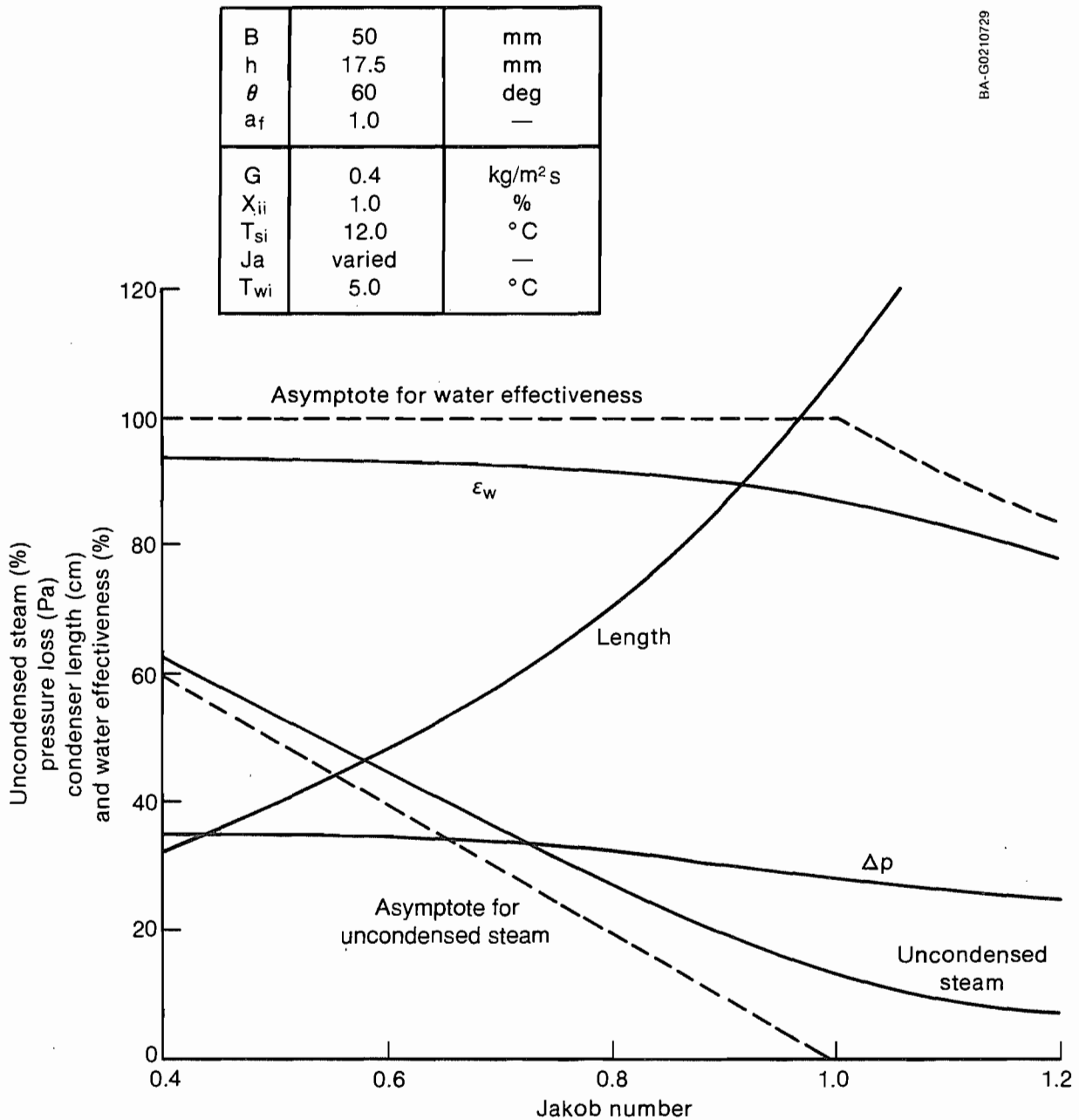


Figure 5-10. Influence of Jakob number varied via water flow rate on cocurrent condenser performance at $G = 0.4 \text{ kg/m}^2 \text{ s}$

Figure 5-11 illustrates the effect of water flow rate on the condensation process in cocurrent flow. This figure shows condenser heat load per unit plan-form area versus steam and water temperatures at $G = 0.6 \text{ kg/m}^2 \text{ s}$. An ideal condenser performance is depicted by an outer envelope, typical of condensation in the presence of inert gases. Lines of constant Jakob numbers originate at zero heat load and water inlet temperature. Low Jakob numbers represent low water flows. The intersection of a constant Jakob number line with the ideal envelope shows the outlet water and steam temperatures and the heat load taken by an ideal condenser. For the ideal envelope, we can achieve

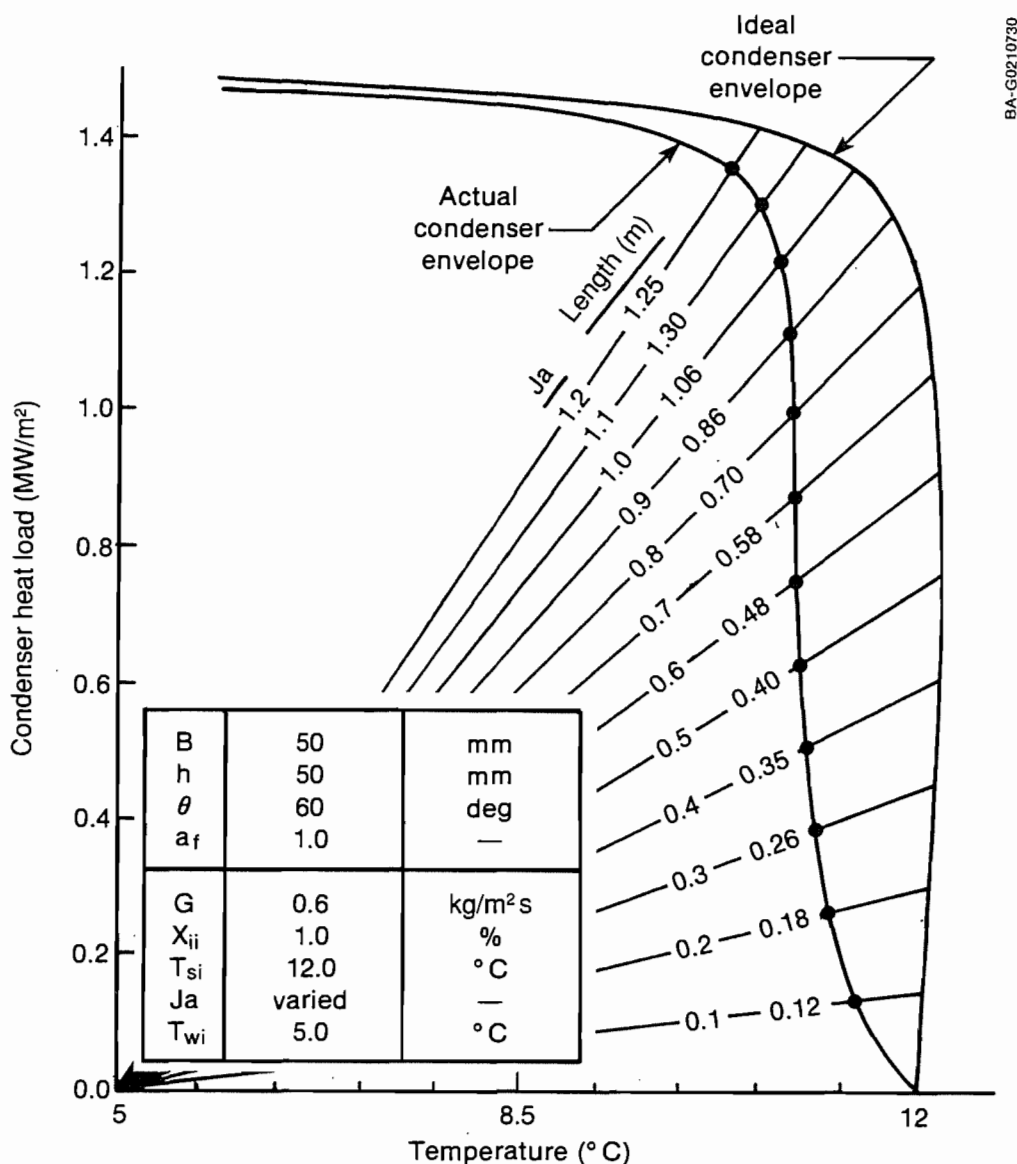


Figure 5-11. Cocurrent condenser operating diagram

outlet water temperatures as high as the steam inlet temperature if Ja is from 0.1 to 0.8. (At higher Ja, sensible cooling of the steam and inert gas mixture begins to take place.)

However, for an actual condenser, the outlet water temperature is considerably lower because of vapor pressure losses. In a range of Ja = 0.4 to 0.8, essentially a constant water outlet temperature is achieved for a real condenser. For Ja < 0.4, higher water outlet temperatures result; for Ja > 0.8, outlet water temperature begins to decrease.

The Jakob number can also be varied with inlet steam saturation temperature for the cocurrent condenser by holding the ratio $\dot{m}_{wi}/\dot{m}_{si}$ constant (at 84.3)

and varying the steam inlet temperature. Figure 5-12 illustrates the variation of the condenser performance with Jakob number from 0.4 to 1.2 for two levels of X_{ii} (0.1% and 1.0%) and $G = 0.6 \text{ kg/m}^2 \text{ s}$. The differences between Figure 5-9 and Figure 5-12 are: Δp increases dramatically with decreasing steam inlet temperature and the Jakob number, causing ϵ_w to reach a maximum at $Ja \approx 1$; and uncondensed steam and ϵ_w deviate farther from their corresponding asymptotes as Ja decreases.

A similar set of features is seen for $G = 0.4 \text{ kg/m}^2 \text{ s}$ in Figure 5-13. However, because of a lower Δp at lower G , deviations from the asymptotes in this figure are smaller.

This series of parametric studies provides a designer with guidelines for choosing cocurrent condenser packing geometry and operating conditions. From the results reported, we can estimate performance parameters at design conditions and the penalties associated with deviations in parameters from chosen values. For optimal design, however, the condenser model should be incorporated into an overall system study to identify appropriate design choices.

5.2 Countercurrent Condenser

The countercurrent condenser, the second stage of the condenser subsystem, condenses the leftover steam flow from the first cocurrent stage and concentrates the inert gases to the maximum extent possible before exhausting them. We expect this second stage will handle approximately 10%-30% of the total steam flow. Since the counterflow operation is generally more efficient, performance does not suffer as significantly in this stage from vapor pressure loss as in the first stage. Despite varying pressure losses, because the water temperature decreases in the direction of steam flow, more than 98% of the incoming steam is condensed in this stage. Thus, the minimum required water flow for this stage always corresponds to a Jakob number greater than one.

5.2.1 Condensation Process

Figure 5-14 illustrates detailed numerical results of steam condensation in counterflow in the presence of inert gases. Results are for packings with the effective area fraction $a_f = 1$. Figure 5-14 also shows the variation of various temperatures with condenser length. The condenser length is measured beginning at the bottom (the condenser bottom is on the left.). In this figure, the condenser is 0.37 m high. The steam and inert gas mixture enters the condenser from below at a nominally saturated condition of 12°C . Cooling water at 5°C corresponding to a Ja of 1.1 enters from the top. (Because numerical integration was carried out from the bottom, a series of iterations are required to match the cooling water temperature at any given height. Details of the integration and iteration processes may be found in Appendix F.) The water temperature rises continuously from the inlet value to approximately 11.3°C as it reaches the bottom.

The saturation temperature of steam decreases continuously; the rate of decrease is gradual in the first part of the condenser over lengths less than 0.27 m, where most of the steam condenses. Farther from the inlet, the gas begins cooling with a sharp decrease in the saturation temperature. The dry-bulb temperature of the gas increases in the first part of the condenser,

B	50	mm
h	50	mm
θ	60	deg
a_f	1.0	—
G	0.6	kg/m ² s
X_{ii}	0.1, 1.0	%
T_{si}	varied	°C
Ja	varied	—
T_{wi}	5.0	°C

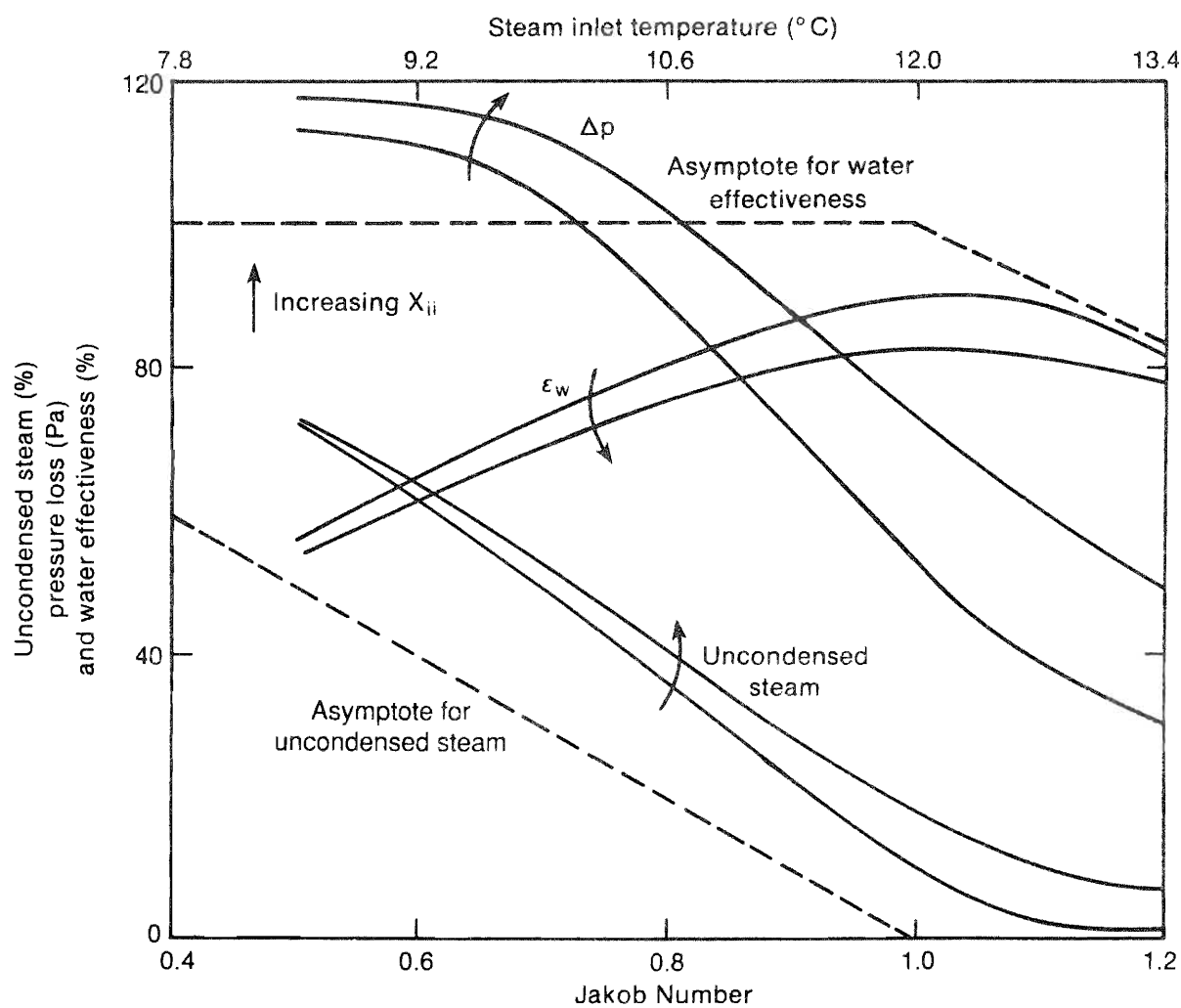


Figure 5-12. Influence of Jakob number varied via inlet steam temperature on cocurrent condenser performance at $G = 0.6 \text{ kg/m}^2 \text{ s}$

B	50	mm
h	50	mm
θ	60	deg
a_f	1.0	—
G	0.4	kg/m ² s
X_{ii}	0.1, 1.0	%
T_{si}	varied	°C
Ja	varied	—
T_{wi}	5.0	°C

BA-G0210732

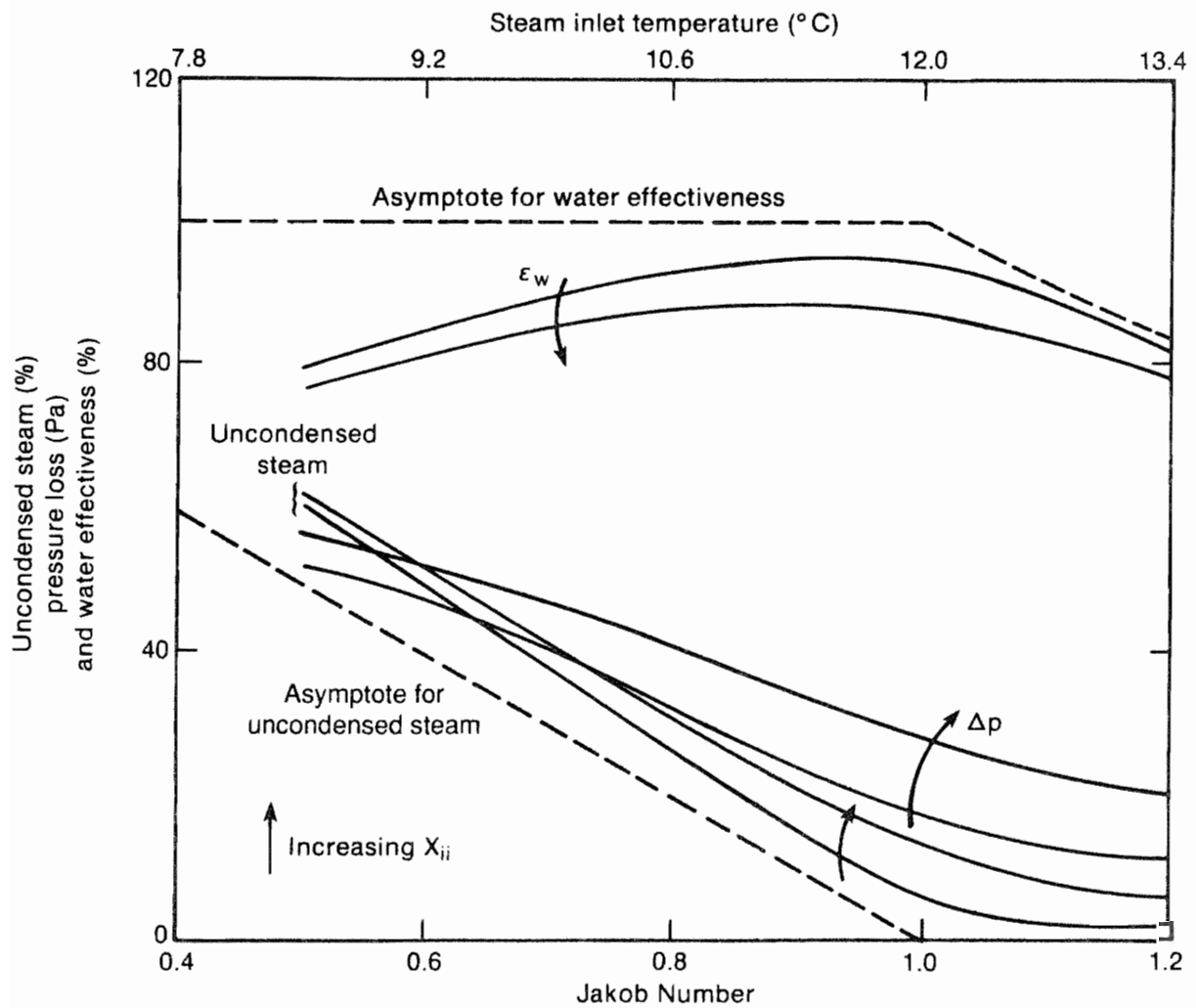


Figure 5-13. Influence of Jakob number varied via inlet steam temperature on cocurrent condenser performance at $G = 0.4 \text{ kg/m}^2 \text{ s}$

B	25	mm
h	25	mm
θ	60	deg
a_f	1.0	—
G	0.4	kg/m ² s
X_{ii}	1.0	%
T_{si}	12.0	°C
Ja	1.1	—
T_{wi}	5.0	°C

BA-G0210733

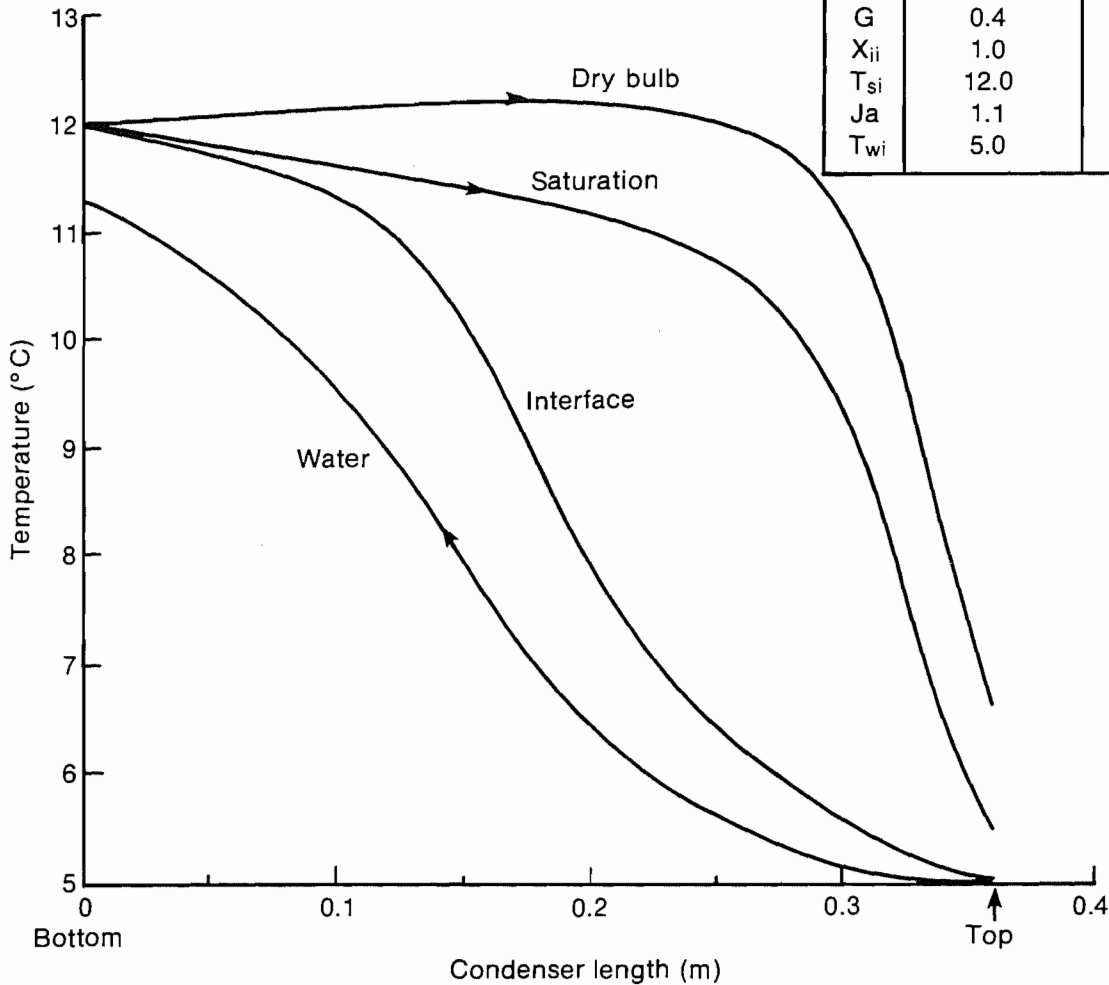


Figure 5-14. Variations of temperatures within the condenser versus downstream distance in countercurrent flow

resulting from decreasing gas velocity and frictional heating. This temperature drops sharply in the latter part of the condenser because of gas cooling.

Also shown in Figure 5-14 is the variation of the gas-liquid interface temperature. This temperature decreases continuously with length, following the water temperature. Again, the relative value of this interface temperature to the water and saturation temperatures indicates the relative value of gas- or liquid-side resistance to condensation. Near the bottom of the condenser, the interface temperature is close to the saturation value, implying a liquid-side-controlled process. As more steam condenses through the length, the interface temperature moves closer to the water temperature, indicating a

dominant gas-side resistance. At the top of the condenser, nearly 99% of the incoming steam was condensed.

Figure 5-15 shows the variations of the interfacial steam flux w_s ($\text{kg/m}^2 \text{ s}$), the pressure loss Δp (Pa), and inert gas mass percentage in steam. The steam flux increases gradually from the bottom of the condenser, reaches a maximum midway, and then begins to decrease at the top. This maximum occurs because the largest driving temperature potential occurs somewhere in the middle of the condenser in countercurrent flow. The pressure loss increases monotonically with length. Initially, the rise in pressure loss is high; this rate is maintained almost halfway through the condenser. In the latter half, however, the pressure loss does not increase as rapidly.

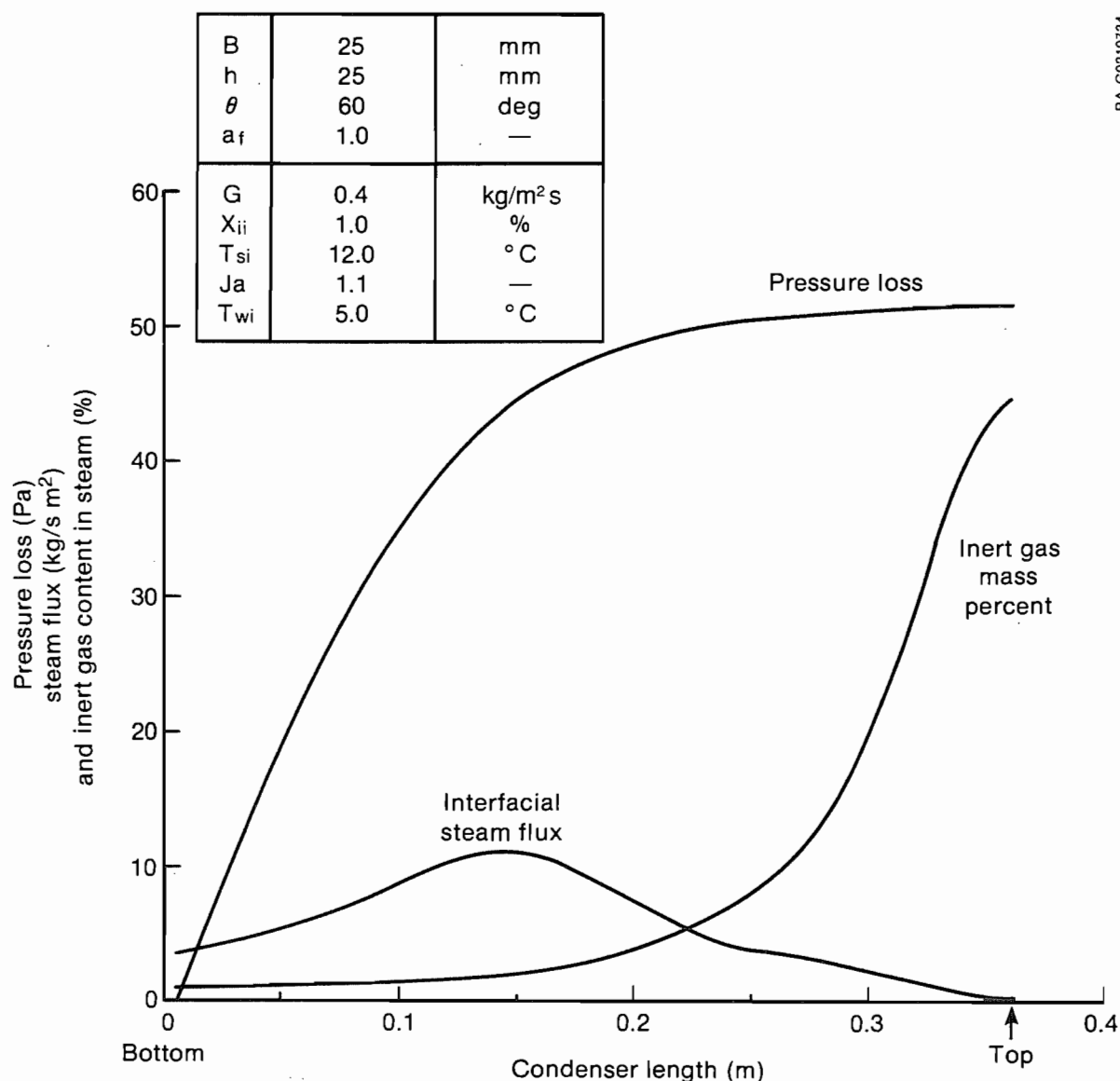
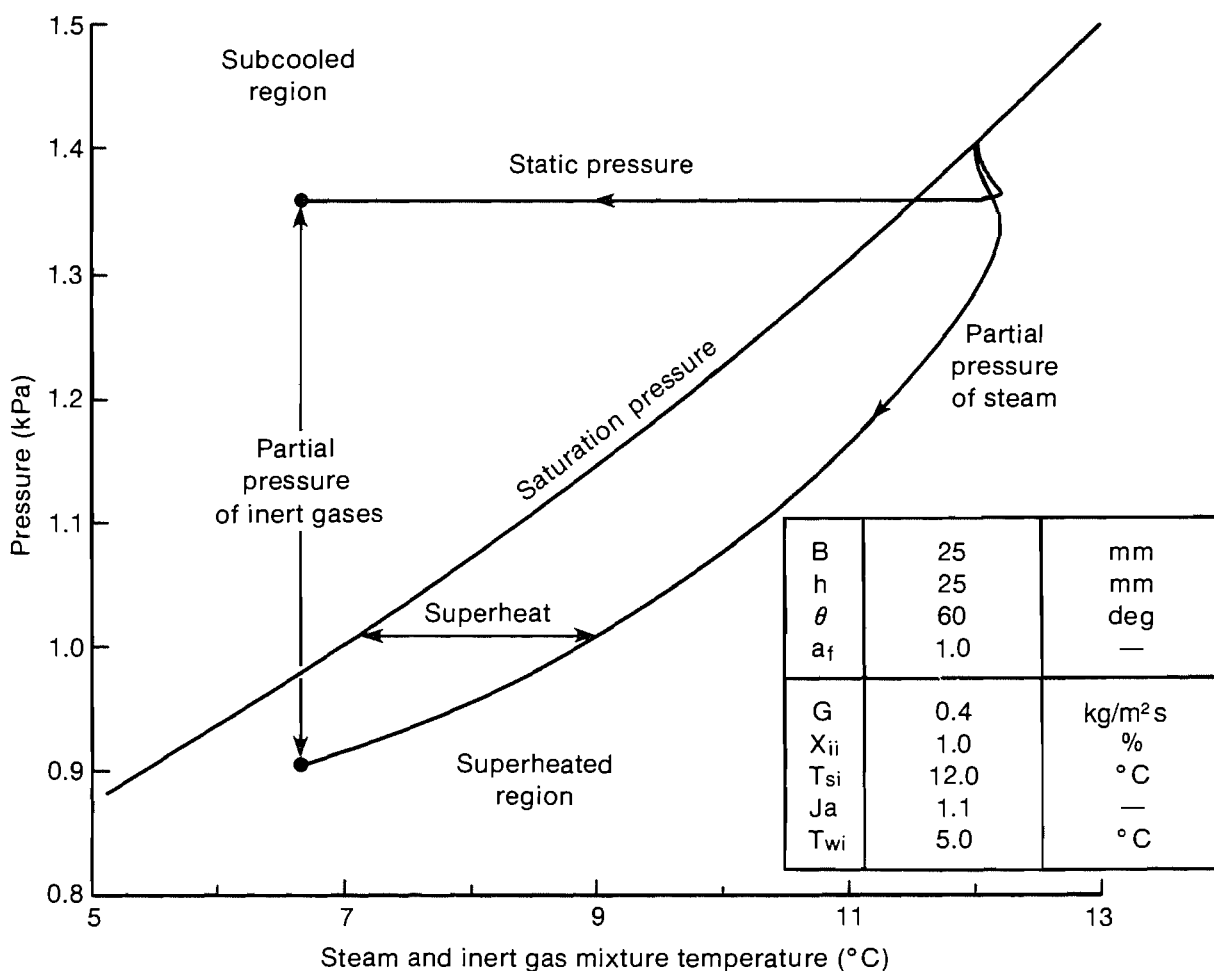


Figure 5-15. Variations of pressure loss, interfacial steam flux, and inert content in steam within condenser versus downstream distance in countercurrent flow

The inert gas mass concentration in the steam increases with condenser length as the steam progressively condenses. This increase is gradual in the first half of the condenser; the latter half concentrates the inert gases by a great amount, starting from almost the initial inlet value of 1% to an outlet concentration of 45%. The counterflow arrangement is efficient in achieving a high concentration of noncondensable gases and, thus, is best suited as the last stage of the condenser subsystem to reduce the load on the inert gas removal system. In fact, the counterflow arrangement is the most efficient, and if the turbine exhaust steam can be routed directly into a countercurrent condenser without other penalties, it should be considered.

Figure 5-16 shows the countercurrent condensation of the steam and inert gas mixture state diagram, including static pressure, partial pressure of steam, and saturation pressure versus temperature. The saturation line splits this figure into subcooled and superheated regions. The gas mixture entering the condenser quickly goes into the superheated region. The static pressure decreases slightly initially and remains essentially constant in the latter half of the condenser. The steam partial pressure decreases continuously until it reaches a value corresponding to the water inlet saturation temperature. The steam and inert gas mixture, however, remains superheated by about 1.5°C as it exits the condenser.



BA-G0210735

Figure 5-16. Steam and inert gas mixture process path in countercurrent flow

5.2.2 Influence of Packing Geometry

5.2.2.1 Effective Area Fraction

Experimental results suggest all surface area is effective for the tested packings in countercurrent flow. Figure 5-17 shows the influence of a_f as it varies from 0.1 to 1.0 for a fixed countercurrent packing length of 0.8 m. With increasingly higher effective fraction, the condensed steam increases monotonically, and the accompanying pressure loss decreases from a high value of 120 Pa down to 50 Pa. Changes in both of these quantities, when a_f is around 0.8, are gradual.

5.2.2.2 Packing Size

We investigated packing size variation (base and height varied together) by varying the base dimension over 10 to 50 mm and holding a height-to-base ratio of 1.0. Calculations were continued to a condenser length where the steam saturation temperature was 0.02°C higher than the water inlet temperature. This condition, in effect, resulted in condensing almost a constant 98.8% of incoming steam for all cases. The results of packing size variation are shown in Figure 5-18. The required condenser length, as expected, increases almost

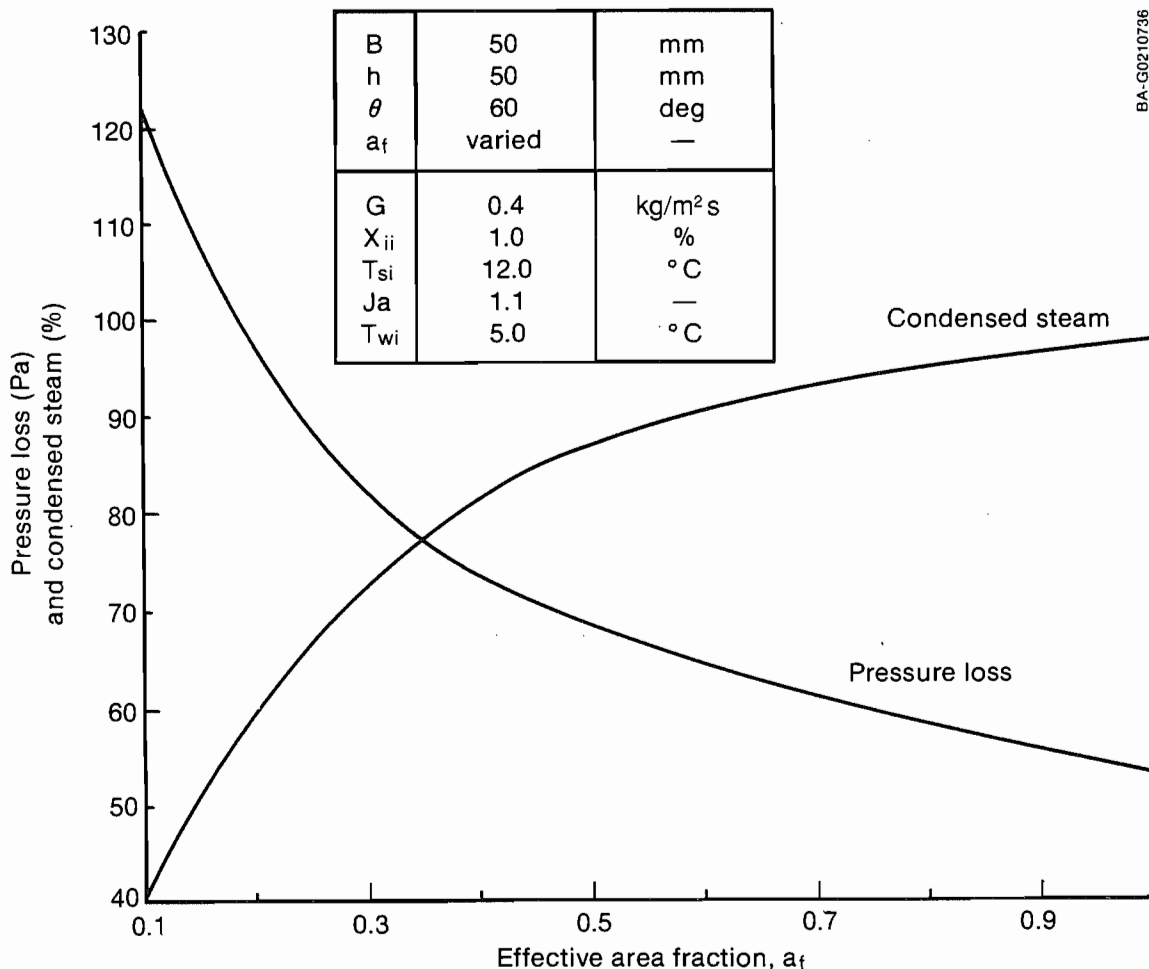


Figure 5-17. Influence of effective area fraction on countercurrent condenser performance

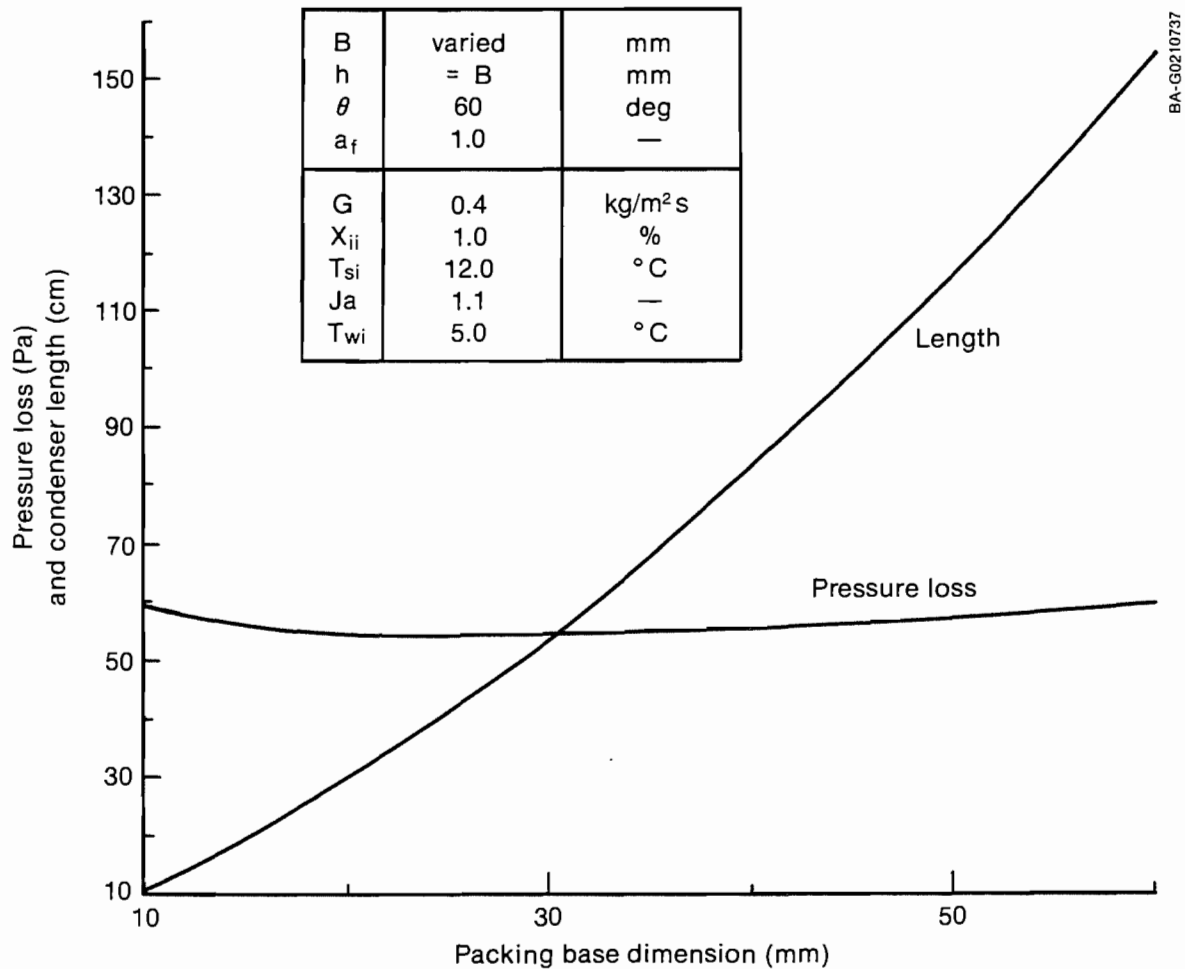


Figure 5-18. Influence of packing size on countercurrent condenser performance

linearly with the packing base dimension. The pressure loss shows a gradual minimum at a base of 25 mm. The variation of pressure loss over the entire range of base variation is less than 10%. Of course, larger packing size will allow for larger gas loadings without flooding.

5.2.2.3 Packing Height

The results of a parametric study varying the packing height-to-base (h/B) ratio from 0.1 to 1.2 at a base of 25 mm are shown in Figure 5-19 as plots of pressure loss, required condenser length, and surface area per volume versus the h/B ratio. Again in all cases, over 98.8% of the incoming steam was condensed. As expected, the required condenser length increases and surface area per volume decreases with increasing h/B ratio. The pressure loss decreases monotonically with increasing h/B ratio within the range investigated. As in cocurrent flow, we could not find a clear-cut choice for the h/B ratio. A trade-off between vapor pressure loss and required condenser length on a system level must be made for an appropriate choice of h/B ratio.

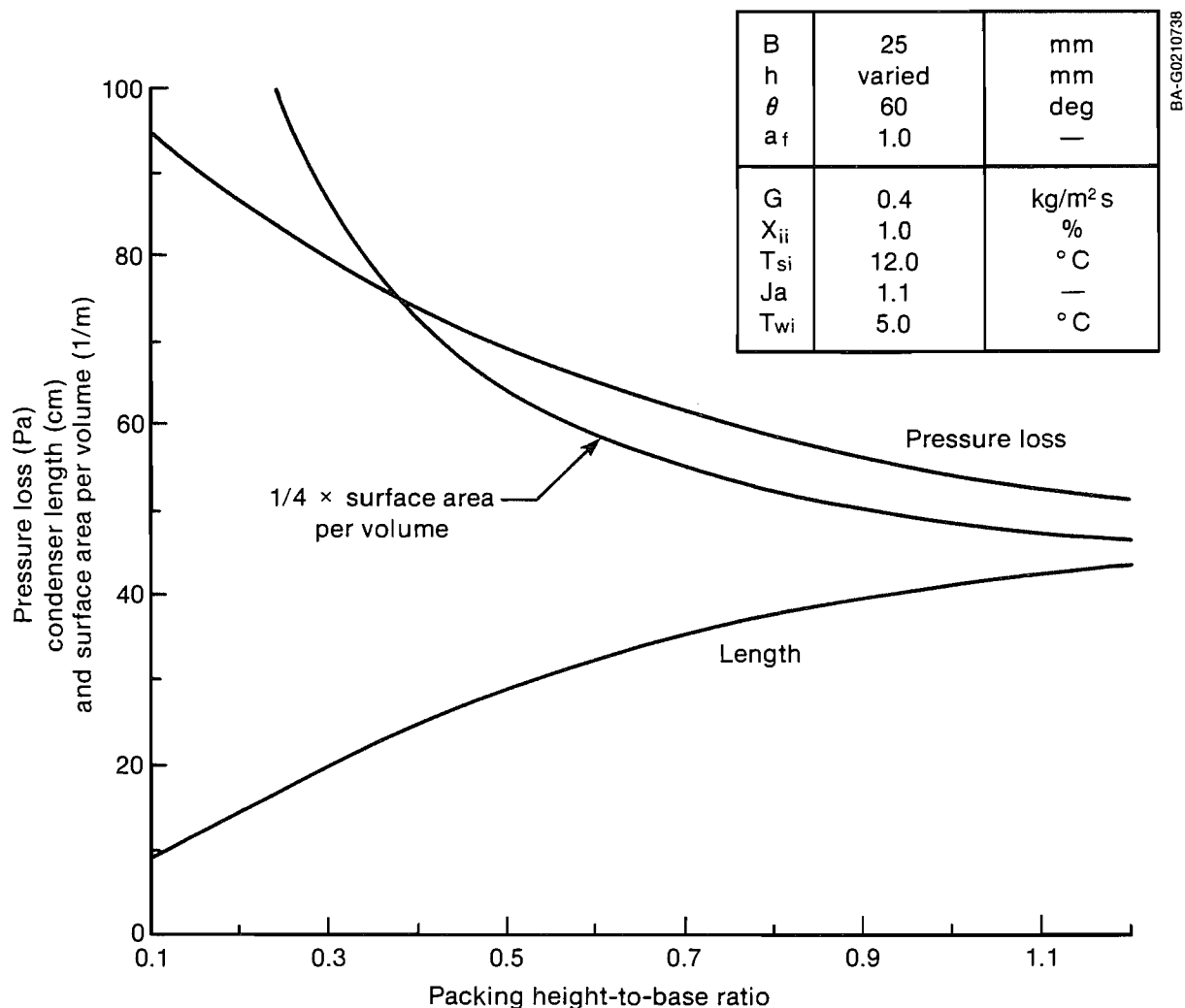


Figure 5-19. Influence of packing height-to-base ratio on countercurrent condenser performance

5.2.2.4 Channel Inclination

Varied channel inclinations provided the most significant influence on countercurrent flow as well. Figure 5-20 shows pressure loss and required condenser length. In all cases, over 96% of the incoming steam was condensed. The pressure loss exhibits a pronounced minimum at $\theta = 65$ deg. Variation of Δp over $55 \leq \theta \leq 70$ is within 6% of the minimum value. The required condenser length also exhibited a rather flat minimum, which occurred over θ values of 35 to 45 deg. At $\theta = 60$ deg, the required length was 6% over its minimum. Since vapor pressure loss is a premium for OTEC applications, a channel inclination from 55 to 70 deg is clearly preferred for achieving optimum condenser performance.

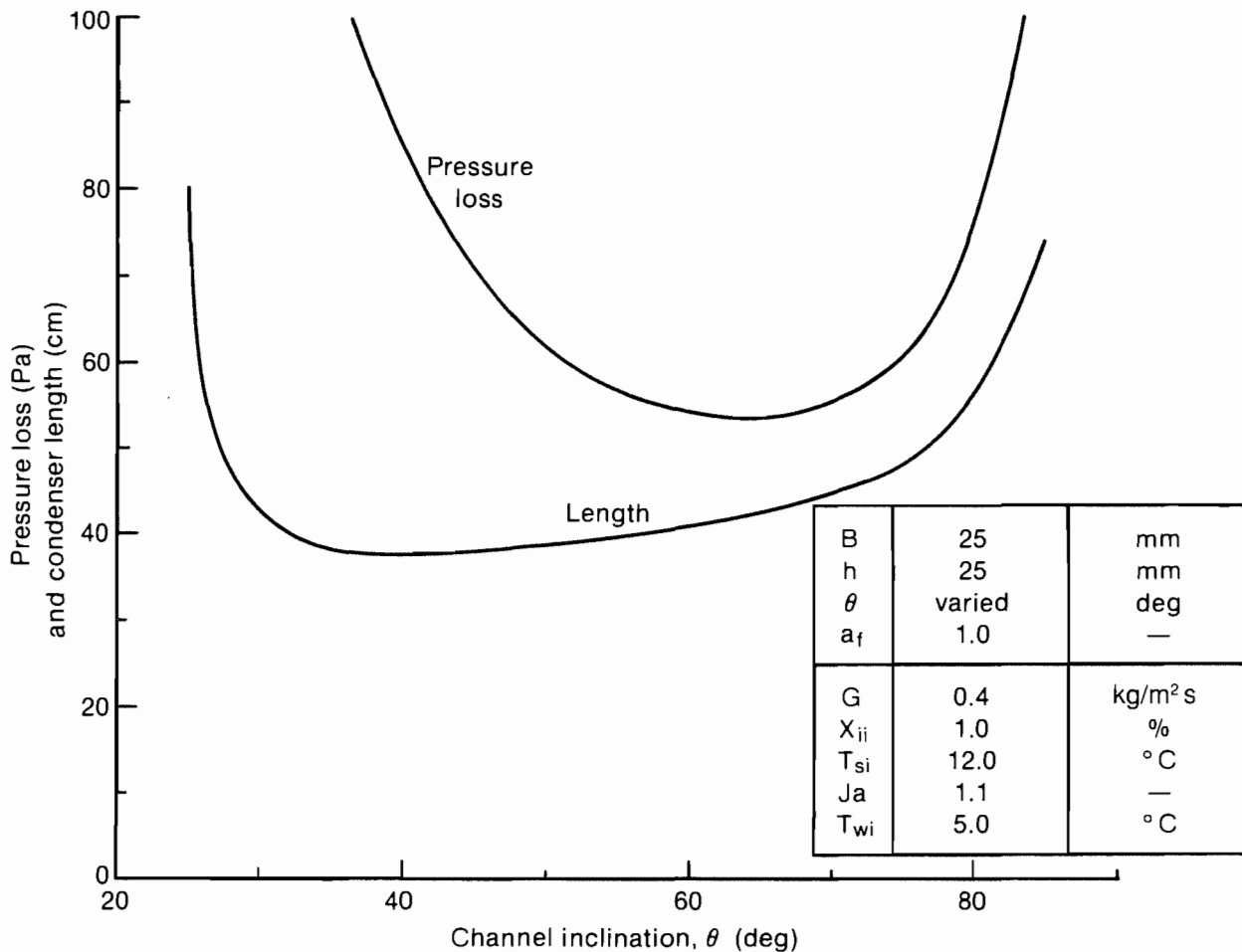


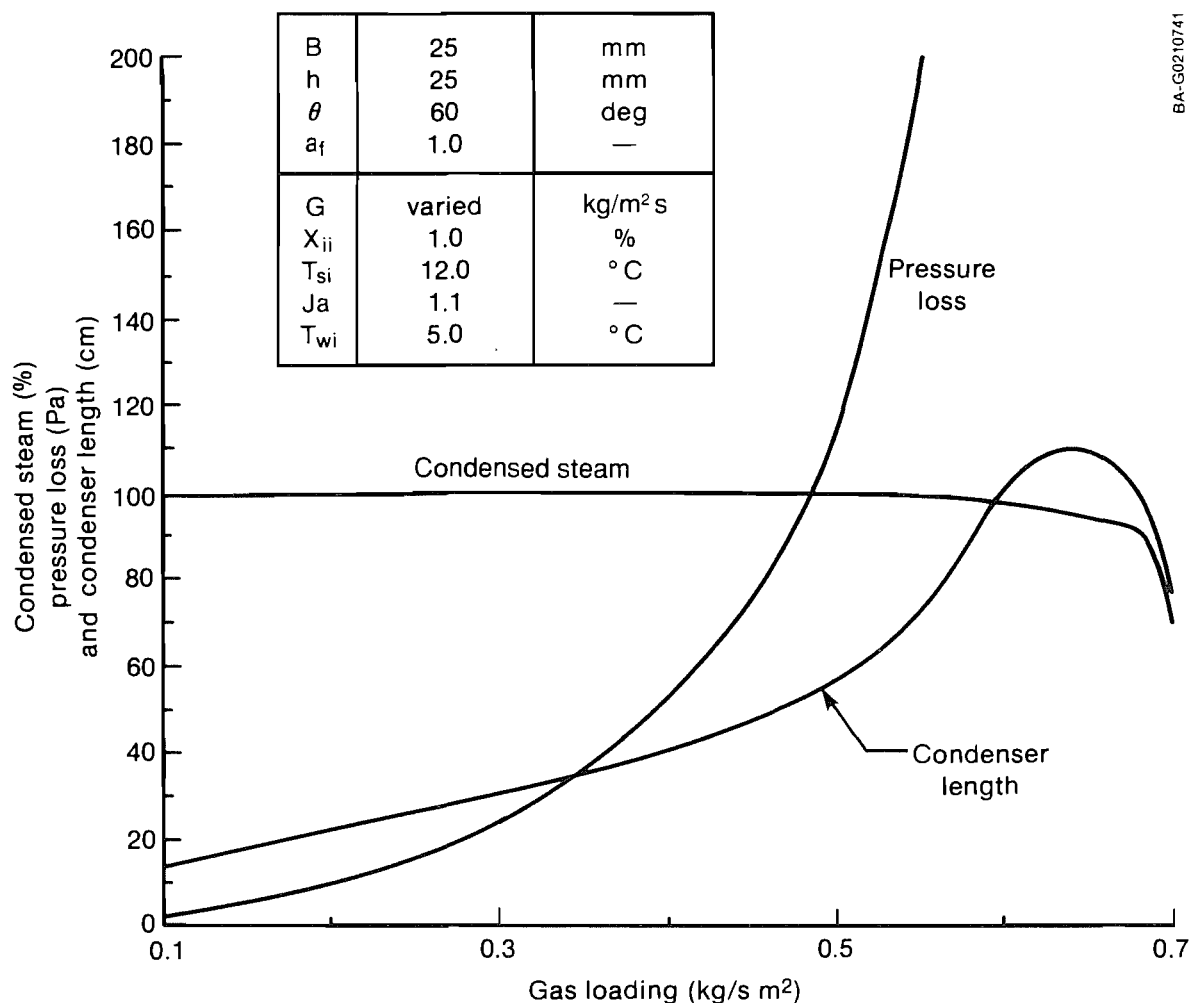
Figure 5-20. Influence of channel inclination on countercurrent condenser performance

5.2.3 Influence of Flow Parameters

In the following studies, the packing geometry was fixed at base $B = 25$ mm, height $h = 25$ mm, $\theta = 60$ deg, and $a_f = 1.0$.

5.2.3.1 Gas Loading

Figure 5-21 shows the influence of increasing gas loading G . The pressure loss increases monotonically with G , while the condensed steam remains close to 100% for G up to 0.55 kg/m² s and then begins to drop off sharply because of increasing pressure losses. The required condenser length increases gradually for G up to 0.5 kg/m² s and then shows a somewhat steeper increase for G up to 0.65 kg/m² s, reaching a maximum of slightly over 1 m here. At higher gas loadings, because of large condenser pressure losses, the required length of the condenser begins to decrease. The results in this figure imply that gas loading perhaps should be limited to a maximum value of 0.65 kg/m² s in practical situations at OTEC conditions.



BA-G0210741

Figure 5-21. Influence of gas loading on countercurrent condenser performance

5.2.3.2 Inert Gas Content

Increased levels of inert gas in the incoming steam resulted in an increase in the required condenser length and also a corresponding increase in the vapor pressure loss. We investigated inert gas content at three levels: $X_{ii} = 1\%$, 3% , and 5% . The following section describes the combined effects of Jakob number and X_{ii} .

5.2.3.3 Jakob number

The Jakob number was parametrically varied via water flow rate at a fixed T_{si} and T_{wi} of 12°C and 5°C , respectively. Figure 5-22 shows the influence of varied Jakob number. Since over 98% of the steam is condensed for $Ja > 1$ in countercurrent flow, the water effectiveness can be related to the Jakob number simply as $\epsilon_w = 0.98/Ja$. Shown in this figure are variations of pressure loss and a required condenser length for three levels of X_{ii} : 1% , 3% , and 5% . Increases in Jakob number cause decreases in both pressure loss and

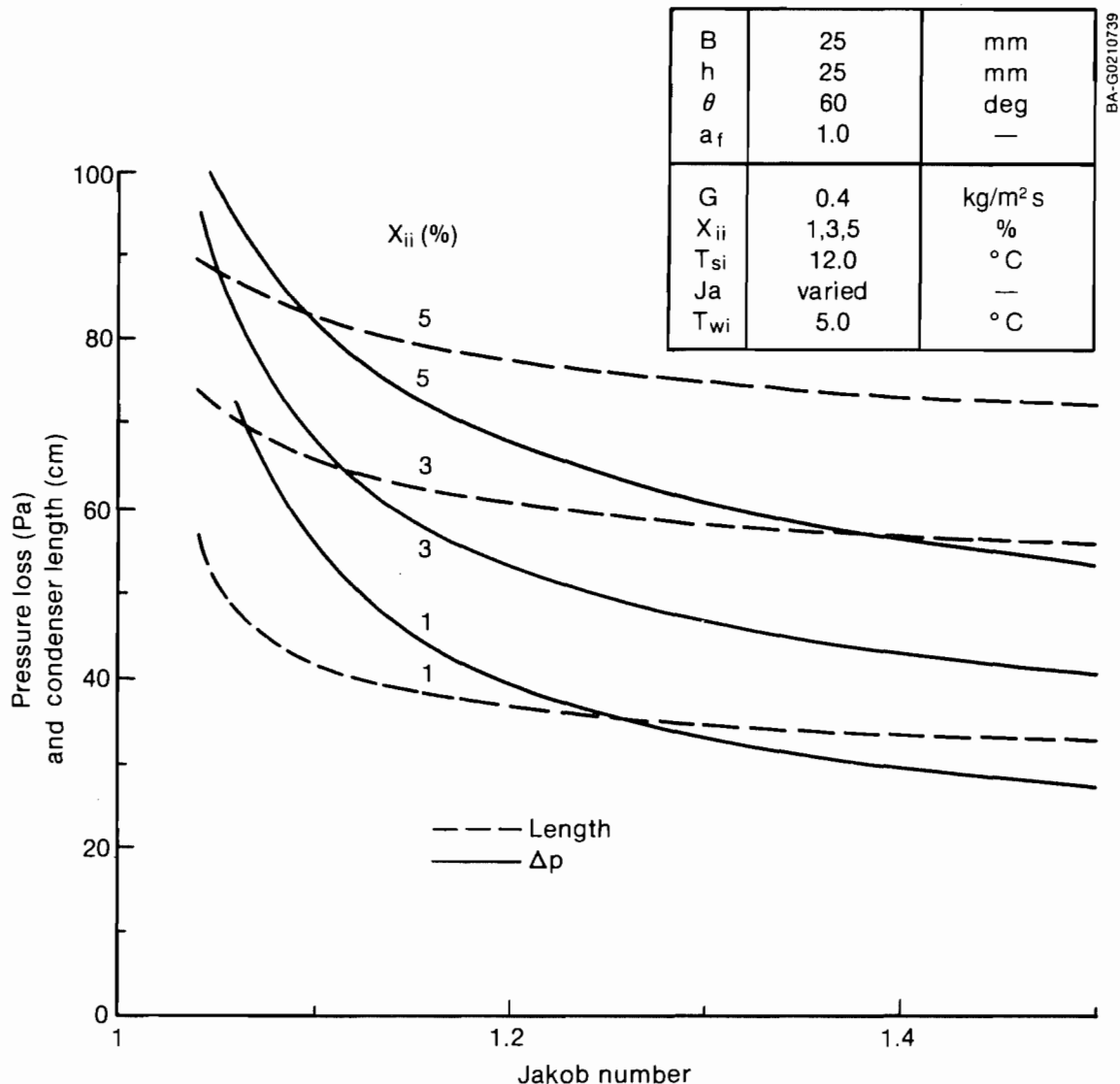


Figure 5-22. Influence of Jakob number varied via water flow on countercurrent condenser performance

condenser length. Higher levels of X_{ii} increase both of these quantities. Operating at conditions equivalent to a Jakob number of 1.2 is common in many mass transfer processes in the chemical industry. Operation at higher Ja results in inefficient use of cooling water. Despite somewhat increased requirements for vapor pressure loss and condenser length, the OTEC condenser is expected to operate over a Jakob number range of 1.05 to 1.15 to efficiently use cold water.

The countercurrent parametric studies presented provide results for preliminary design choices. Critical choices in parameters such as channel

inclination, gas loading, and Jakob number are required to assure optimum condenser subsystem performance. Choices on other parameters may be less critical. Detailed systems analyses should be pursued to arrive at design trade-offs on all the condenser choices as well as other components for a prototype typical OTEC system.

6.0 CONCLUSIONS AND RECOMMENDATIONS

6.1 Conclusions

This work focuses on establishing the feasibility of direct-contact condensers for OC-OTEC applications. We examined a large number of potential packing materials and identified structured packing as the most suitable for the cocurrent and countercurrent stages of the condenser. We also achieved significant progress in the areas of model development, experimental investigation, model validation, and parametric studies. Under each category, the following paragraphs summarize the approach taken and describe the major achievements. These conclusions are based on fresh water tests with injection of noncondensable gases into steam. We anticipate extending these results to seawater in the near future.

Model Development

- We present a model for one-dimensional flow of steam condensing on water in the presence of a noncondensable gas in steam and water for cocurrent and countercurrent flow.
- For flow through structured packings, the model uses established correlations for gas- and liquid-side heat and mass transfer. For liquid flow, we consider turbulent water film flow over an inclined plane.
- For gas flow through one to two layers of packings, we used the friction correlation developed by Bravo, Rocha, and Fair (1986) in a Darcy-Weisbach formulation (see Table 2-2).
- Because we evaluate heat, mass, and momentum transfers independently in the model, we show the vapor process path deviating from the saturation line during condensation and entering a superheated region.
- We model the evolution of inert gas from the coolant during condensation as a diffusional process.
- We implemented numerical schemes for integrating the process differential equations.
- For countercurrent flow, we implemented efficient iteration schemes to match calculated water conditions with specified inlet water conditions.
- We coded the cocurrent and countercurrent models in Turbo-Pascal™ language so the program can be used on a standard IBM personal computer or other compatible computer.

Experimental Investigations

- We tested four different cocurrent condenser geometries and presented the results in tables over a wide range of cocurrent condenser operating conditions that bracket expected conditions for OTEC applications as can be simulated with the facility.
- For countercurrent condensers, we tested four different structured packings and presented their results. The experimental data allowed us to establish flooding limits for the tested packing with the lowest equivalent diameter.

- We tabulated extensive test results for evaluating experimental repeatability, consistency, and uncertainties. We estimated uncertainties for the measured parameters.
- For countercurrent condenser geometries not using structured packings, we provide entire sets of observed measurements in Appendix E. We provide comparisons of tests with and without structured packings to illustrate the advantages of using structured packings.

Model Validation

- We provide extensive sets of comparisons between model predictions and experimental data for condensers using structured packings.
- The model follows a majority of the significant trends observed in the experiments. Some discrepancies exist in pressure loss comparisons, as discussed below.
- The model predictions yielded condensed steam with an average deviation of less than 2.8% and standard deviation of less than 2.4%, as compared with the laboratory data for the tested structured packings.
- The predictions for gas pressure loss yielded an average deviation of less than 4 Pa with a standard deviation of less than 6 Pa; exceptions to these are test data with 3X packing in countercurrent flow where the standard deviation is 12.3 Pa and test data for 19060 packing in cocurrent flow with an average deviation of -17 Pa and a standard deviation of 10.4 Pa. These discrepancies are small compared with the gas pressure losses in the condenser. We believe the discrepancies were caused by the pressure measurement lines becoming clogged with water during some of the experiments.
- With the noted exceptions, the model provides performance estimates of condensers well within an uncertainty acceptable for engineering design of direct-contact condensers. For a two-stage condenser with a $\pm 2\%$ uncertainty in condensed steam for either stage at a design condition of 80% and 98% condensed steam in cocurrent and countercurrent stages, respectively, the resulting uncertainty in the overall condensed steam is less than $\pm 0.5\%$. A designer may opt to use a third stage to reduce this uncertainty even more at the expense of 2% additional water usage, if desired.

The shortcomings of the present model lie primarily in choosing a formulation for a local gas friction coefficient. Similar drawbacks in the experimental data lie in the large uncertainty and possible errors in Δp measurements.

Parametric Studies

- For cocurrent and countercurrent condensers, we present detailed sets of parametric studies with geometrical and flow parameters. These results provide guidance in selecting suitable packing and operating conditions for a particular application.
- The pressure loss in the condenser can be maintained low by choosing a channel inclination θ in a range of $55 \leq \theta \leq 70$ deg. Increasing packing size allows higher admissible gas loadings but requires longer lengths to condense a given amount. The maximum amount condensed is insensitive to the

base dimension in the range of $45 < B < 90$ mm for cocurrent flow (with height = 0.35 times base) and in the range of $30 < B < 60$ mm for counter-current flow (with height = base).

- For optimum use of condenser length, the maximum allowable inlet gas loading for cocurrent flow is limited to less than $0.6 \text{ kg/m}^2 \text{ s}$ for cocurrent flow and perhaps to $0.5 \text{ kg/m}^2 \text{ s}$ for countercurrent flow. These limits arise because of increasing Δp with increased available condenser length.

For the proposed seawater tests of direct-contact condensers at the heat and mass transfer scoping test apparatus, the major uncertainty in the condenser performance resides in the rate at which the dissolved gases may come out of solution within the condenser. Phenomena other than that modeled here, such as nucleation, may come into play. For three assumptions on the rate of deaeration (which are designed to bracket performance in seawater), Table 6-1 summarizes the predictions of condenser performance via condensed steam and pressure losses. We expect to see about 1% difference in the condensed steam; the pressure loss difference under the worst condition of immediate gas release from the coolant is a 16-Pa increase. Thus, the expected performance differences for seawater use are minimal and within the predictive capability of the model. However, confirming this finding will have to await the completion of the proposed tests.

6.2 Recommendations

Based on the present study, the following future efforts are recommended for developing direct-contact condensers for OC-OTEC.

- The two separate codes for the cocurrent and countercurrent stages should be combined to form an integral condenser code. This integration will allow identification of appropriate geometry and flow conditions for both stages in an optimal manner.
- The fresh water properties used in the model should be supplemented with seawater properties such as viscosity, density, and most importantly, boiling point elevation or vapor pressure reduction. The phenomena of independent absorption and desorption of oxygen and nitrogen in cold seawater may require treating noncondensable gases as two individual species.
- The model could be improved further by (1) using a formulation for turbulent film flow over inclined planes that might be expressed in a dimensionless form for use with liquids other than water and (2) a phenomenological model of condensation occurring in free-fall regions above and below the packing.
- Entrance and exit losses should be treated in the model as they occur instead of being lumped together as a local gas friction coefficient. Additionally, adequate care must be exercised in future tests to prevent the Δp measurement lines from becoming waterlogged to reduce the overall Δp measurement uncertainty.
- Integrated staged-condenser designs identified for maximum performance in seawater should be fabricated and tested within the scope of the future experimental plan. Cooling water distribution manifold designs that result in minimum water and steam pressure losses must be pursued. Uniform gas and liquid distributions for cocurrent condensers require further study.

Table 6-1. Comparison of the Influence of Rate Deaeration on a Two-Stage Condenser[†]

	Inert Gas In Steam (%)	In Water (ppm)	Cocurrent Condenser Condensed Steam (%)	Pressure Loss (Pa)	Countercurrent [§] Condenser Condensed Steam (%)	Pressure Loss (Pa)	Overall Condenser Condensed Steam (%)	Pressure Loss (Pa)
Fresh Water, no gas liberation	0.35	0	73.83	45.45	98.13	43.8	99.5	89.3
Freshwater, [¶] gradual gas liberation	0.35	17	73.35	46.20	94.79	54.9	98.6	101.1
Fresh water, immediate gas liberation	0.70	0	72.03	50.59	94.79	54.9	98.5	105.5

[†]Assumed inlet conditions are: $T_{si} = 12.5^{\circ}\text{C}$; $T_{wi} = 5.0^{\circ}\text{C}$;

Gas Loading = $0.5 \text{ kg/m}^2 \text{ s}$ (for cocurrent stage);
 $= 0.4 \text{ kg/m}^2 \text{ s}$ (for countercurrent stage).

Jakob number = 0.8 for cocurrent and 1.2 for countercurrent stage.

[§]Immediate gas release in a countercurrent stage does not affect its performance.

[¶]Assumed gas diffusivity in water is ten times the normal level.

Many potential applications exist for direct-contact condensers. The presented design method may be modified to analyze condensers for other applications. Mass transfer processes occurring in the many gas-liquid contactors can again be modeled using the present approach with suitable modifications.

This study evaluates the suitability of structured packings for use in OTEC direct-contact condensers. At OTEC conditions, these packings can accept gas loadings in a range of 0.4 to 0.55 kg/m² s, translating to a heat rejection capacity of 1 to 2 MW_t/m³ of packing volume. Typical volumetric heat-transfer coefficient ranges from 150 to 300 kW/m³ K. For any power rating, analytical results indicate that the turbine exhaust steam can be condensed by 1-m-high condensers at water-flow rates of less than 10% over a thermodynamically required minimum with gas venting requirements of not over 10% of a thermodynamically required minimum. These results significantly reduce the cold-water flow rate and pumping power requirement and increase the cost-effectiveness of OC-OTEC as a renewable energy resource.

7.0 REFERENCES

- Ackermann, G., 1937, "Wärmeübergang und molekulare Stoffübertragung im gleichen Feld bei grossen Temperatur- und Partialdruck-differenzen," Forschungsheft, No. 382, Berlin: VDI-Verlag.
- Bharathan, D., D. A. Olson, H. J. Green, and D. H. Johnson, 1982, Measured Performance of Direct-Contact Jet Condensers, SERI/TP-252-1437, Golden, CO: Solar Energy Research Institute.
- Bharathan, D., and Penney, T. 1984, "Flash Evaporation from Falling Turbulent Jets," Journal of Heat Transfer, Vol. 106, No. 2, pp. 407-416.
- Bras, G. H., 1953 (Apr.), "Design of Cooler Condensers for Vapor-Gas Mixtures-Part 1," Chemical Engineering, pp. 223-226.
- Bravo, J. L., J. A. Rocha, and J. R. Fair, 1985 (Jan.), "Mass Transfer in Gauze Packings," Hydrocarbon Processing, pp. 91-95.
- Bravo, J. L., J. A. Rocha, and J. R. Fair, 1986 (Mar.), "Pressure Drop in Structures Packing," Hydrocarbon Processing, pp. 45-59.
- Butterworth, D., and G. F. Hewitt, eds., 1978, Two-Phase Flow and Heat Transfer, Harwell Services, Oxford, England: Oxford University Press.
- Chilton, T. H., and A. P. Colburn, 1934 (Nov.), "Mass Transfer (Absorption) Coefficients; Predictions from Data on Heat Transfer and Fluid Friction," Industrial and Engineering Chemistry, Vol. 26, pp. 1183-1187.
- Colburn, A. P., and O. A. Hougen, 1934 (Nov.), "Design of Cooler Condensers for Mixtures of Vapors with Noncondensing Gases," Industrial and Engineering Chemistry, Vol. 26, pp. 1178-1182.
- Dukler, A. E., 1960, "Fluid Mechanics and Heat Transfer in Vertical Falling-Film Systems," Chemical Engineering Progress Symposium series, Heat Transfer, Vol. 56, No. 30, pp. 6-15.
- Fair, J. R., 1961 (Aug.), "Design of Direct-Contact Gas Coolers," Petroleum and Chemical Engineer, Vol. 2, pp. 203-210.
- Fair, J. R., 1972 (June), "Designing Direct-Contact Coolers/Condensers," Chemical Engineering, Vol. 2, pp. 91-100. (See also, "Process Heat Transfer by Direct Fluid Phase Contact," Chemical Engineering Progress Symposium series no. 118, Vol. 68, pp 1-11, 1972.)
- Forsythe, G. E., M. A. Malcolm, and C. B. Moler, 1977, Computer Methods for Mathematical Computations, Englewood Cliffs, NJ: Prentice-Hall, Inc.
- Hasson, D., D. Luss, and R. Peck, 1964, "Theoretical Analysis of Vapor Condensation on Laminar Liquid Jets," International Journal of Heat and Mass Transfer, Vol. 7, pp. 969-981.
- Higbie, R., 1935, "The Rate of Absorption of a Pure Gas into a Still Liquid during Short Periods of Exposure," AIChE Trans., Preprint.

- John, J. E. A., and W. L. Haberman, 1980, Introduction to Fluid Mechanics, Englewood Cliffs, NJ: Prentice-Hall, Inc.
- Johnson, C. M., G. N. Vanderplaats, and P. J. Marto, 1980 (July), "Marine Condenser Design Using Numerical Optimization," Journal of Mechanical Design, Vol. 102, pp. 469-475.
- Kline, S. J., and F. A. McClintock, 1953.(Jan.), "Describing Uncertainties in Single-Sample Experiments," Mechanical Engineering, Vol. 75, No. 1, pp. 3-8.
- Kreith, F., and R. F. Boehm, eds., 1988, Direct Contact Heat Transfer, New York: Hemisphere Publishing Company.
- Kreith, F., and M. Bohn, 1986, Principles of Heat Transfer, 4th ed., New York: Harper and Row.
- Kulic, E., E. Rhodes, and G. Sullivan, 1975 (Jun.), "Heat Transfer Rate Predictions in Condensation on Droplets from Air-Steam Mixtures," The Canadian Journal of Chemical Engineering, Vol. 53, pp. 252-258.
- Kutateladze, S. S., 1959, Heat Transfer in Condensation and Boiling, Chapter 7, 2nd ed., AEC-TR-3370, Moscow-Leningrad, English translation by U.S. Atomic Energy Commission.
- Maa, J. R., 1967, "Evaporation Coefficients of Liquids," Industrial Engineering Chemistry Fundamentals, Vol. 6, No. 4, pp. 504-518.
- Meier, W., 1979, "Sulzer Columns for Rectification and Absorption," Sulzer Technical Review, Vol. 2, pp. 49-61.
- Metre, H., Jr., 1973, "Condensation Heat Transfer," Advances in Heat Transfer, Vol. 9, T. F. Irvine, Jr., and J. P. Hartnelt, eds., New York: Academic Press, pp. 181-272.
- Mills, A. F., and R. A. Seban, 1967, "The Condensation Coefficient for Water," International Journal of Heat and Mass Transfer, Vol. 10, pp. 1815-1827.
- Panchal, C. B., and Bell, K. J., 1984, Theoretical Analysis of Condensation in the Presence of Noncondensable Gases as Applied to Open Cycle OTEC Condensers, ASME paper 84-WA/Sol-27, New York: American Society of Mechanical Engineers.
- Parsons, B. K., D. Bharathan, and J. A. Althof, 1985, Thermodynamic Systems Analysis of Open-Cycle Ocean Thermal Energy Conversion (OTEC), SERI/TR-252-2234, Golden, CO: Solar Energy Research Institute.
- Sherwood, T. K., R. L. Pigford, and C. R. Wilke, 1975, Mass Transfer, New York: McGraw-Hill.
- Sideman, S., and D. Moalern-Maroon, 1982, "Direct-Contact Condensation," Advances in Heat Transfer, Vol. 15, T. F. Irvine and J. P. Hartnett, eds., New York: Academic Press, pp. 227-281.
- Wallis, G. B., 1969, One-dimensional Two-phase Flow, New York: McGraw Hill.

- Wassel, A. T., D. C. Bugby, A. F. Mills, and J. L. Farr, Jr., Science Applications, Inc., 1982 (Feb.), Design Methodology for Direct-Contact Falling Film Evaporators and Condensers for Open-Cycle Ocean Thermal Energy Conversion, SERI/STR-251-2256, Golden, CO: Solar Energy Research Institute.
- Webb, R. L., and A. S. Wanniarachchi, 1980, "The Effects of Noncondensable Gases in Water Chiller Condensers--Literature Survey and Theoretical Predictions," ASHRAE Transactions, Vol. 80, pp. 142-159.

NOMENCLATURE FOR APPENDICES[†]

D	tube diameter (m)
d	probe diameter (m)
E	enthalpy rate (kW)
Gr	Grashof number
h	enthalpy (kJ/kg)
K	pressure loss coefficient
K_c	convective mass-transfer coefficient (m/s)
K_{in}	contribution of kinetic energy (App. H)
k	thermal conductivity (W/m K)
ℓ	probe length (m)
ℓ	packing stack length (m)
M_{out}	vapor momentum
Q	volumetric flow rate (m ³ /s)
R	RTD probe resistance (Ω)
r	recovery factor
Sol	solubility (mole air/mole water)
V	condenser vent fraction
V	velocity (m/s)

Greek

β	coefficient of thermal expansion (1/K)
ϵ	condenser effectiveness
ϵ'	effective emissivity
τ	shear stress (Pa)
σ	surface tension (N/m)
σ	Stefan-Boltzmann constant

Subscripts and Superscripts

adi	adiabatic
atm	atmospheric
D	tube diameter
d	probe diameter
e	exhaust

[†]See Nomenclature on page xiii for additional symbols.

NOMENCLATURE FOR APPENDICES (Concluded)

in	inlet
id	ideal (equilibrium conditions)
nc	natural convection
p	probe, pressure
r	radiative
tip	probe tip

APPENDIX A EXPERIMENTAL FACILITY AND INSTRUMENTATION

A.1 Introduction

The experiments described here were performed in SERI's Low Temperature Heat- and Mass-Transfer Laboratory in Golden, Colo. The laboratory, recently moved to a permanent location, allows us to investigate and improve methods of transferring heat and mass under the small driving potentials that often exist when the sun is the energy source.

Our primary thrust was to examine direct-contact evaporators and condensers for OC-OTEC. The driving force for OTEC systems is a near 20°C temperature difference between warm surface tropical seawater and cold seawater pumped from depths of approximately 1000 m. Direct-contact devices are attractive since the liquid and vapor are not separated by a solid barrier. A solid barrier, such as those used in conventional surface condensers, adds to the thermal resistance that reduces heat transfer and overall performance.

Increased transfer rates can lower component and overall system costs. For a fixed thermal load, lower resistance to heat-transfer results in smaller and less costly heat exchangers and containment vessels. Increased heat exchanger effectiveness also reduces the required liquid flow rate. The cost of the piping and pumps is proportional to the flow rate; therefore, seawater requirements affect the cost of OTEC systems because the seawater system cost is a large portion of the total cost. In addition, reducing the seawater flow lowers the power requirements of the pumps and condenser exhaust system. Because this power is subtracted from the gross generator output, lowering the seawater flow requirement increases the net available power.

The thrust of our laboratory research is to understand the direct-contact heat-exchange mechanism and to simultaneously increase the transfer rates and decrease size and water flow requirements. These objectives are reflected in the research facility's design.

A.2 Capabilities of the Facility

A.2.1 General

A heat rate of up to 300 kW is transferred to the closed warm-water loop through a shell-and-tube heat exchanger. Another closed loop fired by natural gas boilers provides heat to the exchanger. The cold-water loop removes heat by routing the flow through vapor compression chillers. The warm- and cold-water loops exchange heat and mass in an evacuated test cell. Warm water flows through an evaporator in one end of the chamber, and cold water flows through a condenser at the other end, as shown in Figure A-1. Heat and mass are exchanged by evaporation of the warm water and direct-contact condensation of the vapor on the cold water.

The pressure in the O-ring-sealed vacuum chamber is maintained by a three-stage compressor train consisting of a booster, a rotary vane pump, and a liquid-ring vacuum pump. Inert gases, which affect heat- and mass-transfer rates, can be added to the steam through flowmeters to examine the effect vacuum leaks and desorbed gases that may evolve from using seawater have on

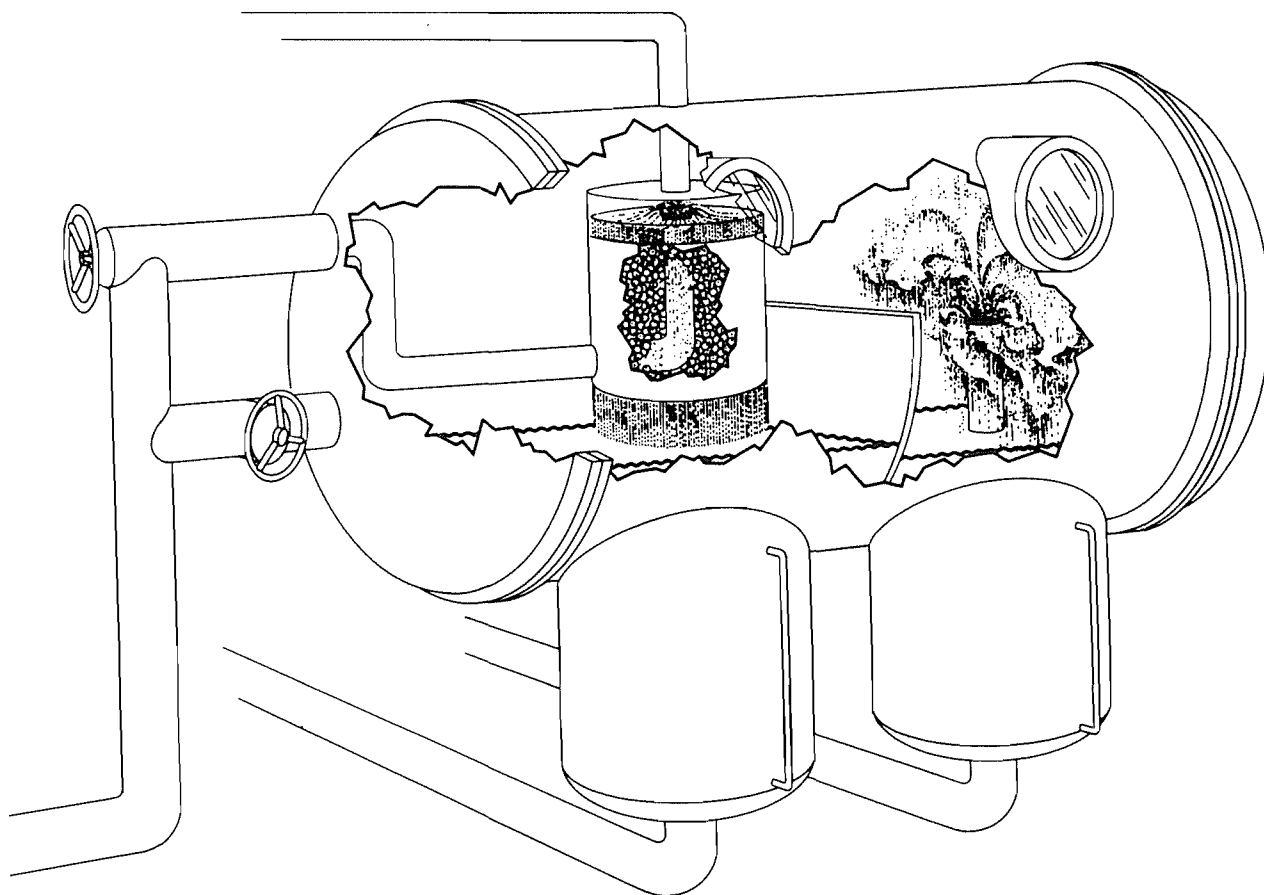


Figure A-1. Heat- and mass-transfer laboratory test chamber: condenser, left; evaporator, right

condenser performance. We can measure the concentration of these noncondensable gases in the vapor at the vacuum exhaust or other points in the test chamber with a gas mass spectrometer. A solenoid butterfly valve in the line between the vacuum tank and the compressor train allows us to vary the venting rate and to seal the tank under vacuum for leak tests and inactive periods. Table A-1 summarizes the facility's capabilities.

A.2.2 Hardware

This section documents the hardware specifications at the time of the reported tests. We modified the laboratory slightly when we moved it to its permanent location, particularly the piping lengths, but replication tests indicate the changes had no measurable effect on experimental results. Table A-2 lists the model numbers and other hardware specifications. Figures A-2 and A-3 show the laboratory in its former location.

Table A-1. SERI Low-Temperature Heat- and Mass-Transfer Laboratory Capabilities

Parameters	Units
Heat rate	0-300 kW
Water temperature	3-30°C
Water flow	0-50 kg/s
Threshold vacuum pressure	700 Pa
Vent capacity	0-0.57 m ³ /s
Inert gas injection	0-200 L/min
Chamber leak rate	0.5 mg/s

A.2.2.1 Flow Loops

The water flow loops are constructed of carbon steel Schedule-40 pipe. Most of the pipes on the high pressure side of the pumps have a nominal pipe diameter of 6 in. The pipes that drain the test section on the suction side are approximately 8 in. in diameter. Pipes to the chillers and the separate boiler loop are 4-in. lines. Near the end of the tests on the countercurrent condenser geometries, we replaced a portion of the 6-in. pipe with a 3-in. pipe downstream of the pumps. This replacement accommodates 3-in. turbine flowmeters, which increased the accuracy of our measurements at lower flow rates over the previous 6-in. flowmeter (see Section A-4). All of the pipe connections, such as to valves and bends, are sealed with O-rings to minimize air leakage into the system. The capacity of the cold-water loop, approximately 4 m³, is large because of the long piping run to the outside chillers. The capacity of the warm-water loop is near 1 m³.

Included in the lines are static mixers, flow straighteners, turbine flowmeters, and numerous valves to control flow rate and water routing. Figure A-4 shows the layout. The water circulation pumps are located in a pit 3 m below the laboratory floor to ensure adequate suction head. The bearings of the centrifugal pumps have double mechanical seals and a stuffing box that is flooded with water to minimize air leakage.

Table A-2. Heat- and Mass-Transfer Laboratory Hardware Model Numbers and Specifications

Hardware	Manufacturer	Model	Remarks
Cold water pump	Cornell	4RFB-6	40-hp electric motor
Warm water pump	Ingersol-Rand	6x5x10 HC	20-hp electric motor
Chiller	McQuay	ALR-110AD	Vapor compression
Boiler	Hydrotherm	MR-1800 B	Natural gas
WW heat exchanger	Young	HF-802-ER-IP	Shell and tube
Lobed blower	Kinney	MB 2000	10-hp electric motor
Rotary compressor	Kinney	KT 500	30-hp electric motor
Liquid-ring pump	Kinney	KLRC-75	3-hp electric motor

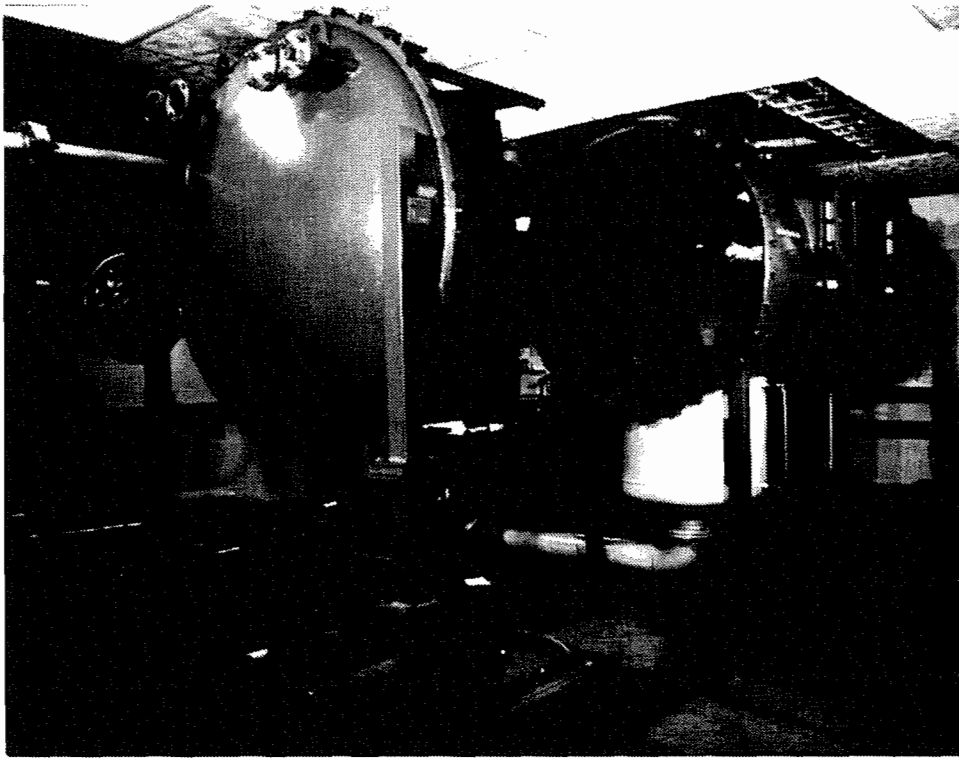


Figure A-2. Vacuum test chamber with end caps rolled back

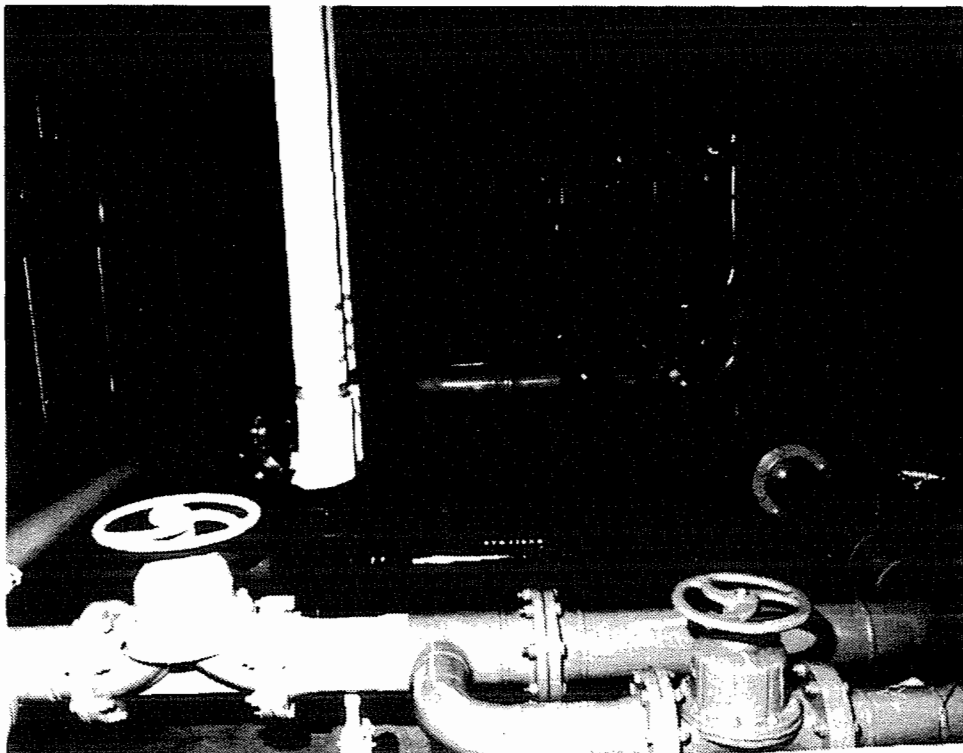


Figure A-3. Water piping and an end view of the test chamber

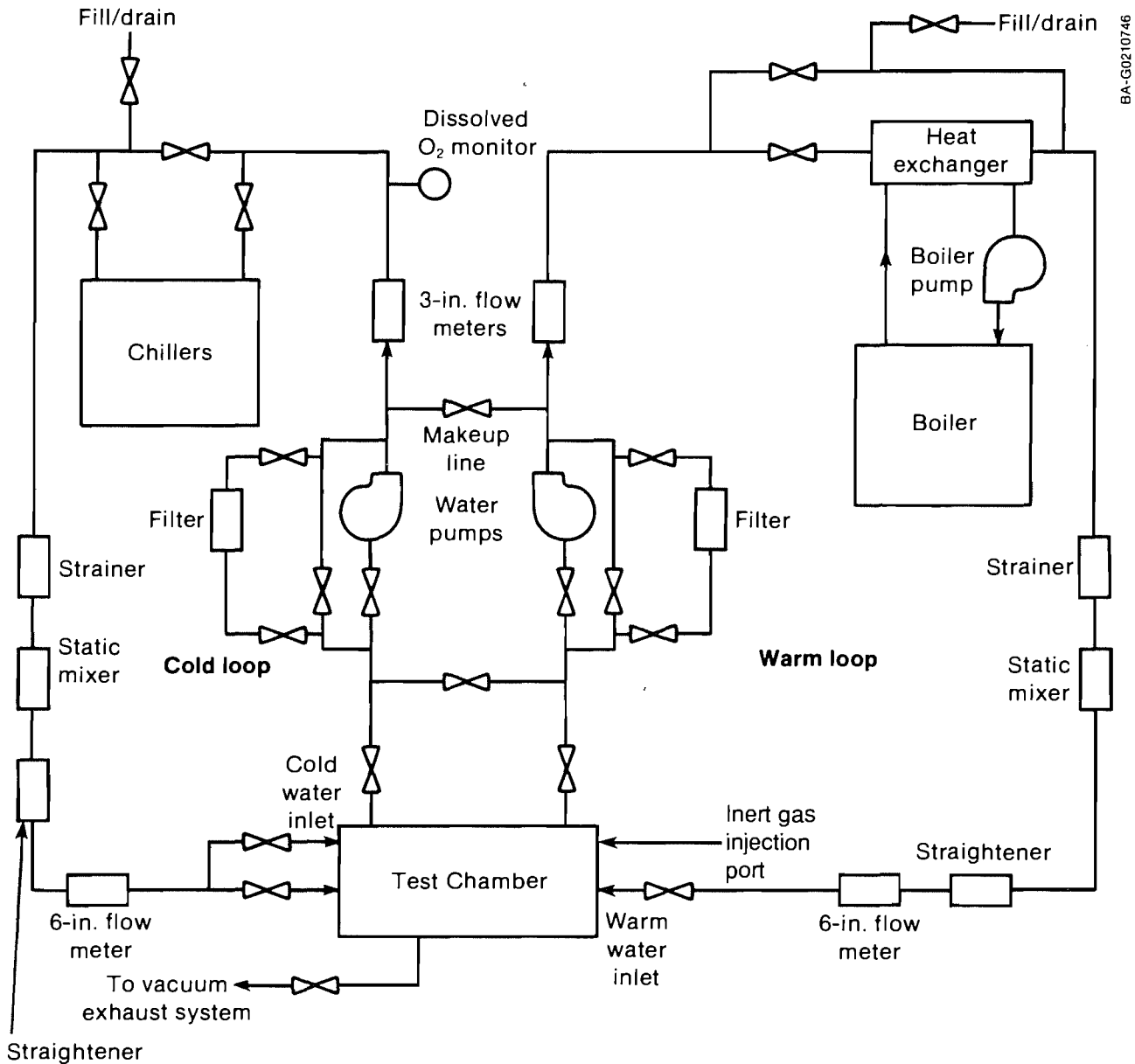


Figure A-4. Schematic of laboratory piping

A.2.2.2 Test Chamber

The test cell is a carbon steel horizontal cylinder 1.8 m long and 1.5 m in diameter with two clamp-on hemispherical end caps. The end caps are mounted on trolleys that can be rolled away from the cylinder. The evaporator and condenser modules with their water inlet manifolds and instrumentation are mounted directly on the end caps for easy fabrication and removal of the test articles. Two reservoirs under the heat exchanger sections of the test cell allow us to collect the warm and cold discharge waters separately. The test cell is equipped with four glass ports, two on top for lighting and two on one side for viewing and photographing.

Two cold-water inlet pipes enter the test chamber, one on the lower part of the end cap and the other on the upper part. The warm-water inlet is on the upper part of the end cap. In addition to the water inlets and drains, six 2.5-in. pipes through the end caps are used for instrumentation wiring.

Because the system operates under vacuum, the closed water loops contain low levels of dissolved oxygen. Low oxygen levels along with a standard practice of keeping the test chamber sealed under vacuum during inactive periods limits corrosion of the test cell interior.

A.2.2.3 Chiller and Boiler

The chiller is composed of two independent refrigerant loops with two compressors each. There is one 25-hp compressor and three 35-hp compressors resulting in a total capacity of around 135 tons of cooling. Various combinations of compressor units are used to achieve stepwise steady-state heat rates from around 75 to 300 kW.

A natural-gas-fired boiler supplies hot water to the heat exchanger in the experimental warm-water loop. The boiler has six independently controlled units with a capacity of around 56 kW each. A butterfly valve in the gas supply line for three of the units allows us to vary the heat rate continuously to match the cooling rate of the chillers and achieve steady-state conditions in the test chamber.

A.2.2.4 Inert Gas Injection System

Two Tylan mass flow controllers are used to control and measure the rate of inert gas added to the tank. Plumbing allows us to use either bottled gas or ambient air. Continuously variable gas flow rates from 0 to 200 standard litres per minute are possible. Coupled with the steam production of the evaporator, these flow rates allow us to test the full range of possible inert gas levels in the steam entering the condenser that are typical for OTEC systems.

A.2.2.5 Vacuum Exhaust System

The test cell is evacuated by a three-stage gas exhaust system consisting of a lobe blower, an oil-sealed rotary vane compressor, and a liquid-ring vacuum pump in series. The nominal venting capacity of the system is $0.57 \text{ m}^3/\text{s}$. A butterfly valve in the 8-in. line between the tank and the vacuum system induces a pressure drop that allows us to vary the actual venting rate at the tank continuously. A threshold pressure of 700 Pa can be attained in the test cell. At operating pressure the air leakage into the cell is less than 0.5 mg/s (0.4 atmospheric cubic centimeters per second). The three stages of the vacuum system are water cooled. The gas passes through a separator to remove sealing and lubrication oil entrained in the exhaust before being vented to ambient. A noise-suppression curtain suspended from the ceiling reduces the noise level in the laboratory.

A.3 Facility Changes after Relocation

Most of the experimental facility description previously presented applies to the existing hardware at the permanent location. This subsection describes the minor changes.

The laboratory is now in its own independent single-level building. The boiler that supplies heat to the evaporator loop is in an attached room. The chiller that supplies cold water to the condenser is now on a pad directly outside the laboratory building. Relocating this equipment resulted in shorter water supply lines. The current warm- and cold-water capacity has not been measured, but we estimate that both loops are currently under 1 m^3 . This change does not affect steady-state experimental results but does affect the response time to changes in operating conditions between runs.

The compressed air supply in the new facility has a smaller capacity than that provided in the earlier facility. Therefore, supply pressure fluctuates more than it did when air was taken from a large building system. This change, however, does not affect the experiments when inert gas enters the chamber because air is introduced through mass flow controllers (see Section A.4.2.2). These controllers deliver constant mass flow under the current pressure fluctuations.

The pump pit in the new building is 1 m deeper (4 m total) than the one at the previous location. This change results in less cavitation at the pump intake at low tank pressures and should not affect experimental results.

A.4 Instrumentation

This section presents an overview of the available instrumentation at the laboratory. We categorize the instrumentation in terms of the primary quantity to be measured, such as pressure, temperature, and flow. We discuss appropriate installation effects of probes and overall uncertainties in the primary measurements.

A.4.1 Temperature

Measuring the temperature is critical for OTEC processes because we are dealing with very low temperature differences; for example, about 3°C for the evaporator. To arrive at acceptable uncertainty in the measured evaporator or condenser effectiveness, the temperatures of the heat-exchange fluids must be measured within an uncertainty limit of a few millikelvins. The overall uncertainty of the temperature measuring system is affected by a variety of factors such as the choice of the probe, its calibration, installation, and environment.

We quickly narrowed our initial choice of a probe down to platinum-resistance temperature detectors (RTD) because of their stable resistance-temperature relationship, inherently low measurement uncertainty of approximately 1 mK (O'Brien and Miller 1983), ruggedness, and reasonable cost. After reviewing various commercially available RTD probes, we chose the Rosemount Model 78S-OIN-0900 as the primary temperature sensor for all applications in the laboratory. Table A-3 summarizes the specification of this probe as quoted by the manufacturers.

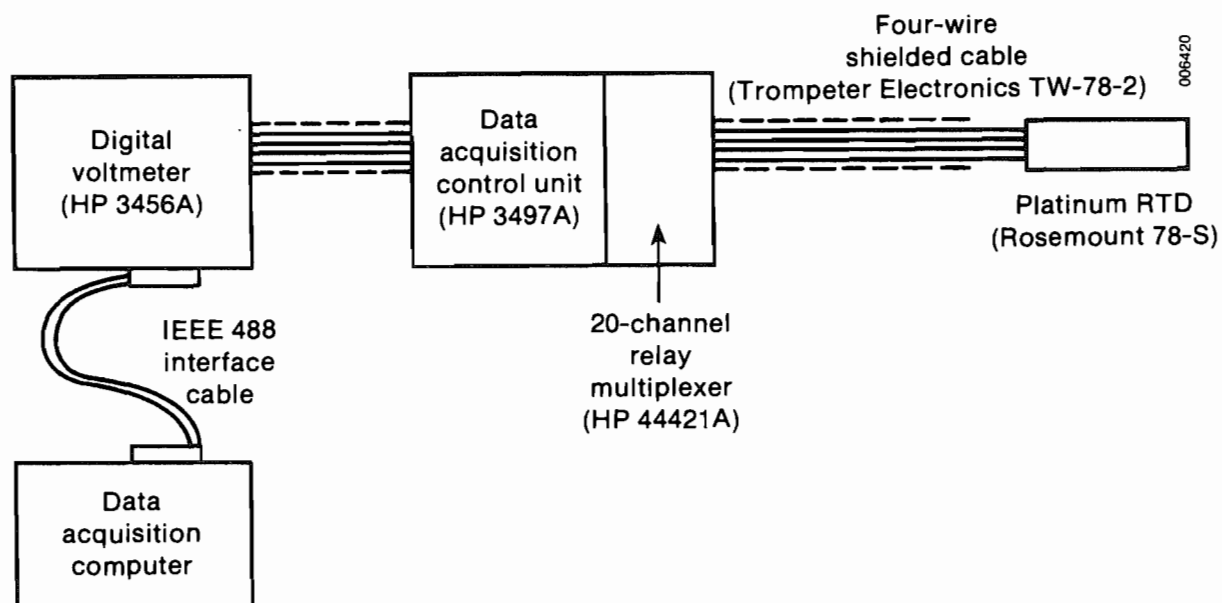
Each RTD is connected in a four-wire ohm configuration to a digital voltmeter (HP model 3456A) via a 20-channel relay multiplexer card housed in a data acquisition and control unit (HP model 3497A). A schematic of the temperature measurement system is shown in Figure A-5. We modified the relay multiplexer internally to allow four contact closures for the four-wire ohm measurement. Two relay cards allow us to monitor 20 RTD channels.

Table A-3. Platinum-Resistance--Temperature-Detector Specifications

Resistance at 0°C	100 Ω
Sensitivity	0.00385/°C
Lead wire configuration	4-wire
Range	-200° to 660°C
Repeatability over range	$\pm 0.05^\circ\text{C}$
Stability over range (1 year)	$\pm 0.25^\circ\text{C}$
Response time (water, 1 m/s)	5.0 s
Material of construction	316SS

Two specific channels monitor the system measurement uncertainty continuously during tests. One channel was connected to a 4-wire ohm short circuit to monitor the zero-offset of the voltmeter. We used a second channel to monitor the voltmeter calibration by connecting a precision 100- Ω resistor (Guideline Model 9330, calibrated 9/10/81, at 25°C, 10 mA test current, 100.0004 $\Omega \pm 0.0003 \Omega$, temperature-coefficient, -0.0001 Ω/K , stability, 0.001 Ω/yr) housed in an insulated isothermal enclosure kept at room temperature within the laboratory. We continually monitored these two channels during the course of the experiments to apply appropriate corrections to the indicated ohm readings of the RTD probes.

We performed a separate series of tests to estimate the uncertainty in the 4-wire ohm measurement of the system using the above two channels. For these tests, the operation of the voltmeter was set for shifted 4-wire ohm function

**Figure A-5. Temperature measurement system**

with Auto-Zero, with the measurement taken over 10 power-line cycles, typical of the conditions during the operation of the experiment. A current of 1 mA is applied to the unknown resistor during the measurement. The standard deviation in the 100- Ω resistance measurement over one month of tests was 0.000223 Ω with a maximum deviation of 0.003526 Ω . Thus, the uncertainty in the ohm measurement is $3\sigma = 0.000669 \Omega$. For 100- Ω platinum RTDs with a resistance-temperature coefficient of 0.385 Ω/K , the uncertainty in the temperature measurement is estimated to be 1.74 mK.

Before installing the apparatus, we calibrated the RTDs using controlled temperature water bath facilities available at the SERI calibration laboratory. The calibration bath temperature is reproducible within ± 5 mK in the calibration range of 0° to 40°C. The temperature was monitored using a high-purity, glass-enclosed platinum resistance RTD with its accuracy traceable to NBS standards. We measured the resistance of the calibrated probes within an uncertainty of ± 1 m Ω . A typical set of calibration data for a particular RTD is shown in Table A-4. The calibration data were then fitted to yield temperature as a function of the measured resistance as

$$T = a + bR + cR^2, \quad (A-1)$$

where T is the temperature in °C and R is the resistance in ohms. For each RTD, the predicted temperature differed from the calibration temperature to within ± 2 mK (see Table A-4).

Table A-4. Typical Calibration Data for RTD

Observation No.	Bath Temperature (°C)	RTD [‡] Probe Resistance R	Predicted Temperature (°C)	Residual [¶] (°C)
1	25.001	109.822	24.999	0.001
2	30.002	111.765	30.003	-0.001
3	35.001	113.702	34.999	0.001
4	40.001	115.638	40.001	-0.000
5	19.999	107.877	19.999	-0.000
6	15.012	105.933	15.010	0.002
7	10.001	103.979	10.003	-0.002
8	5.007	102.026	5.007	-0.000
9	0.005	100.067	0.004	0.001

[‡]Serial No 185225

[¶]Rounded to three-digit fractions.

The combined effect of calibration errors and measurement-system errors in the temperature measurement is estimated to be less than 7 mK.

The installation and environment of the RTD have the largest influence in determining the overall measurement uncertainty. Because these influences vary widely with the fluid media properties and the surroundings, we treat them separately for water and steam temperature measurements.

A.4.1.1 Water Temperature

In fluid applications, the probe faces a complex heat-transfer effect where the convective heat transfer between the fluid is balanced against radiative transfer between the probe, the fluid, and the surrounding and the simultaneous conductive heat transfer between the sensor and its support. Self heating because of the passage of measurement current introduces additional heat generated within the sensor that must be considered in estimating an "effective" sensor temperature. Benedict (1977) provides an excellent treatment of the problem with practical guidelines for evaluating various effects and avoiding installation errors.

It is inherently clear that for obtaining least error, the dominant mode of heat transfer must be convective transfer between the fluid and the probe. Worst-case errors result when the fluid velocity is low and the difference in the temperature of the probe and its environment is large.

Consider a typical water temperature measurement RTD installation as shown in Figure A-6. (Approximate dimensions of the probe, of diameter d , and the flow pipe are also included in this figure.) For a worst case, the water temperature is assumed to be at 5°C; the surrounding ambient air is at 25°C. The emissivity of the wall surrounding the probe is assumed to be unity. Assuming a low water flow rate of 5 kg/s, the flow Reynolds number around the probe is 1180. Assuming a nominal Prandtl number for water of 10, we can estimate the convective Nusselt number as

$$Nu = 0.193 Re_d^{0.618} Pr^{0.31} = 31 . \quad (A-2)$$

With the thermal conductivity for water $k = 0.57 \text{ W/m K}$, the convective heat-transfer coefficient h_c is

$$h_c = \frac{kNu}{d} = 2783 \text{ W/m}^2 \text{ K} . \quad (A-3)$$

Estimating an "effective" radiative heat-transfer coefficient requires estimating the pipe wall temperature.

To estimate pipe wall temperature, we estimate the natural convective air-side heat-transfer coefficient using (Kreith and Bohn 1986)

$$Nu_D = 0.53(Gr_D Pr)^{1/4} , \quad (A-4)$$

where

$$Gr_D = \frac{\rho^2 g \beta (T - T_\infty) D^3}{\mu^2} . \quad (A-5)$$

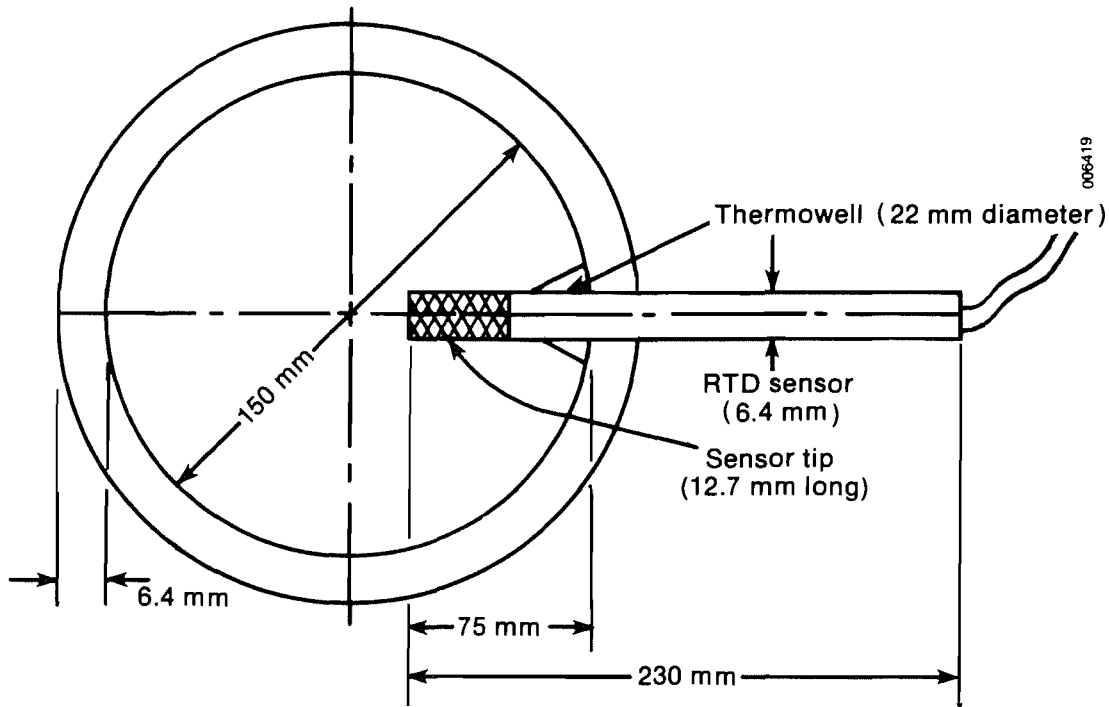


Figure A-6. Typical water temperature measurement RTD installation

With the pipe diameter $D = 165$ mm, at standard atmospheric conditions, and $T - T_{\infty} = 20$ K, we get

$$Gr_D = \frac{(1.225)^2 \cdot 9.81(3.5 \times 10^{-3}) \cdot 20(0.165)^3}{(1.789 \times 10^{-5})^2} = 1.45 \times 10^7. \quad (A-6)$$

Then, for air, using $Pr = 0.7$, we get $Nu_D = 29.9$.

For air, with $k = 26.24 \times 10^{-3}$ W/m K, the effective heat-transfer coefficient is

$$h_{nc} = 29.9 \times \frac{26.24 \times 10^{-3}}{0.165} = 4.76 \text{ W/m}^2 \text{ K}. \quad (A-7)$$

The approximate heat-transfer coefficient through the steel wall of thickness t is

$$h_s = \frac{k_s}{t} = \frac{51.9 \text{ W/m}^2 \text{ K}}{0.0064 \text{ m}} = 8.1 \text{ kW/m}^2 \text{ K}. \quad (A-8)$$

For water flow through the pipe, the effective convective heat-transfer coefficient is

$$Re_D = 27,870; Nu = 220; h_c = 1.67 \text{ kW/m}^2 \text{ K}. \quad (A-9)$$

With these assumptions, we estimate an inner wall temperature of 5.07°C .

The radiative heat-transfer coefficient between the probe and its environment is approximated as

$$h_r = \frac{\sigma \epsilon' (T_p^4 - T_w^4)}{(T_p - T_w)}, \quad (\text{A-10})$$

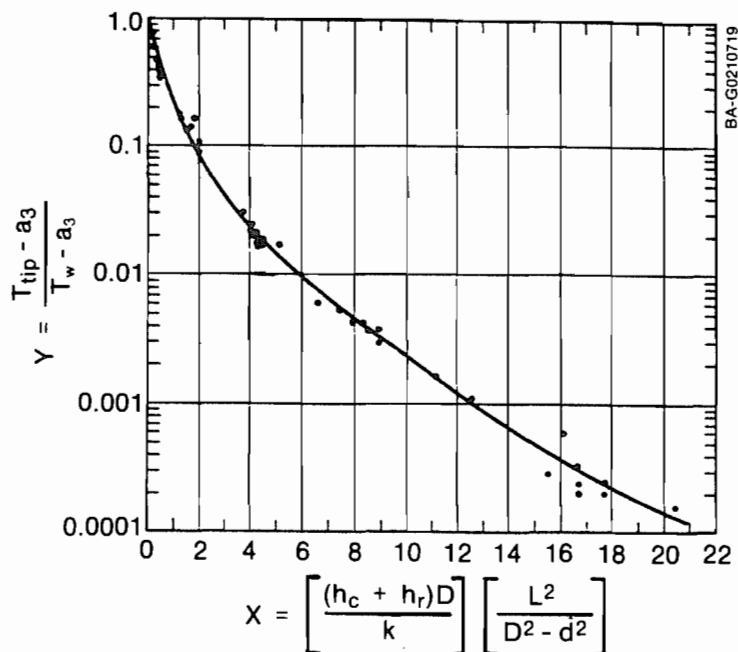
where

σ = the Stefan-Boltzmann constant, $5.67 \times 10^{-8} \text{ W/m}^2 \text{ K}^4$
 T_p, T_w = estimated probe and wall temperatures (K)
 ϵ' = effective emissivity, approximated by (Benedict 1977)

$$\epsilon' = \epsilon_p \left(1 - \epsilon_{f1} \frac{T_{adi}^4 - T_w^4}{T_p^4 - T_w^4} \right). \quad (\text{A-11})$$

For T_p and T_w of 6° and 5°C , respectively, we get $h_r \approx 49 \text{ W/m}^2 \text{ K}$. Using Figure A-7 (Benedict 1977, p. 248), we estimate

$$a_3 = \frac{h_c T_{adi} + h_r T_w}{h_c + h_r} = 5.0012^\circ\text{C}.$$



Source: Benedict 1984

Figure A-7. Summary curve of 20 step-linearized solutions for probe temperature calculations. Limits of variables ($0 < \epsilon_w < 1$), ($0 < \epsilon_{f1} < 1$), ($1 < k < 20$), ($1 < h_c < 1000$), ($2 \text{ in.} < L < 12 \text{ in.}$), ($1/16 \text{ in.} < D < 2 \text{ in.}$), ($0 < d < 1/4 \text{ in.}$), ($70^\circ\text{F} < T < 1200^\circ\text{F}$)

The abscissa x , defined as

$$x = \left[\frac{(h_c + h_r)D}{K} \right] \left[\frac{L^2}{D^2 - d^2} \right]$$

$$= \left[\frac{2.832 \times 0.00635}{0.0519} \right] \left[\frac{9 \text{ in.}^2}{0.875 \text{ in.}^2 - 0.25 \text{ in.}^2} \right] = 115.2 . \quad (\text{A-12})$$

This yields an ordinate value of <0.0001 ; i.e., if

$$y = \frac{T_{\text{tip}} - a_3}{T_w - a_3} < 0.0001 = \frac{T_{\text{tip}} - 5.0012}{0.0688} < 0.0001 ,$$

then $T_{\text{tip}} \approx 5.00^\circ\text{C}$.

Thus, errors in the water temperature measurement because of installation effects are negligible.

For continuous operation with a 1 mA sensing current, self-heating generates 100 μW . Assuming this heat is lost by convection only, the probe temperature rise may be estimated as

$$\Delta T = \frac{Q}{h_c \pi d L} = \frac{100 \times 10^{-6}}{2783 \times 253.3 \times 10^{-6}} = 0.14 \times 10^{-3} \text{ K} . \quad (\text{A-13})$$

Thus, an overall error in the water temperature measurement is estimated to be less than $\pm 0.01 \text{ K}$.

A.4.1.2 Steam Temperature

The uncertainties in the temperature measurement, because of calibration and measurement system errors, are once again less than 7 mK. Installation effects, however, are considerably larger than for water, as we shall note below.

Consider a worst-case steam temperature measurement with an assumed nominal saturated steam temperature of 5°C and a steam flow rate of 0.06 kg/s through the vacuum vessel of 1.52 m diameter, corresponding to a steam velocity of 4.8 m/s. The probe Reynolds number is then

$$\text{Re}_d = \frac{\rho V d}{\mu} = \left(\frac{1}{147.2} \right) 4.84 \left(\frac{0.00635}{8.2 \times 10^{-6}} \right) = 25.47 . \quad (\text{A-14})$$

Note that this Reynolds number is extremely low.

The mean Nusselt number can be expressed as $\text{Nu} = 0.821 \text{Re}^{0.385} \times 1.1 \text{Pr}^{0.31}$ (O'Brien and Miller 1983). With a steam Prandtl number of 0.82, we see that $\text{Nu} = 0.903(25.5)^{0.385}(0.82)^{0.31} = 2.95$.

The corresponding conductive heat-transfer coefficient is

$$h_c = \frac{k \text{Nu}}{d} = \frac{2.95(1.85 \times 10^{-2})}{0.00635} = 8.61 \text{ W/m}^2 \text{ K} . \quad (\text{A-15})$$

The stagnation temperature at the probe may be calculated as

$$T_{adi} = T + r \frac{v^2}{2C_p} ,$$

where r is the recovery factor, $r = (Pr)^{1/2}$, for laminar flow. (A-16)

Then, the adiabatic steam stagnation temperature is

$$T_{adi} = 5 + (0.82)^{1/2} \frac{4.84^2}{21.86 \times 10^3} = 5.0057^\circ\text{C} \quad (\text{A-17})$$

The effective radiative heat-transfer coefficient may be calculated as

$$h_r = \sigma \epsilon' \frac{T_p^4 - T_w^4}{T_p - T_w} . \quad (\text{A-18})$$

Assuming $T_w = 25^\circ\text{C}$, and $\epsilon' \approx 1$, we get $h_r = 5.43 \text{ W/m}^2 \text{ K}$. (A-19)

Assuming that the probe is completely immersed in steam, we can neglect conduction through the probe. In this case, the probe tip temperature can be calculated as

$$T_{tip} = \frac{h_r T_w + h_c T_{adi}}{h_r + h_c} = \frac{5.43(25) + 8.61(5.006)}{5.43 + 8.61} = 12.74^\circ\text{C} . \quad (\text{A-20})$$

Error in dry-bulb steam temperature measurement can be quite high.

Now consider the case of the steam saturation temperature measurement using a wet bulb where the probe tip is covered by a wick constantly kept wet by the internal wicking action from a reservoir containing water.

The typical wet-bulb probe schematic is shown in Figure A-8. The convective heat transfer to the probe is now enhanced by heat transfer associated with mass transfer in the form of evaporation or condensation. Neglecting radial temperature distribution within the probe, we may write a heat balance equation for the probe as

$$h_c(T_s - T_b) + h_{fg}K_c \rho \ln \left(\frac{1 - y_s}{1 - y_b} \right) + h_r(T_w - T_s) = 0 , \quad (\text{A-21})$$

where

K_c = mass-transfer coefficient

y_b = mole fraction of steam in bulk

y_s = the mole fraction of steam at the interface temperature T_s (probe temperature).

We can estimate K_c using the Colburn-Hougen analogy from h_c as

$$\frac{h_c}{K_c \rho C_p} = \left(\frac{Sc}{Pr} \right)^{2/3} , \text{ giving us } K_c = 1.41 \text{ m/s} . \quad (\text{A-22})$$

Solving Eq. 3-21 iteratively then yields a probe surface temperature of $T_s \approx 5.01^\circ\text{C}$.

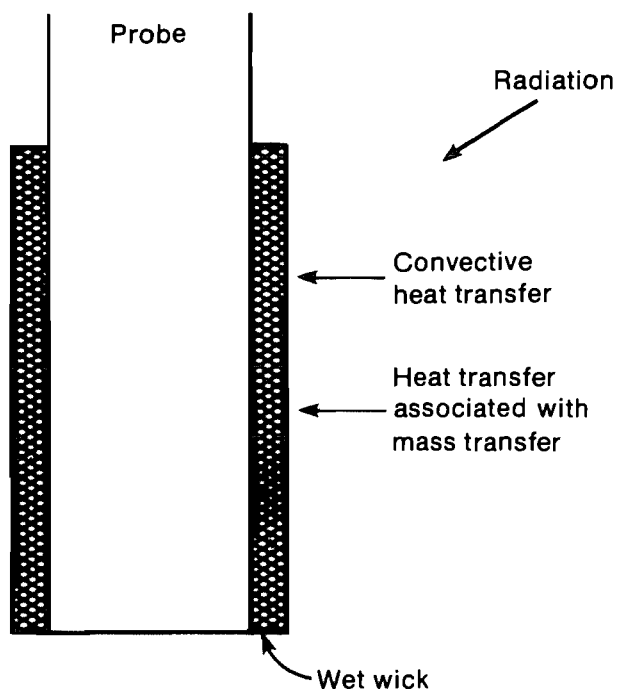


Figure A-8. Wet-bulb steam temperature measurement probe

as the number of turbine revolutions per unit volumetric fluid displacement (e.g., pulses/gal). The flowmeter output is in the form of a scaled 0-5-V pulse per turbine revolution. The manufacturers calibrated the meters regularly once a year. The calibration was repeatable within $\pm 0.2\%$ over the course of five years of operation.

The elapsed time between pulses is measured using an electronic counter (Fluke Model 7260A), time-averaged to yield less than 0.1% error in the overall time measurement.

Sources of error in flow rate measurement arise from errors in estimating the calibration "constant" and in measuring the elapsed time between pulses. Error in the water-flow measurement is estimated to be $\pm 1\%$ over the flow rate range of 5 to 15 kg/s.

A.4.2.2 Inert Gas Injection Rate

Inert gas used in the investigation is compressed air available from the common laboratory utility line. For the tests, we injected gas into the vacuum chamber in the vapor space above the evaporator. The gas flow was monitored using two mass-flow controllers (Tylan Model FC262, 0-50 and 0-150 Std. L/min). Depending upon the requirement, we used either one or both of the controllers. The accuracy of the gas flow injection measurement is $\pm 2\%$ of the full-scale reading as quoted by the controller manufacturers. This specification translates into an uncertainty of ± 0.02 g/s for injection rates of less than 1 g/s, ± 0.06 g/s for injection rates of up to 3 g/s and ± 0.08 g/s for the maximum injection rate of approximately 4.1 g/s.

Thus, the error in steam saturation temperature measurement using a wet bulb, because of installation effect, is significantly smaller than that for the corresponding dry-bulb measurement. Therefore, for all steam temperature measurements in the laboratory, we adopted wet-bulb probes. We estimated the overall system error in steam saturation temperature measurement to be less than ± 0.02 K.

A.4.2 Flow Measurement

Next to temperature, flow measurement is critical in achieving the overall system energy balance in the laboratory.

A.4.2.1 Water Flow Measurement

We measured the cold- and warm-water flow rates going into the heat exchangers using two 3-in. turbine flowmeters (Flow Technology Inc., Model FT-96C3000-LJC(s)). We calibrated the response of the flowmeter

Table A-5. Summary of Uncertainties in Primary Measurements

Condenser inlet conditions	
Steam temperature	$\pm 0.02^{\circ}\text{C}$
Total pressure	$\pm 0.5\%$
Inert gas flow	$\pm 2.0\%$
Water temperature	$\pm 0.01^{\circ}\text{C}$
Water flow rate	$\pm 1.0\%$
Condenser outlet conditions	
Steam temperature	$\pm 0.02^{\circ}\text{C}$
Water temperature	$\pm 0.01^{\circ}\text{C}$
Pressure loss	$\pm 10\text{ Pa}$ or $\pm 10\%$
Exhaust pump conditions	
Steam temperature (dry bulb)	$\pm 20\text{--}0^{\circ}\text{C}$
Total pressure	$\pm 0.5\%$
Volumetric flow	$\pm 7\%$

A.4.2.3 Exhaust Volumetric Flow

Inert gas and uncondensed steam are exhausted from the vacuum exhaust pumps as described earlier. The volumetric flow upstream of the first-stage rotary blower is constant within $\pm 3\%$ over a range of inlet pressures from 1000 Pa to 3000 Pa. We verified this constant volumetric flow rate by injecting known amounts of inert gas into the vacuum system under dry (completely void of water spots) conditions and by measuring the pressure and temperature of the gas upstream of the blower inlet. The measurements indicate that the volumetric flow of the blower remained constant at $0.56\text{ m}^3/\text{s}$ within $\pm 3\%$ over an inlet pressure and temperature ranges of 1000 to 3000 Pa, and 6° to 27°C , respectively. We then inferred the volumetric flow of the exhaust gases just downstream of

the condenser by correcting the volumetric flow upstream of the blower for pressure and temperature changes in the exhaust gas between the two stations.

We estimate overall uncertainty in the inferred volumetric flow downstream of the condenser to be $\pm 7\%$. The large uncertainty in this measurement arises primarily because of uncertainties in estimating Δp between the two stations.

A.4.3 Pressure

For these tests, we measured absolute pressure of the steam at three different locations; namely, above the evaporator, at the condenser outlet and at the vacuum pump inlet. Three absolute pressure transducers (MKS, Inc., model 222BHS-A-0-100, 0-100-mm Hg range) were used with three digital indicators. Errors in absolute pressure measurement arise from calibration errors, zero-shifts of the transducers, and reading errors. As quoted by the manufacturers, the overall error in the absolute pressure measurement is estimated to be $\pm 0.5\%$ of the reading over the tested range of 1000 to 3000 Pa of absolute pressure.

We also used two differential pressure transducers to measure pressure losses in the steam flow. One of these was connected across the condenser packing to yield losses from condenser inlet to the vapor outlet. The second transducer measured the pressure difference between the condenser inlet to the inert gas exit location above the vacuum chamber.

Errors in the differential pressure measurement arise from calibration errors, zero-shifts, and reading errors. Large zero-shift turned out to be a severe problem with these transducers. To compensate for zero-drift errors, all zero readings were recorded both at the beginning and end of each test run. The differential pressure readings were corrected using an average zero-reading

for each run. Estimated errors in the differential pressure measurements are large, about ± 10 Pa or $\pm 10\%$ of the quoted results, whichever is larger.

A.4.4 Summary

Table A-5 summarizes the uncertainties in the primary measurements. These uncertainties are then carried forward to provide uncertainty estimates for the deduced or inferred quantities such as water effectiveness and modified vent fraction. Analyses for inferring uncertainties in the deduced quantities are provided in Appendix B and summarized in Section 3.2.

A.5 References

- Benedict, R. P., 1984, Fundamentals of Temperature, Pressure, and Flow Measurements, New York: John Wiley & Sons.
- Kreith, F., and M. Bohn, 1986, Principles of Heat Transfer, 4th ed., New York: Harper and Row.
- O'Brien, B., and S. Miller, 1983 (Nov.) "Thermocouples, RTDs Can Boost Temperature Measurement Accuracy," Ind. R&D, Vol 25. No. 11, pp. 96-100.

APPENDIX B MEASUREMENT UNCERTAINTIES AND THEIR PROPAGATION

In this appendix we discuss experimental measurements and the parameters we used to describe condenser performance. We discuss the primary data taken for each of the condenser configurations, such as temperature and pressure, and define the derived parameters. In addition, we present the uncertainties or errors in the numerical values of these derived quantities arising from the primary measurement errors discussed in Appendix A.

B.1 Primary Data Measurements

At every test condition, the raw experimental data include temperatures, flow rates, and pressures. We measured temperatures with platinum RTDs as discussed in Appendix A. We measured steam saturation temperatures at the top and bottom of the test articles using cotton wicks for wetting. At the bottom, we placed the RTD nominally 0.2 m above the water drain pool, which eliminated direct splashing of the temperature probe. The upper steam temperature probe was placed around 0.15 m above the water distribution plate for similar reasons. In both cases, the end of the wick trailed directly in the water resulting in full wetting. Water inlet and outlet temperatures were measured by probes placed in the inlet and drain piping just upstream and downstream of the test article. We measured the water flow rate by a turbine-type flow meter placed in the inlet piping. Inert gas injection ports were located near an upper corner of the tank on the evaporator side to allow the gas to fully mix with the steam before the mixture entered the condenser.

We took three primary gas pressure measurements, the inlet pressure, the pressure drop through the test article, and the exhaust pressure at the vacuum pump inlet. In the first and last measurement points, we used absolute pressure transducers but measured the pressure drop with a differential instrument. Experiments varied the inert gas injection rate, the heat removal rate (reflected in varying water flow rate because inlet water temperature was nearly constant), and volumetric venting rate (achieved by closing the butterfly valve in the line between the condenser exit and the exhaust vacuum pump). The measured data are presented in Appendices D and E for all performed tests along with performance parameters.

B.2 Consistency of Data

The experimental data have a definite uncertainty associated with the measurements. These intrinsic uncertainties result in inconsistencies in redundant data. For our applications, these inconsistencies can be significant because of the small driving forces and pressure drops. To minimize confusion, we chose a set of nonredundant data as the baseline results and derived other results from them. We tried several schemes for eliminating data inconsistencies with varying results. The following scheme resulted in good agreement between derived and measured results and minimized errors in computing condenser performance parameters.

The primary measurements are inlet steam temperature T_{si} , inlet water temperature T_{wi} , outlet water temperature T_{wo} , water flow rate m_w , inert gas flow rate m_i , pressure drop in the condenser Δp , and the temperature and pressure at the vacuum exhaust T_{ex} and P_{ex} , respectively. The following procedure

finds the inlet and outlet absolute pressure and the outlet steam temperature from these values.

We assume the steam is saturated, and saturation pressure can be calculated using the following equation:

$$P_{\text{sat}}(T) = A \exp [B - C/(T + D)] + E , \text{ in Pascals for } T \text{ in } ^\circ\text{C} , \quad (\text{B-1})$$

where $A = 161.7574$, $B = 18.4779$, $C = 4026.976$, $D = 234.738$, and $E = 3.73835$.

Therefore, the partial pressure of steam at the inlet is

$$PP_{\text{si}} = P_{\text{sat}}(T_{\text{si}}) . \quad (\text{B-2})$$

The amount of steam condensed can be found from a heat balance, assuming the sensible heat content of the inert gas and the condensed steam is small compared with the latent heat of condensation:

$$\dot{m}_{\text{sc}} = \dot{m}_{\text{w}} C_{\text{pw}} (T_{\text{wo}} - T_{\text{wi}}) / h_{\text{fg}} , \quad (\text{B-3})$$

where C_{pw} is an average specific heat of water, nominally $4.186 \text{ kJ/kg } ^\circ\text{C}$, and h_{fg} is an average heat of vaporization, nominally 2470 kJ/kg .

We made an initial guess of the steam flow rate at the condenser outlet of $\dot{m}_{\text{so}} = \dot{m}_{\text{sc}}/10$. The total inlet steam flow rate is then

$$\dot{m}_{\text{si}} = \dot{m}_{\text{sc}} + \dot{m}_{\text{so}} . \quad (\text{B-4})$$

The steam outlet mole fraction is found as

$$y_{\text{so}} = \frac{\dot{m}_{\text{so}}/M_{\text{s}}}{\dot{m}_{\text{so}}/M_{\text{s}} + \dot{m}_{\text{i}}/M_{\text{i}}} . \quad (\text{B-5})$$

We guessed a new outlet flow rate by using the measurements made at the exhaust pump. First, we used the mole fraction of steam at the condenser exit to find the partial pressure of steam at the exhaust (at this point the steam is no longer saturated):

$$PP_{\text{sx}} = P_{\text{ex}} y_{\text{so}} , \quad (\text{B-6})$$

where P_{ex} is the measured exhaust pressure. The steam outlet mass flow is then found using a known exhaust volumetric flow rate Q_{ex} as

$$\dot{m}_{\text{so}} = \frac{Q_{\text{ex}} PP_{\text{sx}}}{T_{\text{sx}} R_{\text{s}}} . \quad (\text{B-7})$$

The variable R_{s} is the gas constant for steam. The process of making calculations using Eqs. B-4 through B-7 is continued until the condenser outlet steam mass flow rate converges within $10^{-4}\%$.

Other condenser parameters are calculated as follows. The inlet steam mole fraction is

$$y_{si} = \frac{\dot{m}_{si}/M_s}{\dot{m}_{si}/M_s + \dot{m}_i/M_i} \quad (B-8)$$

The total inlet pressure is now inferred as

$$P_i = PP_{si}/y_{si} \quad (B-9)$$

The total outlet pressure is found using the measured pressure drop

$$P_o = P_i - \Delta p \quad (B-10)$$

Outlet steam partial pressure is found from this and the calculated mole fraction

$$PP_{so} = P_o y_{so} \quad (B-11)$$

The outlet steam temperature is found by using an inverse of Eq. B-1, as

$$T_{sat}(P) = \frac{C}{B - \ln[(P - E)/A]} - D \quad (B-12)$$

$$T_{so} = T_{sat}(PP_{so}) \quad (B-13)$$

For establishing the consistency of the data, in Figure B-1, the calculated T_{so} is compared with the measured T_{so} for the cocurrent condenser tests using 19060 packing. Variations are minimal and within the derived uncertainty of the calculations (presented in Section B.4). Similar variations are found for all experimental data sets. The following condenser performance parameter calculations use the derived absolute pressures and steam outlet temperatures to avoid inconsistencies because of measurement redundancies and errors. These inconsistencies are well within the derived error bands presented in Section B.4.

B.3 Condenser Performance Parameters

The data analysis presented here uses several common heat exchanger parameters as well as several less common parameters that we found to be particularly useful in understanding the performance of direct-contact devices for OC-OTEC applications.

Effectiveness

Effectiveness is defined as the ratio of the actual heat-transfer rate to the maximum possible heat-transfer rate. This parameter varies from zero to one with a value of one indicating a perfect device, such as an infinitely long countercurrent heat exchanger. For a condenser with noncondensable gases in the vapor, the maximum possible heat transfer is if the water outlet temperature is equal to the steam inlet temperature. Assuming a constant liquid specific heat and low condensate to coolant flow ratios, the effectiveness ϵ can be defined as

$$\epsilon = \frac{T_{wo} - T_{wi}}{T_{si} - T_{wi}} \quad (B-14)$$

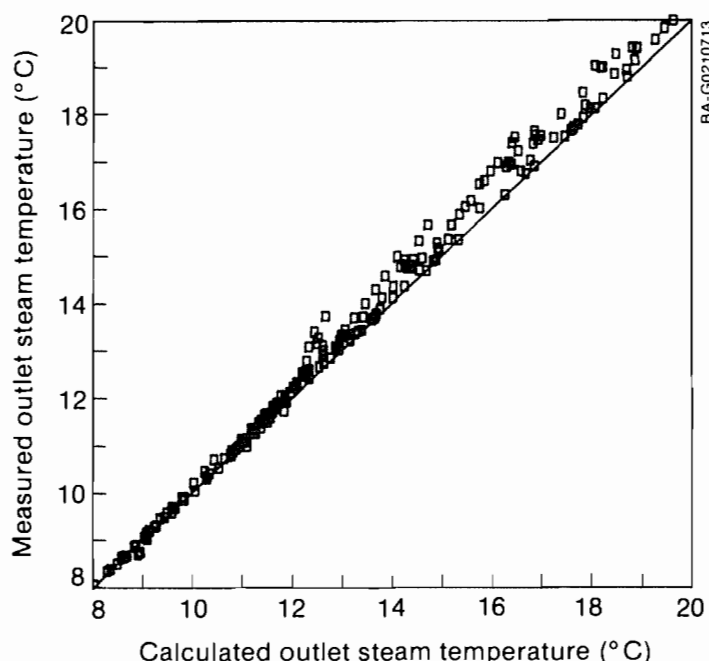


Figure B-1. Comparison of measured and calculated steam outlet temperature for cocurrent packing 19060

This definition does not account for heat exchanger geometry. In a cocurrent condenser where the streams flow in the same direction, the maximum possible heat transfer results in equal vapor and liquid outlet temperatures. It is possible to find this equilibrium outlet temperature T^* from a heat balance:

$$\dot{m}_w C_{pw} (T_{wi} - T^*) = \dot{m}_{sc, \max} h_{fg} \quad (B-15)$$

The maximum amount of steam that can be condensed for a given set of conditions, $\dot{m}_{sc, \max}$ (where $T_{so} = T_{wo}$), is a function of the inert flow rate, inlet steam temperature, and condenser pressure. We have assumed no pressure drop in the condenser for these ideal calculations. The solution method is as follows: for a guessed T_{so} , the outlet steam partial pressure is found using Eq. B-2. The outlet inert gas partial pressure and known mass flow rate can then be used to determine the amount of steam condensed:

$$P = P_{\text{sat}}(T_{si}) / (1 - y_{ii}) \quad (B-16)$$

$$pp_{io} = P - P_{\text{sat}}(T_{so}) \quad (B-17)$$

$$\dot{m}_{so} = (M_s / M_i) \dot{m}_i (1 - P / pp_{io}) \quad (B-18)$$

$$\dot{m}_{sc} = \dot{m}_{si} - \dot{m}_{so} \quad (B-19)$$

The amount of steam condensed is then used in the heat balance of Eq. B-15. These equations are solved iteratively until T_{so} and T_{wo} agree.

A modified effectiveness ϵ^* can then be defined that considers that the maximum possible temperature difference in a countercurrent geometry is less than $T_{si} - T_{wi}$:

$$\epsilon^* = \frac{T_{wo} - T_{wi}}{T^* - T_{wi}} . \quad (B-20)$$

Mass Fractions

Inlet and outlet inert mass fractions are easily found from mass flow rates

$$X_{ii} = \dot{m}_i / (\dot{m}_i + \dot{m}_{si}) \quad (B-21)$$

$$X_{io} = \dot{m}_i / (\dot{m}_i + \dot{m}_{so}) . \quad (B-22)$$

Gas Loading

The gas loading is simply the inlet steam and inert gas mixture flow divided by the cross-sectional area:

$$G = (\dot{m}_{si} + \dot{m}_i) / A . \quad (B-23)$$

Area represents the cross-sectional area of the gas-liquid contacting device.

Percentage of Steam Condensed

The percentage of steam condensed is on a mass basis

$$\% \text{ Cond} = (\dot{m}_{sc} / \dot{m}_{si}) 100 . \quad (B-24)$$

Jakob Number

A Jakob number is defined as

$$Ja = \frac{\dot{m}_w C_{pw} (T_{si} - T_{wi})}{\dot{m}_{si} h_{fg}} . \quad (B-25)$$

B.4 Derived Parameter Error Analysis

The uncertainty in the primary measurements discussed in Appendix A has a definite effect on the certainty of derived condenser performance parameters. It is possible to estimate these derived parameter uncertainties. This section presents error estimates for both cocurrent and countercurrent experimental tests with 19060 packing; errors are similar for the other packing media.

The method for estimating the propagation of errors, as well as the errors associated with the primary variables, is taken from Kline and McClintock[†]. Table B-1 shows the error ranges for the 19060 packing in countercurrent

[†]Kline, S. J., and F. A. McClintock, 1953 (Jan.), "Describing Uncertainties in Single-Sample Experiments," Mechanical Engineering, Vol. 75, No. 1, pp. 3-8.

tests. Briefly, the errors are estimated as the sum of the squares of the partial derivatives of the equations with respect to the primary variables times the errors in the primary variables. For example, if a derived parameter Y is a function of other variables A, B, and C:

$$Y = f(A, B, C),$$

and the error estimates of A, B, and C are known and represented by ΔA , ΔB , and ΔC , respectively, the error of derived parameter Y with approximately the same confidence level is

$$\Delta y = \left[\left(\frac{\partial Y}{\partial A} \Delta A \right)^2 + \left(\frac{\partial Y}{\partial B} \Delta B \right)^2 + \left(\frac{\partial Y}{\partial C} \Delta C \right)^2 \right]^{1/2}. \quad (B-26)$$

This error estimation is commonly used and gives a good estimate of the actual errors. As an example, the error in effectiveness defined in Eqs. B-14 is computed as

$$\begin{aligned} \Delta \epsilon = & \left\{ \left(\frac{\Delta T_{wo}}{T_{si} - T_{wi}} \right)^2 \right. \\ & + \left[\frac{(T_{wo} - T_{si}) \Delta T_{wi}}{(T_{si} - T_{wi})^2} \right]^2 \\ & \left. + \left[\frac{(T_{wi} - T_{wo}) \Delta T_{si}}{(T_{si} - T_{wi})^2} \right]^2 \right\}^{1/2}. \end{aligned} \quad (B-27)$$

The relative error can be found by dividing by the actual value of computed effectiveness as $(\Delta \epsilon / \epsilon)$.

This process assumes that the functional form of Eq. B-26 is correct. Errors resulting from assumptions in the equations are not included. In our case, the only assumptions affecting the analysis are that the sensible heat capacity of the vapor and condensate is negligible compared with the latent heat

**Table B-1. Countercurrent Derived Parameter
Uncertainty Estimates 19060 Packing**

Derived Parameter	Error Range (%)
Gas loading	2.4-2.6
Jakob number	1.8-2.0
Inlet inert mass fraction	2.3-2.5
Outlet inert mass fraction	2.0-4.5
Effectiveness	0.2-0.7
Percentage condensed	1.7-2.0
Inlet pressure	0.1-0.2
Outlet pressure	0.4-0.9

of condensation, that the ideal gas law holds (used for volumetric flow calculations), and that the curve fits for saturation temperature and pressure are accurate (standard deviation for our data ranges was 0.3%).

The primary uncertainties in the experimental measurements are presented in Appendix A. Table B-2 presents these values again along with the uncertainties in several other parameters used in the analysis.

It can be seen that the derived uncertainty depends on the value of the experimentally measured variables. We computed the errors for every experimental condition along with the derived results. We also computed uncertainties for every parameter in intermediate calculations. Tables B-3 and B-4 show the complete results of the error analysis for a data point for each of the countercurrent and cocurrent tests using 19060 packing. The range of relative error for all the experimental data with these configurations are presented in Table B-5 for cocurrent flow and Table B-1 for countercurrent flow.

Table B-2. Primary Uncertainties

Temperature	
Water inlet	0.01°C
Water outlet	0.01°C
Steam inlet	0.02°C
Steam outlet	0.02°C
Exhaust	10.00°C
Pressure	
Condenser inlet	0.5%
Condenser differential	10 Pa or 10%
Exhaust	0.5%
Flow rates	
Water	1.0%
Inert gas	2.0%
Other	
Exhaust volumetric flow (0.5668 m ³ /s)	3.0%
Water specific heat (4.186 kJ/kg °C)	0.5%
Heat of vaporization (2470 kJ/kg)	0.6%
Column diameter (0.6096 m in 8 cases)	1.0%
Supply pipe diameter (0.1524 m)	0.5%

The only parameter with large errors is the pressure loss. These errors are the result of the large uncertainty in the pressure drop measurement. For these tests, the measured vapor pressure drop is very low, usually between 2 and 20 Pa. The error in the pressure drop is 10 Pa.

Table B-3. Uncertainties in Countercurrent Condenser Experimental Results

Parameter	Value	Units	Absolute Error	Relative Error
<u>Measured Parameters</u>				
Steam inlet temperature	283.07	K	0.020	0.00007
Steam outlet temperature	281.82	K	0.020	0.00007
Water inlet temperature	278.18	K	0.010	0.00004
Water outlet temperature	282.54	K	0.010	0.00004
Steam exhaust temperature	297.39	K	10.000	0.03363
Inert mass flow rate	0.3450×10^{-3}	kg/s	0.6900×10^{-5}	0.02000
Water mass flow rate	0.6140×10	kg/s	0.6140×10^{-1}	0.01000
Total inlet pressure	1153.00	Pa	5.765	0.00500
Pressure drop	11.14	Pa	10.000	0.89767
Exhaust pressure	437.23	Pa	2.186	0.00500
<u>Input Parameters</u>				
Exhaust volumetric flow	0.56680	m ³ /s	0.0170040	0.03000
Heat of vaporization	2470.00	kJ/kg	14.8200	0.00600
Water specific heat	4.18600	kJ/kg °C	0.020930	0.00500
<u>Intermediate Calculated Results</u>				
Cross-section area	0.27386	m ²	0.00584	0.02132
P _{sat} (TSI)	1221.08	Pa	1.64	0.00134
P _{sat} (TSOC)	1071.09	Pa	10.96	0.01024
Exhaust steam partial pressure	385.28	Pa	2.99	0.00776
Steam flow in	0.4696×10^{-1}	kg/s	0.59863×10^{-3}	0.01275
Steam flow out	0.1591×10^{-2}	kg/s	0.72751×10^{-4}	0.04573
Steam condensed	0.4537×10^{-1}	kg/s	0.59418×10^{-3}	0.01310
Inlet gas constant	460.75	Pa-m ³ /kg-C	0.06	0.00013
Outlet gas constant	440.80	Pa-m ³ /kg-C	2.84	0.00645
<u>Intermediate Calculated Results</u>				
Steam inlet ρ	0.9346×10^{-2}	kg/m ³	0.12537×10^{-4}	0.00134
Gas inlet velocity	18.347	m/s	0.45648	0.02488
<u>Calculated Results</u>				
Total inlet pressure	1226.66	Pa	1.65	0.00135
Total outlet pressure	1215.52	Pa	10.14	0.00834
Steam outlet temperature	281.13	K	0.150	0.00053
Steam loading	0.1715	kg/m ² s	0.00426	0.02484

**Table B-3. Uncertainties in Countercurrent Condenser Experimental Results
(Concluded)**

Parameter	Value	Units	Absolute Error	Relative Error
Fraction condensed	0.9661	---	0.0177	0.01828
Jakob number	1.0836	---	0.0201	0.01856
Inlet inert mass fraction	0.7293×10^{-2}	---	0.1717×10^{-3}	0.02354
Outlet inert mass fraction	0.1782	---	0.7309×10^{-2}	0.04102
Inlet inert mole fraction	0.4548×10^{-2}	---	0.1074×10^{-3}	0.02361
Outlet inert mole fraction	0.1188	---	0.5226×10^{-2}	0.04398
Inlet steam mole fraction	0.9955	---	0.1074×10^{-3}	0.00011
Outlet steam mole fraction	0.8812	---	0.5233×10^{-2}	0.00594
Effectiveness (water)	0.8916	---	0.00419	0.00470
Inlet volumetric flow	5.02969	m ³ /s	0.06402	0.01273
Outlet volumetric flow	0.19738	m ³ /s	0.00774	0.03919

Table B-4. Uncertainties in Cocurrent Condenser Experimental Results

Parameter	Value	Units	Absolute Error	Relative Error
<u>Measured Parameters</u>				
Steam inlet temperature	284.15	K	0.020	0.00007
Steam outlet temperature	283.99	K	0.020	0.00007
Water inlet temperature	278.42	K	0.010	0.00004
Water outlet temperature	282.86	K	0.010	0.00004
Steam exhaust temperature	295.28	K	10.000	0.03387
Inert mass flow rate	0.3100×10^{-4}	kg/s	0.6200×10^{-6}	0.02000
Water mass flow rate	0.5760×10	kg/s	0.5760×10^{-1}	0.01000
Total inlet pressure	1318.00	Pa	6.590	0.00500
Pressure drop	16.50	Pa	10.000	0.60606
Exhaust pressure	1284.09	Pa	6.420	0.00500
<u>Input Parameters</u>				
Exhaust volumetric flow	0.56680	m ³ /s	0.0170040	0.03000
Equilibrium outlet temperature	283.37	K	0.020	0.00007
Water specific heat	4.18600	kJ/kg °C	0.020930	0.00500
<u>Intermediate Calculated Results</u>				
Cross-section area	0.27386	m ²	0.00584	0.02132
P _{sat} (TSI)	1312.40	Pa	1.75	0.00133
P _{sat} (TSOC)	1291.74	Pa	10.96	0.00783
Exhaust steam partial pressure	1279.45	Pa	6.40	0.00500

Table B-4. Uncertainties in Cocurrent Condenser Experimental Results
(Concluded)

Parameter	Value	Units	Absolute Error	Relative Error
Steam flow in	0.4866×10^{-1}	kg/s	0.61662×10^{-3}	0.01267
Steam flow out	0.5321×10^{-2}	kg/s	0.24221×10^{-3}	0.04552
Steam condensed	0.4334×10^{-1}	kg/s	0.56701×10^{-3}	0.01308
Inlet gas constant	461.47	Pa-m ³ /kg °C	0.01	0.00001
Outlet gas constant	460.91	Pa-m ³ /kg °C	0.10	0.00021
Intermediate Calculated Results				
Steam inlet ρ	0.1001×10^{-1}	kg/m ³	0.13309×10^{-4}	0.00133
Gas inlet velocity	17.757	m/s	0.44110	0.02484
Calculated Results				
Total inlet pressure	1312.92	Pa	1.65	0.00133
Total outlet pressure	1296.42	Pa	10.14	0.00783
Steam outlet temperature	283.91	K	0.118	0.00041
Steam loading	0.1777	kg/m ² s	0.00441	0.02481
Fraction condensed	0.8907	---	0.0162	0.01821
Jakob number	1.1494	---	0.0211	0.01835
Inlet inert mass fraction	0.6366×10^{-3}	---	0.1506×10^{-4}	0.02366
Outlet inert mass fraction	0.5792×10^{-2}	---	0.2863×10^{-3}	0.04946
Inlet inert mole fraction	0.3960×10^{-3}	---	0.9372×10^{-5}	0.02367
Outlet inert mole fraction	0.3610×10^{-2}	---	0.1788×10^{-3}	0.04954
Inlet steam mole fraction	0.9964	---	0.1789×10^{-3}	0.00018
Outlet steam mole fraction	0.9996	---	0.9372×10^{-5}	0.00001
Effectiveness (water)	0.7749	---	0.00324	0.00418
Inlet volumetric flow	4.86331	m ³ /s	0.06192	0.01273
Outlet volumetric flow	0.54024	m ³ /s	0.02481	0.04593

Table B-5. Cocurrent Derived Parameter
Uncertainty Estimates
19060 Packing

Derived Parameter	Error Range (%)
Gas loading	2.4-2.7
Jakob number	1.8-2.0
Inlet inert mass fraction	2.3-5.5
Outlet inert mass fraction	3.4-5.0
Effectiveness	0.17-0.75
Percentage condensed	1.7-5.0
Inlet pressure	0.12-0.14
Outlet pressure	0.38-0.93

APPENDIX C RELATIVE RANKING OF TESTED CONTACT DEVICES

C.1 Direct-Contact Design Considerations

Several physical factors influence the design of direct-contact condensers. In selecting our test articles, we looked at liquid-vapor interfacial area, liquid renewal, inert gas influences, liquid and vapor pressure drops, and other factors.

Vapor-liquid interfacial area affects the overall transfer process rates. Gas- and liquid-phase heat- and mass-transfer coefficients, which are defined per unit area, are relatively insensitive to packing characteristic diameter (typical published correlations include an exponent of less than one for the Reynolds number). Therefore, maximizing the liquid-gas interfacial area results in the largest overall heat- and mass-transfer rates. Increasing the interfacial area usually means decreasing the characteristic packing dimension and results in smaller, more contorted vapor passageways that cause a larger frictional vapor pressure drop. In OTEC systems where the overall driving potential is only around 20°C, condenser vapor pressure drop should be minimized so the turbine can extract more energy. The trade-offs between increasing pressure drop and increasing condensation efficiency falls into the systems analysis area. We used a preliminary systems analysis to guide the design for the test articles described in this section. These results showed that pressure drops between 0 and 200 Pa were acceptable; that around 75%-90% of the steam should be condensed in the cocurrent section; and that the maximum possible of the remaining steam should be condensed in the second-stage countercurrent section.

For open-cycle OTEC conditions, the transfer coefficients in the gas and liquid phases are of the same magnitude. High heat-transfer rates associated with direct-contact processes result in quick warming of the coolant surface. To maintain high transfer rates, the liquid surface needs to be renewed with the cooler liquid either by turbulent mixing within the liquid or by bulk remixing. Renewal of the liquid interface temperature is an obvious design feature of the test articles.

Inert gases affect the performance of direct-contact condensers in several ways. First, the presence of inert gases lowers the bulk steam partial pressure, which is the driving force for mass transfer. Second, the inert gases are carried by bulk vapor flow to the coolant surface, and a gradient of non-condensable gases builds up. The diffusion of steam through this gradient is reflected by an increase in the gas-side resistance to mass transfer. Finally, the inert gases must be continuously removed from the condenser to prevent pressure buildup. Removing the inert gases from all portions of the condenser is a major design consideration. Any pockets where inert gases are allowed to build up are ineffective and reduce the overall effectiveness of the device. Inactive areas can be prevented by designs that do not allow local vapor velocities to drop and by intelligent placement of the exhaust intake. The first two effects are examined experimentally by controlling the inert gas content in the inlet steam. We discuss the effects of our exhaust system on the experimental conditions in Sections C.4 and C.5. The location

of the exhaust intake and the vapor velocities in our experiments ensure that the effects of localized noncondensable-gas buildup are minimized or eliminated.

All other factors being equal, a condenser with lower vapor and liquid pressure drop is desirable, especially in OC-OTEC applications. As previously mentioned, any reduction in condenser vapor pressure drop allows the turbine to extract a larger amount of useful energy. The liquid pressure drop is a function of the frictional losses in the water piping, the height of the contacting device, and the height of the water distribution and collection systems. The pressure drop must be overcome by pumps, and the power required to run the pumps reduces the electric energy available from the complete power system. In OTEC systems this is especially critical since the turbine-generator requires around 1600 kg/s of cold water per megawatt of electricity produced. Every meter of liquid head loss in the condenser results in a reduction of around 2% in the net power delivery of the system.

Other factors to consider in designing the test articles are cost of materials and fabrication; modularity or ability to scale up to larger units; biofouling potential, which may be low for all cases because of low oxygen content in deep, cold seawater (Panchal et al. 1984); and potential maintenance problems.

C.2 Existing Contact Devices

Direct-contact devices are used extensively in chemical process industries. Direct-contact separators include many familiar types of hardware such as absorbers, strippers, distillation columns, and liquid extractors where mass exchange is the primary purpose. Cooling tower, flasher, and direct-contact condenser processes include heat and mass transfer. Many of the same principles apply for all the devices. For example, most designs incorporate methods for increasing interfacial area. Some of the designs suitable for our application of condensation are baffle trays (both segmental and disc-donut), spray columns, packed columns, tray columns, and pipeline contactors. Most of these designs can be used in cocurrent and countercurrent flow geometries. Several are also amenable to cross-flow. Literature on the performance and design of these devices are mainly limited to mass transfer alone. A review of the material available on direct-contact heat transfer was done by Fair (1961, 1972). Most of the methods and experiments described in those articles and in applications are limited to conditions where the sensible and latent loads are of nearly equal magnitude. Little data are available for conditions where the latent load is the majority of the heat duty.

Another factor of deviation from routine applications is the possibility of high levels of noncondensable gases in the steam. If seawater deaeration is not used upstream of the heat exchangers, the steam entering the condenser may have inert gas mass fractions near 0.2%. For the high-performance condensers considered in OC-OTEC applications, the inert gas mass fraction will increase up to 50% through the condenser stages. These levels of inert gases are much greater than those usually encountered in conventional power-plant surface condensers. The geometries we selected for this report are the next logical progression in developing direct-contact condensers for open-cycle applications.

C.3 Test Configurations

C.3.1 General

To ascertain the relative merits among configurations, we tested a set of eight different methods of gas-liquid contact in countercurrent flow. The first seven condenser test sections have several common features. We used a central 127-mm ID PVC pipe to supply cold water to the unit. The pipe was centrally located as shown in the cross sections of Figure C-1. A cylindrical enclosure was used to contain the steam and water flow.

For the countercurrent tests, outlet gas venting was through a centrally located 152-mm (inside diameter) pipe mounted nominally 0.2 m above the top of the water delivery pipe. The first four countercurrent condenser configurations did not use a water distribution plate. Water exiting the distribution pipe cascaded freely onto the spiral screen or onto the first baffle plate. The last three countercurrent geometries used a water distribution plate located 25 mm below the outlet of the cold-water pipe. The plate was 0.61 m in diameter and made of Plexiglas®. Water flowed downward through 9.5-mm-diameter holes drilled on a square pitch of 25 mm. Six 70-mm-long, 70-mm (inside diameter) plastic tubes mounted on the plate allowed upward vapor escape. For the eighth configuration, a 50-mm nozzle located nominally 100 mm above the packing was used to distribute the water.

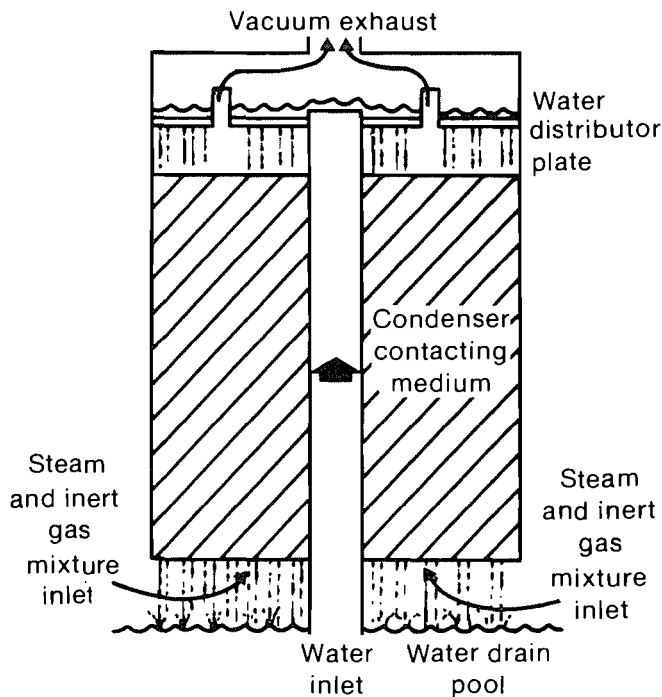


Figure C-1. Countercurrent condenser

C.3.2 Countercurrent Test Article Designs

Table C-1 describes the eight test-article configurations tested. Performance figures for all of the configurations were measured and calculated in countercurrent flow. Configurations 7 and 8 were tested in cocurrent flow as well. Figures C-2 through C-6 show the different condenser types. The first configuration is an innovative design with relatively unrestricted spiral vapor flow paths to minimize pressure drop, yet the screens renew the water surface temperatures by mixing and distributing the water evenly through the holes. The baffle plates of configuration 2 through 4 are a common contactor design that is simple to construct and has features that make it of interest for OTEC applications such as simple vapor paths. Configuration 5 is a variation of configuration 1 but is easier to construct. The water falls more freely downward without following the screw spirals because of a larger void area in the rubber screen.

Configuration 7 uses a commercial structured packing used for contacting devices. Corrugated plastic sheets are attached with angles of 60 deg between

Table C-1. Summary of Countercurrent Condenser Configurations

Configuration	Description	Length (m)	Diameter (m)	Remarks
1	Spiral screen	0.61	0.46	Perforated metal screens with 4.7 mm diam. holes, triangular pitch of 6.4 mm, triple lead screw spiral with pitch of 20 cm.
2	Three baffles	0.58	0.61	Disc-donut baffles with 50% steam blockage and 20 cm spacing.
3	Two baffles	0.58	0.61	Same as 2 except bottom disc and donut was removed.
4	One baffle	0.58	0.61	Same as 3 except bottom disc and donut was removed.
5	Spiral rubber	0.78	0.61	Rubber screen with 7.1 mm holes at 10.7 mm pitch, 6 lead screw spiral with 60-cm pitch.
6	Munters pack 27060	0.78	0.61	Commercial cooling tower fill polyethylene PLASdek 27060, surface area ratio $98 \text{ m}^2/\text{m}^3$
7	Munters pack 19060	0.78	0.61	Same as 6 with smaller corrugation height PLASdek 19060, surface area ratio $138 \text{ m}^2/\text{m}^3$
8	Jaeger Tri-Pack no. 1	0.18, 0.36, 0.66	0.64	Random packing polypropylene surface area ratio $157 \text{ m}^2/\text{m}^3$, equivalent diameter 50 mm, 98% void

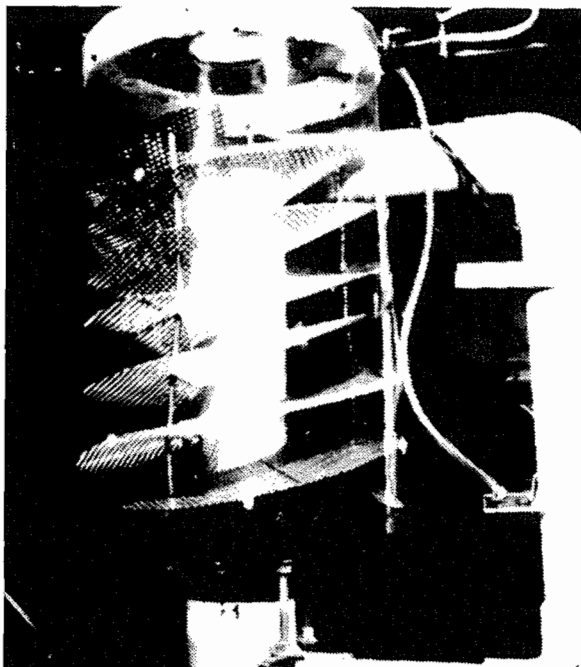


Figure C-2. Spiral screen, condenser configuration 1

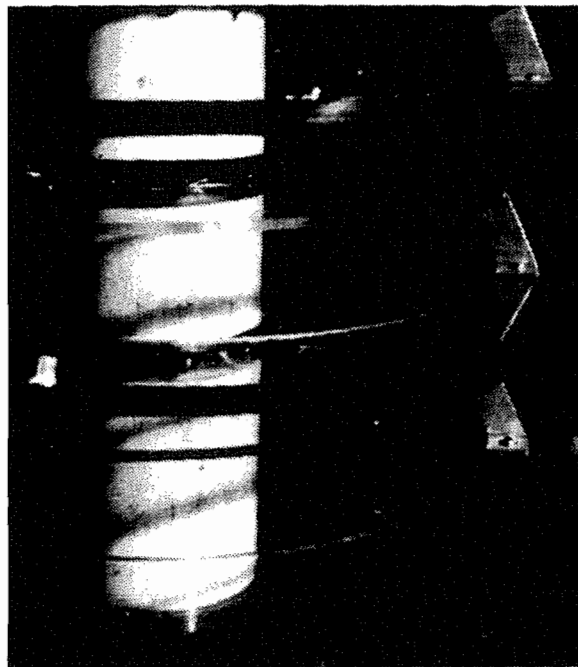


Figure C-3. Baffle plate, disc donut, condenser configurations 2 through 4

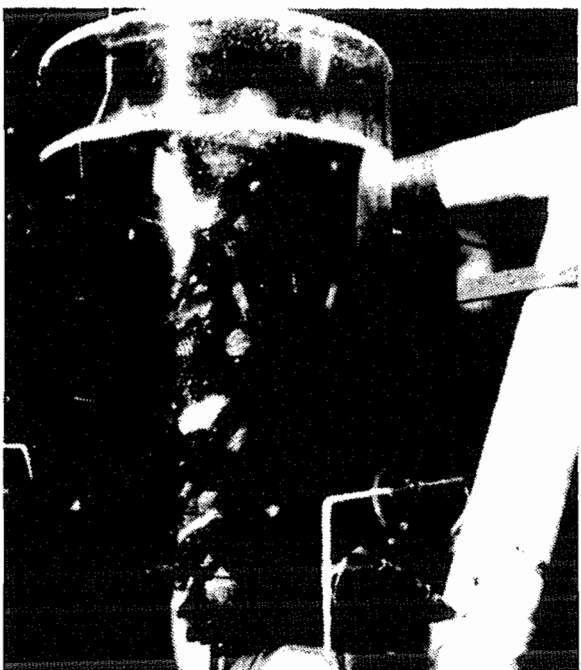


Figure C-4. Spiral rubber mat, condenser configuration 5



Figure C-5. Munters packing, condenser configurations 6 and 7

adjacent sheets. The resulting matrix has relatively simple vapor flow areas, and the interfacial surface area is large. Dimples on the sheets promote liquid mixing. Configuration 8 used random packings (Jaeger Tri-Pack no. 1, nominal 50 mm diameter) with an active surface area per volume of $157 \text{ m}^2/\text{m}^3$ and made of polypropylene. This packing was dumped into a 0.64-m-diameter cylinder. We used three different packing depths, 0.18, 0.36, and 0.66 m, in the tests.

These test articles are not meant to be all inclusive of the options available for OTEC direct-contact condensers. Other geometries may be included in future tests.

C.4 Performance Measures

The relative performance of the tested condenser configurations is quantified by two parameters: a water effectiveness ϵ and a vent fraction V . Considering that in a gas-liquid contact device, we aim to maximize the heat- and mass-transfer rates at a minimum pressure loss penalty, the above two parameters allow us to quantify the efficiency with which these two objectives are met in a device. Both of these parameters are defined to illustrate the deviation of a countercurrent condenser from its potentially maximum possible performance.

The water effectiveness ϵ is defined as

$$\epsilon = \frac{T_{wo} - T_{wi}}{T_{si} - T_{wi}} \quad (\text{C-1})$$

and represents the efficiency with which the available temperature difference potential is used. An ideal countercurrent condenser can operate at a minimum water flow (corresponding to a Jakob number of unity) and yield $\epsilon = 1$, in the absence of noncondensable gas.

An ideal condenser, again, incurs no pressure loss. If P_i and P_o represent the static pressures at the condenser inlet and outlet, then for an ideal condenser we have $P_i = P_o^\dagger$. This condenser also reduces the partial pressure of the outgoing vapor to the minimum possible, in other words, to a saturation value at the coolant inlet temperature. In our case, this condition results in

$$pp_{so} = P_{sat}(T_{wi}) \quad (\text{C-2})$$

and causes a minimum amount of vapor to be carried away from the condenser by the venting system designed to remove the noncondensable gases.

[†]Recovery of kinetic energy from the incoming vapor may result in $P_o > P_i$, but this effect is currently ignored.



Figure C-6. Condenser configuration 8 with random packing

The volume flow rate requirement Q for the venting system is then inversely proportional to the partial pressure of noncondensable gases at the exit and is proportional to the gas absolute temperature

$$\frac{1}{Q} \propto \frac{PP_{io}}{T_{io}} \quad (C-3)$$

For the ideal condenser, we may write the volume flow requirement as

$$\frac{1}{Q_{id}} \propto \frac{[P_i - P_{sat}(T_{wi})]}{(T_{wi} + 273.15)} \quad (C-4)$$

The venting volume flow requirement increases for an actual condenser. Because of incomplete condensation within a finite length, the outgoing vapor does not come to equilibrium with the incoming water, in other words, $T_{so} > T_{wi}$. This results in lower partial pressure for the noncondensable gases at the exit. In

addition the exit static pressure is reduced by Δp , the incurred pressure loss. Thus, for the actual condenser, we write

$$\frac{1}{Q} \propto \frac{[P_i - \Delta p - P_{sat}(T_{so})]}{(T_{so} + 273.15)} \quad (C-5)$$

Here T_{so} is the saturation temperature of the outgoing steam.

Now the condenser vent fraction is defined as

$$V = \frac{Q_{id}}{Q} = \frac{[P_i - \Delta p - P_{sat}(T_{so})](T_{wi} + 273.15)}{[P_i - P_{sat}(T_{wi})](T_{so} + 273.15)} \quad (C-6)$$

We note that $\epsilon = 1$ and $V = 1$ represent the maximum ideal performance we may expect from the condenser. The condenser effectiveness ϵ provides a measure of the heat- and mass-transfer efficiencies and V a measure of the pressure loss penalty.

For the tested condenser configurations, we find that as ϵ approaches one, V tends to be much smaller than one and vice versa. An efficient operating point lies where both ϵ and V approach unity; this point must be found based on a study of overall system trade-offs.

C.5 Relative Performance

The relative performance of the various tested condenser configurations are compared in a plot of water effectiveness versus vent fraction at similar gas loadings and noncondensable gas concentrations. For the disc and donut baffle contactors (configurations 2 through 4 of Table C-1), measured performances at $0.35 < G < 0.45 \text{ kg/m}^2 \text{ s}$ and $0.7 < X_{i1} < 2.0$ are shown in Figure C-7. For each geometry, the test data show that as ϵ increases, V decreases and vice versa. The top righthand corner of this figure with $\epsilon = 1$ and $V = 1$ represents an ideal condenser with possible maximum performance. The farther away from this corner a condenser performance falls, the worse it is. Within the set of data shown for the three configurations, the single pair disc-donut baffle yields the lowest performance, limited to a region of $\epsilon < 0.6$ and $V < 0.4$. Using a second pair of baffles improves the performance considerably, expanding the operating range to $\epsilon < 0.7$ and $V < 0.65$. For the tests with three pairs of baffles, the improvement in performance from the two pairs is only minimal. The three pairs allow operation at a vent fraction of up to 0.75. For the entire set of data for these types of contactors, the performance was limited to ϵ and V less than about 0.8.

Similar comparisons of performance configurations 1, 5, 6, and 8 of Table C-1 are shown in Figure C-8. Features similar to those shown in Figure C-7 are seen here as well. All sets of data in this figure yield performance measures higher than those for the disc-donut baffles shown in Figure C-7. Increasingly better performance was observed with the configurations in the following sequence: spiral screen, random packing, spiral mat, and structured packing. The data range for the random packing is limited to $V < 0.4$; although the data for rubber mat and random packing appear to be equivalent in this figure, the random packings yielded substantially higher vapor pressure loss (see tables

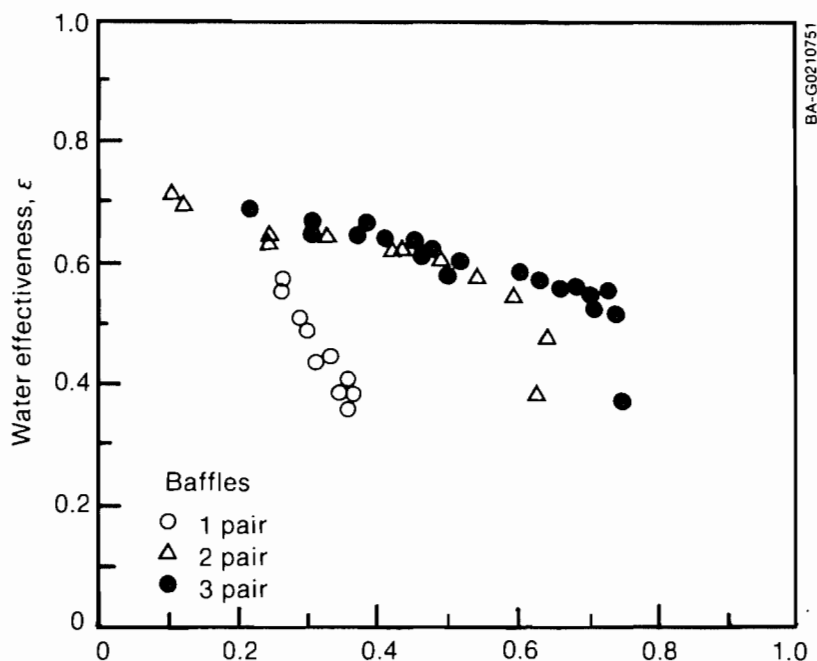


Figure C-7. Performance of countercurrent disc-donut baffle condensers

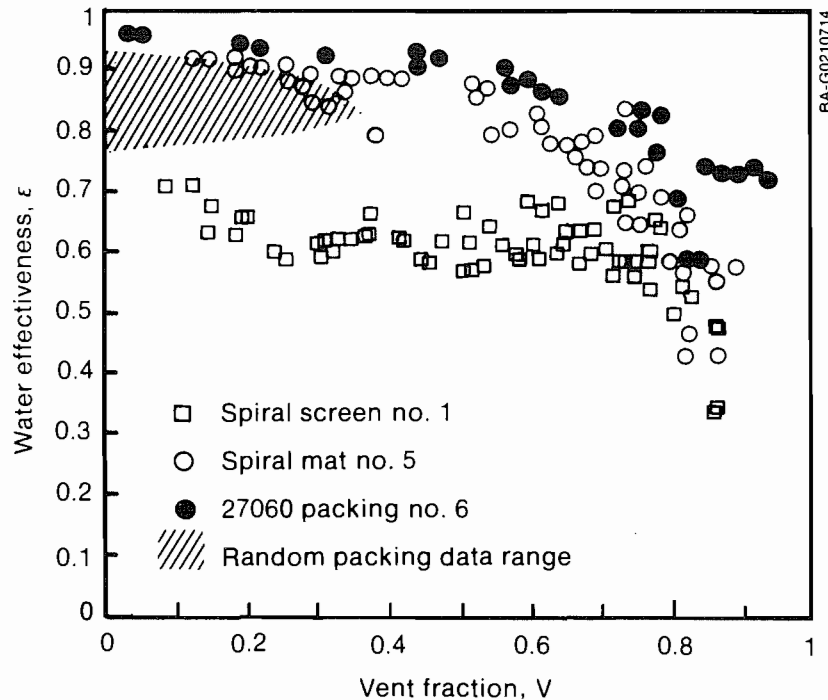


Figure C-8. Relative performance comparisons of countercurrent condenser configurations

in Appendix E). Among the four sets of data shown for $0.35 < G < 0.5 \text{ kg/m}^2 \text{ s}$ in Figure C-8, the use of structured packing as the gas-liquid contactor yields the highest performance, with ϵ falling in the range of $0.7 < \epsilon < 0.95$ for a vent fraction of up to $V = 0.95$.

Entire test data for the structured packings are tabulated in Appendix D. The data for configurations not using structured packings, namely, configurations 1 through 5 and 8 listed in Table C-1 are provided in Appendix E.

Early test results, such as shown in Figures C-7 and C-8, guided us to identify the structured packings as the most promising method for steam-water contact in a direct-contact condenser application and allowed us to concentrate our modeling efforts for condensers using structured packings.

C.6 References

- Fair, J. R., 1961 (Aug.), "Design of Direct-Contact Gas Coolers," Petroleum and Chemical Engineer, Vol. 2, pp. 203-210.
- Fair, J. R., 1972 (June), "Designing Direct-Contact Coolers/Condensers," Chemical Engineering, Vol. 2, pp. 91-100. (See also, "Process Heat Transfer by Direct Fluid Phase Contact," Chemical Engineering Progress Symposium series no. 118, Vol. 68, pp 1-11, 1972.)
- Panchal, C. B., and Bell, K. J., 1984, Theoretical Analysis of Condensation in the Presence of Noncondensable Gases as Applied to Open Cycle OTEC Condensers, ASME paper 84-WA/Sol-27, New York: American Society of Mechanical Engineers.

APPENDIX D DATA TABLES FOR EXPERIMENTS USING STRUCTURED PACKINGS

A complete set of experimental data and model predictions for structured packings are provided in the accompanying tables. Cocurrent test data are contained in Tables D-1 through D-4 for AX, 19060, 4X packings, and for free-falling jets, respectively. Tables D-5 through D-8 contain data for counter-current condensers using AX, 19060, 3X, and 27060 packings, respectively. Details of the packing geometry may be found in Section 3.0.

Most of the tables have 10 columns. Column 1 refers to a serial number. Column 2, labeled T_{si} , represents the measured saturation temperature of the incoming steam and inert gas mixture in degrees Celsius. The uncertainty in this measurement is $\pm 0.02^\circ\text{C}$. Column 3, labeled T_{wi} , represents the measured water inlet temperature in degrees Celsius with an uncertainty of $\pm 0.01^\circ\text{C}$.

Column 4, labeled G , is the condenser gas loading defined as the entire mass flow rate of the steam and inert gas mixture divided by the planform area of the condenser. This quantity is expressed in kilograms per square meter per second and possesses an uncertainty of $\pm 2.5\%$ of the measured value.

Column 5, labeled Ja , is the Jakob number, defined in Eq. 4-1, with an uncertainty of $\pm 1.9\%$. Column 6, labeled X_{ii} , is the inert gas mass concentration in the incoming steam expressed as a percentage of the total steam and inert gas mixture flow. This quantity is estimated to possess an uncertainty of $\pm 2.4\%$ of the quoted value.

Column 7 represents the amount of steam condensed within the contactor expressed as a percentage of the incoming steam flow with an uncertainty of $\pm 1.9\%$ of the incoming steam flow. Column 8 represents the measured overall condenser pressure loss (static pressure difference between inlet and outlet gas streams) expressed in Pascals with an uncertainty of ± 10 Pa or $\pm 10\%$ of the quoted value, whichever is greater. Columns 9 and 10 represent the predicted condensed steam and pressure loss directly comparable to columns 7 and 8, respectively.

Columns 11 and 12, where present, show a second set of comparisons of predictions made that assume the packing extends the full free-fall height of water.

A list of minimum, maximum, average, and standard deviation for each column is provided at the end of each table. Also provided are the average and standard deviation of the difference between model prediction (length is specified) and the experimental data for condensed steam and pressure loss.

Note that Table D-4 for free-falling jets does not contain any predictions.

Table D-1. Cocurrent Condenser Data for AX Packing

No	T _{si} (C)	T _{wi} (C)	G kg/sm ²	Ja	X _{ii} (%)	Measured	Model (l=0.18m)	Cond- ensed Steam (%)	Press- ure Loss (Pa)
						Cond- ensed Steam (%)	Cond- ensed Steam (%)		
1	12.89	5.24	0.266	0.864	0.508	80.68	11.04	81.25	14.70
2	12.84	5.12	0.268	0.879	0.500	81.88	12.02	82.32	14.64
3	13.03	5.44	0.259	0.892	0.519	82.69	9.97	82.96	13.72
4	12.87	5.09	0.261	0.895	0.517	83.03	9.21	83.27	13.90
5	12.67	5.25	0.252	0.898	0.532	82.97	9.34	83.12	13.57
6	12.40	5.00	0.248	0.906	0.540	83.41	9.75	83.47	13.44
7	12.69	5.16	0.253	0.907	0.531	83.72	9.88	83.71	13.44
8	12.70	5.26	0.249	0.907	0.538	83.63	9.38	83.62	13.24
9	12.25	4.86	0.248	0.908	0.541	83.54	9.74	83.55	13.52
10	12.50	5.05	0.246	0.908	0.548	83.72	8.83	83.62	13.19
11	12.79	5.44	0.242	0.916	0.553	84.17	8.87	83.98	12.67
12	13.23	5.13	0.265	0.920	0.510	85.10	10.06	84.93	13.41
13	12.80	5.51	0.239	0.923	0.561	84.55	8.82	84.22	12.40
14	12.35	4.80	0.246	0.923	0.548	84.81	9.11	84.46	13.08
15	13.04	4.93	0.263	0.925	0.513	85.40	8.97	85.17	13.40
16	13.50	5.31	0.263	0.931	0.513	85.94	8.57	85.55	12.95
17	12.73	4.98	0.250	0.933	0.539	85.67	8.81	85.16	12.89
18	12.48	5.25	0.231	0.948	0.581	85.83	7.89	85.24	11.92
19	13.73	5.29	0.262	0.964	0.515	88.31	7.83	87.16	12.32
20	11.02	4.97	0.267	0.969	0.507	85.02	13.53	84.53	16.58
21	12.49	5.17	0.228	0.969	0.588	87.20	6.95	86.13	11.52
22	11.08	4.98	0.267	0.975	0.503	85.41	13.52	84.90	16.37
23	11.16	5.05	0.267	0.976	0.503	85.40	13.18	84.94	16.28
24	11.15	5.08	0.263	0.984	0.511	85.73	12.73	85.16	15.93
25	12.16	4.95	0.253	0.985	0.531	87.44	9.37	86.69	13.42
26	11.28	5.29	0.260	0.987	0.518	85.78	12.71	85.18	15.56
27	11.10	5.11	0.257	0.994	0.522	86.09	12.98	85.39	15.49
28	11.04	4.98	0.260	0.995	0.517	86.19	12.33	85.53	15.70
29	11.08	4.97	0.259	1.008	0.518	86.97	11.81	86.02	15.43
30	12.49	5.19	0.249	1.011	0.540	88.72	8.47	87.59	12.69
31	12.72	5.11	0.227	1.014	0.590	89.64	6.46	87.85	10.94
32	12.48	5.31	0.244	1.018	0.553	88.98	8.36	87.61	12.34
33	12.31	5.25	0.235	1.035	0.572	89.59	7.36	87.91	11.89
34	12.13	5.15	0.230	1.043	0.584	89.82	7.25	87.98	11.69
35	12.12	5.13	0.227	1.059	0.593	90.41	7.67	88.33	11.39
36	12.13	5.22	0.223	1.065	0.604	90.48	7.20	88.33	11.15
37	11.47	4.96	0.261	1.066	0.514	89.86	10.38	88.16	14.52
38	11.93	5.07	0.220	1.070	0.612	90.73	6.85	88.37	11.11
39	11.73	5.12	0.259	1.090	0.519	90.85	9.40	88.78	13.93
40	13.20	4.94	0.227	1.100	0.591	93.41	5.76	90.31	10.01
41	12.23	5.09	0.215	1.136	0.627	92.85	5.87	89.78	10.25
42	12.64	5.14	0.213	1.204	0.630	94.71	5.43	90.95	9.63

Table D-1. Cocurrent Condenser Data for AX Packing (Concluded)

No	Tai (C)	Twi (C)	G kg/sm ²	Ja	Xii (%)	Measured		Model (l=0.18m)	
						Cond- ensed Steam (%)	Press- ure Loss (Pa)	Cond- ensed Steam (%)	Press- ure Loss (Pa)
43	12.37	5.06	0.257	1.210	0.522	94.65	7.47	91.26	12.42
44	13.63	4.70	0.223	1.212	0.602	95.97	4.98	92.16	9.07
45	12.91	5.05	0.212	1.271	0.635	95.91	5.45	91.84	9.15
46	12.81	5.04	0.257	1.289	0.523	96.23	6.47	92.33	11.66
47	14.22	4.54	0.219	1.335	0.612	97.32	4.22	93.41	8.24
48	12.29	4.86	0.239	1.075	1.116	87.70	9.61	85.01	13.95
49	12.88	5.09	0.241	1.122	1.110	89.84	9.02	86.31	13.22
50	12.60	5.28	0.209	1.211	1.277	90.94	7.11	86.58	11.31
51	12.98	4.98	0.203	1.361	1.311	93.88	6.11	88.64	10.19
Minimum:									
	11.02	4.54	0.203	0.864	0.500	80.68	4.22	81.25	8.24
Maximum:									
	14.22	5.51	0.268	1.361	1.311	97.32	13.53	93.41	16.58
Average:									
	12.42	5.10	0.245	1.023	0.599	87.90	8.90	86.48	12.85
Standard Deviation:									
	0.74	0.18	0.018	0.124	0.182	4.16	2.32	2.82	1.96

Difference Between Predictions and Experiment:

	No. of Points	Average	Standard Deviation
Condensed Steam (%)	51	-1.40	1.50
Pressure Loss (Pa)	51	4.00	0.60

Table D-2. Cocurrent Condenser Data for 19060 Packing

No	Tsi (C)	Twi (C)	G kg/sm ²	Ja	Xii (%)	Measured	Model (l=0.61m)	Cond- ensed Steam (%)	Press- ure Loss (Pa)	Cond- ensed Steam (%)	Press- ure Loss (Pa)
						Cond- ensed Steam (%)	Press- ure Loss (Pa)				
1	11.00	5.27	0.178	1.144	0.064	89.05	16.50	97.14	4.61		
2	11.10	5.47	0.169	1.179	0.067	89.77	14.39	96.96	4.20		
3	11.11	5.45	0.167	1.200	0.068	90.69	13.71	96.97	4.09		
4	11.13	5.46	0.162	1.241	0.070	91.69	11.79	96.85	3.85		
5	11.21	5.45	0.156	1.304	0.072	92.98	11.23	96.75	3.55		
6	11.29	5.40	0.154	1.354	0.074	93.98	10.13	96.67	3.40		
7	13.40	5.20	0.243	1.204	0.078	90.54	17.81	97.70	5.92		
8	13.62	5.35	0.239	1.236	0.079	91.38	15.14	97.62	5.61		
9	8.50	4.96	0.223	1.238	0.085	92.71	27.49	97.32	10.43		
10	13.84	5.43	0.236	1.267	0.080	92.15	14.29	97.58	5.36		
11	8.73	5.07	0.224	1.274	0.085	93.72	24.28	97.47	10.07		
12	13.90	5.49	0.230	1.299	0.082	93.09	12.46	97.49	5.10		
13	9.00	5.20	0.226	1.311	0.084	94.96	19.98	97.45	9.59		
14	13.80	5.47	0.220	1.339	0.086	93.82	9.85	97.43	4.81		
15	9.24	5.35	0.222	1.367	0.086	95.97	16.93	97.37	8.85		
16	17.98	4.99	0.367	1.231	0.096	91.65	20.38	98.13	8.27		
17	17.88	5.05	0.358	1.241	0.099	92.19	17.91	98.08	8.01		
18	16.94	4.76	0.342	1.243	0.103	91.60	19.77	98.09	7.97		
19	17.86	5.21	0.347	1.266	0.102	92.65	15.66	98.04	7.64		
20	17.82	5.09	0.338	1.305	0.105	93.36	14.02	98.00	7.28		
21	18.09	4.92	0.337	1.354	0.105	94.18	13.14	97.95	6.98		
22	10.94	5.34	0.321	1.359	0.110	94.05	41.62	98.05	13.80		
23	10.93	5.22	0.322	1.378	0.110	94.80	40.54	98.07	13.65		
24	14.28	5.05	0.648	1.110	0.630	88.69	88.94	91.50	56.80		
25	14.40	5.04	0.644	1.130	0.630	89.23	88.60	92.16	54.54		
26	14.63	5.08	0.646	1.150	0.630	89.86	86.10	92.75	52.95		
27	15.01	5.25	0.649	1.170	0.620	90.75	82.91	93.36	50.90		
28	15.40	5.18	0.646	1.230	0.630	92.30	78.07	94.45	47.11		
29	13.93	5.60	0.510	0.950	0.790	82.64	78.17	84.53	44.89		
30	14.24	5.84	0.511	0.960	0.790	82.94	63.07	85.26	43.52		
31	14.42	5.79	0.514	0.980	0.790	84.01	65.38	86.55	42.10		
32	14.73	5.76	0.512	1.020	0.790	86.27	57.27	88.73	38.82		
33	14.96	5.79	0.507	1.050	0.800	87.97	49.53	89.97	36.46		
34	15.46	6.04	0.508	1.070	0.800	89.37	41.22	90.82	34.62		
35	16.51	6.84	0.509	1.100	0.790	90.87	20.47	91.86	31.63		
36	13.96	5.11	0.519	1.190	0.780	92.76	63.87	92.74	38.11		
37	14.18	5.29	0.522	1.190	0.780	92.88	63.94	92.76	37.95		
38	14.10	5.22	0.516	1.210	0.780	93.05	62.55	93.08	37.00		

Table D-2. Cocurrent Condenser Data for 19060 Packing (Concluded)

No	T _{si} (C)	T _{wi} (C)	G kg/sm ²	Ja	X _{ii} (%)	Measured	Model (l=0.61m)	Cond- ensed Steam (%)	Press- ure Loss (Pa)	Cond- ensed Steam (%)	Press- ure Loss (Pa)
						Cond- ensed Steam (%)	Press- ure Loss (Pa)				
39	14.49	5.33	0.523	1.230	0.770	93.46	63.27	93.57	36.18		
40	14.56	5.32	0.518	1.250	0.780	93.93	61.76	93.82	35.11		
41	14.68	5.30	0.518	1.270	0.780	94.26	60.17	94.12	34.40		
42	15.35	5.08	0.514	1.400	0.790	96.37	55.61	95.46	30.48		
43	13.40	5.72	0.463	1.080	0.870	89.13	64.53	89.08	36.85		
44	12.97	5.35	0.461	1.080	0.880	88.86	63.64	88.89	37.81		
45	13.05	5.34	0.456	1.110	0.890	89.57	61.77	89.82	36.09		
46	13.36	5.53	0.459	1.110	0.880	90.12	60.55	90.03	35.47		
47	13.48	5.32	0.451	1.180	0.890	92.11	57.85	91.80	32.38		
48	13.99	5.56	0.452	1.220	0.890	93.03	58.78	92.64	30.60		
Minimum:											
	8.50	4.76	0.15	0.95	0.06	82.64	9.85	84.53	3.40		
Maximum:											
	18.09	6.84	0.65	1.40	0.89	96.37	88.94	98.13	56.80		
Average:											
	13.73	5.36	0.39	1.20	0.45	91.36	42.02	94.23	24.08		
Standard Deviation:											
	2.40	0.34	0.15	0.11	0.35	3.00	25.78	3.76	17.26		

Difference Between Predictions and Experiment:

	No. of Points	Average	Standard Deviation
Condensed Steam (%)	48	2.80	2.40
Pressure Loss (Pa)	48	-17.60	10.40

Table D-3. Cocurrent Condenser Data for 4X Packing

No	T _{ai} (C)	T _{wi} (C)	G kg/sm ²	Ja	X _{ii} (%)	Measured	Press-	Model (l=1.08m)	Press-
						Cond- ensed Steam (%)	ure Loss (Pa)	Cond- ensed Steam (%)	ure Loss (Pa)
1	11.95	4.57	0.266	0.843	0.504	80.32	12.27	80.53	12.73
2	11.36	5.29	0.227	0.847	0.590	79.40	10.81	79.72	10.86
3	12.31	4.83	0.267	0.847	0.502	80.66	12.20	80.97	12.39
4	12.55	4.81	0.275	0.847	0.487	80.86	12.57	81.17	12.67
5	12.80	5.02	0.273	0.856	0.492	81.50	11.70	81.93	12.14
6	13.30	5.49	0.269	0.865	0.498	82.25	11.07	82.70	11.32
7	11.45	5.39	0.220	0.867	0.607	80.80	10.23	81.14	10.00
8	11.66	5.51	0.219	0.880	0.610	81.77	10.04	82.12	9.60
9	11.81	5.58	0.217	0.899	0.616	83.26	9.37	83.40	9.13
10	9.84	4.03	0.193	0.947	0.692	85.41	8.73	85.16	8.38
11	10.42	4.55	0.191	0.977	0.701	87.17	8.04	86.52	7.77
12	10.92	4.13	0.187	1.141	0.713	93.49	7.09	91.69	6.34
13	12.43	5.08	0.394	0.905	0.680	82.13	25.50	81.91	27.13
14	12.30	4.95	0.394	0.907	0.681	82.16	25.97	81.99	27.31
15	12.43	5.13	0.387	0.914	0.694	82.77	24.50	82.40	26.09
16	12.64	5.27	0.387	0.921	0.693	83.29	24.08	82.94	25.43
17	12.67	5.21	0.381	0.946	0.704	85.01	23.27	84.39	23.95
18	13.13	4.93	0.378	1.048	0.710	90.96	18.91	89.12	20.41
19	12.06	4.99	0.451	0.979	0.744	84.95	38.25	83.62	36.52
20	12.32	5.09	0.452	0.999	0.743	86.47	36.21	84.78	35.10
21	12.36	4.93	0.455	1.016	0.737	87.67	35.61	85.75	34.51
22	12.29	4.60	0.458	1.045	0.733	89.44	34.44	87.09	33.84
23	13.10	5.12	0.458	1.079	0.732	91.23	31.65	88.54	30.93
24	13.21	4.82	0.457	1.137	0.734	93.60	28.13	90.27	29.03
25	13.67	4.72	0.464	1.196	0.724	95.40	26.32	91.73	27.56
26	14.58	4.23	0.462	1.389	0.726	97.78	22.33	94.25	23.17
27	13.26	5.13	0.502	0.933	0.668	83.41	40.71	82.87	40.36
28	13.40	5.26	0.498	0.942	0.674	84.18	41.03	83.44	38.99
29	13.30	5.03	0.496	0.963	0.676	85.55	39.29	84.67	37.86
30	13.27	5.21	0.496	1.060	0.675	90.35	36.16	88.07	35.92
31	14.45	4.29	0.500	1.175	0.671	95.68	27.42	92.43	28.69
32	14.54	4.94	0.504	1.223	0.665	96.33	27.39	92.65	29.29
33	13.82	5.20	0.528	0.916	0.636	82.65	43.19	82.46	42.52
34	13.70	5.23	0.519	0.917	0.647	82.69	43.53	82.37	41.72
35	12.91	5.13	0.518	0.965	0.647	84.66	45.47	83.76	43.88
36	13.10	5.29	0.514	0.975	0.652	85.66	44.92	84.39	42.18
37	13.49	5.59	0.514	0.987	0.652	86.62	42.18	85.17	40.45

Table D-3. Cocurrent Condenser Data for 4X Packing (Concluded)

No	T _{ai} (C)	T _{wi} (C)	G kg/sm^2	Ja	X _{ii} (%)	Measured		Model (l=1.08m)	
						Cond- ensed Steam (%)	Press- ure Loss (Pa)	Cond- ensed Steam (%)	Press- ure Loss (Pa)
Minimum:									
	9.84	4.03	0.187	0.843	0.487	79.40	7.09	79.72	6.34
Maximum:									
	14.58	5.59	0.528	1.389	0.744	97.78	45.47	94.25	43.88
Average:									
	12.67	4.99	0.388	0.982	0.657	86.15	25.69	85.08	25.57
Standard Deviation:									
	1.04	0.38	0.116	0.122	0.074	5.01	12.55	3.81	12.04

Difference Between Predictions and Experiment:

	No. of Points	Average	Standard Deviation
Condensed Steam (%)	37	-1.10	1.30
Pressure Loss (Pa)	37	-0.10	1.20

Table D-4. Cocurrent Condenser Data for Falling Jets

No	T _{ai} (C)	T _{wi} (C)	G kg/sm ²	Ja	X _{ii} (%)	Measured	
						Cond- ensed Steam (%)	Press- ure Loss (Pa)
1	14.08	5.41	0.155	1.999	0.604	85.08	3.96
2	13.95	5.16	0.151	2.080	0.618	86.13	3.53
3	14.43	4.91	0.157	2.174	0.597	87.92	3.15
4	14.91	4.84	0.161	2.242	0.582	89.74	3.29
5	16.08	4.93	0.171	2.326	0.546	91.56	1.84
6	16.86	5.14	0.169	2.481	0.554	93.13	2.09
7	17.91	5.38	0.173	2.582	0.541	94.57	1.82
8	16.53	5.11	0.173	2.344	1.608	84.78	3.78
9	17.25	5.10	0.178	2.430	1.570	86.19	3.71
10	17.79	5.20	0.179	2.496	1.557	87.83	2.46
11	18.57	5.35	0.179	2.611	1.554	89.26	2.56
12	19.03	5.43	0.179	2.687	1.557	90.87	2.26
13	13.35	5.15	0.187	2.048	0.503	88.18	6.10
14	13.46	5.25	0.181	2.119	0.520	89.30	4.60
15	13.51	5.30	0.177	2.164	0.532	90.42	3.77
16	13.46	5.36	0.165	2.292	0.571	91.39	3.69
17	13.44	5.27	0.155	2.448	0.604	92.59	2.66
18	13.60	5.14	0.151	2.621	0.624	93.86	2.32
19	14.03	5.00	0.145	2.909	0.649	95.34	1.71
20	18.66	5.49	0.226	2.050	0.690	86.40	6.03
21	17.89	5.39	0.206	2.133	0.758	87.01	5.30
22	17.61	5.37	0.197	2.189	0.793	87.44	4.26
23	17.56	5.21	0.191	2.268	0.816	88.53	3.17
24	17.91	5.08	0.188	2.398	0.830	89.89	3.75
25	18.45	4.85	0.192	2.488	0.812	91.66	2.99
26	19.06	4.79	0.196	2.569	0.798	92.89	2.41
27	20.66	5.09	0.236	2.308	1.961	85.84	6.36
28	20.94	5.22	0.230	2.395	2.010	86.99	5.26
29	21.14	5.37	0.220	2.507	2.100	87.76	4.52
30	21.36	5.39	0.216	2.584	2.136	88.83	4.17
31	21.50	5.40	0.208	2.706	2.217	89.59	2.95
32	21.74	5.47	0.202	2.811	2.282	90.37	2.44
33	21.95	5.42	0.194	2.979	2.378	91.38	1.93
34	15.72	4.91	0.242	2.086	0.647	89.53	6.94
35	16.02	5.02	0.238	2.151	0.655	90.34	5.38
36	16.26	5.10	0.234	2.220	0.666	91.30	4.61
37	16.53	5.12	0.230	2.308	0.678	92.23	4.48

Table D-4. Cocurrent Condenser Data for Falling Jets (Concluded)

No	Tsi (C)	Twi (C)	G kg/sm ²	Ja	Xii (%)	Measured	
						Cond- ensed Steam (%)	Press- ure Loss (Pa)
38	16.78	5.15	0.224	2.413	0.696	93.18	4.20
39	17.12	5.17	0.219	2.545	0.714	94.12	2.93
40	17.56	5.12	0.215	2.694	0.726	95.08	2.80
41	18.20	5.06	0.208	2.944	0.751	96.12	1.97
42	14.49	5.31	0.154	2.800	1.809	87.54	5.10
43	14.57	5.14	0.149	2.984	1.871	88.92	3.86
44	15.04	4.90	0.151	3.145	1.837	90.57	3.94
45	15.87	4.76	0.155	3.369	1.794	92.50	3.71
46	13.06	5.12	0.320	1.927	0.489	93.45	15.89
47	13.05	4.94	0.316	1.992	0.495	94.07	14.60
48	13.17	4.87	0.313	2.055	0.499	94.60	14.14
49	13.36	4.79	0.314	2.116	0.498	95.29	10.85
50	13.73	4.86	0.313	2.197	0.500	95.86	11.32
51	14.37	4.92	0.323	2.265	0.484	96.61	10.53
52	14.79	5.02	0.314	2.410	0.498	97.20	8.92
53	15.31	5.00	0.311	2.571	0.504	97.75	8.19
54	15.58	5.12	0.336	2.064	0.466	92.55	11.53
55	15.76	5.10	0.335	2.109	0.468	93.19	10.50
56	16.03	5.19	0.329	2.180	0.475	93.73	9.47
57	16.31	5.11	0.332	2.235	0.472	94.59	8.45
58	16.68	5.16	0.323	2.362	0.485	95.36	7.68
59	17.04	5.10	0.326	2.420	0.479	96.08	7.30
60	17.49	5.07	0.320	2.567	0.489	96.72	6.52
61	18.32	5.06	0.310	2.830	0.505	97.54	5.69
Minimum:							
	13.05	4.76	0.14	1.93	0.47	84.78	1.71
Maximum:							
	21.95	5.49	0.34	3.37	2.38	97.75	15.89
Average:							
	16.51	5.13	0.22	2.42	0.94	91.46	5.35
Standard Deviation:							
	2.44	0.19	0.06	0.31	0.59	3.45	3.37

Table D-5. Countercurrent Condenser Data for AX Packing

No	T _{ai} (C)	T _{wi} (C)	G kg/sm ²	J _a	X _{ii} (%)	Measured	Press-	Model (l=0.36m)	Press-
						Cond- ensed Steam (%)	ure Loss (Pa)	Cond- ensed Steam (%)	ure Loss (Pa)
1	11.29	5.63	0.100	1.062	6.225	89.88	6.85	89.90	12.45
2	11.34	5.63	0.076	1.427	8.102	89.33	5.87	88.90	8.63
3	12.30	5.23	0.074	3.667	8.276	91.70	5.76	91.80	6.93
4	11.48	5.29	0.068	4.727	8.941	89.97	7.47	89.93	7.17
5	11.27	5.81	0.093	1.087	12.496	81.82	7.11	81.22	15.06
6	10.89	5.56	0.061	1.615	17.830	78.19	6.11	78.14	10.00
7	11.40	5.63	0.056	1.957	10.701	86.61	5.43	86.99	6.55
8	11.32	5.61	0.043	2.524	13.518	83.49	5.45	84.65	5.44
9	10.81	5.38	0.027	3.803	19.832	77.50	5.44	79.32	4.20
10	12.04	4.99	0.044	6.094	13.066	87.58	4.98	88.46	5.00
11	11.34	5.25	0.048	6.583	12.232	86.90	6.47	87.09	5.81
12	11.59	4.83	0.029	8.907	18.674	83.04	4.22	84.36	4.11
13	10.67	5.27	0.046	2.191	22.515	74.11	5.58	75.86	8.01
14	10.58	5.25	0.040	2.461	24.822	71.95	5.45	74.37	7.23
15	10.23	5.31	0.031	2.941	29.966	67.25	4.89	69.82	6.26
16	10.26	5.34	0.027	3.433	33.286	65.59	4.52	68.26	5.68
17	10.11	4.95	0.015	6.391	30.433	69.50	4.87	72.09	3.10
18	10.89	4.45	0.018	13.368	26.564	76.94	3.49	79.22	3.33
19	11.58	5.68	0.115	0.967	5.461	86.03	7.25	90.32	15.83
20	11.52	5.71	0.107	1.028	5.861	88.60	7.67	90.37	13.46
21	11.50	5.75	0.104	1.039	6.004	89.55	7.20	90.18	12.98
22	11.96	5.46	0.144	1.730	4.416	94.91	6.95	94.12	13.15
23	12.13	5.39	0.116	2.222	5.418	94.09	6.46	93.60	10.25
24	10.98	5.18	0.130	2.300	4.850	93.90	10.38	92.97	12.72
25	11.20	5.34	0.117	2.598	5.393	93.34	9.40	92.53	11.36
26	11.89	5.62	0.121	0.968	9.944	81.66	9.02	84.60	19.47
27	16.92	5.13	0.141	6.111	10.526	94.21	15.43	94.08	11.48
28	12.37	5.72	0.189	1.344	3.395	95.03	8.87	95.05	18.10
29	12.36	5.80	0.182	1.380	3.522	95.33	8.82	94.86	17.28
30	11.94	5.06	0.184	1.393	3.502	93.25	20.28	95.21	17.49
31	12.64	5.19	0.189	1.473	3.409	95.49	16.75	95.83	16.38
32	12.31	5.24	0.177	1.497	3.646	94.97	15.86	95.31	15.86
33	10.76	5.30	0.185	1.534	3.472	93.51	12.73	93.70	20.09
34	12.01	5.54	0.161	1.535	3.958	95.32	7.89	94.45	15.03
35	10.89	5.51	0.182	1.540	3.529	93.74	12.71	93.51	19.71
36	13.08	5.57	0.182	1.543	3.537	96.11	13.35	95.80	15.10
37	10.70	5.33	0.176	1.582	3.633	94.03	12.98	93.41	19.06

Table D-5. Countercurrent Condenser Data for AX Packing (Continued)

No	Tai (C)	Twi (C)	G kg/sm ²	Ja	Xii (%)	Measured		Model (l=0.36m)	
						Cond- ensed Steam (%)	Press- ure Loss (Pa)	Cond- ensed Steam (%)	Press- ure Loss (Pa)
38	10.64	5.19	0.177	1.595	3.623	94.26	12.33	93.55	19.08
39	10.66	5.18	0.166	1.710	3.844	94.40	11.81	93.42	17.47
40	13.28	5.55	0.151	1.922	4.241	96.06	8.58	95.49	11.78
41	13.06	5.54	0.184	1.360	8.284	90.99	35.30	89.69	23.51
42	16.57	5.15	0.161	5.195	9.350	94.62	18.50	94.28	13.16
43	12.66	5.72	0.220	1.204	2.926	89.40	9.97	95.58	22.36
44	12.28	5.53	0.211	1.221	3.046	90.25	9.34	95.32	21.74
45	12.49	5.33	0.218	1.232	2.974	89.30	33.13	95.76	21.66
46	11.99	5.29	0.203	1.264	3.170	92.15	9.75	95.22	20.68
47	11.85	5.14	0.201	1.277	3.197	93.23	9.74	95.22	20.45
48	12.09	5.32	0.197	1.283	3.274	89.94	27.44	95.20	19.61
49	12.30	5.55	0.201	1.286	3.201	94.40	9.38	95.27	19.81
50	12.30	5.45	0.203	1.293	3.174	93.72	9.88	95.40	19.85
51	12.84	5.39	0.194	1.434	3.323	95.79	16.22	95.88	16.82
52	10.79	5.28	0.192	1.494	3.347	91.81	13.18	93.89	20.98
53	10.70	5.20	0.192	1.498	3.350	91.88	13.52	93.87	21.09
54	13.02	5.75	0.204	1.188	7.525	86.17	37.02	89.34	28.27
55	12.92	5.58	0.204	1.203	7.546	88.79	37.97	89.49	28.16
56	15.93	4.92	0.210	3.803	7.348	95.60	18.94	94.83	17.53
57	16.07	5.16	0.198	4.049	7.757	95.24	24.33	94.59	16.50
58	15.73	5.40	0.304	2.462	5.188	96.49	33.73	95.36	27.13
59	15.68	5.32	0.290	2.582	5.417	96.43	30.49	95.28	25.67
60	15.84	5.15	0.250	3.104	6.243	96.09	24.36	95.11	21.27
Minimum:									
	10.11	4.45	0.015	0.967	2.926	65.59	3.49	68.26	3.10
Maximum:									
	16.92	5.81	0.304	13.368	33.286	96.49	37.97	95.88	28.27
Average:									
	12.17	5.37	0.142	2.545	8.705	89.19	12.75	90.12	14.91
Standard Deviation:									
	1.63	0.26	0.071	2.184	7.611	7.65	8.97	7.06	6.61

Table D-5. Countercurrent Condenser Data for AX Packing (Concluded)

No	T _{si} (C)	T _{wi} (C)	G kg/sm ²	J _a	X _{ii} (%)	Measured	Model (l=0.36m)	Condensed Steam (%)	Press- ure Loss (Pa)
						Cond- ensed Steam (%)	Press- ure Loss (Pa)		

Difference Between Predictions and Experiment:

	No. of Points	Average	Standard Deviation
Condensed Steam (%)	60	0.90	1.90
Pressure Loss (Pa)	60	2.20	6.00

Table D-6. Countercurrent Condenser Data for 19060 Packing

No	T _{ai} (C)	T _{wi} (C)	G kg/sm ²	J _a	X _{ii} (%)	Measured		Model (l=0.61m)	
						Cond- ensed Steam (%)	Press- ure Loss (Pa)	Cond- ensed Steam (%)	Press- ure Loss (Pa)
1	9.93	5.19	0.175	1.018	0.357	96.02	13.97	98.87	20.75
2	9.93	5.27	0.172	1.018	0.364	95.93	13.56	98.96	18.61
3	9.93	5.19	0.177	1.018	0.354	96.04	14.66	98.91	20.82
4	9.98	5.30	0.172	1.029	0.364	96.55	11.71	99.12	16.65
5	9.93	5.25	0.170	1.034	0.368	97.22	10.13	99.08	16.70
6	9.97	5.27	0.168	1.055	0.373	97.85	8.34	99.22	14.32
7	9.98	5.26	0.167	1.067	0.373	98.33	7.37	99.28	12.85
8	10.03	5.28	0.165	1.079	0.378	98.62	6.16	99.27	12.28
9	9.98	5.22	0.163	1.097	0.384	98.87	4.98	99.32	10.17
10	10.04	5.16	0.161	1.141	0.389	99.17	2.90	99.34	9.07
11	9.98	4.98	0.175	1.063	0.713	96.31	11.04	98.22	15.59
12	10.02	5.09	0.174	1.074	0.717	96.26	12.61	98.30	13.55
13	9.92	5.03	0.170	1.080	0.730	96.24	11.14	98.29	13.29
14	10.17	5.13	0.174	1.082	0.717	97.23	8.47	98.41	12.83
15	10.20	5.11	0.174	1.094	0.720	97.77	6.59	98.47	12.37
16	10.26	5.09	0.172	1.123	0.728	98.21	5.24	98.56	11.39
17	10.35	5.20	0.166	1.160	0.755	98.47	3.83	98.56	10.64
18	10.49	5.11	0.166	1.212	0.755	98.66	2.32	98.70	9.66
19	11.16	5.11	0.153	1.484	0.819	98.85	0.58	98.92	6.25
20	10.02	5.00	0.173	1.095	1.081	96.65	8.78	97.37	13.27
21	10.27	5.17	0.174	1.098	1.074	96.48	8.22	97.48	12.94
22	10.05	5.07	0.170	1.111	1.100	96.59	8.21	97.32	13.10
23	10.22	5.14	0.169	1.119	1.106	97.15	6.51	97.41	12.62
24	10.46	5.09	0.172	1.164	1.087	97.78	5.90	97.78	11.31
25	11.32	5.08	0.165	1.409	1.127	98.43	1.43	98.35	8.44
26	10.71	5.07	0.186	1.127	1.337	96.88	8.21	97.02	14.59
27	10.52	5.22	0.174	1.159	1.430	96.90	6.74	96.82	12.20
28	10.48	5.29	0.168	1.177	1.481	96.80	5.89	96.63	12.20
29	10.89	5.19	0.178	1.189	1.393	97.39	6.09	97.21	12.20
30	11.07	5.24	0.178	1.216	1.395	97.59	5.02	97.33	11.63
31	11.20	5.27	0.175	1.260	1.419	97.75	4.13	97.50	10.11
32	11.06	4.90	0.183	1.269	1.692	97.26	5.45	96.97	11.57
33	11.44	4.96	0.184	1.349	1.685	97.65	3.40	97.30	10.57
34	11.48	5.22	0.166	1.400	1.497	97.93	2.05	97.64	9.20
35	10.54	4.81	0.166	1.312	1.856	97.11	2.87	96.41	11.30
36	10.59	4.91	0.162	1.334	1.908	97.01	2.28	96.39	10.24
37	11.79	5.07	0.180	1.422	1.720	97.78	2.70	97.41	10.00
38	11.48	5.10	0.180	1.488	2.061	97.25	16.14	96.59	10.86

Table D-6. Countercurrent Condenser Data for 19060 Packing (Continued)

No	T _{ai} (C)	T _{wi} (C)	G kg/sm ²	Ja	X _{ii} (%)	Measured	Model (l=0.61m)	Cond- ensed Steam (%)	Press- ure Loss (Pa)
						Cond- ensed Steam (%)	Cond- ensed Steam (%)		
39	11.50	5.17	0.176	1.501	2.097	97.19	14.17	96.48	10.94
40	12.20	5.21	0.173	1.534	1.791	97.86	1.94	97.57	8.62
41	12.53	5.25	0.172	1.603	1.800	97.98	1.21	97.72	8.22
42	12.19	4.93	0.170	1.606	2.174	97.58	1.53	97.12	8.95
43	12.38	4.97	0.169	1.659	2.186	97.64	2.14	97.19	8.74
44	11.28	4.89	0.176	1.785	2.099	97.24	13.36	96.68	10.43
45	11.29	4.90	0.173	1.821	2.135	97.19	15.21	96.73	9.55
46	11.74	5.50	0.160	1.474	2.311	96.87	1.62	96.18	9.40
47	11.15	4.91	0.152	1.542	2.418	96.88	0.26	96.14	8.78
48	11.15	4.95	0.150	1.571	2.459	96.81	0.79	96.05	8.81
49	12.06	5.20	0.157	1.651	2.345	97.23	1.30	96.69	8.60
50	11.33	5.14	0.155	2.227	2.381	96.79	13.21	96.44	8.05
51	11.37	5.25	0.151	2.267	2.441	96.67	13.56	96.29	8.14
52	11.96	5.30	0.249	1.022	0.379	96.83	26.40	99.06	29.50
53	11.90	5.14	0.249	1.033	0.378	96.86	26.40	99.26	26.38
54	11.87	5.03	0.253	1.034	0.372	96.91	26.87	99.31	26.21
55	11.96	4.97	0.256	1.048	0.368	97.28	25.95	99.43	23.93
56	12.07	4.97	0.259	1.054	0.364	97.67	25.89	99.48	23.42
57	12.19	4.99	0.258	1.065	0.365	98.06	23.84	99.50	21.69
58	12.30	4.96	0.258	1.081	0.365	98.49	21.64	99.57	19.22
59	12.42	5.00	0.261	1.092	0.361	98.79	20.70	99.59	18.20
60	12.86	5.25	0.258	1.127	0.365	99.08	17.09	99.63	15.42
61	13.01	5.33	0.258	1.137	0.365	99.21	15.34	99.64	14.83
62	13.13	5.37	0.252	1.178	0.374	99.46	10.36	99.65	12.55
63	12.63	5.40	0.256	1.068	0.731	97.08	21.95	98.68	21.55
64	12.55	5.47	0.250	1.073	0.750	97.59	19.10	98.64	20.29
65	12.26	4.98	0.259	1.076	0.723	97.25	26.44	98.76	21.14
66	12.24	4.99	0.261	1.078	0.717	97.26	31.66	98.75	21.22
67	12.33	5.37	0.243	1.081	0.770	97.88	16.12	98.65	18.53
68	12.12	5.32	0.235	1.095	0.796	98.09	14.83	98.58	18.06
69	12.15	5.10	0.238	1.137	0.786	98.55	13.30	98.79	16.09
70	12.37	5.01	0.233	1.203	0.803	98.89	9.77	98.96	13.07
71	12.99	4.80	0.237	1.303	0.788	99.13	8.57	99.17	11.73
72	13.25	5.50	0.267	1.106	1.049	97.44	21.42	98.22	20.31
73	12.72	5.39	0.251	1.111	1.116	97.45	18.56	98.01	18.81
74	13.24	5.54	0.265	1.112	1.058	97.44	20.69	98.24	18.96
75	12.59	5.28	0.250	1.113	1.121	97.47	18.92	98.00	18.98
76	12.48	4.92	0.255	1.122	1.096	97.51	17.82	98.11	19.76

Table D-6. Countercurrent Condenser Data for 19060 Packing (Continued)

No	T _{si} (C)	T _{wi} (C)	G kg/sm ²	Ja	X _{ii} (%)	Measured		Model (l=0.61m)	
						Cond- ensed Steam (%)	Press- ure Loss (Pa)	Cond- ensed Steam (%)	Press- ure Loss (Pa)
77	12.48	5.18	0.266	1.135	1.053	97.66	20.97	98.10	20.72
78	12.55	4.95	0.254	1.140	1.104	97.92	15.80	98.25	17.52
79	12.46	5.16	0.262	1.149	1.069	97.62	22.14	98.15	19.00
80	12.69	5.01	0.247	1.171	1.134	98.22	13.54	98.28	16.61
81	11.62	5.23	0.249	1.177	1.127	97.79	20.09	97.67	19.31
82	11.57	5.27	0.242	1.195	1.159	97.73	19.99	97.67	17.72
83	12.86	4.99	0.249	1.197	1.126	98.45	12.38	98.40	15.64
84	11.54	5.11	0.259	1.215	1.083	97.87	21.61	97.81	19.87
85	11.48	5.07	0.254	1.235	1.104	97.84	22.12	97.86	18.20
86	11.05	5.07	0.245	1.278	1.142	97.88	21.71	97.58	18.69
87	11.07	5.19	0.239	1.290	1.170	97.82	20.39	97.53	17.43
88	10.98	5.24	0.239	1.343	1.171	97.81	19.12	97.50	17.14
89	11.00	5.30	0.234	1.363	1.195	97.77	18.20	97.52	15.77
90	10.99	5.17	0.252	1.373	1.111	97.93	22.51	97.68	17.74
91	13.72	5.04	0.240	1.380	1.168	98.88	7.18	98.74	11.69
92	11.02	5.26	0.245	1.399	1.144	97.86	21.99	97.66	16.36
93	14.16	4.98	0.238	1.468	1.177	98.98	5.78	98.87	10.79
94	11.01	5.28	0.246	1.476	1.139	97.88	20.53	97.64	17.05
95	11.00	5.33	0.243	1.545	1.153	97.85	19.69	97.69	15.56
96	10.90	5.18	0.244	1.652	1.149	97.91	13.81	97.78	15.13
97	10.85	5.23	0.234	1.857	1.197	97.81	17.85	97.74	13.80
98	12.88	4.76	0.264	1.185	1.410	97.90	17.97	97.85	17.95
99	12.92	5.34	0.238	1.188	1.564	97.65	11.92	97.46	16.26
100	12.88	4.78	0.262	1.192	1.420	97.87	18.83	97.84	17.80
101	13.10	5.10	0.248	1.217	1.499	98.12	10.17	97.77	16.20
102	13.29	5.10	0.245	1.249	1.516	98.25	9.54	97.92	14.40
103	13.81	5.11	0.262	1.265	1.770	97.97	14.16	97.57	16.32
104	13.60	5.11	0.247	1.308	1.504	98.44	8.06	98.07	14.31
105	14.04	5.07	0.249	1.359	1.493	98.63	7.02	98.28	13.23
106	14.67	5.12	0.238	1.523	1.563	98.74	5.23	98.47	11.13
107	13.82	5.17	0.258	1.274	1.800	97.93	14.35	97.51	16.33
108	13.73	5.35	0.241	1.314	1.926	97.83	10.20	97.36	14.43
109	13.88	5.29	0.238	1.362	1.945	98.01	8.60	97.49	13.83
110	14.75	5.06	0.267	1.372	2.083	98.09	12.86	97.54	15.65
111	14.79	5.00	0.269	1.378	2.065	98.10	13.79	97.60	15.45
112	14.82	5.34	0.280	1.383	1.987	98.17	14.75	97.54	16.47
113	14.83	5.41	0.276	1.384	2.015	98.15	13.22	97.49	16.57
114	14.20	5.33	0.228	1.465	2.034	98.11	7.08	97.61	12.16
115	14.43	5.25	0.227	1.523	2.036	98.23	6.73	97.75	11.70
116	14.60	5.14	0.234	1.543	1.983	98.36	6.04	97.94	11.28

Table D-6. Countercurrent Condenser Data for 19060 Packing (Continued)

No	T _{s1} (C)	T _{w1} (C)	G kg/sm ²	Ja	X _{ii} (%)	Measured	Model (l=0.61m)	Cond- ensed Steam (%)	Press- ure Loss (Pa)	Cond- ensed Steam (%)	Press- ure Loss (Pa)
						Cond- ensed Steam (%)	Press- ure Loss (Pa)				
117	13.99	5.18	0.254	1.568	2.184	98.08	7.47	97.29	14.20		
118	14.46	5.30	0.273	1.648	2.038	98.21	11.86	97.57	14.92		
119	14.45	5.23	0.277	1.650	2.010	98.24	13.73	97.58	15.77		
120	14.87	5.12	0.223	1.660	2.078	98.39	5.89	98.00	10.15		
121	14.35	5.20	0.263	1.948	2.111	98.15	10.84	97.63	13.66		
122	14.36	5.22	0.259	1.975	2.143	98.12	11.00	97.59	13.69		
123	14.22	4.96	0.255	2.153	2.177	98.11	10.51	97.63	13.62		
124	14.39	5.25	0.262	2.220	2.121	98.11	10.97	97.68	13.37		
125	14.41	5.30	0.255	2.279	2.182	98.05	11.06	97.65	12.61		
126	14.35	5.21	0.255	2.403	2.182	98.06	10.59	97.69	12.56		
127	14.38	5.23	0.255	2.405	2.181	98.06	11.27	97.69	12.53		
128	14.44	5.21	0.249	1.418	2.226	97.99	9.62	97.30	14.29		
129	14.10	4.94	0.245	1.425	2.262	97.99	7.90	97.22	14.67		
130	14.40	5.09	0.252	1.428	2.199	98.03	10.12	97.39	14.15		
131	14.23	5.16	0.237	1.455	2.338	97.89	8.27	97.17	13.64		
132	14.06	5.40	0.233	1.669	2.378	97.89	6.96	97.11	12.55		
133	14.34	5.40	0.236	1.734	2.344	97.95	8.98	97.26	12.89		
134	14.25	5.26	0.236	1.741	2.349	97.98	8.78	97.27	12.92		
135	14.03	5.25	0.252	1.805	2.203	98.04	9.12	97.36	13.68		
136	13.95	5.12	0.248	1.834	2.234	98.01	6.56	97.35	13.72		
137	14.10	4.89	0.250	1.931	2.223	98.12	9.68	97.55	13.20		
138	14.09	4.86	0.243	1.994	2.277	98.08	8.88	97.55	12.39		
139	14.21	5.01	0.248	2.211	2.236	98.06	10.78	97.59	12.88		
140	14.37	5.26	0.252	2.538	2.205	98.05	4.97	97.66	12.55		
141	14.39	5.30	0.251	2.546	2.213	98.03	9.97	97.66	12.54		
142	14.38	5.31	0.247	2.694	2.244	98.00	10.81	97.63	12.56		
143	14.41	5.43	0.243	2.715	2.288	97.95	10.25	97.59	11.87		
144	14.39	5.30	0.253	2.785	2.197	98.04	6.97	97.70	12.42		
145	14.40	5.31	0.252	2.802	2.205	98.02	9.97	97.69	12.43		
146	16.05	5.32	0.377	1.061	0.663	97.48	42.43	99.14	31.80		
147	16.10	5.08	0.389	1.063	0.642	97.56	44.11	99.20	32.92		
148	16.72	5.45	0.386	1.083	0.969	97.72	33.01	98.71	30.46		
149	16.80	5.43	0.389	1.088	0.961	97.73	34.65	98.79	29.21		
150	16.54	5.16	0.392	1.089	0.955	97.83	36.54	98.78	29.63		
151	16.62	5.16	0.395	1.089	0.947	97.82	36.54	98.82	29.32		
152	16.65	4.81	0.404	1.101	0.926	97.86	38.94	98.92	29.36		
153	15.83	4.94	0.403	1.108	0.930	98.05	37.70	98.75	31.59		
154	16.81	4.87	0.403	1.109	0.929	98.05	36.73	98.97	28.21		
155	15.92	5.00	0.401	1.109	0.934	98.00	38.20	98.75	31.37		

Table D-6. Countercurrent Condenser Data for 19060 Packing (Continued)

No	T _{ai} (C)	T _{wi} (C)	G kg/sm ²	Ja	X _{ii} (%)	Measured	Model (l=0.61m)	Cond- ensed Steam (%)	Press- ure Loss (Pa)
						Cond- ensed Steam (%)	Cond- ensed Steam (%)		
156	15.02	4.81	0.413	1.120	0.907	98.30	42.69	98.59	35.40
157	16.94	4.93	0.400	1.124	0.937	98.31	33.72	98.99	27.31
158	17.06	4.90	0.405	1.134	0.925	98.53	31.07	99.06	26.24
159	15.14	5.15	0.393	1.139	0.951	98.19	41.04	98.61	30.82
160	14.69	5.22	0.406	1.150	0.923	98.32	44.60	98.45	35.54
161	14.61	5.19	0.400	1.156	0.934	98.32	43.84	98.49	33.38
162	17.30	4.92	0.402	1.160	0.932	98.77	28.26	99.13	24.29
163	13.77	5.36	0.370	1.186	1.010	98.40	36.26	98.18	30.81
164	13.69	5.34	0.366	1.192	1.021	98.38	37.00	98.13	31.15
165	13.66	5.13	0.395	1.214	0.947	98.52	44.41	98.31	32.99
166	13.53	5.22	0.379	1.229	0.987	98.48	41.43	98.22	31.42
167	13.11	5.18	0.371	1.266	1.007	98.53	37.05	98.14	30.09
168	13.14	5.32	0.364	1.271	1.028	98.49	37.14	98.11	28.74
169	13.32	5.47	0.389	1.277	0.960	98.56	41.95	98.15	32.68
170	13.44	5.44	0.391	1.293	0.956	98.56	43.59	98.23	31.76
171	12.89	5.37	0.368	1.373	1.016	98.56	27.10	98.09	28.98
172	12.81	5.35	0.357	1.397	1.045	98.53	28.97	98.07	27.33
173	12.96	5.17	0.390	1.412	0.959	98.64	42.51	98.29	30.22
174	12.52	5.01	0.363	1.527	1.030	98.60	36.08	98.24	25.80
175	12.47	5.04	0.358	1.532	1.042	98.59	29.97	98.19	26.10
176	12.65	5.20	0.369	1.563	1.012	98.60	37.78	98.24	26.68
177	17.42	5.16	0.407	1.126	1.222	98.01	35.12	98.57	28.53
178	17.42	5.25	0.401	1.130	1.241	97.97	34.55	98.56	27.31
179	17.56	5.15	0.395	1.180	1.571	98.24	26.73	98.21	26.27
180	17.57	5.32	0.391	1.183	1.587	98.23	27.42	98.19	25.22
181	18.28	5.26	0.399	1.230	1.863	98.35	25.90	98.03	24.53
182	18.30	5.22	0.404	1.230	1.839	98.37	26.36	98.07	24.37
183	17.88	5.26	0.383	1.253	1.936	98.42	22.31	97.94	22.96
184	17.87	5.07	0.388	1.254	1.915	98.45	23.36	97.96	23.91
185	17.58	5.21	0.405	1.258	1.834	98.58	23.73	97.95	25.36
186	17.61	5.26	0.408	1.264	1.821	98.59	23.75	97.91	26.55
187	18.89	5.14	0.400	1.293	2.146	98.45	21.53	97.91	23.14
188	18.86	5.26	0.391	1.297	2.208	98.40	20.99	97.85	22.27
189	18.99	4.85	0.386	1.360	1.920	98.88	16.44	98.37	20.12
190	16.88	5.06	0.384	1.392	1.930	98.69	22.01	97.89	22.97
191	16.85	5.16	0.373	1.408	1.986	98.66	19.73	97.83	22.03
192	19.60	4.96	0.382	1.424	1.940	99.00	15.22	98.52	17.92
193	16.75	4.96	0.402	1.445	1.847	98.77	22.51	97.95	24.66
194	16.67	4.83	0.399	1.453	1.859	98.77	22.50	97.95	24.66
195	20.14	4.64	0.388	1.491	1.913	99.15	13.87	98.68	17.37
196	16.75	5.36	0.381	1.546	1.947	98.69	19.14	97.86	22.31

Table D-6. Countercurrent Condenser Data for 19060 Packing (Concluded)

No	T _{ai} (C)	T _{wi} (C)	G kg/sm ²	Ja	X _{ii} (%)	Measured		Model (l=0.61m)	
						Cond- ensed Steam (%)	Press- ure Loss (Pa)	Cond- ensed Steam (%)	Press- ure Loss (Pa)
197	16.63	5.19	0.377	1.566	1.965	98.70	18.36	97.87	22.33
198	16.64	5.31	0.384	1.662	1.929	98.71	18.08	97.93	21.82
199	16.63	5.26	0.384	1.670	1.929	98.71	17.56	97.94	21.76
200	16.79	5.40	0.404	1.768	1.837	98.71	20.46	98.04	22.88
201	16.80	5.55	0.398	1.776	1.866	98.69	19.97	97.96	23.08
202	16.56	5.14	0.372	1.826	1.993	98.67	17.80	97.98	20.41
203	16.55	5.18	0.367	1.836	2.020	98.65	16.66	97.93	20.54
204	16.64	5.29	0.385	1.975	1.926	98.68	16.78	98.01	21.77
205	16.64	5.32	0.374	2.030	1.982	98.65	16.92	98.03	19.89
206	16.56	5.01	0.402	2.033	1.846	98.75	18.60	98.14	22.29
207	16.59	5.14	0.394	2.044	1.883	98.73	18.97	98.12	21.42
208	16.57	5.16	0.391	2.252	1.897	98.70	14.97	98.13	21.17
209	16.57	5.28	0.369	2.263	2.010	98.63	16.09	98.04	19.71
Minimum:									
	9.92	4.64	0.150	1.018	0.354	95.93	0.26	96.05	6.25
Maximum:									
	20.14	5.55	0.413	2.802	2.459	99.46	44.60	99.65	35.54
Average:									
	13.50	5.16	0.273	1.412	1.413	97.98	17.07	98.03	18.10
Standard Deviation:									
	2.42	0.17	0.084	0.384	0.621	0.67	11.14	0.74	6.87
Difference Between Predictions and Experiment:									
						No. of		Standard	
						Points		Average	
								Deviation	
Condensed Steam (%)						209	0.10	1.00	
Pressure Loss (Pa)						209	0.80	5.10	

Table D-7. Countercurrent Condenser Data for 3X Packing

No	Tsi (C)	Twi (C)	G kg/sm ²	Ja	Xii (%)	Measured		Model (l=0.61m)		Model (l=0.80m)	
						Cond- ensed Steam (%)	Press- ure Loss (Pa)	Cond- ensed Steam (%)	Press- ure Loss (Pa)	Cond- ensed Steam (%)	Press- ure Loss (Pa)
1	9.72	4.20	0.060	3.584	9.935	87.58	7.09	86.25	4.36	87.88	5.08
2	13.29	5.10	0.091	6.942	15.408	86.64	27.39	86.22	6.81	88.23	7.95
3	11.34	4.40	0.050	10.520	24.813	78.33	22.33	79.13	4.86	80.87	5.92
4	11.33	5.57	0.197	1.159	3.260	91.13	10.04	91.34	17.18	94.12	18.88
5	11.46	5.65	0.179	1.280	3.568	93.12	9.37	91.65	13.85	94.13	15.07
6	9.38	4.10	0.139	1.483	4.557	92.22	8.73	89.99	11.14	92.42	12.25
7	9.90	4.62	0.121	1.717	5.216	91.87	8.04	89.54	8.95	91.80	9.92
8	12.40	5.14	0.168	2.578	7.324	92.67	18.91	89.46	12.55	91.91	13.88
9	12.48	5.29	0.198	2.781	7.763	91.50	31.65	88.25	16.64	91.03	18.39
10	12.43	4.98	0.144	3.958	10.358	89.59	28.13	87.30	11.40	89.80	12.88
11	12.57	4.89	0.105	5.584	13.671	87.03	26.32	86.02	8.20	88.26	9.48
12	13.54	4.33	0.106	7.162	13.512	89.70	27.42	88.84	7.41	90.73	8.54
13	11.14	5.44	0.209	1.081	3.082	88.76	10.23	90.77	20.56	93.85	23.09
14	12.53	5.10	0.248	1.101	2.602	92.12	11.70	93.89	21.55	96.27	23.59
15	13.02	5.56	0.235	1.165	2.742	93.95	11.07	94.20	17.91	96.36	19.30
16	12.19	5.42	0.281	1.439	4.517	93.48	23.27	89.67	28.17	92.89	30.58
17	11.81	5.09	0.276	1.862	5.683	92.25	35.61	88.31	28.48	91.57	30.98
18	11.72	4.76	0.238	2.234	6.535	92.21	34.44	88.46	22.48	91.47	24.58
19	12.72	5.34	0.236	2.261	6.581	92.80	36.16	89.15	20.49	92.04	22.37
20	12.00	5.28	0.347	1.154	3.691	89.10	25.50	88.63	46.00	92.49	51.47
21	11.87	5.15	0.346	1.161	3.701	89.34	25.97	88.68	45.87	92.52	51.24
22	11.99	5.33	0.328	1.209	3.894	90.58	24.50	88.88	40.35	92.59	44.59
23	12.20	5.47	0.319	1.259	4.006	92.02	24.08	89.25	36.81	92.82	40.34
24	12.44	5.29	0.391	1.411	4.071	90.96	45.47	89.25	49.23	92.87	53.34

Table D-7. Countercurrent Condenser Data for 3X Packing (Continued)

No	Tai (C)	Twi (C)	G kg/sm ²	Ja	Xii (%)	Measured	Model (l=0.61m)	Model (l=0.80m)	Cond- ensed Steam (%)	Press- ure Loss (Pa)	Cond- ensed Steam (%)	Press- ure Loss (Pa)
						Cond- ensed Steam (%)	Press- ure Loss (Pa)	Cond- ensed Steam (%)				
25	11.53	5.15	0.335	1.467	4.740	89.85	38.25	87.44	42.28	91.23	46.16	
26	12.63	5.45	0.363	1.528	4.373	92.25	44.92	89.50	41.58	92.93	44.86	
27	12.95	5.29	0.388	1.638	4.111	94.00	41.03	90.67	42.77	93.86	45.75	
28	11.78	5.25	0.301	1.660	5.241	91.60	36.21	87.93	33.61	91.42	36.57	
29	13.02	5.74	0.339	1.662	4.675	93.35	42.18	89.75	35.34	93.01	38.06	
30	12.84	5.07	0.353	1.821	4.501	94.61	39.29	90.86	35.84	93.86	38.34	
31	12.80	5.17	0.410	1.539	3.894	93.14	40.71	90.54	48.37	93.84	51.81	
32	13.39	5.31	0.451	1.582	3.555	92.40	43.19	91.47	52.46	94.61	55.81	
33	13.27	5.34	0.442	1.587	3.625	92.21	43.53	91.24	51.51	94.42	54.87	
Minimum:												
	9.38	4.10	0.050	1.081	2.602	78.33	7.09	79.13	4.36	80.87	5.080	
Maximum:												
	13.54	5.74	0.451	10.520	24.813	94.61	45.47	94.20	52.46	96.36	55.810	
Average:												
	12.11	5.13	0.254	2.441	6.339	90.98	27.36	89.17	26.82	92.06	29.271	
Standard Deviation:												
	0.99	0.40	0.112	2.104	4.586	2.99	12.29	2.57	15.42	2.78	16.552	

Table D-7. Countercurrent Condenser Data for 3X Packing (Concluded)

No	Tsi (C)	Twi (C)	G kg/sm ²	Ja	Xii (%)	Measured	Press- ure Loss (Pa)	Model (l=0.61m)	Press- ure Loss (Pa)	Model (l=0.80m)	Press- ure Loss (Pa)
						Cond- ensed Steam (%)		Cond- ensed Steam (%)		Cond- ensed Steam (%)	

Difference Between Predictions (l=0.8m) and Experiment:

	No. of Points	Average	Standard Deviation
Condensed Steam (%)	33	1.10	1.50
Pressure Loss (Pa)	33	1.90	12.30

Table D-8. Countercurrent Condenser Data for 27060 Packing

No	Tsi (C)	Twi (C)	G kg/sm ²	Ja	Xii (%)	Measured		Model (l=0.61m)		Model (l=0.80m)	
						Cond- ensed Steam (%)	Press- ure Loss (Pa)	Cond- ensed Steam (%)	Press- ure Loss (Pa)	Cond- ensed Steam (%)	Press- ure Loss (Pa)
1	9.81	5.34	0.172	0.988	0.365	95.94	8.78	94.74	16.06	96.64	23.12
2	10.16	5.52	0.191	0.995	0.330	96.33	13.01	94.94	18.40	96.90	26.28
3	9.79	5.32	0.165	1.011	0.379	96.36	8.32	95.99	13.48	98.16	17.68
4	9.86	5.25	0.170	1.028	0.368	97.18	7.28	96.68	13.08	98.73	15.95
5	9.95	5.22	0.172	1.046	0.365	97.72	6.60	97.26	12.24	99.04	14.02
6	10.21	5.24	0.175	1.066	0.357	98.42	6.56	97.88	11.28	99.26	12.35
7	10.43	5.33	0.177	1.080	0.354	98.89	4.74	98.15	10.72	99.34	11.51
8	10.55	5.38	0.173	1.117	0.362	99.16	2.56	98.54	9.11	99.39	9.53
9	9.90	5.33	0.165	1.041	0.758	96.12	7.05	94.49	11.67	97.29	13.73
10	9.91	5.29	0.184	1.054	0.681	96.53	11.73	94.63	13.78	97.46	16.08
11	9.88	5.33	0.180	1.059	0.696	96.59	11.32	94.65	13.17	97.46	15.21
12	9.92	5.18	0.168	1.059	0.745	96.76	6.55	95.09	11.34	97.68	12.95
13	10.03	5.15	0.170	1.082	0.736	97.35	5.76	95.64	10.79	97.98	11.99
14	10.19	5.13	0.173	1.097	0.724	97.97	4.84	96.04	10.51	98.19	11.51
15	10.28	5.01	0.197	1.098	0.947	97.12	11.18	94.38	13.52	97.23	15.08
16	10.85	5.68	0.196	1.102	0.952	97.01	10.64	94.30	12.99	97.18	14.47
17	9.90	5.21	0.181	1.138	1.029	97.08	9.92	93.90	11.84	96.81	13.02
18	9.98	5.30	0.179	1.154	1.043	96.94	9.41	94.01	11.35	96.86	12.40
19	9.85	5.30	0.197	1.194	0.949	97.33	12.14	94.08	13.11	96.95	14.23
20	9.82	5.40	0.190	1.207	0.983	97.19	11.56	93.94	12.35	96.82	13.37
21	9.50	4.97	0.179	1.212	1.045	97.10	11.55	94.15	11.16	96.88	12.04
22	9.44	5.13	0.167	1.233	1.118	96.99	10.44	93.84	10.05	96.60	10.83
23	9.38	5.39	0.182	1.301	1.027	97.15	11.13	93.60	11.51	96.48	12.35
24	9.36	5.48	0.174	1.322	1.075	97.13	10.20	93.42	10.71	96.30	11.48
25	9.11	5.24	0.159	1.329	1.170	96.85	9.28	93.36	9.36	96.16	10.04

Table D-8. Countercurrent Condenser Data for 27060 Packing (Continued)

No	T _{s1} (C)	T _{w1} (C)	G kg/sm ²	J _a	X ₁₁ (%)	Measured	Model (l=0.61m)	Model (l=0.80m)	Cond- ensed Steam (%)	Press- ure Loss (Pa)	Cond- ensed Steam (%)	Press- ure Loss (Pa)
						Cond- ensed Steam (%)	Press- ure Loss (Pa)	Cond- ensed Steam (%)				
26	9.01	5.09	0.162	1.332	1.150	96.82	9.64	93.49	9.62	96.27	10.31	
27	9.13	5.19	0.181	1.368	1.032	97.21	12.35	93.78	11.18	96.54	11.93	
28	9.15	5.24	0.177	1.387	1.057	97.21	11.40	93.76	10.71	96.49	11.42	
29	8.98	5.04	0.188	1.411	0.992	97.41	12.47	93.97	11.74	96.67	12.48	
30	9.08	5.16	0.186	1.417	1.002	97.23	13.29	93.95	11.47	96.64	12.19	
31	9.11	5.40	0.168	1.546	1.108	97.07	2.69	93.77	9.52	96.36	10.10	
32	8.90	5.10	0.180	1.566	1.040	97.29	11.77	94.06	10.55	96.60	11.16	
33	8.95	5.19	0.178	1.567	1.052	97.10	11.72	93.97	10.39	96.53	11.00	
34	9.07	5.42	0.162	1.570	1.152	96.81	10.49	93.62	9.04	96.21	9.61	
35	8.80	5.03	0.178	1.707	1.048	97.34	12.92	94.29	10.07	96.68	10.61	
36	8.74	4.95	0.178	1.724	1.050	97.33	1.69	94.34	10.04	96.70	10.58	
37	8.63	4.92	0.160	1.799	1.166	97.00	10.98	94.12	8.57	96.44	9.06	
38	10.62	5.21	0.181	1.128	1.374	96.92	5.78	93.30	11.29	96.37	12.44	
39	10.60	5.10	0.199	1.156	1.248	97.31	9.73	93.73	12.74	96.70	13.92	
40	10.69	5.22	0.197	1.160	1.261	97.30	9.64	93.72	12.44	96.68	13.57	
41	10.76	5.37	0.169	1.186	1.466	97.23	3.89	93.68	9.45	96.49	10.24	
42	10.69	5.32	0.169	1.199	1.471	97.34	3.50	93.70	9.41	96.49	10.18	
43	11.05	5.41	0.191	1.221	1.621	97.39	7.54	92.98	11.33	96.06	12.27	
44	10.94	5.42	0.184	1.237	1.678	97.27	6.84	92.84	10.73	95.92	11.60	
45	10.79	4.93	0.178	1.238	1.739	97.18	4.24	93.28	10.00	96.19	10.78	
46	10.64	5.30	0.156	1.270	1.588	97.27	2.09	93.89	7.97	96.49	8.55	
47	10.88	4.95	0.173	1.281	1.789	97.19	3.61	93.52	9.23	96.29	9.91	
48	10.59	5.20	0.152	1.306	1.626	97.42	1.98	94.06	7.51	96.55	8.03	
49	10.62	5.02	0.153	1.362	1.623	97.52	1.58	94.49	7.26	96.80	7.73	
50	10.78	4.82	0.163	1.368	1.519	97.81	2.20	95.05	7.64	97.21	8.09	
51	8.71	5.06	0.151	1.871	1.233	96.90	10.28	93.99	7.81	96.27	8.28	

Table D-8. Countercurrent Condenser Data for 27060 Packing (Continued)

No	Tsi (C)	Twi (C)	G kg/sm ²	Ja	Xii (%)	Measured	Model (l=0.61m)	Model (l=0.80m)	Cond- ensed Steam (%)	Press- ure Loss (Pa)	Cond- ensed Steam (%)	Press- ure Loss (Pa)
						Cond- ensed Steam (%)	Press- ure Loss (Pa)	Cond- ensed Steam (%)				
52	11.52	5.31	0.194	1.333	1.913	97.43	6.38	93.11	10.64	96.05	11.39	
53	11.55	5.31	0.192	1.346	1.925	97.48	6.30	93.20	10.36	96.10	11.08	
54	11.08	5.03	0.165	1.364	1.869	97.39	1.93	93.88	8.12	96.44	8.66	
55	11.32	5.02	0.163	1.443	1.895	97.57	1.94	94.33	7.53	96.69	8.00	
56	11.64	5.34	0.182	1.449	2.039	97.30	5.88	93.43	9.15	96.16	9.75	
57	11.65	5.36	0.180	1.461	2.053	97.35	5.95	93.45	8.96	96.16	9.55	
58	11.49	4.96	0.165	1.491	1.871	97.70	1.31	94.69	7.37	96.93	7.81	
59	11.35	4.91	0.184	1.557	2.013	97.46	3.97	93.84	9.08	96.41	9.63	
60	11.76	4.95	0.164	1.564	1.885	97.85	1.39	95.06	6.95	97.14	7.36	
61	11.45	5.07	0.182	1.568	2.031	97.30	4.23	93.79	8.90	96.35	9.45	
62	11.98	4.90	0.163	1.601	1.896	97.90	1.39	95.33	6.65	97.31	7.03	
63	11.54	5.27	0.180	1.798	2.054	97.22	4.21	93.96	8.44	96.40	8.94	
64	11.56	5.34	0.176	1.828	2.099	97.27	4.22	93.89	8.17	96.32	8.66	
65	11.50	5.22	0.184	1.881	2.012	97.35	4.60	94.11	8.62	96.49	9.12	
66	11.62	5.42	0.180	1.903	2.061	97.31	4.70	93.98	8.34	96.38	8.84	
67	11.34	4.90	0.187	2.039	1.982	97.51	4.37	94.45	8.66	96.71	9.14	
68	11.39	5.00	0.185	2.061	2.005	97.42	4.58	94.38	8.52	96.65	9.01	
69	11.43	5.13	0.178	2.482	2.078	97.31	4.44	94.49	7.90	96.64	8.36	
70	11.49	5.27	0.177	2.586	2.084	97.28	4.08	94.47	7.81	96.60	8.27	
71	11.60	5.25	0.176	1.353	2.106	97.17	3.57	93.16	9.00	96.00	9.64	
72	11.74	5.20	0.172	1.414	2.146	97.30	2.05	93.54	8.34	96.21	8.90	
73	11.99	5.31	0.167	1.488	2.210	97.37	2.18	93.79	7.66	96.33	8.16	
74	12.18	5.21	0.166	1.558	2.219	97.48	1.89	94.22	7.26	96.59	7.72	
75	12.39	5.25	0.168	1.581	2.200	97.63	1.81	94.43	7.20	96.74	7.64	
76	12.59	5.19	0.171	1.604	2.159	97.75	1.68	94.74	7.15	96.95	7.58	

Table D-8. Countercurrent Condenser Data for 27060 Packing (Continued)

No	Tsi (C)	Twi (C)	G kg/sm ²	Ja	Xii (%)	Measured	Model (l=0.61m)	Model (l=0.80m)	Cond- ensed Steam (%)	Press- ure Loss (Pa)	Cond- ensed Steam (%)	Press- ure Loss (Pa)	Cond- ensed Steam (%)	Press- ure Loss (Pa)
						Cond- ensed Steam (%)	Cond- ensed Steam (%)	Cond- ensed Steam (%)						
77	12.91	5.20	0.174	1.640	2.120	97.87	2.05	95.08	7.03	97.19	7.44			
78	11.14	4.67	0.173	1.795	2.131	97.38	4.83	94.09	8.05	96.46	8.54			
79	11.13	4.83	0.158	1.915	2.334	96.99	4.12	93.79	7.12	96.16	7.58			
80	11.31	5.03	0.163	2.417	2.270	97.00	4.23	94.21	7.11	96.38	7.56			
81	11.38	5.10	0.172	2.461	2.155	97.20	3.79	94.36	7.59	96.53	8.05			
82	11.37	5.20	0.156	2.482	2.364	96.96	3.55	94.02	6.73	96.21	7.17			
83	11.34	5.04	0.169	2.490	2.188	97.23	4.28	94.37	7.41	96.51	7.86			
84	11.43	5.19	0.171	2.560	2.166	97.24	5.01	94.36	7.50	96.51	7.95			
85	11.51	5.32	0.169	2.698	2.181	97.19	4.04	94.38	7.33	96.49	7.78			
86	11.46	5.31	0.161	2.951	2.296	96.93	3.93	94.30	6.88	96.38	7.32			
87	11.22	4.85	0.170	3.037	2.177	97.25	4.22	94.68	7.36	96.68	7.80			
88	11.40	5.24	0.156	3.063	2.368	96.95	4.01	94.26	6.61	96.32	7.05			
89	11.24	4.94	0.160	3.182	2.312	96.97	4.27	94.51	6.81	96.51	7.25			
90	12.26	5.14	0.264	1.027	0.357	97.11	26.16	96.98	22.70	99.00	27.94			
91	12.26	5.05	0.267	1.030	0.353	97.54	24.04	97.10	22.81	99.07	27.72			
92	12.36	5.12	0.268	1.044	0.352	97.89	23.45	97.47	21.43	99.27	24.78			
93	12.45	5.10	0.268	1.051	0.351	98.21	21.94	97.71	20.54	99.37	23.23			
94	12.57	5.19	0.262	1.068	0.360	98.56	20.61	98.06	18.14	99.46	19.80			
95	12.68	5.19	0.261	1.077	0.360	98.83	19.80	98.25	17.15	99.51	18.47			
96	12.76	5.20	0.268	1.078	0.352	99.10	17.28	98.25	17.90	99.52	19.29			
97	12.92	5.34	0.257	1.119	0.366	99.36	14.19	98.67	14.36	99.58	15.00			
98	13.07	5.24	0.253	1.168	0.372	99.52	11.00	98.98	12.15	99.63	12.52			
99	12.52	5.08	0.269	1.050	0.696	97.35	21.86	95.75	20.53	98.26	23.81			
100	12.66	5.20	0.265	1.069	0.707	97.61	20.69	96.13	18.70	98.46	21.03			
101	12.67	5.14	0.265	1.071	0.706	97.96	19.01	96.22	18.50	98.51	20.73			

Table D-8. Countercurrent Condenser Data for 27060 Packing (Continued)

No	Tsi (C)	Twi (C)	G kg/sm ²	Ja	Xii (%)	Measured	Model (l=0.61m)	Model (l=0.80m)	Cond- ensed Steam (%)	Press- ure Loss (Pa)	Cond- ensed Steam (%)	Press- ure Loss (Pa)
						Cond- ensed Steam (%)	Cond- ensed Steam (%)	Cond- ensed Steam (%)				
102	12.70	5.15	0.263	1.094	0.713	98.40	18.18	96.53	17.18	98.64	18.81	
103	12.82	5.18	0.261	1.110	0.718	98.63	16.76	96.76	16.13	98.74	17.44	
104	12.96	5.16	0.261	1.134	0.719	98.90	15.08	97.06	15.11	98.86	16.13	
105	13.24	5.17	0.255	1.207	0.734	99.15	11.70	97.60	12.56	99.04	13.13	
106	13.98	5.09	0.243	1.393	0.770	99.33	5.68	98.32	9.11	99.26	9.40	
107	12.52	4.80	0.298	1.085	0.940	97.82	19.76	94.77	23.21	97.66	26.17	
108	10.34	4.96	0.203	1.091	0.922	97.12	11.48	94.41	14.28	97.27	16.01	
109	12.74	4.95	0.268	1.093	1.047	97.70	20.05	95.07	18.25	97.77	20.25	
110	10.85	5.51	0.203	1.097	0.923	97.00	11.19	94.45	13.77	97.30	15.37	
111	12.55	5.02	0.287	1.099	0.977	97.76	18.51	94.82	21.18	97.67	23.60	
112	12.08	4.93	0.290	1.109	0.968	97.88	18.27	94.52	22.40	97.48	24.95	
113	12.84	5.14	0.262	1.113	1.070	97.87	18.02	95.23	16.87	97.84	18.48	
114	12.08	4.96	0.285	1.119	0.984	97.87	17.49	94.63	21.33	97.53	23.59	
115	12.93	5.04	0.263	1.122	1.068	98.13	16.57	95.46	16.46	97.97	17.92	
116	13.06	5.07	0.261	1.153	1.075	98.43	14.79	95.79	15.30	98.12	16.43	
117	11.45	5.02	0.268	1.160	1.048	97.92	17.81	94.29	19.52	97.25	21.31	
118	11.44	4.98	0.268	1.160	1.047	97.86	19.18	94.33	19.48	97.27	21.26	
119	11.20	4.95	0.275	1.187	1.019	98.03	17.71	94.27	20.42	97.24	22.17	
120	11.20	4.97	0.273	1.191	1.029	98.03	16.81	94.27	20.09	97.23	21.78	
121	11.03	5.06	0.270	1.214	1.036	98.00	19.75	94.12	19.81	97.11	21.41	
122	11.05	5.11	0.270	1.218	1.038	98.03	19.46	94.10	19.77	97.10	21.35	
123	11.00	5.24	0.276	1.236	1.017	98.05	17.00	93.95	20.64	97.01	22.27	
124	10.93	5.22	0.269	1.241	1.040	98.05	16.61	93.94	19.74	96.98	21.27	
125	10.63	5.13	0.263	1.308	1.065	97.95	18.57	94.01	18.63	96.96	19.89	
126	10.60	5.04	0.265	1.311	1.055	98.08	19.24	94.12	18.77	97.03	20.01	
127	10.43	4.91	0.275	1.344	1.020	98.13	16.65	94.18	19.93	97.07	21.18	

Table D-8. Countercurrent Condenser Data for 27060 Packing (Continued)

No	T _{s1} (C)	T _{w1} (C)	G kg/sm ²	J _a	X ₁₁ (%)	Measured		Model (l=0.61m)		Model (l=0.80m)	
						Cond- ensed Steam (%)	Press- ure Loss (Pa)	Cond- ensed Steam (%)	Press- ure Loss (Pa)	Cond- ensed Steam (%)	Press- ure Loss (Pa)
128	10.50	5.02	0.271	1.355	1.034	98.15	17.08	94.19	19.26	97.06	20.45
129	10.51	5.17	0.268	1.393	1.044	98.11	19.38	94.15	18.69	97.01	19.80
130	10.52	5.19	0.269	1.394	1.041	98.09	20.15	94.13	18.82	97.00	19.94
131	10.30	5.02	0.269	1.456	1.041	98.14	18.64	94.27	18.56	97.05	19.58
132	10.36	5.06	0.270	1.456	1.037	98.07	18.69	94.30	18.58	97.07	19.60
133	10.41	5.23	0.267	1.499	1.051	98.11	18.57	94.25	18.05	97.01	19.01
134	10.45	5.30	0.264	1.507	1.063	98.04	15.80	94.22	17.65	96.98	18.59
135	10.33	5.20	0.264	1.572	1.063	98.08	18.14	94.36	17.38	97.04	18.25
136	10.37	5.28	0.257	1.595	1.089	98.06	18.91	94.36	16.48	97.01	17.30
137	12.05	5.09	0.238	1.115	1.175	97.43	14.34	94.58	15.47	97.38	17.02
138	12.09	4.98	0.241	1.117	1.164	97.40	14.71	94.73	15.59	97.48	17.11
139	11.92	5.03	0.249	1.141	1.124	97.52	16.75	94.72	16.39	97.47	17.86
140	11.80	4.94	0.249	1.141	1.124	97.62	16.01	94.68	16.54	97.45	18.03
141	11.24	5.20	0.230	1.188	1.214	97.59	13.42	94.10	14.91	96.99	16.14
142	11.24	5.10	0.234	1.194	1.198	97.60	14.52	94.25	15.17	97.09	16.38
143	11.27	5.26	0.244	1.203	1.147	97.68	15.86	94.15	16.34	97.06	17.65
144	11.32	5.24	0.244	1.212	1.148	97.70	17.13	94.29	16.06	97.14	17.29
145	10.92	5.43	0.226	1.272	1.237	97.57	14.32	93.82	14.38	96.73	15.41
146	10.88	5.34	0.228	1.273	1.227	97.66	14.55	93.89	14.56	96.79	15.59
147	11.01	5.44	0.242	1.284	1.156	97.70	17.82	94.01	15.86	96.91	16.96
148	10.95	5.33	0.244	1.284	1.149	97.75	17.97	94.07	16.08	96.95	17.19
149	10.58	5.20	0.246	1.392	1.138	97.82	18.71	94.19	15.94	96.96	16.89
150	10.38	5.02	0.230	1.393	1.217	97.71	14.69	94.12	14.40	96.86	15.26
151	10.65	5.33	0.242	1.399	1.160	97.81	17.94	94.10	15.48	96.89	16.40
152	10.36	5.10	0.219	1.423	1.274	97.66	14.91	94.05	13.21	96.76	14.00
153	10.44	5.31	0.229	1.497	1.224	97.74	16.02	94.08	13.93	96.78	14.71

Table D-8. Countercurrent Condenser Data for 27060 Packing (Continued)

No	Tsl (C)	Twi (C)	G kg/sm ²	Ja	Xii (%)	Measured	Model (l=0.61m)	Model (l=0.80m)	Cond- ensed Steam (%)	Press- ure Loss (Pa)	Cond- ensed Steam (%)	Press- ure Loss (Pa)
						Cond- ensed Steam (%)	Press- ure Loss (Pa)	Cond- ensed Steam (%)			Cond- ensed Steam (%)	Press- ure Loss (Pa)
154	10.44	5.32	0.228	1.498	1.225	97.69	16.51	94.09	13.83	96.78	14.60	
155	10.44	5.28	0.238	1.533	1.176	97.73	18.80	94.26	14.61	96.91	15.39	
156	10.20	5.07	0.225	1.612	1.243	97.73	16.69	94.33	13.21	96.88	13.90	
157	10.17	5.08	0.221	1.636	1.268	97.72	15.89	94.28	12.83	96.82	13.50	
158	10.25	5.13	0.238	1.675	1.175	97.83	18.39	94.50	14.21	97.01	14.90	
159	10.07	4.95	0.226	1.687	1.240	97.84	1.96	94.44	13.17	96.92	13.82	
160	10.18	5.06	0.233	1.704	1.199	97.83	18.60	94.53	13.68	97.00	14.34	
161	10.12	5.06	0.218	1.716	1.283	97.67	15.32	94.37	12.38	96.84	13.01	
162	13.16	5.11	0.261	1.152	1.427	97.90	15.45	94.48	15.98	97.31	17.33	
163	13.22	5.09	0.258	1.179	1.442	98.15	13.76	94.73	15.08	97.43	16.21	
164	14.11	5.33	0.273	1.196	1.699	98.05	12.55	94.23	15.76	97.12	16.94	
165	13.39	5.10	0.256	1.215	1.456	98.31	12.62	95.04	14.12	97.59	15.06	
166	14.24	5.40	0.262	1.242	1.768	98.22	10.57	94.48	14.03	97.22	14.97	
167	13.60	4.98	0.257	1.257	1.446	98.57	11.29	95.47	13.33	97.82	14.10	
168	14.06	5.03	0.249	1.348	1.494	98.68	9.54	95.97	11.45	98.06	12.01	
169	14.84	5.14	0.261	1.390	1.781	98.62	6.59	95.47	11.98	97.77	12.58	
170	14.90	4.90	0.253	1.495	1.472	98.95	6.81	96.73	10.14	98.46	10.56	
171	16.19	4.90	0.286	1.496	1.303	99.22	7.17	97.31	10.91	98.84	11.30	
172	14.46	5.36	0.255	1.312	1.819	98.36	8.32	94.88	12.56	97.42	13.28	
173	14.34	5.09	0.262	1.342	2.122	98.05	8.51	94.12	13.60	96.93	14.42	
174	14.36	5.26	0.258	1.357	2.154	98.00	8.58	94.03	13.27	96.86	14.07	
175	14.39	5.21	0.257	1.366	2.164	98.03	9.18	94.11	13.07	96.90	13.85	
176	14.79	5.33	0.255	1.376	1.815	98.51	7.54	95.30	11.76	97.65	12.38	
177	14.07	5.07	0.258	1.438	2.154	98.09	7.16	94.16	13.14	96.90	13.88	
178	14.11	5.19	0.254	1.443	2.186	98.03	6.91	94.09	12.83	96.85	13.56	

Table D-8. Countercurrent Condenser Data for 27060 Packing (Continued)

No	T _{ai} (C)	T _{wi} (C)	G kg/sm ²	J _a	X _{ii} (%)	Measured	Model (l=0.61m)	Model (l=0.80m)	Cond- ensed Steam (%)	Press- ure Loss (Pa)	Cond- ensed Steam (%)	Press- ure Loss (Pa)
						Cond- ensed Steam (%)	Cond- ensed Steam (%)	Cond- ensed Steam (%)				
179	15.28	5.05	0.253	1.508	1.833	98.75	5.61	95.94	10.48	98.00	10.96	
180	15.49	5.11	0.254	1.563	2.185	98.48	5.81	95.25	10.82	97.57	11.36	
181	14.04	5.35	0.259	1.642	2.145	98.06	5.48	94.31	12.75	96.93	13.42	
182	14.02	5.32	0.255	1.663	2.180	98.07	0.69	94.31	12.42	96.92	13.06	
183	15.89	4.89	0.242	1.683	1.914	98.83	4.21	96.44	8.89	98.25	9.28	
184	16.62	4.99	0.255	1.750	2.177	98.74	4.70	96.05	9.50	98.05	9.93	
185	13.89	5.16	0.260	1.891	2.133	98.14	5.46	94.64	12.41	97.10	13.01	
186	13.90	5.24	0.253	2.171	2.193	98.04	5.52	94.77	11.64	97.13	12.20	
187	14.64	5.31	0.252	1.415	2.200	98.12	8.31	94.33	12.18	97.02	12.88	
188	14.81	5.25	0.252	1.458	2.202	98.22	7.72	94.57	11.79	97.16	12.43	
189	15.02	5.20	0.252	1.490	2.201	98.31	7.41	94.80	11.42	97.30	12.02	
190	13.95	5.15	0.251	1.589	2.210	98.04	6.79	94.26	12.29	96.90	12.95	
191	13.96	5.14	0.252	1.589	2.206	98.03	6.29	94.27	12.35	96.91	13.01	
192	16.13	5.08	0.251	1.697	2.216	98.57	4.56	95.72	9.79	97.84	10.25	
193	13.80	5.04	0.245	1.879	2.263	98.03	5.14	94.54	11.42	97.01	12.00	
194	13.80	5.06	0.238	1.916	2.328	97.99	4.98	94.51	10.92	96.97	11.48	
195	13.96	5.30	0.251	1.943	2.214	98.03	5.78	94.57	11.71	97.03	12.30	
196	13.89	5.24	0.245	2.092	2.260	97.96	6.02	94.66	11.19	97.05	11.74	
197	13.91	5.28	0.241	2.135	2.304	97.97	4.72	94.63	10.90	97.01	11.45	
198	13.84	5.15	0.252	2.196	2.206	98.07	1.49	94.78	11.58	97.14	12.14	
199	13.77	5.12	0.234	2.448	2.367	97.91	4.51	94.78	10.31	97.07	10.84	
200	13.80	5.09	0.247	2.490	2.243	98.04	5.82	94.95	11.06	97.20	11.60	
201	13.83	5.27	0.226	2.507	2.448	97.82	4.23	94.69	9.80	96.98	10.32	
202	13.76	5.04	0.245	2.512	2.266	97.95	2.19	94.94	10.95	97.19	11.49	
203	13.85	5.27	0.238	2.640	2.331	97.86	5.23	94.86	10.47	97.11	11.00	
204	13.86	5.26	0.238	2.648	2.325	97.92	4.87	94.89	10.44	97.13	10.97	

Table D-8. Countercurrent Condenser Data for 27060 Packing (Continued)

No	Tsi (C)	Twi (C)	G kg/sm ²	Ja	Xii (%)	Measured		Model (l=0.61m)		Model (l=0.80m)	
						Cond- ensed Steam (%)	Press- ure Loss (Pa)	Cond- ensed Steam (%)	Press- ure Loss (Pa)	Cond- ensed Steam (%)	Press- ure Loss (Pa)
205	13.76	5.11	0.240	2.777	2.307	97.93	4.86	94.99	10.55	97.19	11.08
206	13.77	5.13	0.236	2.821	2.350	97.95	1.59	94.96	10.30	97.16	10.82
207	14.69	5.12	0.389	1.020	0.322	97.49	39.45	96.56	40.37	98.75	52.34
208	14.70	5.20	0.389	1.020	0.321	97.49	38.81	96.52	40.49	98.72	52.65
209	14.65	5.10	0.383	1.040	0.652	97.73	33.70	95.39	34.88	98.13	41.94
210	16.43	5.16	0.375	1.042	0.995	98.80	23.05	95.26	27.76	98.03	32.38
211	14.76	5.25	0.378	1.051	0.660	97.69	34.31	95.66	32.60	98.31	38.23
212	16.50	5.45	0.382	1.064	0.978	97.67	28.67	95.46	27.34	98.17	31.02
213	15.04	4.95	0.390	1.083	0.958	98.07	31.27	95.05	31.12	97.92	35.09
214	15.02	4.92	0.391	1.084	0.956	98.08	31.66	95.06	31.24	97.93	35.20
215	16.87	5.26	0.371	1.027	1.008	99.04	20.79	95.18	27.33	97.95	32.65
216	17.18	5.41	0.359	1.064	1.040	99.26	14.27	95.94	22.50	98.42	25.20
217	15.58	5.48	0.354	1.066	1.054	97.83	26.23	95.00	25.66	97.86	29.17
218	15.52	5.28	0.359	1.073	1.038	98.07	25.18	95.17	25.90	97.97	29.21
219	15.63	5.21	0.354	1.102	1.054	98.34	24.95	95.64	23.38	98.21	25.68
220	15.32	4.56	0.396	1.146	1.255	98.38	27.64	94.91	28.31	97.77	30.77
221	15.24	4.73	0.382	1.155	1.302	98.35	27.55	94.85	26.51	97.71	28.72
222	15.98	5.16	0.366	1.169	1.020	98.53	25.53	96.35	21.58	98.56	22.97
223	14.38	5.25	0.357	1.231	1.391	98.42	25.58	94.40	24.21	97.36	25.91
224	14.30	5.10	0.360	1.235	1.381	98.40	25.85	94.47	24.53	97.40	26.22
225	13.97	5.10	0.373	1.307	1.334	98.56	28.77	94.55	25.73	97.43	27.27
226	14.00	5.25	0.363	1.318	1.371	98.49	28.90	94.50	24.42	97.38	25.85
227	13.73	5.39	0.363	1.434	1.371	98.51	26.25	94.56	23.83	97.37	25.04
228	13.69	5.34	0.362	1.441	1.373	98.52	26.21	94.60	23.67	97.38	24.85
229	13.42	5.25	0.373	1.696	1.332	98.61	28.86	94.99	23.52	97.56	24.46

Table D-8. Countercurrent Condenser Data for 27060 Packing (Continued)

No	Tai (C)	Twi (C)	G kg/sm ²	Ja	Xii (%)	Measured	Model (l=0.61m)	Model (l=0.80m)	Cond- ensed Steam (%)	Press- ure Loss (Pa)	Cond- ensed Steam (%)	Press- ure Loss (Pa)
						Cond- ensed Steam (%)	Press- ure Loss (Pa)	Cond- ensed Steam (%)				
230	13.49	5.36	0.367	1.709	1.355	98.58	29.01	94.97	22.75	97.54	23.67	
231	16.95	5.21	0.350	1.155	2.114	98.42	16.04	93.61	21.03	96.88	22.84	
232	17.21	4.82	0.361	1.201	2.053	98.59	15.91	94.26	20.50	97.28	21.95	
233	15.79	5.14	0.371	1.206	1.672	98.43	22.12	94.20	23.86	97.26	25.61	
234	15.73	5.03	0.369	1.209	1.681	98.44	22.73	94.25	23.58	97.28	25.29	
235	21.15	4.91	0.372	1.228	1.990	99.25	8.32	95.92	15.22	98.31	16.05	
236	17.67	4.78	0.356	1.270	2.082	98.75	14.08	94.78	18.26	97.57	19.33	
237	19.43	4.83	0.351	1.294	2.108	99.06	9.30	95.55	15.18	98.03	15.97	
238	18.34	4.80	0.356	1.294	2.080	98.89	12.58	95.15	17.01	97.79	17.92	
239	17.72	5.30	0.392	1.330	2.215	98.51	19.38	94.01	22.06	97.10	23.34	
240	17.69	5.23	0.389	1.346	2.217	98.54	20.13	94.11	21.57	97.15	22.78	
241	13.08	4.66	0.352	1.688	1.410	98.61	25.34	95.12	21.40	97.61	22.26	
242	13.10	4.77	0.340	1.729	1.463	98.57	23.67	95.08	20.07	97.55	20.88	
243	16.08	5.13	0.409	1.112	1.220	98.24	30.83	94.68	30.17	97.68	33.35	
244	15.95	5.27	0.400	1.117	1.245	98.23	28.66	94.59	29.19	97.61	32.20	
245	17.69	5.45	0.424	1.191	1.755	98.44	25.80	94.15	27.09	97.29	29.16	
246	17.72	5.54	0.422	1.195	1.763	98.43	26.00	94.14	26.77	97.29	28.79	
Minimum:												
	8.63	4.56	0.151	0.988	0.321	95.94	0.69	92.84	6.61	95.92	7.03	
Maximum:												
	21.15	5.68	0.424	3.182	2.448	99.52	39.45	98.98	40.49	99.63	52.65	
Average:												
	12.37	5.15	0.244	1.455	1.418	97.83	12.54	94.76	14.77	97.27	16.12	

Table D-8. Countercurrent Condenser Data for 27060 Packing (Concluded)

No	Tsi (C)	Twi (C)	G kg/sm ²	Ja	Xii (%)	Measured	Model (l=0.61m)	Model (l=0.80m)	Cond- ensed Steam (%)	Press- ure Loss (Pa)	Cond- ensed Steam (%)	Press- ure Loss (Pa)
						Cond- ensed Steam (%)	Press- ure Loss (Pa)	Press- ure Loss (Pa)				

Standard Deviation:

2.29 0.17 0.069 0.444 0.590 0.63 8.31 1.11 6.35 0.81 7.53

Difference Between Predictions (l=0.8m) and Experiment:

	No. of Points	Average	Standard Deviation
Condensed Steam (%)	246	-0.60	0.70
Pressure Loss (Pa)	246	3.60	3.40

APPENDIX E DATA TABLES FOR COUNTERCURRENT CONDENSER GEOMETRIES OTHER THAN STRUCTURED PACKING

This appendix provides a complete set of experimental data for countercurrent condensers not using structured packing. Their geometries are described and performances are evaluated in Appendix C.

Table E-1 contains the data for spiral screen configuration 1 in Table C-1. Tables E-2 through E-4 contain the data for disc-donut baffle contactors, configurations 2 through 4. Table E-5 contains data for configuration 5. Table E-6 summarizes the data for configuration 8 using random packings tested at three different packing fill depths.

All the tables contain 9 columns. Column 1 refers to a serial number. Column 2, labeled T_{si} , represents the measured saturation temperature of the incoming steam and inert gas mixture in degrees Celsius; the uncertainty in this measurement is $\pm 0.02^\circ\text{C}$. Column 3, labeled T_{wi} , represents the measured water inlet temperature in degrees Celsius with an uncertainty of $\pm 0.01^\circ\text{C}$.

Column 4, labeled G , is the condenser gas loading defined as the entire mass flow rate of the steam and inert gas mixture divided by the flow planform area of the condenser; this quantity is expressed in $\text{kg/m}^2 \text{ s}$ and possesses an uncertainty of $\pm 2.5\%$ of the measured value. Column 5, labeled Ja , is the Jakob number with an uncertainty of $\pm 1.9\%$.

Column 6, labeled X_{ii} , is the inert gas mass concentration in the incoming steam expressed as a percentage of the total steam and inert gas mixture flow. This quantity is estimated to possess an uncertainty of $\pm 2.4\%$ of the quoted value.

Column 7 represents the amount of steam condensed within the contactor expressed as a percentage of the incoming steam flow with an uncertainty of $\pm 1.9\%$ of the incoming steam flow. Column 8 represents the measured overall condenser pressure loss (static pressure difference between inlet and outlet gas streams) expressed in Pascals, with an uncertainty of $\pm 10 \text{ Pa}$ or $\pm 10\%$ of the quoted value, whichever is greater. Column 9 refers to the vent fraction of Eq. C-6 and possesses an uncertainty of less than 10%.

**Table E-1. Countercurrent Condenser Data for Configuration 1
with Spiral Metal Screen**

S.No.	T _{si} (C)	T _{wi} (C)	G (kg/m ² s)	Ja	X _{ii} (%)	Cond- ensed Steam (%)	Press- ure Loss (Pa)	Vent Fraction
1	15.98	5.90	0.331	2.346	3.307	93.34	63.20	0.876
2	15.47	5.67	0.314	2.363	2.913	93.09	60.77	0.849
3	14.87	4.98	0.329	2.307	2.245	93.79	75.54	0.837
4	14.28	5.41	0.379	1.793	1.469	94.41	167.16	0.634
5	14.23	5.66	0.384	1.699	0.971	94.36	169.80	0.589
6	14.02	5.69	0.386	1.614	0.485	94.35	196.14	0.504
7	14.56	6.06	0.450	1.394	0.415	94.99	171.75	0.640
8	14.62	5.92	0.458	1.419	0.407	95.08	236.21	0.510
9	14.66	5.86	0.447	1.476	0.418	94.96	230.71	0.541
10	14.68	5.73	0.450	1.493	0.415	95.07	140.45	0.692
11	14.64	5.39	0.443	1.561	0.843	95.17	188.53	0.607
12	14.74	5.35	0.449	1.552	0.832	95.18	248.06	0.560
13	14.85	5.26	0.459	1.560	0.813	95.34	171.59	0.646
14	15.30	5.30	0.460	1.616	1.214	95.34	240.00	0.611
15	15.38	5.44	0.461	1.598	1.212	95.30	210.95	0.637
16	15.83	5.58	0.446	1.708	1.668	95.13	170.26	0.717
17	15.95	5.64	0.447	1.706	1.664	95.12	144.67	0.748
18	15.74	5.53	0.466	1.631	1.597	95.35	191.45	0.674
19	16.21	5.36	0.454	1.776	2.036	95.27	140.17	0.770
20	16.95	5.45	0.446	1.902	2.476	95.10	115.52	0.808
21	8.98	5.03	0.219	1.476	0.854	90.81	92.27	0.582
22	9.02	5.10	0.209	1.513	0.894	90.31	91.83	0.589
23	9.71	4.69	0.219	1.896	1.695	91.02	44.02	0.781
24	9.75	4.75	0.210	1.944	1.765	90.60	41.09	0.793
25	10.79	4.27	0.217	2.446	2.543	91.16	25.53	0.894
26	10.79	4.38	0.204	2.579	2.699	90.54	24.16	0.899
27	10.30	4.48	0.220	2.166	2.096	91.18	34.53	0.850
28	10.39	4.65	0.207	2.269	2.226	90.52	30.97	0.866
29	9.46	4.96	0.219	1.662	1.272	90.88	72.34	0.716
30	9.08	5.29	0.223	1.370	0.420	90.76	144.01	0.398
31	9.09	5.26	0.228	1.372	0.411	91.02	144.58	0.163
32	15.58	5.53	0.498	1.539	0.750	95.28	451.02	0.326
33	15.55	5.54	0.497	1.534	0.751	95.32	442.16	0.357
34	15.44	5.78	0.487	1.513	1.528	95.51	235.63	0.653
35	15.46	5.78	0.490	1.501	1.519	95.53	230.37	0.666
36	16.38	5.56	0.471	1.758	2.350	95.40	115.65	0.820
37	16.40	5.60	0.454	1.798	2.432	95.23	113.85	0.827
38	17.05	5.10	0.460	1.990	2.821	95.42	92.61	0.861
39	17.08	5.16	0.457	2.005	2.838	95.38	95.96	0.860

**Table E-1. Countercurrent Condenser Data for Configuration 1
with Spiral Metal Screen (Continued)**

S.No.	T _{si} (C)	T _{wi} (C)	G (kg/m ² s)	Ja	X _{ii} (%)	Cond- ensed Steam (%)	Press- ure Loss (Pa)	Vent Fraction
40	15.66	5.54	0.468	1.628	1.978	95.39	158.23	0.769
41	15.62	5.43	0.491	1.606	1.888	95.65	153.52	0.769
42	15.27	5.50	0.484	1.544	1.153	95.44	338.77	0.516
43	15.28	5.54	0.481	1.546	1.159	95.40	339.63	0.475
44	15.09	5.58	0.483	1.505	0.386	94.94	475.77	0.188
45	15.11	5.61	0.479	1.512	0.391	94.88	475.20	0.184
46	14.99	4.76	0.494	1.622	0.474	95.42	472.72	0.257
47	14.92	4.75	0.497	1.602	0.472	95.49	469.29	0.244
48	14.87	4.77	0.487	1.632	0.959	95.67	367.28	0.449
49	14.94	4.77	0.487	1.638	0.958	95.65	369.78	0.457
50	15.08	4.87	0.502	1.590	1.455	95.92	193.66	0.710
51	15.15	4.99	0.493	1.612	1.481	95.81	192.44	0.686
52	15.49	4.96	0.504	1.634	1.607	95.89	173.74	0.731
53	15.71	4.95	0.510	1.646	1.587	95.94	177.44	0.736
54	15.93	5.12	0.501	1.682	1.163	95.70	349.36	0.505
55	15.94	5.17	0.500	1.673	1.163	95.69	352.72	0.519
56	15.34	5.18	0.506	1.552	0.694	95.48	450.89	0.303
57	15.24	5.22	0.488	1.587	0.719	95.32	436.53	0.325
58	14.89	5.24	0.496	1.508	0.236	95.18	514.17	0.144
59	14.92	5.18	0.502	1.513	0.234	95.25	524.72	0.145
60	14.84	5.18	0.485	1.533	0.724	95.35	425.25	0.342
61	14.80	5.08	0.483	1.545	0.727	95.35	423.01	0.316
62	14.80	5.05	0.492	1.532	0.714	95.51	362.29	0.420
63	14.89	5.10	0.492	1.537	0.713	95.44	367.99	0.415
64	15.06	5.52	0.493	1.487	0.712	95.55	107.05	0.781
65	15.02	5.46	0.501	1.470	0.701	95.63	104.21	0.776
66	15.16	5.57	0.477	1.526	0.735	95.15	412.81	0.362
67	15.16	5.65	0.480	1.513	0.732	95.15	412.47	0.370
68	14.66	5.56	0.494	1.419	0.711	95.58	232.17	0.616
69	14.57	5.56	0.488	1.407	0.720	95.54	223.28	0.600
70	14.44	5.51	0.489	1.399	0.718	95.59	140.21	0.741
71	14.55	5.74	0.477	1.411	0.735	95.42	138.75	0.720
72	11.25	5.29	0.173	2.597	3.298	88.02	11.87	0.900
73	11.28	5.29	0.171	2.633	3.326	87.93	12.03	0.902
74	14.31	4.31	0.146	5.149	7.454	86.51	62.94	0.881
75	14.30	4.25	0.148	5.123	7.384	86.65	65.19	0.862
76	16.62	5.39	0.160	5.737	8.657	86.85	31.36	0.936
77	16.64	5.40	0.162	5.716	8.590	86.96	28.83	0.939

**Table E-1. Countercurrent Condenser Data for Configuration 1
with Spiral Metal Screen (Concluded)**

S.No.	T _{si} (C)	T _{wi} (C)	G (kg/m ² s)	Ja	X _{ii} (%)	Cond- ensed Steam (%)	Press- ure Loss (Pa)	Vent Fraction
78	13.27	5.99	0.438	1.342	0.143	94.78	447.21	0.088
79	13.24	5.96	0.436	1.340	0.144	94.77	450.86	0.125
80	13.50	5.67	0.430	1.450	0.436	94.81	445.19	0.192
81	13.49	5.64	0.433	1.446	0.434	94.84	448.71	0.202
82	14.15	5.42	0.429	1.628	1.733	95.11	142.45	0.742
83	14.18	5.44	0.434	1.624	1.710	95.15	142.56	0.754
84	16.98	5.15	0.471	1.994	2.721	95.57	98.88	0.863
85	16.96	5.25	0.470	1.991	2.721	95.54	99.23	0.865
86	17.50	6.38	0.414	2.790	3.092	94.59	106.82	0.859
87	17.37	6.16	0.422	2.745	3.026	94.77	107.39	0.863
88	13.03	5.43	0.390	1.507	0.481	94.41	344.24	0.232
89	12.57	5.70	0.374	1.827	0.501	94.40	276.69	0.391
90	11.71	5.50	0.364	2.050	0.515	94.40	234.89	0.392
91	12.07	5.53	0.364	1.972	0.515	94.37	249.52	0.404
92	12.88	5.26	0.384	1.776	0.488	94.63	314.28	0.361
93	14.48	5.57	0.418	1.397	0.449	94.08	380.30	0.150
94	14.60	5.97	0.399	1.419	0.937	93.92	305.09	0.375
95	13.64	5.73	0.360	1.944	1.037	94.12	184.77	0.590
96	12.48	5.28	0.353	2.255	1.057	94.27	157.55	0.657
97	12.88	5.38	0.355	2.562	1.052	94.28	167.34	0.634
98	13.06	5.20	0.383	2.057	0.974	94.72	188.02	0.612
99	13.19	5.32	0.385	1.587	0.970	94.56	229.93	0.520
100	16.63	5.78	0.512	1.612	0.731	95.06	471.86	0.304
101	15.52	6.01	0.454	1.608	0.823	94.84	388.39	0.313
102	15.58	5.66	0.464	1.641	0.806	95.27	285.01	0.535
103	15.54	5.62	0.473	1.617	0.790	95.37	246.96	0.584
104	15.54	5.64	0.477	1.600	0.785	95.37	254.95	0.581
105	15.83	5.92	0.461	1.632	0.812	94.37	113.98	0.535

**Table E-2. Countercurrent Condenser Data for Configuration 2
with Three Pairs of Baffles**

S.No.	T _{si} (C)	T _{wi} (C)	G (kg/m ² s)	Ja	X _{ii} (%)	Cond- ensed Steam (%)	Press- ure Loss (Pa)	Vent Fraction
1	12.89	4.98	0.198	2.088	1.874	92.37	160.52	0.618
2	12.89	5.09	0.193	2.119	1.924	92.11	128.22	0.677
3	10.78	5.64	0.201	1.328	0.311	92.21	242.20	0.206
4	10.79	5.69	0.196	1.352	0.319	91.99	237.14	0.248
5	12.30	5.18	0.191	1.939	1.622	92.03	152.16	0.629
6	12.29	5.20	0.186	1.979	1.664	91.83	158.12	0.624
7	11.11	5.48	0.198	1.462	0.632	92.18	215.47	0.344
8	11.06	5.49	0.195	1.461	0.640	92.07	203.56	0.388
9	11.70	5.02	0.195	1.793	1.275	92.31	156.62	0.605
10	11.73	5.08	0.189	1.833	1.313	92.04	170.67	0.583
11	11.37	5.33	0.189	1.643	0.987	91.92	191.75	0.496
12	11.37	5.33	0.189	1.643	0.987	91.92	191.75	0.496
13	11.41	5.17	0.200	1.611	0.933	92.43	195.60	0.441
14	15.98	4.91	0.378	1.477	0.660	96.07	565.32	0.329
15	16.01	4.91	0.381	1.467	0.655	96.10	589.30	0.306
16	17.18	4.90	0.378	1.626	1.317	96.00	474.78	0.507
17	17.20	4.91	0.379	1.637	1.315	96.01	491.82	0.497
18	18.06	5.23	0.375	1.704	1.978	95.76	318.79	0.663
19	18.05	5.14	0.383	1.693	1.938	95.88	318.41	0.666
20	18.76	5.27	0.376	1.775	2.340	95.68	274.62	0.705
21	18.79	5.23	0.381	1.771	2.313	95.74	255.38	0.721
22	17.80	5.26	0.377	1.633	1.645	95.84	455.98	0.549
23	17.78	5.41	0.371	1.654	1.670	95.74	455.72	0.541
24	16.16	5.06	0.362	1.526	1.030	95.81	481.65	0.444
25	16.16	5.12	0.360	1.534	1.037	95.76	481.09	0.445
26	15.26	4.98	0.362	1.396	0.346	95.87	633.96	0.216
27	15.34	5.01	0.364	1.393	0.345	95.90	638.38	0.214
28	18.15	4.78	0.341	2.570	2.601	95.53	242.15	0.751
29	18.48	4.89	0.329	3.225	2.684	95.41	321.49	0.715
30	19.34	6.90	0.420	1.447	0.890	95.88	758.79	0.303
31	18.32	6.09	0.419	1.445	0.893	96.07	656.54	0.380
32	18.26	6.29	0.402	1.473	0.931	95.86	663.11	0.370
33	17.04	5.01	0.396	1.504	0.943	96.14	576.79	0.410
34	17.08	5.16	0.391	1.511	0.955	96.06	560.96	0.422
35	15.74	3.96	0.389	1.520	0.960	96.36	477.51	0.454
36	15.71	4.25	0.371	1.547	1.008	96.11	458.40	0.469
37	18.21	3.93	0.391	1.831	2.245	96.16	240.68	0.728
38	18.24	4.03	0.389	1.844	2.234	96.15	225.89	0.743
39	18.97	5.43	0.386	1.737	2.261	95.72	275.45	0.704

**Table E-2. Countercurrent Condenser Data for Configuration 2
with Three Pairs of Baffles (Concluded)**

S.No.	T _{si} (C)	T _{wi} (C)	G (kg/m ² s)	Ja	X _{ii} (%)	Cond- ensed Steam (%)	Press- ure Loss (Pa)	Vent Fraction
40	18.76	5.22	0.386	1.718	2.273	95.78	244.75	0.727
41	19.71	5.88	0.403	1.688	2.165	95.84	350.20	0.680
42	19.67	5.79	0.408	1.685	2.163	95.91	366.47	0.671
43	20.86	6.91	0.406	1.654	2.137	95.58	490.06	0.609
44	20.77	6.82	0.409	1.659	2.163	95.62	457.45	0.628

**Table E-3. Countercurrent Condenser Data for Configuration 3
with Two Pairs of Baffles**

S.No.	T _{si} (C)	T _{wi} (C)	G (kg/m ² s)	Ja	X _{ii} (%)	Cond- ensed Steam (%)	Press- ure Loss (Pa)	Vent Fraction
1	13.15	4.75	0.166	2.566	2.227	90.73	84.87	0.600
2	13.18	4.71	0.174	2.499	2.127	91.15	84.14	0.597
3	10.39	5.37	0.179	1.436	0.350	91.25	98.00	0.183
4	10.35	5.35	0.178	1.439	0.352	91.23	128.60	0.083
5	12.63	4.97	0.176	2.232	1.760	91.19	86.60	0.550
6	12.62	5.00	0.169	2.285	1.828	90.86	79.29	0.571
7	11.12	5.37	0.185	1.575	0.674	91.47	115.60	0.264
8	11.17	5.47	0.179	1.628	0.699	91.13	112.06	0.272
9	12.19	5.38	0.166	2.076	1.491	90.54	72.35	0.562
10	12.18	5.32	0.171	2.029	1.452	90.79	85.20	0.539
11	11.64	5.47	0.175	1.788	1.064	90.98	73.08	0.457
12	11.62	5.43	0.177	1.778	1.055	91.06	91.74	0.406
13	15.85	4.93	0.356	1.583	0.700	95.66	495.06	0.262
14	15.93	4.90	0.350	1.630	0.713	95.46	450.66	0.302
15	16.21	4.81	0.367	1.596	1.354	95.50	199.64	0.546
16	16.24	4.96	0.358	1.622	1.388	95.32	186.96	0.558
17	18.53	5.39	0.384	1.746	1.929	95.27	147.65	0.624
18	18.55	5.47	0.367	1.804	2.017	95.02	148.01	0.620
19	19.51	5.21	0.365	1.999	2.415	94.90	135.62	0.645
20	19.54	5.24	0.365	1.989	2.410	94.86	148.90	0.631
21	17.44	5.31	0.364	1.687	1.704	95.14	174.92	0.576
22	17.51	5.38	0.354	1.717	1.748	94.97	167.76	0.585
23	16.67	5.45	0.362	1.575	1.031	95.57	417.49	0.420
24	16.59	5.40	0.364	1.566	1.026	95.59	408.93	0.387
25	15.46	5.40	0.362	1.413	0.345	95.23	471.48	0.144
26	15.41	5.39	0.358	1.415	0.349	95.18	465.59	0.170
27	17.15	4.63	0.460	1.369	0.272	96.57	788.31	0.119
28	17.42	4.59	0.475	1.359	0.263	96.69	807.25	0.108
29	18.07	4.21	0.470	1.480	0.531	97.06	845.04	0.244
30	18.09	4.24	0.460	1.502	0.544	96.98	847.51	0.244
31	18.77	4.63	0.469	1.508	0.797	96.93	785.31	0.325
32	18.72	4.49	0.473	1.507	0.792	97.00	768.88	0.326
33	18.76	4.46	0.466	1.534	1.072	96.90	630.08	0.439
34	18.79	4.42	0.466	1.540	1.071	96.90	650.23	0.425
35	19.23	4.32	0.465	1.611	1.339	96.83	564.23	0.491
36	19.26	4.33	0.461	1.611	1.348	96.80	551.54	0.488
37	19.74	4.21	0.464	1.677	1.604	96.76	501.86	0.540
38	19.69	4.25	0.460	1.672	1.616	96.72	492.75	0.540
39	20.09	4.22	0.455	1.743	1.949	96.53	378.45	0.598

**Table E-3. Countercurrent Condenser Data for Configuration 3
with Two Pairs of Baffles (Concluded)**

S.No.	T _{si} (C)	T _{wi} (C)	G (kg/m ² s)	Ja	X _{ii} (%)	Cond- ensed Steam (%)	Press- ure Loss (Pa)	Vent Fraction
40	20.12	4.15	0.460	1.732	1.928	96.62	402.68	0.594
41	20.02	4.85	0.463	2.032	1.901	96.72	401.47	0.634
42	19.98	4.91	0.461	2.032	1.921	96.70	388.49	0.643
43	20.34	5.29	0.444	2.530	2.007	96.66	467.98	0.622
44	20.33	5.21	0.450	2.512	1.987	96.70	464.66	0.629
45	19.61	5.04	0.482	1.071	0.519	95.06	452.31	0.154
46	19.60	5.00	0.477	1.082	0.525	94.98	477.07	0.137
47	19.60	5.00	0.477	1.082	0.525	94.98	477.07	0.137
48	21.22	5.40	0.457	1.207	1.092	94.45	336.64	0.299
49	21.22	5.34	0.466	1.196	1.071	94.48	358.72	0.275
50	21.82	5.36	0.468	1.228	1.591	94.31	167.30	0.376
51	21.80	5.37	0.471	1.228	1.580	94.38	169.42	0.383
52	22.70	5.19	0.476	1.295	1.881	94.25	123.75	0.421
53	22.68	5.18	0.477	1.297	1.876	94.25	122.28	0.419
54	22.35	5.38	0.471	1.222	1.322	94.30	325.02	0.302
55	22.40	5.37	0.495	1.225	1.257	94.19	361.77	0.217
56	20.15	5.72	0.436	1.151	0.859	93.83	230.66	0.209
57	20.06	5.79	0.431	1.150	0.869	93.81	265.86	0.193
58	18.90	5.26	0.458	1.045	0.273	94.83	498.50	0.058
59	18.87	5.33	0.454	1.048	0.276	94.79	485.80	0.077
60	13.77	5.79	0.143	2.057	2.573	88.15	30.25	0.610
61	13.61	5.70	0.147	1.989	2.512	88.51	42.29	0.590
62	9.38	5.26	0.123	1.263	0.508	87.40	60.15	0.093
63	9.42	5.25	0.121	1.285	0.515	87.20	43.70	1.237
64	13.08	5.63	0.149	1.861	2.070	88.67	51.28	0.524
65	13.05	5.59	0.154	1.820	2.007	89.05	53.95	0.519
66	10.75	5.79	0.128	1.438	0.977	87.27	58.50	0.294
67	10.68	5.77	0.129	1.417	0.965	87.45	57.28	0.294
68	12.23	5.18	0.156	1.691	1.586	89.47	58.07	0.455
69	12.32	5.26	0.157	1.679	1.578	89.44	26.51	0.514
70	11.64	5.94	0.134	1.565	1.388	87.57	37.38	0.440
71	11.63	5.89	0.135	1.574	1.375	87.76	54.03	0.402

**Table E-4. Countercurrent Condenser Data for Configuration 4
with One Pair of Baffles**

S.No.	T _{si} (C)	T _{wi} (C)	G (kg/m ² s)	Ja	X _{ii} (%)	Cond- ensed Steam (%)	Press- ure Loss (Pa)	Vent Fraction
1	15.91	5.52	0.180	2.982	2.051	88.11	19.58	0.391
2	15.94	5.62	0.171	3.115	2.162	87.53	15.97	0.407
3	10.86	5.41	0.171	1.654	0.366	89.52	21.11	0.080
4	10.85	5.46	0.165	1.680	0.379	89.14	21.16	0.085
5	14.75	5.05	0.182	2.770	1.698	88.82	17.94	0.390
6	11.36	4.81	0.169	2.022	0.740	89.53	15.27	0.230
7	13.01	5.21	0.191	2.112	0.979	89.89	15.52	0.278
8	17.00	4.80	0.374	1.653	0.677	93.51	40.40	0.259
9	17.06	4.91	0.365	1.672	0.694	93.29	44.16	0.262
10	20.03	4.95	0.364	2.096	1.366	92.43	22.59	0.319
11	20.03	4.76	0.374	2.072	1.331	92.67	28.37	0.327
12	22.75	4.90	0.377	2.394	1.965	91.75	35.56	0.350
13	22.78	4.91	0.381	2.365	1.945	91.83	19.11	0.360
14	24.22	5.49	0.381	2.470	2.280	91.11	18.79	0.359
15	21.51	5.40	0.346	2.310	1.793	91.49	22.44	0.358
16	21.49	5.20	0.355	2.271	1.748	91.72	28.50	0.358
17	19.02	5.55	0.360	1.847	1.036	92.53	31.53	0.288
18	19.01	5.65	0.349	1.883	1.069	92.30	23.47	0.297
19	15.32	5.41	0.345	1.419	0.364	93.38	65.86	0.183
20	15.31	5.34	0.344	1.428	0.364	93.37	65.28	0.189

**Table E-5. Countercurrent Condenser Data for Configuration 5
with Spiral Matted Screen**

S.No.	T _{si} (C)	T _{wi} (C)	G (kg/m ² s)	Ja	X _{ii} (%)	Cond- ensed Steam (%)	Press- ure Loss (Pa)	Vent Fraction
1	9.90	5.47	0.165	1.192	1.130	91.19	40.38	0.559
2	9.86	5.40	0.165	1.200	1.129	91.25	40.92	0.565
3	9.53	5.05	0.172	1.091	0.725	91.35	44.53	0.335
4	12.08	5.75	0.174	1.532	2.127	91.71	40.46	0.807
5	9.54	5.05	0.176	1.084	0.712	91.48	44.55	0.323
6	12.05	5.70	0.176	1.496	2.096	91.87	40.48	0.811
7	9.85	5.02	0.177	1.229	1.056	92.08	40.67	0.618
8	10.59	5.08	0.177	1.300	1.052	92.27	40.43	0.756
9	9.82	4.96	0.179	1.221	1.043	92.20	41.51	0.615
10	10.06	4.90	0.179	1.281	1.041	92.38	40.04	0.701
11	10.89	4.84	0.180	1.502	1.038	92.60	36.59	0.818
12	10.05	4.86	0.181	1.280	1.030	92.48	39.54	0.701
13	10.82	4.77	0.182	1.500	1.025	92.72	37.03	0.816
14	10.40	5.16	0.188	1.171	0.993	92.33	42.96	0.603
15	10.34	5.14	0.189	1.149	0.989	92.14	44.61	0.498
16	10.34	5.13	0.191	1.147	0.978	92.21	44.85	0.492
17	11.11	4.92	0.192	1.352	1.612	92.82	43.30	0.752
18	10.59	4.85	0.195	1.230	1.274	92.77	42.87	0.649
19	11.12	4.94	0.195	1.342	1.586	92.92	42.27	0.753
20	13.99	5.16	0.196	2.003	0.952	92.98	34.42	0.879
21	10.55	4.83	0.197	1.218	1.262	92.82	43.97	0.635
22	13.93	5.07	0.199	1.988	0.942	93.10	34.16	0.879
23	15.55	5.24	0.205	2.081	1.812	92.43	16.18	0.798
24	12.64	5.32	0.212	1.419	1.173	93.26	27.32	0.817
25	11.82	5.06	0.214	1.301	1.164	93.33	30.06	0.762
26	11.48	4.98	0.216	1.245	1.152	93.30	31.16	0.696
27	11.19	5.07	0.217	1.166	1.149	92.96	35.06	0.550
28	11.24	4.95	0.217	1.196	1.149	93.15	33.12	0.614
29	12.75	5.38	0.219	1.384	1.698	92.98	15.70	0.720
30	15.06	5.53	0.219	1.789	1.692	92.90	15.87	0.796
31	10.67	4.78	0.220	1.117	0.851	92.90	37.56	0.397
32	10.67	4.78	0.220	1.117	0.851	92.90	37.56	0.397
33	10.75	4.77	0.221	1.131	0.847	93.04	37.12	0.449
34	10.75	4.77	0.221	1.131	0.847	93.04	37.12	0.449
35	12.63	5.52	0.222	1.319	1.675	92.93	21.69	0.669
36	13.12	5.19	0.227	1.445	1.639	93.32	22.01	0.733
37	11.08	4.76	0.230	1.151	0.815	93.40	36.78	0.520
38	11.08	4.76	0.230	1.151	0.815	93.40	36.78	0.520

Table E-5. Countercurrent Condenser Data for Configuration 5
with Spiral Matted Screen (Continued)

S.No.	T _{si} (C)	T _{wi} (C)	G (kg/m ² s)	Ja	X _{ii} (%)	Cond- ensed Steam (%)	Press- ure Loss (Pa)	Vent Fraction
39	14.63	5.38	0.233	1.630	0.803	93.78	25.15	0.855
40	13.38	5.10	0.236	1.445	0.532	93.92	26.28	0.821
41	13.38	5.10	0.236	1.445	0.532	93.92	26.28	0.821
42	11.11	5.09	0.236	1.051	0.531	92.31	42.05	0.045
43	11.11	5.09	0.236	1.051	0.531	92.31	42.05	0.045
44	11.45	5.12	0.237	1.096	0.529	93.14	37.86	0.415
45	11.45	5.12	0.237	1.096	0.529	93.14	37.86	0.415
46	11.58	5.11	0.237	1.118	0.528	93.48	35.86	0.555
47	11.58	5.11	0.237	1.118	0.528	93.48	35.86	0.555
48	14.51	5.47	0.238	1.559	1.564	93.50	17.63	0.782
49	11.20	5.02	0.239	1.065	0.524	92.72	40.10	0.175
50	11.20	5.02	0.239	1.065	0.524	92.72	40.10	0.175
51	11.15	5.01	0.241	1.057	0.520	92.59	41.98	0.093
52	11.15	5.01	0.241	1.057	0.520	92.59	41.98	0.093
53	11.63	4.86	0.241	1.177	0.777	93.87	35.01	0.640
54	11.63	4.86	0.241	1.177	0.777	93.87	35.01	0.640
55	11.32	5.04	0.242	1.074	0.518	93.03	39.51	0.293
56	11.32	5.04	0.242	1.074	0.518	93.03	39.51	0.293
57	12.40	5.19	0.242	1.234	0.773	93.97	32.62	0.745
58	12.40	5.19	0.242	1.234	0.773	93.97	32.62	0.745
59	12.20	5.05	0.244	1.203	0.513	94.09	32.86	0.750
60	12.20	5.05	0.244	1.203	0.513	94.09	32.86	0.750
61	13.32	5.46	0.244	1.332	0.767	94.03	29.83	0.813
62	13.78	5.11	0.253	1.414	1.474	93.95	23.25	0.741
63	11.22	5.23	0.332	1.402	0.752	95.51	72.03	0.531
64	11.37	5.50	0.332	1.433	0.751	95.47	69.83	0.547
65	11.30	5.44	0.333	1.424	0.749	95.48	74.08	0.528
66	11.19	5.18	0.334	1.390	0.745	95.55	72.28	0.524
67	11.55	5.37	0.335	1.349	0.743	95.40	74.01	0.481
68	11.70	5.35	0.337	1.264	0.739	95.34	72.39	0.458
69	11.26	4.93	0.339	1.327	0.736	95.56	73.74	0.486
70	12.67	5.19	0.339	1.142	0.736	94.94	74.32	0.361
71	16.29	5.54	0.340	1.877	2.176	95.36	49.79	0.774
72	12.62	5.13	0.340	1.141	0.733	95.02	74.10	0.378
73	11.55	5.34	0.341	1.335	0.732	95.48	75.26	0.483
74	11.28	4.93	0.342	1.320	0.729	95.60	74.17	0.482
75	13.69	5.57	0.344	1.901	1.447	95.76	43.49	0.839

**Table E-5. Countercurrent Condenser Data for Configuration 5
with Spiral Matted Screen (Continued)**

S.No.	T _{si} (C)	T _{wi} (C)	G (kg/m ² s)	Ja	X _{ii} (%)	Cond- ensed Steam (%)	Press- ure Loss (Pa)	Vent Fraction
76	16.03	5.19	0.347	2.531	2.138	95.72	38.02	0.834
77	16.01	5.14	0.347	2.538	2.136	95.73	50.08	0.819
78	16.04	5.19	0.347	2.311	2.135	95.66	48.47	0.804
79	12.28	5.28	0.347	1.184	0.718	95.21	78.96	0.377
80	13.68	5.53	0.347	1.886	1.431	95.82	31.97	0.841
81	16.24	5.41	0.349	1.853	2.124	95.50	49.41	0.772
82	16.07	5.17	0.350	2.090	2.119	95.68	49.92	0.798
83	17.01	5.50	0.350	1.480	2.115	95.16	51.81	0.714
84	16.11	5.25	0.350	2.294	2.116	95.69	48.74	0.807
85	16.05	5.12	0.352	2.080	2.107	95.72	49.40	0.802
86	13.70	5.38	0.353	1.746	1.409	95.89	54.31	0.791
87	16.94	5.34	0.353	1.495	2.096	95.24	51.25	0.711
88	12.28	5.24	0.353	1.179	0.706	95.30	79.68	0.378
89	15.97	4.90	0.354	1.973	2.093	95.90	49.46	0.826
90	13.63	5.34	0.354	1.816	1.404	95.94	54.07	0.823
91	13.63	5.34	0.354	1.820	1.405	95.93	53.59	0.816
92	16.01	4.98	0.354	1.977	2.091	95.89	49.48	0.827
93	16.25	5.51	0.354	2.151	2.091	95.75	49.91	0.828
94	14.69	4.97	0.355	1.230	1.402	95.53	60.11	0.665
95	13.71	5.39	0.356	1.731	1.400	95.91	54.68	0.790
96	16.38	5.47	0.356	1.710	2.081	95.61	19.50	0.817
97	14.69	4.97	0.356	1.232	1.396	95.57	60.04	0.670
98	13.81	5.42	0.357	1.561	1.393	95.84	56.47	0.758
99	13.86	5.47	0.358	1.564	1.392	95.82	56.09	0.755
100	13.66	5.21	0.358	1.672	1.391	95.94	55.65	0.795
101	17.27	5.37	0.359	1.504	1.386	95.94	107.82	0.817
102	16.33	5.35	0.359	1.694	2.064	95.67	51.21	0.779
103	15.48	5.87	0.361	1.193	1.379	95.25	115.28	0.568
104	15.54	5.64	0.361	1.225	1.377	95.55	112.80	0.651
105	16.07	5.48	0.362	1.316	1.375	95.79	110.68	0.732
106	13.94	5.07	0.362	1.376	1.373	95.89	58.45	0.755
107	13.69	5.21	0.363	1.658	1.373	96.00	55.71	0.800
108	16.24	5.47	0.363	2.107	2.044	95.85	50.20	0.823
109	14.21	5.00	0.363	1.313	1.371	95.78	61.14	0.693
110	12.26	5.31	0.363	1.210	0.687	95.44	81.22	0.383
111	15.39	5.69	0.363	1.190	1.372	95.34	115.41	0.570
112	12.30	5.35	0.363	1.204	0.687	95.44	82.00	0.386

Table E-5. Countercurrent Condenser Data for Configuration 5
with Spiral Matted Screen (Continued)

S.No.	T _{si} (C)	T _{wi} (C)	G (kg/m ² s)	Ja	X _{ii} (%)	Cond- ensed Steam (%)	Press- ure Loss (Pa)	Vent Fraction
113	16.06	5.46	0.363	1.319	1.370	95.82	110.22	0.736
114	13.96	5.11	0.364	1.083	0.685	94.74	76.60	0.284
115	13.76	5.20	0.365	1.490	1.366	95.91	58.01	0.731
116	15.58	5.58	0.365	1.236	1.362	95.55	113.24	0.634
117	13.99	5.11	0.366	1.079	0.682	94.74	76.73	0.275
118	14.17	4.95	0.366	1.299	1.362	95.83	60.92	0.693
119	13.72	5.14	0.366	1.491	1.360	95.95	57.93	0.758
120	14.03	5.42	0.366	1.393	1.360	95.77	59.83	0.699
121	16.28	5.47	0.366	2.273	2.027	95.89	52.23	0.823
122	14.40	4.90	0.366	1.263	1.360	95.72	60.93	0.661
123	13.98	5.06	0.367	1.365	1.357	95.92	59.33	0.730
124	19.32	5.29	0.367	1.675	2.018	95.85	45.26	0.860
125	19.27	5.26	0.368	1.668	2.012	95.87	44.76	0.861
126	16.30	5.52	0.369	2.257	2.007	95.91	9.66	0.870
127	14.02	5.38	0.370	1.377	1.347	95.82	61.42	0.693
128	17.21	5.13	0.370	1.469	1.344	96.10	108.30	0.817
129	14.35	4.82	0.370	1.259	1.345	95.80	61.32	0.663
130	19.15	5.17	0.371	1.698	1.343	96.10	46.48	0.891
131	13.96	5.49	0.372	1.096	0.671	94.85	36.80	0.350
132	16.59	5.08	0.373	1.598	1.990	95.67	52.86	0.731
133	16.58	5.06	0.374	1.612	1.986	95.69	53.91	0.734
134	16.85	5.13	0.374	1.388	1.984	95.84	54.26	0.784
135	15.44	4.99	0.376	1.173	1.323	95.53	61.93	0.614
136	16.84	5.10	0.379	1.385	1.960	95.91	53.74	0.787
137	19.12	5.09	0.380	1.675	1.310	96.20	46.64	0.889
138	18.21	4.71	0.380	1.455	2.322	96.03	50.49	0.824
139	18.16	4.76	0.380	1.451	2.325	96.02	50.39	0.822
140	15.93	5.27	0.381	1.152	1.308	95.42	61.66	0.608
141	15.42	4.92	0.382	1.164	1.306	95.58	61.96	0.606
142	15.96	5.31	0.382	1.150	1.305	95.42	61.24	0.610
143	20.46	5.21	0.382	1.774	1.941	96.00	43.95	0.870
144	13.78	5.19	0.384	1.083	0.649	95.06	81.62	0.268
145	13.04	5.12	0.385	1.140	0.649	95.42	87.16	0.315
146	20.45	5.18	0.387	1.750	1.915	96.04	43.50	0.868
147	16.98	5.23	0.388	1.462	1.912	95.81	55.26	0.741
148	18.47	5.46	0.388	1.472	1.912	95.96	49.14	0.829
149	13.04	5.10	0.388	1.134	0.642	95.44	88.13	0.305
150	15.64	5.61	0.389	1.051	0.642	94.26	71.58	0.200

**Table E-5. Countercurrent Condenser Data for Configuration 5
with Spiral Matted Screen (Concluded)**

S.No.	T _{si} (C)	T _{wi} (C)	G (kg/m ² s)	Ja	X _{ii} (%)	Cond- ensed Steam (%)	Press- ure Loss (Pa)	Vent Fraction
151	18.44	5.49	0.389	1.469	1.909	95.96	50.31	0.828
152	15.64	5.64	0.389	1.046	0.642	94.25	72.10	0.198
153	17.39	4.96	0.391	1.298	1.898	95.96	55.23	0.770
154	17.44	5.03	0.391	1.300	1.897	95.95	55.03	0.770
155	16.49	4.67	0.395	1.218	1.571	95.90	59.86	0.697
156	15.19	5.07	0.400	1.064	0.625	94.81	76.19	0.259
157	17.54	5.20	0.400	1.295	1.857	95.63	55.57	0.679
158	17.62	5.30	0.401	1.293	1.851	95.62	55.85	0.679
159	15.16	4.99	0.401	1.058	0.622	94.86	76.10	0.265
160	16.80	4.81	0.402	1.452	1.846	96.04	56.11	0.735
161	16.45	4.58	0.406	1.211	1.531	96.01	60.59	0.693
162	15.23	4.87	0.407	1.067	0.613	94.99	75.40	0.289
163	15.20	4.87	0.408	1.068	0.612	95.03	75.39	0.294
164	17.25	5.62	0.409	1.100	1.220	95.17	63.01	0.526
165	15.41	5.13	0.409	1.053	0.611	94.66	78.96	0.194
166	15.36	5.07	0.409	1.051	0.611	94.75	79.07	0.217
167	16.93	5.40	0.412	1.164	0.605	96.07	61.28	0.737
168	16.95	5.42	0.414	1.155	0.603	96.07	60.60	0.733
169	15.41	5.07	0.414	1.047	0.603	94.76	80.40	0.203
170	17.18	5.34	0.418	1.091	1.193	95.30	65.02	0.522
171	15.66	4.95	0.418	1.075	0.597	95.15	76.23	0.336
172	15.75	4.99	0.418	1.077	0.597	95.16	77.07	0.345
173	16.42	5.37	0.421	1.088	0.593	95.61	69.98	0.541
174	15.42	5.02	0.424	1.037	0.589	94.84	80.97	0.191
175	16.41	5.37	0.425	1.089	0.588	95.67	69.98	0.550
176	18.48	5.33	0.425	1.210	1.751	95.17	60.16	0.544
177	16.16	5.23	0.425	1.079	0.587	95.34	74.20	0.420
178	18.45	5.30	0.426	1.203	1.747	95.18	59.39	0.540
179	16.10	5.16	0.426	1.077	0.586	95.39	73.71	0.427
180	16.17	4.89	0.427	1.082	0.877	95.29	73.74	0.398
181	16.12	4.81	0.427	1.081	0.876	95.29	74.12	0.391
182	16.65	5.00	0.443	1.030	0.564	94.45	80.43	0.135
183	16.61	4.97	0.443	1.031	0.564	94.50	79.67	0.144
184	17.89	4.69	0.460	1.083	1.085	95.37	122.43	0.397
185	18.02	4.80	0.460	1.085	1.085	95.37	122.95	0.400

Table E-6. Countercurrent Condenser Data for Configuration 8 with Random Packing

S.No.	Tsi (C)	Tw (C)	G (kg/m ² s)	Ja	Xii (%)	Cond- ensed Steam (%)	Press- ure Loss (Pa)	Vent Fraction
Packing Depth 18 cm.								
1	11.64	5.14	0.243	1.141	0.892	90.74	43.87	0.133
2	10.41	5.25	0.243	1.118	0.891	90.53	131.97	0.171
3	11.76	5.16	0.245	1.156	1.758	90.57	43.57	0.257
4	11.06	5.02	0.245	1.052	0.885	89.90	95.87	0.144
5	11.59	5.15	0.248	1.110	1.734	90.00	56.37	0.263
6	11.09	5.05	0.248	1.085	0.873	90.15	116.17	0.144
7	10.82	4.99	0.249	1.103	0.872	90.41	125.47	0.151
8	11.62	5.23	0.249	1.099	0.872	90.12	53.47	0.134
9	11.24	5.06	0.250	1.056	0.868	90.02	106.87	0.140
10	10.36	5.05	0.250	1.143	1.721	90.83	123.77	0.330
11	11.58	5.17	0.251	1.094	1.716	89.93	65.17	0.264
12	11.19	4.93	0.251	1.068	0.866	90.10	93.17	0.139
13	10.62	5.07	0.251	1.113	1.715	90.60	113.87	0.313
14	11.21	4.91	0.251	1.073	1.713	90.11	97.87	0.272
15	10.92	5.15	0.252	1.091	1.711	90.37	105.17	0.298
16	10.63	4.95	0.252	1.116	0.862	90.74	137.27	0.156
17	11.18	5.14	0.252	1.077	1.706	90.19	98.77	0.282
18	11.32	5.01	0.252	1.072	1.706	90.07	97.37	0.270
19	11.18	4.80	0.253	1.080	1.700	90.22	92.77	0.270
20	11.63	5.21	0.254	1.080	0.854	90.03	68.37	0.133
21	11.67	5.22	0.255	1.081	1.686	89.99	74.27	0.261
22	11.36	4.93	0.256	1.076	0.849	90.20	87.37	0.135
23	11.55	5.07	0.256	1.081	0.847	90.12	79.47	0.133
24	11.07	4.82	0.257	1.030	0.423	90.51	115.97	0.071
25	11.81	5.29	0.259	1.075	1.660	90.05	87.57	0.257
26	10.56	5.22	0.261	1.135	0.045	91.58	342.87	0.009
27	10.61	4.77	0.262	1.102	0.045	91.49	193.97	0.008
28	10.92	4.72	0.263	1.060	0.415	90.95	138.17	0.072
29	10.54	4.94	0.263	1.120	0.045	91.63	349.87	0.009
30	11.44	4.92	0.264	1.049	0.413	90.57	129.27	0.067
31	11.38	5.03	0.264	1.020	0.045	90.61	132.07	0.007
32	11.70	5.00	0.266	1.070	0.410	90.54	69.37	0.065
33	11.69	4.86	0.266	1.089	0.409	90.88	58.97	0.064
34	11.70	5.09	0.266	1.054	0.409	90.40	80.57	0.065
35	11.45	4.88	0.267	1.046	0.409	90.63	122.77	0.066

**Table E-6. Countercurrent Condenser Data for Configuration 8
with Random Packing (Continued)**

S.No.	T _{si} (C)	T _{wi} (C)	G (kg/m ² s)	Ja	X _{ii} (%)	Cond- ensed Steam (%)	Press- ure Loss (Pa)	Vent Fraction
36	10.84	4.78	0.267	1.085	0.409	91.28	154.57	0.074
37	11.42	4.89	0.267	1.039	0.044	90.58	86.27	0.007
38	11.41	4.96	0.267	1.026	0.044	90.55	98.67	0.007
39	10.49	5.06	0.267	1.137	0.408	91.72	182.87	0.083
40	11.21	5.01	0.268	1.084	0.044	91.26	193.27	0.008
41	11.73	5.12	0.268	1.047	0.407	90.43	91.77	0.065
42	11.43	4.98	0.268	1.020	0.044	90.65	117.67	0.007
43	10.78	4.89	0.269	1.104	0.406	91.50	171.97	0.076
44	11.56	5.11	0.269	1.018	0.044	90.73	143.07	0.007
45	10.71	5.04	0.270	1.120	0.404	91.63	180.97	0.079
46	11.61	4.92	0.270	1.053	0.404	90.65	116.87	0.065
47	11.49	4.95	0.270	1.029	0.044	90.74	129.27	0.007
48	11.76	5.05	0.271	1.051	0.402	90.56	106.47	0.064
49	11.56	5.06	0.272	1.061	0.044	91.08	181.97	0.007
50	11.71	5.04	0.273	1.038	0.043	90.91	166.87	0.007
51	13.37	4.81	0.366	1.172	0.444	93.40	329.47	0.072
52	13.81	5.08	0.367	1.137	0.445	93.09	311.57	0.070
53	15.02	4.88	0.374	1.161	0.438	93.58	76.47	0.059
54	14.51	5.24	0.374	1.118	0.435	92.84	314.37	0.064
55	15.01	5.02	0.383	1.115	0.427	92.55	132.27	0.059
56	15.10	4.95	0.386	1.124	0.421	92.92	338.07	0.057
57	15.18	5.16	0.387	1.107	0.422	92.43	166.37	0.058
58	15.36	5.23	0.391	1.109	0.420	92.63	276.47	0.057
59	15.38	5.23	0.391	1.111	0.417	92.46	204.57	0.057
60	15.42	5.20	0.392	1.116	0.417	92.57	251.27	0.056
61	15.08	4.91	0.394	1.106	0.074	93.24	409.37	0.010
62	14.80	4.85	0.394	1.125	0.074	93.47	425.97	0.011
63	15.25	5.20	0.394	1.091	0.074	92.47	167.27	0.010
64	15.51	5.18	0.395	1.120	0.416	92.81	330.27	0.056
65	15.53	5.24	0.395	1.115	0.414	92.73	304.97	0.056
66	14.61	5.03	0.395	1.144	0.074	93.66	437.17	0.011
67	15.27	5.10	0.395	1.100	0.074	93.15	403.17	0.010
68	13.78	4.90	0.396	1.222	0.073	94.28	472.07	0.012
69	15.23	5.03	0.397	1.101	0.073	93.16	393.27	0.010
70	15.24	5.00	0.398	1.102	0.073	93.10	371.07	0.010
71	14.31	5.02	0.399	1.167	0.073	93.94	455.67	0.011

Table E-6. Countercurrent Condenser Data for Configuration 8 with Random Packing (Continued)

S.No.	Tsi (C)	Twi (C)	G (kg/m ² s)	Ja	Xii (%)	Cond- ensed Steam (%)	Press- ure Loss (Pa)	Vent Fraction
72	15.39	5.23	0.399	1.090	0.073	92.59	235.97	0.010
73	15.30	5.03	0.400	1.101	0.073	93.03	355.77	0.010
74	15.39	5.10	0.401	1.099	0.073	92.90	327.17	0.010
75	15.46	5.18	0.401	1.096	0.072	92.76	292.27	0.010
Packing Depth 36 cm.								
1	10.74	5.14	0.244	1.001	0.048	90.64	343.04	0.009
2	10.63	4.88	0.247	1.015	0.048	90.88	350.04	0.009
3	10.74	4.91	0.253	1.028	0.047	91.14	200.74	0.008
4	10.56	4.86	0.254	1.037	0.046	91.36	202.64	0.009
5	10.37	5.35	0.255	1.090	0.046	91.59	216.94	0.010
6	10.24	5.31	0.255	1.119	0.428	91.66	208.44	0.091
7	10.28	5.40	0.255	1.102	0.046	91.68	220.84	0.010
8	10.70	5.34	0.256	1.056	0.046	91.39	212.44	0.009
9	10.59	5.35	0.258	1.066	0.046	91.56	217.74	0.009
10	10.38	5.13	0.259	1.110	0.420	91.77	214.74	0.086
11	10.89	5.26	0.260	1.059	0.045	91.46	221.74	0.009
12	11.70	5.45	0.261	1.023	0.418	92.00	81.44	0.069
13	10.74	4.94	0.261	1.058	0.045	91.61	223.64	0.008
14	11.25	5.11	0.262	1.002	0.417	90.89	135.84	0.072
15	11.48	5.25	0.267	0.997	0.409	90.94	151.54	0.070
16	11.48	5.13	0.267	1.016	0.408	91.00	132.24	0.069
17	11.39	4.82	0.267	1.052	1.613	91.24	171.74	0.263
18	11.44	4.94	0.268	1.040	1.610	91.20	177.14	0.264
19	11.15	4.85	0.268	1.059	1.610	91.45	183.64	0.276
20	10.51	4.84	0.268	1.101	0.407	92.06	226.64	0.080
21	11.67	5.32	0.269	1.010	0.406	90.96	171.34	0.068
22	10.76	4.92	0.269	1.086	0.406	91.89	224.34	0.077
23	10.31	4.82	0.269	1.199	0.809	92.41	244.74	0.166
24	11.47	4.97	0.269	1.033	1.602	91.23	175.94	0.264
25	11.64	5.14	0.271	1.020	0.403	91.17	201.54	0.066
26	11.68	5.24	0.271	1.017	0.402	91.12	186.54	0.067
27	10.71	4.97	0.272	1.166	0.802	92.22	244.14	0.156
28	11.94	5.44	0.272	1.020	0.401	91.51	102.04	0.066
29	11.30	4.98	0.272	1.092	0.799	91.72	224.94	0.138
30	11.22	5.11	0.272	1.059	0.400	91.67	222.04	0.072

**Table E-6. Countercurrent Condenser Data for Configuration 8
with Random Packing (Continued)**

S.No.	Tsi (C)	Tw (C)	G (kg/m ² s)	Ja	Xii (%)	Cond- ensed Steam (%)	Press- ure Loss (Pa)	Vent Fraction
31	11.71	5.16	0.273	1.025	0.400	91.26	119.54	0.066
32	11.28	4.93	0.274	1.047	0.398	91.66	216.74	0.069
33	11.48	4.98	0.274	1.071	0.795	91.59	215.64	0.134
34	11.12	5.19	0.274	1.134	0.793	92.01	237.64	0.148
35	11.79	5.12	0.275	1.039	0.793	91.28	196.74	0.129
36	11.90	5.21	0.275	1.042	0.792	91.24	207.24	0.127
37	11.10	4.84	0.275	1.087	1.568	91.87	204.24	0.279
38	11.71	5.02	0.275	1.039	0.789	91.35	185.24	0.129
39	11.15	5.00	0.276	1.111	0.790	91.99	234.94	0.143
40	11.92	5.12	0.277	1.052	1.560	91.28	173.64	0.249
41	11.69	4.97	0.277	1.039	0.787	91.39	176.84	0.129
42	10.85	5.25	0.278	1.175	1.554	92.29	232.14	0.310
43	12.04	5.13	0.278	1.064	1.554	92.26	105.24	0.246
44	11.05	4.94	0.278	1.114	1.552	92.09	217.64	0.285
45	10.87	5.01	0.280	1.151	1.544	92.32	230.44	0.299
46	11.98	5.13	0.280	1.048	1.544	91.38	157.44	0.247
47	10.95	4.95	0.280	1.132	1.544	92.24	224.04	0.291
48	11.80	4.97	0.280	1.045	0.778	91.46	168.84	0.127
49	12.02	5.12	0.281	1.050	1.536	91.48	146.84	0.245
50	12.36	5.31	0.282	1.071	0.773	92.69	104.34	0.121
51	12.08	5.13	0.282	1.054	1.531	91.64	132.94	0.243
52	12.02	5.06	0.284	1.049	0.767	91.53	160.04	0.123
53	12.20	5.20	0.286	1.048	0.762	91.61	141.14	0.122
54	13.85	5.31	0.339	1.075	1.283	92.66	215.84	0.189
55	13.88	4.95	0.340	1.123	1.279	94.18	161.14	0.185
56	13.77	5.07	0.340	1.092	1.279	93.23	190.94	0.188
57	14.46	5.23	0.341	1.155	2.533	94.32	123.24	0.345
58	13.97	5.14	0.343	1.103	2.526	92.78	288.34	0.360
59	13.79	5.06	0.343	1.126	2.520	92.96	302.84	0.366
60	13.51	5.15	0.344	1.155	2.516	93.22	308.94	0.385
61	13.87	4.81	0.345	1.125	2.509	92.98	309.74	0.354
62	13.36	5.12	0.345	1.080	0.634	93.09	344.44	0.100
63	13.73	5.09	0.347	1.142	2.497	93.16	317.34	0.371
64	13.12	5.00	0.349	1.126	0.629	93.48	370.64	0.103
65	14.04	4.78	0.350	1.133	2.474	93.10	301.64	0.347
66	14.49	5.25	0.351	1.127	2.466	93.67	195.24	0.342
67	13.04	5.15	0.354	1.161	0.622	93.73	387.94	0.107

**Table E-6. Countercurrent Condenser Data for Configuration 8
with Random Packing (Continued)**

S.No.	T _{si} (C)	T _{wi} (C)	G (kg/m ² s)	Ja	X _{ii} (%)	Cond- ensed Steam (%)	Press- ure Loss (Pa)	Vent Fraction
68	14.19	5.26	0.355	1.071	0.622	92.99	368.94	0.091
69	14.51	5.15	0.355	1.127	2.436	93.21	241.54	0.336
70	14.35	4.93	0.356	1.134	2.434	93.15	288.64	0.337
71	14.30	5.11	0.357	1.103	1.223	93.01	372.34	0.172
72	14.05	4.97	0.357	1.084	0.616	93.10	365.14	0.090
73	14.17	5.18	0.357	1.072	0.610	93.04	377.14	0.089
74	14.22	4.98	0.358	1.105	1.220	93.08	354.74	0.173
75	14.43	5.24	0.358	1.093	0.617	94.19	186.24	0.089
76	15.27	5.06	0.359	1.213	1.800	94.66	74.64	0.229
77	14.39	5.24	0.362	1.076	0.613	93.27	226.94	0.089
78	14.18	4.92	0.362	1.091	0.610	93.18	364.34	0.088
79	14.64	5.27	0.363	1.106	1.201	93.00	323.64	0.167
80	13.88	5.11	0.363	1.174	1.197	93.60	408.74	0.183
81	14.22	5.06	0.363	1.142	1.200	93.39	406.04	0.174
82	14.82	5.53	0.363	1.094	1.199	92.91	278.54	0.167
83	14.40	4.97	0.364	1.112	1.198	93.18	353.64	0.169
84	14.39	5.23	0.364	1.073	0.605	93.02	271.14	0.088
85	14.37	5.04	0.365	1.090	0.603	93.13	350.84	0.087
86	13.77	4.88	0.365	1.175	1.772	93.73	391.54	0.272
87	14.19	4.99	0.365	1.145	1.769	93.46	387.54	0.258
88	14.43	5.17	0.366	1.079	0.603	93.07	318.04	0.087
89	13.34	4.94	0.366	1.232	1.189	94.04	421.94	0.196
90	13.54	4.83	0.366	1.220	1.764	93.97	402.14	0.280
91	14.59	5.06	0.367	1.104	0.888	93.18	391.44	0.124
92	14.58	4.83	0.368	1.133	1.756	93.35	387.74	0.241
93	14.72	5.02	0.368	1.125	1.755	93.24	402.74	0.239
94	14.45	4.80	0.368	1.119	0.885	93.33	388.94	0.124
95	14.32	4.98	0.368	1.081	0.442	93.37	414.74	0.064
96	14.27	4.87	0.369	1.087	0.088	93.53	459.44	0.013
97	14.63	4.91	0.370	1.119	1.749	93.35	397.54	0.242
98	12.85	5.09	0.370	1.206	0.087	94.30	453.44	0.016
99	15.08	5.23	0.370	1.132	1.746	94.33	217.44	0.237
100	14.18	5.00	0.371	1.104	0.439	93.58	431.74	0.066
101	13.94	5.15	0.371	1.122	0.439	93.73	432.14	0.069
102	13.73	5.20	0.372	1.144	0.439	93.88	435.14	0.072
103	14.44	4.97	0.372	1.084	0.437	93.43	427.84	0.063

Table E-6. Countercurrent Condenser Data for Configuration 8
with Random Packing (Continued)

S.No.	Tsi (C)	Tw (C)	G (kg/m ² s)	Ja	Xii (%)	Cond- ensed Steam (%)	Press- ure Loss (Pa)	Vent Fraction
104	14.41	4.95	0.372	1.083	0.087	93.50	453.74	0.013
105	14.12	5.00	0.372	1.109	0.087	93.76	475.74	0.013
106	14.73	5.13	0.373	1.096	0.435	94.53	206.94	0.062
107	13.06	4.82	0.374	1.192	0.086	94.34	471.84	0.015
108	14.58	5.10	0.374	1.078	0.087	93.38	437.34	0.012
109	13.87	5.12	0.375	1.145	0.085	93.99	483.34	0.014
110	14.47	4.81	0.376	1.096	0.433	93.50	425.64	0.062
111	14.90	4.82	0.376	1.143	1.720	93.46	402.74	0.232
112	15.03	5.18	0.376	1.119	0.867	94.16	260.04	0.119
113	14.78	4.82	0.376	1.128	0.867	93.45	399.04	0.119
114	14.77	5.27	0.376	1.074	0.086	93.25	422.64	0.012
115	14.96	5.59	0.376	1.057	0.086	92.94	363.94	0.012
116	14.72	5.13	0.377	1.084	0.431	93.80	252.54	0.062
117	15.16	5.25	0.377	1.122	1.714	93.61	282.94	0.233
118	14.91	5.45	0.378	1.064	0.086	93.12	397.54	0.012
119	15.09	5.01	0.378	1.137	1.709	93.44	374.44	0.230
120	15.03	5.12	0.379	1.114	0.859	93.56	314.74	0.118
121	15.18	5.11	0.379	1.130	1.706	93.48	325.44	0.229
122	14.74	5.14	0.380	1.078	0.431	93.31	321.04	0.062
123	14.62	4.83	0.380	1.098	0.429	93.52	420.24	0.061
124	14.99	4.96	0.381	1.123	0.858	93.47	377.54	0.117
125	14.82	5.12	0.382	1.083	0.427	93.33	360.64	0.061
126	15.32	5.29	0.382	1.119	0.854	93.30	455.04	0.114
127	14.80	4.97	0.383	1.095	0.425	93.43	398.04	0.060
128	15.36	5.15	0.384	1.133	0.850	93.44	492.24	0.112
129	14.84	5.25	0.385	1.061	0.075	93.27	387.14	0.011
130	14.78	5.13	0.385	1.067	0.075	93.25	360.54	0.011
131	15.13	5.13	0.386	1.158	0.846	93.66	502.34	0.115
132	14.16	5.07	0.386	1.286	0.844	94.34	519.94	0.132
133	14.91	5.26	0.386	1.192	0.843	93.85	510.54	0.120
134	14.35	4.97	0.387	1.246	0.842	94.22	517.44	0.127
135	15.06	5.32	0.389	1.066	0.075	93.36	426.24	0.011
136	15.05	5.26	0.390	1.070	0.075	93.34	307.74	0.011
137	14.96	5.12	0.390	1.075	0.075	93.29	356.04	0.011
138	15.08	5.05	0.391	1.095	0.074	93.82	534.84	0.010
139	13.75	4.91	0.391	1.186	0.074	94.49	521.24	0.012
140	14.35	4.95	0.391	1.138	0.074	94.21	534.14	0.011

**Table E-6. Countercurrent Condenser Data for Configuration 8
with Random Packing (Continued)**

S.No.	Tsi (C)	Twi (C)	G (kg/m ² s)	Ja	Xii (%)	Cond- ensed Steam (%)	Press- ure Loss (Pa)	Vent Fraction
141	14.94	5.16	0.392	1.112	0.074	93.94	542.34	0.011
142	15.21	5.28	0.392	1.079	0.074	93.52	469.24	0.010
143	15.15	5.11	0.393	1.092	0.074	93.77	524.74	0.010
144	14.25	5.15	0.393	1.158	0.074	94.28	529.44	0.012
145	15.22	5.19	0.394	1.086	0.074	93.67	505.84	0.010
146	13.71	5.10	0.394	1.204	0.074	94.54	522.34	0.013
147	18.80	4.86	0.486	1.228	0.903	95.87	83.54	0.102
148	18.12	5.23	0.489	1.184	1.784	94.62	697.44	0.218
149	17.82	5.31	0.490	1.207	1.779	94.80	701.04	0.227
150	18.46	5.12	0.490	1.161	1.778	94.47	695.54	0.209
151	18.23	5.02	0.496	1.130	0.437	94.56	744.34	0.053
152	18.78	5.25	0.497	1.163	1.755	95.74	411.24	0.207
153	18.10	4.76	0.499	1.138	0.444	94.63	730.04	0.054
154	18.46	4.99	0.501	1.149	0.874	95.74	449.64	0.106
155	18.81	5.27	0.502	1.152	1.740	94.85	519.14	0.205
156	18.50	5.23	0.503	1.121	0.436	94.58	779.24	0.052
157	18.94	5.33	0.503	1.155	1.732	94.51	592.74	0.201
158	18.61	5.13	0.504	1.145	0.870	94.78	548.84	0.104
159	18.42	4.90	0.506	1.137	0.427	94.55	722.94	0.052
160	18.77	5.26	0.506	1.143	0.868	94.50	615.04	0.103
161	19.11	5.43	0.507	1.155	1.721	94.44	646.24	0.199
162	18.46	4.87	0.508	1.138	0.433	94.54	692.24	0.052
163	16.85	5.09	0.508	1.214	0.433	95.42	761.84	0.063
164	18.63	5.05	0.508	1.136	0.431	95.73	446.44	0.052
165	18.96	5.34	0.510	1.143	0.859	94.45	662.24	0.100
166	18.30	4.81	0.510	1.126	0.435	94.81	780.74	0.053
167	18.58	4.86	0.511	1.143	0.430	94.53	665.34	0.051
168	19.33	5.45	0.513	1.158	1.701	94.43	686.54	0.194
169	19.17	5.37	0.514	1.148	0.853	94.43	710.94	0.098
170	17.50	5.32	0.514	1.181	0.428	95.25	779.44	0.060
171	18.72	4.99	0.514	1.135	0.426	94.76	561.54	0.051
172	19.43	5.33	0.516	1.168	1.692	94.48	736.44	0.190
173	18.78	4.94	0.516	1.139	0.426	94.55	633.64	0.051
174	18.82	5.28	0.516	1.116	0.062	94.52	771.34	0.007
175	18.24	5.06	0.516	1.137	0.062	95.14	878.64	0.008
176	19.23	5.32	0.517	1.151	0.849	94.48	743.64	0.097

**Table E-6. Countercurrent Condenser Data for Configuration 8
with Random Packing (Continued)**

S.No.	Tsi (C)	Twi (C)	G (kg/m ² s)	Ja	Xii (%)	Cond- ensed Steam (%)	Press- ure Loss (Pa)	Vent Fraction
177	18.79	5.29	0.518	1.109	0.062	94.77	837.64	0.007
178	18.75	5.24	0.518	1.109	0.062	94.71	811.54	0.007
179	19.28	4.99	0.520	1.177	1.680	94.71	777.94	0.190
180	18.26	4.93	0.520	1.149	0.423	95.05	813.94	0.054
181	18.89	5.24	0.521	1.115	0.062	94.50	758.54	0.007
182	19.29	5.31	0.521	1.148	0.842	94.57	789.14	0.097
183	18.13	5.33	0.524	1.155	0.421	95.14	807.34	0.056
184	18.69	4.92	0.524	1.120	0.061	95.07	899.54	0.007
185	18.87	5.18	0.524	1.111	0.061	94.92	871.84	0.007
186	17.26	5.12	0.525	1.276	0.061	95.76	893.44	0.009
187	19.29	5.51	0.526	1.112	0.061	94.23	693.34	0.007
188	18.14	5.10	0.527	1.170	0.061	95.41	903.74	0.008
189	17.88	5.26	0.527	1.198	0.061	95.51	899.44	0.008
190	19.17	5.37	0.527	1.113	0.061	94.39	747.14	0.007
191	17.58	5.11	0.528	1.235	0.061	95.67	900.64	0.008
192	17.58	5.11	0.528	1.235	0.061	95.67	900.64	0.008
193	19.38	5.27	0.529	1.142	0.831	94.76	840.84	0.096
194	18.35	5.27	0.531	1.160	0.060	95.35	906.44	0.008
195	19.28	5.42	0.532	1.163	0.826	94.90	855.74	0.097
196	18.19	5.00	0.534	1.243	0.824	95.49	864.64	0.107
197	17.89	5.10	0.536	1.294	0.820	95.64	866.64	0.112
198	19.11	5.47	0.536	1.185	0.818	95.09	875.14	0.099
Packing Depth 66 cm.								
1	10.75	5.10	0.233	1.027	1.843	90.85	205.74	0.309
2	10.73	5.03	0.233	1.041	1.842	91.50	175.74	0.310
3	10.93	5.31	0.233	1.022	1.841	90.76	217.04	0.306
4	10.68	5.02	0.233	1.027	1.841	90.94	199.34	0.311
5	10.66	4.96	0.234	1.033	1.835	91.15	191.94	0.310
6	10.91	5.12	0.235	1.045	0.925	92.27	134.94	0.155
7	11.37	5.49	0.238	1.048	1.363	92.18	121.24	0.221
8	10.84	5.08	0.240	1.022	0.907	91.58	185.34	0.155
9	10.59	5.32	0.240	1.069	0.907	91.31	240.74	0.168
10	11.31	5.51	0.240	1.023	1.349	91.37	181.44	0.223
11	10.89	5.13	0.241	1.016	0.904	91.23	207.04	0.154
12	10.89	4.93	0.241	1.048	1.342	91.26	243.04	0.221

Table E-6. Countercurrent Condenser Data for Configuration 8
with Random Packing (Continued)

S.No.	T _{si} (C)	T _{wi} (C)	G (kg/m ² s)	Ja	Xii (%)	Cond- ensed Steam (%)	Press- ure Loss (Pa)	Vent Fraction
13	11.34	5.51	0.242	1.021	1.336	91.21	197.94	0.221
14	11.05	5.23	0.243	1.019	0.893	91.07	228.24	0.150
15	11.41	5.46	0.246	1.027	1.320	91.10	216.14	0.216
16	11.15	5.16	0.246	1.037	0.884	91.27	252.74	0.146
17	11.32	5.30	0.246	1.039	1.315	91.13	237.34	0.215
18	10.94	4.93	0.251	1.064	0.864	91.70	268.34	0.147
19	11.19	4.88	0.262	1.015	0.083	91.98	287.54	0.014
20	11.66	5.41	0.267	0.983	0.081	91.51	227.54	0.014
21	12.18	5.29	0.268	1.077	0.407	93.00	72.34	0.063
22	11.01	5.04	0.270	1.056	0.080	92.32	298.04	0.015
23	10.92	4.89	0.271	1.062	0.080	92.31	287.44	0.015
24	11.85	5.42	0.272	0.998	0.043	91.55	243.64	0.007
25	11.52	4.93	0.272	1.026	0.043	92.21	314.74	0.007
26	11.49	4.87	0.272	1.026	0.080	92.10	292.34	0.013
27	11.77	5.28	0.274	1.000	0.043	91.80	236.44	0.007
28	11.74	5.19	0.274	1.006	0.079	92.00	236.14	0.013
29	11.54	5.12	0.274	1.050	0.397	92.26	311.14	0.068
30	11.65	4.99	0.275	1.024	0.043	92.09	303.24	0.007
31	11.93	5.42	0.275	0.998	0.043	91.67	267.14	0.007
32	11.35	5.10	0.278	1.073	0.043	92.57	330.84	0.008
33	11.87	5.16	0.278	1.019	0.078	92.00	287.34	0.013
34	12.01	5.33	0.278	1.015	0.042	91.90	293.14	0.007
35	11.57	5.02	0.279	1.054	0.391	92.34	290.54	0.067
36	11.96	5.11	0.279	1.028	0.391	92.59	239.94	0.063
37	10.93	4.71	0.279	1.068	0.078	92.56	292.34	0.014
38	11.45	5.29	0.280	1.047	0.042	92.27	257.74	0.008
39	11.47	5.32	0.280	1.044	0.042	92.17	271.04	0.008
40	12.03	5.19	0.280	1.032	0.389	92.07	281.94	0.063
41	11.76	5.09	0.280	1.048	0.389	92.27	285.14	0.065
42	11.48	5.32	0.280	1.046	0.042	92.23	288.24	0.008
43	11.37	5.10	0.281	1.064	0.042	92.49	315.94	0.008
44	11.68	5.16	0.281	1.042	0.077	92.56	246.34	0.013
45	11.50	5.23	0.282	1.061	0.042	92.37	305.24	0.008
46	12.26	5.36	0.282	1.024	0.387	92.34	247.24	0.062
47	11.16	4.85	0.283	1.069	0.077	92.52	290.24	0.014
48	11.49	5.17	0.283	1.069	0.077	93.05	247.14	0.014
49	12.18	5.25	0.284	1.025	0.385	92.16	268.74	0.062

**Table E-6. Countercurrent Condenser Data for Configuration 8
with Random Packing (Continued)**

S.No.	T _{si} (C)	T _{wi} (C)	G (kg/m ² s)	Ja	X _{ii} (%)	Cond- ensed Steam (%)	Press- ure Loss (Pa)	Vent Fraction
50	12.30	5.47	0.284	1.014	0.076	91.88	286.14	0.012
51	11.85	4.83	0.284	1.027	0.021	92.50	343.54	0.003
52	11.32	4.98	0.285	1.066	0.076	92.48	277.24	0.014
53	11.70	4.93	0.286	1.056	0.021	92.66	351.84	0.003
54	11.80	4.77	0.286	1.026	0.021	92.41	326.44	0.003
55	10.89	4.83	0.287	1.129	0.021	93.15	344.84	0.004
56	11.63	5.23	0.289	1.059	0.020	92.66	330.44	0.004
57	11.62	5.20	0.290	1.060	0.020	92.61	320.54	0.004
58	12.23	5.28	0.290	1.023	0.102	92.59	260.04	0.017
59	12.20	5.23	0.290	1.023	0.102	92.35	274.04	0.017
60	12.70	5.19	0.291	1.107	2.356	92.58	307.54	0.347
61	11.51	5.00	0.294	1.048	0.020	92.72	312.94	0.004
62	12.27	5.23	0.294	1.021	0.100	92.37	292.54	0.016
63	12.39	5.32	0.295	1.021	0.100	92.31	306.34	0.016
64	12.61	5.41	0.296	1.013	0.020	92.18	329.54	0.003
65	12.23	4.93	0.296	1.055	0.100	92.79	371.94	0.016
66	12.43	4.90	0.297	1.078	1.168	92.76	351.64	0.179
67	11.42	4.78	0.297	1.058	0.020	92.88	308.24	0.004
68	12.66	4.93	0.298	1.114	2.301	92.83	335.44	0.340
69	12.52	5.35	0.298	1.003	0.020	92.19	313.54	0.003
70	12.56	5.39	0.299	1.026	0.099	92.40	328.64	0.016
71	12.43	4.83	0.299	1.081	1.157	92.85	340.94	0.178
72	12.61	5.31	0.299	1.041	0.099	92.57	358.94	0.016
73	12.03	4.79	0.301	1.020	0.020	92.60	312.04	0.003
74	12.47	4.90	0.302	1.071	0.098	92.95	395.44	0.015
75	13.14	5.47	0.303	1.082	1.699	92.98	299.24	0.253
76	12.64	5.14	0.303	1.055	0.078	92.73	376.74	0.012
77	12.79	5.32	0.306	1.043	0.077	92.55	340.24	0.012
78	12.71	5.21	0.307	1.047	0.077	92.67	359.54	0.012
79	12.89	5.48	0.307	1.032	0.077	92.48	317.94	0.012
80	12.91	5.22	0.307	1.062	0.569	92.81	371.94	0.087
81	12.80	4.88	0.308	1.097	1.127	93.22	344.14	0.170
82	12.80	5.10	0.308	1.062	0.566	92.99	356.44	0.088
83	13.28	5.37	0.308	1.098	1.670	92.84	348.34	0.244
84	12.67	4.69	0.309	1.111	2.223	93.69	316.14	0.335
85	12.85	4.92	0.309	1.100	2.221	93.39	323.44	0.333

**Table E-6. Countercurrent Condenser Data for Configuration 8
with Random Packing (Continued)**

S.No.	Tsi (C)	Twi (C)	G (kg/m ² s)	Ja	Xii (%)	Cond- ensed Steam (%)	Press- ure Loss (Pa)	Vent Fraction
86	13.06	5.35	0.309	1.059	0.563	92.82	391.04	0.085
87	13.12	4.96	0.309	1.128	1.664	93.04	393.34	0.240
88	12.76	4.99	0.311	1.066	0.562	93.39	336.34	0.088
89	13.14	5.12	0.311	1.098	1.117	93.89	306.54	0.166
90	12.78	4.64	0.312	1.122	2.203	93.89	320.14	0.329
91	12.79	4.92	0.312	1.075	0.559	93.94	309.04	0.087
92	12.88	5.19	0.314	1.037	0.125	93.08	324.54	0.020
93	13.27	5.11	0.314	1.107	1.104	93.08	416.74	0.160
94	13.14	5.25	0.321	1.041	0.123	93.03	357.34	0.019
95	13.27	5.21	0.322	1.058	0.122	93.05	401.14	0.019
96	13.27	5.22	0.323	1.054	0.122	93.05	385.94	0.019
97	13.32	5.18	0.323	1.067	0.122	93.17	433.04	0.018
98	13.35	5.09	0.325	1.079	0.121	93.36	462.24	0.018
99	15.69	5.02	0.389	1.171	1.846	94.48	647.04	0.237
100	15.89	5.00	0.391	1.188	2.401	94.83	619.04	0.304
101	16.21	5.22	0.392	1.194	2.352	95.29	460.84	0.294
102	15.95	5.06	0.392	1.188	2.312	95.01	600.64	0.294
103	16.06	5.11	0.393	1.192	2.411	95.27	550.74	0.305
104	15.90	5.04	0.393	1.184	2.373	94.64	650.04	0.301
105	15.99	5.20	0.393	1.169	1.222	95.32	411.84	0.158
106	15.74	4.88	0.394	1.180	1.825	94.66	650.34	0.234
107	15.85	4.97	0.394	1.183	2.313	94.73	634.04	0.295
108	15.88	5.03	0.395	1.175	1.819	94.89	620.84	0.234
109	15.94	5.05	0.395	1.179	1.818	95.19	591.24	0.234
110	15.82	4.94	0.395	1.177	1.817	94.78	640.34	0.234
111	15.89	5.18	0.396	1.154	1.213	94.83	610.34	0.158
112	15.90	5.30	0.397	1.143	1.211	94.60	616.44	0.159
113	16.07	5.46	0.397	1.139	1.211	94.39	638.54	0.157
114	15.94	5.18	0.397	1.160	1.210	95.18	581.24	0.158
115	16.03	5.05	0.397	1.184	1.810	95.39	499.04	0.232
116	16.38	5.29	0.405	1.168	1.186	94.48	719.64	0.148
117	17.99	4.94	0.472	1.198	0.052	95.35	991.64	0.006
118	17.99	5.01	0.472	1.177	0.108	95.32	975.04	0.013
119	18.28	5.26	0.473	1.176	0.070	95.20	991.14	0.008
120	17.99	4.83	0.474	1.188	0.113	95.35	978.64	0.013
121	18.06	4.95	0.475	1.196	0.052	95.35	993.14	0.006

Table E-6. Countercurrent Condenser Data for Configuration 8
with Random Packing (Concluded)

S.No.	T _{si} (C)	T _{wi} (C)	G (kg/m ² s)	Ja	X _{ii} (%)	Cond- ensed Steam (%)	Press- ure Loss (Pa)	Vent Fraction
122	18.33	5.19	0.476	1.180	0.069	95.22	993.64	0.008
123	18.07	4.82	0.476	1.190	0.103	95.36	979.94	0.012
124	18.76	5.01	0.478	1.228	0.506	95.44	983.54	0.057
125	18.17	4.89	0.478	1.188	0.112	95.35	974.04	0.013
126	18.39	5.29	0.479	1.169	0.069	95.65	905.64	0.008
127	18.29	5.15	0.479	1.187	0.051	95.24	982.24	0.006
128	18.17	5.03	0.479	1.189	0.051	95.32	988.14	0.006
129	18.44	5.21	0.480	1.181	0.069	95.21	990.74	0.008
130	18.40	5.30	0.480	1.167	0.069	95.38	921.14	0.008
131	18.87	5.10	0.480	1.227	0.504	95.73	961.34	0.057
132	18.46	5.14	0.481	1.183	0.051	95.20	986.84	0.006
133	18.53	5.30	0.481	1.175	0.069	95.17	976.24	0.008
134	18.72	5.41	0.482	1.180	0.108	95.98	858.24	0.013
135	18.46	5.33	0.482	1.164	0.069	95.18	948.24	0.008
136	18.35	4.97	0.482	1.188	0.103	95.34	977.74	0.012
137	18.50	5.10	0.483	1.184	0.110	95.32	965.14	0.013
138	18.59	5.24	0.484	1.178	0.051	95.18	975.74	0.006
139	18.64	5.31	0.485	1.177	0.105	95.35	951.24	0.012
140	18.78	5.25	0.485	1.192	0.498	96.16	752.94	0.058
141	18.78	5.37	0.486	1.182	0.051	95.34	956.34	0.006

APPENDIX F COMPUTER PROGRAM LISTINGS

This appendix lists the computer codes, written in PASCAL, used for condenser modeling. We used the commercially available PASCAL computer program compiler code Turbo-Pascal™ (version 3.0) to run the codes. The code can be run on any IBM or compatible personal computer.

The first part of the list is for modeling a cocurrent condenser; the second part is for modeling a countercurrent operation. Brief explanations and comments are included in the listings. A detailed table of the variables and their descriptions follows in Table F-1.

```
PROGRAM Cocurrent_Condenser;
```

```
{ $U+ } { User Interrupt enabled }
```

```
{ This algorithm contains routines which model a cocurrent direct
  contact condenser with a packed column geometry for use in an open
  cycle ocean thermal energy conversion (OTEC) system. Packings
  modelled are of the structured type. Details of the modeling and
  the accompanying study can be found in this report (SERI/TR-252-3108).
  This version is set up to run with the TURBO-Pascal compiler (version
  3.0, Borland International Inc.) on an IBM or compatible
  personal computer.
```

```
In case of you may find errors or problems in using this code,
please contact the authors at SERI:
```

```
1617 Cole Boulevard
Golden, Colorado, 80401
Tel: (303)-231-1000
```

```
***** -----
Main Routine --Cocond-- version 871015, Revisions 10-15-87
***** -----}
```

```
CONST
```

```
{ Physical Constants }
Molwts=18.015; Molwti=28.97;
G=9.81; Sigma=0.072;
{ Water Saturation Pressure Curve Fit Constants }
p1=161.75743178; p2=18.477911547; p3=4026.97587317;
p4=234.73842369; p5=3.73834517667;
{ Water Viscosity Curve Fit Constants }
an1=241.4; an2=0.382809486; an3=0.2162830218;
{ Accuracy Tolerance Limit for Integration }
Tol=1e-12;
{ Mathematical Constants }
Pi=3.1415927;
Neqn=11 { Number of Equations to be Integrated };
Nseg=200 { Number of Segments the condenser is divided into };
```

```
TYPE
```

```
State = ARRAY[1..11] of Real;
Lable = String[20];
Vector = ARRAY[1..20] of Real;
```

```
VAR
```

```
Istep : Integer;
Nrun, Serial : Integer;
Cond_Len, Pckdia, C_S_Area, Saperv, Corliq, Corgas,
Corfr, Void, Theta, Sinalpha : Real;
Run_Lable : String[15];
Xin, Velin, Pstgin, Tstgin, Super_In : Real;
```

```

X,X_Est,Tdew,Xend                                : Real;
Kliq,Muliq,Cpli,Prliq,Sccliq,Rholiq,Diffaw       : Real;
Lhtc,Lmtc,Ghtc,Gmtc,Frcgas,Frcliq,Rel,Reg        : Real;
Tsurf,Ovhtc,Ovmtc,SteamFlux,Czero,Cht1,Cht2,Cht3,
Ackerh,Ackf                                       : Real;
Xeq,Veleq,Pstgeq,Tstgeq,Supreq                   : Real;
Temp,Press,Volw,Vols,Enthw,Enths                 : Real;
Y,Yin,Yeqlbm,Y_Est,Prime,Yprime                 : State;
Filein,Filot1,Filot2                             : Lable;
Geometry                                           : String[4];
Form6,Form7                                       : Char;
InFile,OutFile1,OutFile2,OutFile3               : Text;
TgasDB,Tsat,Tliq                                 : Real;
Ptotal,Satpr,ppsteam                             : Real;
Xmass,Ymole                                       : Real;
AirMu,AirK,AirCp                                 : Real;
StmMu,StmK,StmCp                                 : Real;
StmRho,StmDiff                                   : Real;
MixMu,MixK,MixCp,MixPr,MixSc,MixMwt,MixRho       : Real;
Phi12,Phi21                                      : Real;
MixEnth,Enthliq                                  : Real;
I                                                  : Integer;
Epsilon,Toll,T,Tolzer,Tolerance                 : Real;
Tot_In_Enth,Wat_In_Enth,Gas_In_Enth             : Real;
U_Bulk,Gamma,A,Mach                             : Real;
Tzbyt,Pzbyp                                       : Real;
Vel_Eqlbm,Super_Eqlbm,X_Eqlbm                   : Real;
Mom_In,Vel_In,K_E_In                             : Real;
T_Stg_In,T_Dew_In,P_Stg_In                     : Real;
T_Stg_Eq,P_Stg_Eq                               : Real;
Yacob,PpmIn                                       : Real;
Gas_Load,Xinprc                                  : Real;
RhoUb                                             : Real;
Step,Afraction,Xfinal                           : Real;
Base,Height,Side,Apgeom,Sprime                  : Real;
Wateff,Cond_prc,Pdrop,Nusselt_Gas               : Real;
U_G_Eff,U_L_Eff                                  : Real;
Iprint,Setflag                                    : Boolean;

{ A TURBO-Pascal support file }
TYPE
    RegPack =
        RECORD { register pack Used in MSDos call }
            AX, BX, CX, DX, BP, SI, DI, DS, ES, Flags : Integer;
        END;
    TimeStr = String[8] ; DateStr = String[10] ;
VAR
    RecPack : RegPack;
    Ctime,Cdate : String[10];

FUNCTION Time: Timestr;
{ returns the current time in string format HH:MM:SS }
VAR
    Hour,Min,Sec,Frac : String[2];

```

```

BEGIN
    WITH RecPack DO
        BEGIN AX := $2C00 ; MsDos(RecPack) ;
            AX := hi(CX); Str(AX,Hour);
            IF AX < 10 THEN Insert(' ',Hour,1);
            AX := lo(CX); Str(AX,Min );
            IF AX < 10 THEN Insert('0',Min ,1);
            AX := hi(DX); Str(AX,Sec );
            IF AX < 10 THEN Insert('0',Sec ,1);
            AX := lo(DX); Str(AX,Frac);
            IF AX < 10 THEN Insert('0',Frac,1);
            Time := Hour + ':' + Min + ':' + Sec;
            {+ '.' + Frac}
        END;
    END;

FUNCTION Date: DateStr;
{ returns the current date in string format : MM/DD/YYYY }
VAR
    Year : String[4] ; Month,Day : String[2] ;
BEGIN
    WITH RecPack DO
        BEGIN
            AX := $2A shl 8 ; MsDos(Recpack);
            AX := DX shr 8; Str(AX,Month);
            IF AX < 10 THEN Insert(' ',Month,1);
            AX := DX mod 256; Str(AX,Day);
            IF AX < 10 THEN Insert('0',Day ,1);
            Str (CX,Year);
            Date := Month + '/' + Day + '/' + Year;
        END;
    END;

PROCEDURE MachineAccuracy;
{ Calculates the smallest discernable real number
  for the machine }
BEGIN
    Epsilon:=1.0;
    REPEAT
        Epsilon:=Epsilon/2.0;
        Tolerance:=1.0 + Epsilon;
    UNTIL (Tolerance< =1.0);
END;

FUNCTION InertMasstoMoleFraction(xm: Real): Real;
{ Converts inert mass fraction to mole fraction }
BEGIN
    InertMasstoMoleFraction:=xm/Molwti/(xm/Molwti+(1-xm)/Molwts);
END;

FUNCTION InertMoletomassFraction(ym1: Real): Real;
{ Converts inert mole fraction to mass fraction }
BEGIN

```

```
InertMoletoMassFraction:=yml*Molwti/(yml*Molwti+(1-yml)*Molwts);
END;

FUNCTION SatTemperature(Satpr: Real): Real;
{ Returns saturation temperature (C) as a function of
saturation pressure (Pa) }
VAR
ak                                     : real;
BEGIN
  IF (Satpr>p5) THEN
    BEGIN
      ak:=(Satpr-p5)/p1;
      SatTemperature:=p3/(p2-ln(ak))-p4;
    END else
      SatTemperature:=-270.15;
END { SatTemperature };

FUNCTION SatPressure(SatT: Real): Real;
{ Returns saturation pressure as a function of
saturation temperature (C) }
BEGIN
  SatPressure:=p1*exp(p2-p3/(SatT+p4))+p5;
END { SatPressure };

FUNCTION Henry(Twater: Real): Real;
{ Returns Henry's Law constant for air solubility in
fresh water in (Pa/Mole Fraction) of Dissolved Air as a
function of Twater in Celcius. Curve fit from 0 to 40 C,
Taken from data in the Saline Water Conversion Engineering
Data Book, M.W. Kellogg Company, Office of Water Research
and Technology, PB-250 907, October 1975, p136. }
VAR
sol                                     : real;
BEGIN
  sol:=(2.3333 + Twater*( -0.05425579 + Twater*0.00623618))/100000.0;
  Henry:=101325.0/sol;
END { Henry };

FUNCTION MixtureEnthalpy(TmixDB,IMF: Real): Real;
{ Returns mixture enthalpy (kJ/kg) as function of gas
mixture temperature (C), and inert mass fraction }
BEGIN
  MixtureEnthalpy:=(1-IMF)*(2501.6+1.866*TmixDB)+
    IMF*1.005*TmixDB;
END { MixtureEnthalpy };

FUNCTION LiquidEnthalpy(Tw: Real): Real;
{ Returns water enthalpy (kJ/kg) as a function of
water temperature (C) }
BEGIN
  LiquidEnthalpy:=4.186*Tw;
END { LiquidEnthalpy };

PROCEDURE AirTransProp(Tair: Real);
```

```

{ Air Transport Properties as functions of temperature Tair (K)}
BEGIN
    AirK:=26.464e-4*exp(1.5*ln(Tair))/
        (Tair+245.4*exp((-12.0/Tair)*ln(10.0)));
    { Thermal Conductivity in (W/mK)}
    AirMu:=1.458e-6*exp(1.5*ln(Tair))/(Tair+110.4);
    { Dynamic Viscosity in (kg/ms) }
    AirCp:=1.005;
    { Specific Heat in (kJ/kg.K)}
END { AirTransProp};

PROCEDURE SteamTransProp(Tstm: Real);
{ Steam Transport Properties as functions of temperature (K)}
BEGIN
    StmK:=(1.82+0.006*(Tstm-273.15))/100;
    { Thermal Conductivity in (W/mK)}
    StmMu:=(8.02+0.04*(Tstm-273.15))*1.0e-6;
    { Dynamic Viscosity in (kg/ms) }
    StmCp:=1.854+0.000775*(Tstm-273.15);
    { Specific Heat in (kJ/kg.K)}
END { SteamTransProp};

PROCEDURE MixTransProp(TDB,Pt,IMF: Real);
{ Given    TDB = Dry-Bulb Steam Temperature in Celcius.
           Pt  = Total Mixture Pressure in Pascals.
           IMF = Inert Gas Mass Fraction.}

VAR
    Tabs,Gmolfr                                : Real;
BEGIN
    Tabs:=TDB+273.15;
    AirTransProp(Tabs);
    SteamTransProp(Tabs);
    { Calculate Mixture Properties, Wilke's Method
    { Section 9-5, p410, Reid et. al.,
      The properties of Gases and Liquids, McGraw Hill, 1977.}
    Gmolfr:=InertMasstoMoleFraction(IMF);
    StmDiff:=2.918*exp(1.75*ln(Tabs/313.0))/Pt;
    { Diffusivity in (m*m/s), p557, Reid et. al.,
      The properties of Gases and Liquids, McGraw Hill, 1977.}
    MixMwt:=1/(IMF/Molwti+(1.0-IMF)/Molwts);
    MixCp:=IMF*AirCp+(1.0-IMF)*StmCp;
    MixRho:=Pt*MixMwt/(8314.3*Tabs);
    Phil2:=sqr(1.0+exp(0.25*ln(Molwti/Molwts))*sqr(Stmmu/AirMu))
        /sqr(8.0+8.0*Molwts/Molwti);
    Phi21:=sqr(1.0+exp(0.25*ln(Molwts/Molwti))*sqr(AirMu/Stmmu))
        /sqr(8.0+8.0*Molwti/Molwts);
    MixMu:=(1.0-Gmolfr)*Stmmu/((1.0-Gmolfr)+Gmolfr*Phil2)+
        Gmolfr*AirMu/(Gmolfr+(1.0-Gmolfr)*Phi21);
    Phil2:=sqr(1.0+exp(0.25*ln(Molwti/Molwts))*sqr(StmK/AirK))
        /sqr(8.0+8.0*Molwts/Molwti);
    Phi21:=sqr(1.0+exp(0.25*ln(Molwts/Molwti))*sqr(AirK/StmK))
        /sqr(8.0+8.0*Molwti/Molwts);
    MixK:=(1.0-Gmolfr)*StmK/((1.0-Gmolfr)+Gmolfr*Phil2)+Gmolfr*AirK/
        (Gmolfr+(1.0-Gmolfr)*Phi21);

```

```

    MixPr:=1000.0*MixCp*MixMu/MixK;
    MixSc:=MixMu/(MixRho*StmDiff);
END { MixTransProp };

PROCEDURE WaterTransProp(WaterTemp: Real);
{ as function of temperature, WaterTemp in Celcius }
VAR
    DelRho,en1,en2                : real;
BEGIN
    DelRho:=-0.69224607+WaterTemp*
        (-0.00175714+WaterTemp*0.00557143);
    IF (WaterTemp< 11.85) THEN DelRho:=0.0;
    Rholiq:=1000.0-DelRho;
    { Specific Heat in (kJ/kg.K) }
    CpLiq:=(4217044.18+WaterTemp*
        (-3504.246+WaterTemp*(113.174+
        WaterTemp*(-1.309))))/1.0e6;
    { Dynamic Viscosity in (kg/m.s) }
    en1:=an2/((WaterTemp+273.15)/647.3-an3);
    en2:=exp(en1*ln(10.0));
    Muliq:=an1*en2*1.0e-7;
    { Thermal Conductivity of Fresh Water in (W/m.K) }
    Kliq:=0.569+0.001575*WaterTemp;
    { Prandtl Number }
    Prliq:=1000.0*Cpliqliq/Muliq/Kliq;
    { Schmidt Number }
    Scliq:=372.7*(sqr(muliq)/(watertemp+273.15))/(2.71e-9);
    { Derived from oxygen diffusivity in water,
        p576, Reid et. al.,
        The properties of Gases and Liquids, McGraw Hill, 1977.}
END { WaterTransProp };

PROCEDURE PackingCharacteristics;
{ Calculates Structured Packing Characteristics, given
    Base, Height, and angle of inclination Theta; All length
    dimensions are in meters; Theta is in degrees; }
VAR
    Sheet,Contactloss            : Real;
BEGIN
    Base:=0.050;
    Height:=Base*1.00;
    Theta:=60.0;
    Side:=Sqrt(Sqr(Base/2) + Sqr(Height)); { slant length }
    Sprime:=Sqrt(Sqr(Base/(2.0*Cos(Theta*Pi/180.0))+Sqr(Height)));
    { distance over which liquid renewal occurs }
    Sinalpha:=Base/(2.0*Sprime*Cos(Theta*Pi/180.0));
    { Sine of angle of inclination of liquid flow with
        respect to horizontal }
    Pckdia:=Base*Height*(1/(Base+2*Side) + 1/(2*Side));
    { Equivalent Packing diameter }
    Sheet:=0.381/1000.0;
    { Packing sheet thickness }
    Void:=1.0-4.0*Sheet/Pckdia;
    { Packing void fraction }

```

```

Contactloss:=0.0; {%}
{ loss of area due to contact between adjacent sheets }
ApGeom:=(1.0-Contactloss/100.0)*4.0*Void/Pckdia;
{ Total available geometric area per volume (1/m) }
END;

FUNCTION Equil_Pressure_Balance(OneFrac: Real): Real;
{function used by zeroin to find equilibrium conditions
at the condenser exit. }
VAR
Mom_Out,OneCompFlow,TwoCompFlow           : Real;
K_E_Term,K_E_Term_New                     : Real;
Inert_Out_Eqlbm,Stm_Out_Eqlbm              : Real;
TwoFrac,TwoFracnew                        : Real;
T_Eqlbm,Ysoeq,Pout1,Pout2,Pp_Inert         : Real;
XiW,YiW,X_Out_Eqlbm                       : Real;

{total inlet inert in (water+steam) is TwoCompFlow,
total inlet (water+steam) is OneCompFlow}
BEGIN
OneCompFlow:=Yin[1]+Yin[4];
TwoCompFlow:=Yin[3]+Yin[6];
{TwoFrac is ratio of outlet inerts in water to total inlet inerts, and
OneFrac is ratio of steam at outlet to total inlet water flow}
{first guess of inert Release and
steam kinetic energy at the outlet}
TwoFrac:=Yin[6]/TwoCompFlow;
K_E_Term_New:=0.0;
REPEAT
K_E_Term:=K_E_Term_New;
{iteration loop for equilibrium temperature}
{energy balance for equilibrium temperature
with the above assumptions}
T_Eqlbm:=(Tot_In_Enth-K_E_Term-OneCompFlow*OneFrac*2501.3)/
(OneCompFlow*4.186+
TwoCompFlow*1.006+
OneCompFlow*OneFrac*(1.866-4.186));
{outlet equilibrium saturation pressure and
steam flow using above temperature and
saturated steam properties}
PpSteam:=SatPressure(T_Eqlbm);
Stm_Out_Eqlbm:=OneFrac*OneCompFlow;
TwoFracnew:=TwoFrac;
REPEAT
TwoFrac:=TwoFracnew;
{iteration loop for equilibrium gas
Release and pressure outlet inert flow
in steam with the assumed Release and
steam outlet mole fraction}
Inert_Out_Eqlbm:=(1.0-TwoFrac)*TwoCompFlow;
Ysoeq:=Stm_Out_Eqlbm/Molwts/
(Stm_Out_Eqlbm/Molwts+Inert_Out_Eqlbm/Molwti);
{total outlet equilibrium pressure and
inert partial pressure}

```

```

Pout1:=PpSteam/Ysoeq;
Pp_Inert:=Pout1-PpSteam;
{inert gas Release using inert
partial pressure and Henry's law}
Yiw:=Pp_Inert/Henry(T_Eqlbm);
Xiwi:=Yiw*Molwti/(Yiw*Molwti+(1.0-Yiw)*Molwts);
{find new TwoFrac and iterate to get correct gas Release
for the assumed temperature}
TwoFracnew:=Xiwi*Yin[1]/TwoCompFlow;
UNTIL (abs((TwoFrac-TwoFracnew)/TwoFracnew)< 1e-3);
{using above gas Release find outlet gas mixture properties}
X_Out_Eqlbm:=Inert_Out_Eqlbm/(Inert_Out_Eqlbm+Stm_Out_Eqlbm);
MixTransProp(T_Eqlbm,Pout1,X_Out_Eqlbm);
{find gas outlet velocity and kinetic energy term,
check for kinetic energy convergence}
U_Bulk:=(Stm_Out_Eqlbm+Inert_Out_Eqlbm)/Mixrho/C_S_Area;
K_E_Term_New:=(Stm_Out_Eqlbm+Inert_Out_Eqlbm)
*Sqr(U_Bulk)/(2.0*1000.0);
UNTIL (abs((K_E_Term_New-K_E_Term)/K_E_Term_New)< 1e-3);
{go back and revise temperature calculation}
{find new outlet pressure, pressure difference
is zero function for zero in}
Mom_Out:=(Stm_Out_Eqlbm+Inert_Out_Eqlbm)*U_Bulk/C_S_Area;
Pout2:=Yin[7]+Mom_In-Mom_Out;

Equil_Pressure_Balance:=Pout1-Pout2;

{stagnation equilibrium conditions
from compressible gas equations}
Gamma:=Mixcp/(Mixcp-8.3143/Mixmwt);
A:=Sqrt(Gamma*8214.3/Mixmwt*(T_Eqlbm+273.15));
Mach:=U_Bulk/A;
Tzbyt:=(1.0+(Gamma-1.0)*Sqr(Mach)/2.0);
Pzbyp:=Exp((Gamma/(Gamma-1.0))*Ln(Tzbyt));
T_Stg_Eq:=(T_Eqlbm+273.15)*Tzbyt-273.15;
P_Stg_Eq:=Pout1*Pzbyp;
{set array of equilibrium conditions}
Yeqlbm[1]:=Yin[1]+Yin[4]-Stm_Out_Eqlbm;
Yeqlbm[2]:=4.186*(T_Eqlbm-Yin[8])*Yin[1];
Yeqlbm[3]:=Yin[1]*Xiwi;
Yeqlbm[4]:=Stm_Out_Eqlbm;
Yeqlbm[5]:=T_Eqlbm;
Yeqlbm[6]:=Inert_Out_Eqlbm;
Yeqlbm[7]:=Pout1;
Yeqlbm[8]:=T_Eqlbm;
Yeqlbm[9]:=PpSteam;
Yeqlbm[10]:=1e5;
Yeqlbm[11]:=0.0;
Vel_Eqlbm:=U_Bulk;
Super_Eqlbm:=0.0;
X_Eqlbm:=1e20;
END { Equil_Pressure_Balance };

FUNCTION Colburn_Hougen(Tinterface: Real): Real;

```

```

    { evaluates the Colburn Hougen equation at any
      assumed interface temperature, Tinterface in Celcius
      that lies between the steam saturation temperature and
      water temperature }

VAR
    Stmlfr,Xbulk,Ybulk                : Real;
BEGIN
    { Find steam properties at the interface temperature and
      Steam Mole fraction at the interface and bulk }
    Stmlfr:=SatPressure(Tinterface)/Y_Est[7];
    Xbulk:=Y_Est[4]/(Y_Est[4]+Y_Est[6]);
    Ybulk:=Xbulk/Molwts/(Xbulk/Molwts+(1.0-Xbulk)/Molwti);
    { Steam flux in kg/s/m^2 }
    SteamFlux:=-Gmtc*ln((1.0-Ybulk)/(1.0-Stmlfr));
    { Ackermann correction factors for high mass flux
      to heat and friction, Ref: Butterworth and Hewitt:
      Two-phase Flow and Heat Transfer, Oxford University Press, 1978 }
    Czero:=SteamFlux*StmCp/Ghtc;
    Ackerh:=Czero/(1.0-exp(-Czero));
    RhoUb:=(Y_Est[4]+Y_Est[6])/C_S_Area;
    Ackf:=2.0*SteamFlux/(RhoUb*Frcgas)/
        (1.0-exp(-2.0*SteamFlux/(RhoUb*Frcgas)));
    { Liquid and Gas Side heat balance - via Colburn Hougen equation.
      If interface temperature and coefficients are correct, the
      function value of Colburn-Hougen=ZERO }
    Cht1:=Lhtc*(Tinterface-Y_Est[8]);
    Cht2:=Ghtc*Ackerh*(Y_Est[5]-Tinterface);
    Enths:=MixtureEnthalpy(Tinterface,0);
    Enthw:=LiquidEnthalpy(Tinterface);
    Cht3:=(Enths-Enthw)*SteamFlux;

    Colburn_Hougen:=Cht1-Cht2-Cht3;

END { Colburn_Hougen};

PROCEDURE CocurrentZeroin (ax,bx: Real;Flag:Lable;VAR Tint: Real);
    { finds value of x at which a nonlinear function f(x)=0;
      this procedure was adopted from Forsythe et al,
      Computer Methods for Mathematical Computations,
      Prentice-Hall, 1977, Chapter 7. }
VAR
    a,b,c,d,e,fa,fb,fc                : Real;
    p,q,r,s,Xm                        : Real;
BEGIN
    IF (Flag='inter') THEN
        BEGIN
            a:=ax+1e-6;
            b:=bx-1e-6;
            fa:=Colburn_Hougen(a);
            fb:=Colburn_Hougen(b);
        END ELSE
        BEGIN
            a:=ax;
            b:=bx;
        END
    END

```

```

{ evaluates the Colburn Hougen equation at any
  assumed interface temperature, Tinterface in Celcius
  that lies between the steam saturation temperature and
  water temperature }

VAR
  Stmlfr,Xbulk,Ybulk                : Real;
BEGIN
  { Find steam properties at the interface temperature and
    Steam Mole fraction at the interface and bulk }
  Stmlfr:=SatPressure(Tinterface)/Y_Est[7];
  Xbulk:=Y_Est[4]/(Y_Est[4]+Y_Est[6]);
  Ybulk:=Xbulk/Molwts/(Xbulk/Molwts+(1.0-Xbulk)/Molwti);
  { Steam flux in kg/s/m^2 }
  SteamFlux:=-Gmtc*ln((1.0-Ybulk)/(1.0-Stmlfr));
  { Ackermann correction factors for high mass flux
    to heat and friction, Ref: Butterworth and Hewitt:
    Two-phase Flow and Heat Transfer, Oxford University Press, 1978 }
  Czero:=SteamFlux*StmCp/Ghtc;
  Ackerh:=Czero/(1.0-exp(-Czero));
  RhoUb:=(Y_Est[4]+Y_Est[6])/C_S_Area;
  Ackf:=2.0*SteamFlux/(RhoUb*Frcgas)/
    (1.0-exp(-2.0*SteamFlux/(RhoUb*Frcgas)));
  { Liquid and Gas Side heat balance - via Colburn Hougen equation.
    If interface temperature and coefficients are correct, the
    function value of Colburn-Hougen=ZERO }
  Cht1:=Lhtc*(Tinterface-Y_Est[8]);
  Cht2:=Ghtc*Ackerh*(Y_Est[5]-Tinterface);
  Enths:=MixtureEnthalpy(Tinterface,0);
  Enthw:=LiquidEnthalpy(Tinterface);
  Cht3:=(Enths-Enthw)*SteamFlux;

  Colburn_Hougen:=Cht1-Cht2-Cht3;

END { Colburn_Hougen};

PROCEDURE CocurrentZeroin (ax,bx: Real;Flag:Lable;VAR Tint: Real);
{ finds value of x at which a nonlinear function f(x)=0;
  this procedure was adopted from Forsythe et al,
  Computer Methods for Mathematical Computations,
  Prentice-Hall, 1977, Chapter 7. }
VAR
  a,b,c,d,e,fa,fb,fc                : Real;
  p,q,r,s,Xm                        : Real;
BEGIN
  IF (Flag='inter') THEN
    BEGIN
      a:=ax+1e-6;
      b:=bx-1e-6;
      fa:=Colburn_Hougen(a);
      fb:=Colburn_Hougen(b);
    END ELSE
    BEGIN
      a:=ax;
      b:=bx;
    END
  END

```

```

        fa:=Equil_Pressure_Balance(a);
        fb:=Equil_Pressure_Balance(b);
    END;
    c:=a;
    fc:=fa;
    d:=b-a;
    e:=d;
    { convergence test }
    Toll:=2.0*Epsilon*abs(b)+0.5*Tol;
    Xm:=0.5*(c-b);
    WHILE (abs(Xm)>Toll) AND
        (fb<>0.0) AND
        (fb*(fc/abs(fc))< 0.0) DO
    BEGIN
        IF (abs(fc)< abs(fb)) THEN
        BEGIN
            a:=b;
            b:=c;
            c:=a;
            fa:=fb;
            fb:=fc;
            fc:=fa;
        END;
        Xm:=0.5*(c-b);
        Toll:=2.0*Epsilon*abs(b)+0.5*Tol;
        IF (abs(e)< Toll) AND (abs(fa)<=abs(fb)) THEN
        BEGIN { bisection }
            d:=Xm;
            e:=d;
        END ELSE
        BEGIN
            { is quadratic interpolation possible }
            IF (a=c) THEN
            BEGIN
                { linear interpolation }
                s:=fb/fa;
                p:=2.0*Xm*s;
                q:=1.0-s;
            END ELSE
            BEGIN
                { inverse quadratic interpolation }
                q:=fa/fc;
                r:=fb/fc;
                s:=fb/fa;
                p:=s*(2.0*Xm*q*(q-r)-(b-a)*(r-1.0));
                q:=(q-1.0)*(r-1.0)*(s-1.0);
            END;
            { adjust signs }
            IF (p>0.0) THEN q:=-q;
            p:=abs(p);
            { is interpolation acceptable }
            IF ((2.0*p)< (3.0*Xm*q-abs(Toll*q))) AND
                (p< abs(0.5*e*q)) THEN
            BEGIN

```

```

                e:=d;
                d:=p/q;
            END ELSE
            BEGIN
                { bisection }
                d:=Xm;
                e:=d;
            END;
        END;
    { Complete Step }
    a:=b;
    fa:=fb;
    IF (abs(d)>Tol1) THEN b:=b+d;
    IF (abs(d)<=Tol1) THEN b:=b+Tol1*Xm/abs(Xm);
    IF (Flag='inter') THEN fb:=Colburn_Hougen(b) ELSE
                                fb:=Equil_Pressure_Balance(b);
    IF ((fb*(fc/abs(fc)))>0.0) THEN
    BEGIN
        c:=a;
        fc:=fa;
        d:=b-a;
        e:=d;
    END;
    { convergence test }
    Tol1:=2.0*Epsilon*abs(b)+0.5*Tol;
    Xm:=0.5*(c-b);
END { While };
Tint:=b;
END { CocurrentZeroin };

PROCEDURE CocurrentEquilibrium;
{finds equilibrium outlet conditions (infinite length)
 for the cocurrent condenser}
VAR
    Op_Flag,Zero_Flag           : Lable;
    T_Tol                       : Real;
    Term1,Term2,Term3           : Real;
    OneFrac,Lolimit,Hilimit     : Real;
BEGIN
    {set temperature tolerance and
    operating conditions to Superheat}
    T_Tol:=1e-3;
    Op_Flag:='Super';
    {find steam and liquid properties
    at the inlet (assumed to be saturated)}
    Tdew:=SatTemperature(Yin[9]);
    {check for Superheat or saturated conditions}
    IF (abs(Tdew-Yin[5])>T_Tol) THEN
    BEGIN
        Writeln (OutFile1,' inlet conditions super saturated',
                ' or equilibrium Superheated.',
                '***** calculations aborted *****');
    END ELSE
    BEGIN

```

```

        IF (abs((Tdew-Yin[5]))< T_Tol) THEN
        BEGIN
            Op_Flag:='Satur';
            Tdew:=Yin[5];
            Super_In:=0;
        END;
    END;

    {calculate inlet gas Mixture properties}
    Xmass:=Yin[6]/(Yin[6]+Yin[4]);
    MixTransProp(Yin[5],Yin[7],Xmass);
    {calculate inlet stagnation temperature
    and pressure using compressible gas equations}
    Gamma:=Mixcp/(Mixcp-8.3143/Mixmw);
    Vel_In:=(Yin[4]+Yin[6])/C_S_Area/Mixrho;
    A:=Sqrt(Gamma*8314.3/Mixmw*(Yin[5]+273.15));
    Mach:=Vel_In/A;
    Tzbyt:=(1.0+(Gamma-1.0)*Sqr(Mach)/2.0);
    Pzbyp:=Exp((Gamma/(Gamma-1.0))*Ln(Tzbyt));
    T_Stg_In:=(Yin[5]+273.15)*Tzbyt-273.15;
    P_Stg_In:=Yin[7]*Pzbyp;
    {inlet gas enthalpy}
    Gas_In_Enth:=(Yin[6]+Yin[4])*MixtureEnthalpy(Yin[5],Xmass);
    {water inlet enthalpy, total inlet enthalpy,
    and inlet momentum flux}
    Enthw:=LiquidEnthalpy(Yin[8]);
    Wat_In_Enth:=Yin[1]*Enthw+Yin[3]*AirCp*Yin[8];
    K_E_In:=(Yin[6]+Yin[4])*Sqr(Vel_In)/(2*1000.0);
    Tot_In_Enth:=Wat_In_Enth+Gas_In_Enth+K_E_In;
    Mom_In:=(Yin[4]+Yin[6])*Vel_In/C_S_Area;
    {check for saturatated equilibrium conditions,
    i.e. there is adequate water flow to cool the steam
    down to saturation conditions at the outlet}
    WaterTransProp(Yin[8]);
    Term1:=Yin[4]*StmCp*(Yin[5]-Tdew);
    Term2:=Yin[6]*AirCp*(Yin[5]-Tdew);
    Term3:=Yin[1]*Cpliq*(Tdew-Yin[8])+
            Yin[3]*AirCp*(Tdew-Yin[8]);
    IF ((Term1+Term2)>Term3) THEN
        Writeln (Con,' inlet conditions super saturated',
                ' or equilibrium Superheated.',
                '***** calculations aborted *****')
    Else
    BEGIN
        {find equilibrium conditions
        using zeroin function solver}
        Zero_Flag:='equil';
        Hilimit:=Yin[4]/(Yin[4]+Yin[1]);
        Lolimit:=Hilimit/1000.0;
        CocurrentZeroin (Lolimit,Hilimit,Zero_Flag,OneFrac);
    END;

END { CocurrentEquilibrium };

PROCEDURE FileSetup;

```

```
{ sets up input and output files for the calculations }
BEGIN
  { Interactive reading of input and output file names }
  Form6:=Char(012);
  Form7:=Char(012);
  { Writeln('Input File Name???
    - (EG. A:Cctml.Doc ', '-- 20 characters max)');
  ReadLn (Kbd,Filein);
  Writeln('First Output File Name??? - (EG. C:Tape6.Out)');
  ReadLn (Kbd,Filot1);
  Writeln('Second Output File Name??? - (EG. C:Tape7.Out)');
  ReadLn (Kbd,Filot2);}
  Assign (InFile, 'd:coinput.par');
  Assign (OutFile1,'d:CoTape6.out');
  Assign (OutFile2,'d:CoTape7.out');
  Assign (OutFile3,'d:CoTape8.out');
  IF (Filot1='Lst') THEN Form6:='1';
  IF (Filot2='Lst') THEN Form7:='1';
  Reset (InFile);
  Rewrite(OutFile1);
  Rewrite(OutFile2);
  Rewrite(OutFile3);
  { Read the number of condenser runs to be made
    from the first line of the input file }
  ReadLn (Infile);
  ReadLn (InFile,Nrun);

END { FileSetup };

PROCEDURE Cocurrentinput;
  {This procedure contains the input and output routines
   for the direct contact condenser routine -cocond-.
   Input routine for cocurrent condenser reads from the InFile
   assigned earlier.}

VAR
  Verbage          : String[80];
  Ipos             : Integer;
BEGIN
  {initialize condenser starting length to zero}
  Xin:=0.0;
  {Verbage is a dummy character variable which reads comment
   lines in the input file}
  ReadLn (InFile,Run_Lable,Serial,T_Dew_In,Yin[8],
    Gas_Load,Yacob,Xinprc);
  Ipos:=Pos('-',Run_Lable);
  Delete(Run_Lable,1,Ipos-7);
  Ipos:=Pos('T-',Run_Lable);
  Delete(Run_Lable,Ipos+3,15);
  Insert('','',Run_Lable,1);
  Insert('','',Run_Lable,11);
  Writeln (CON,Run_Lable,T_Dew_In:10:2,Yin[8]:10:2,
    Gas_Load:10:4,Yacob:10:4,Xinprc:10:4);
  Geometry:='Pack';
```

```

    { Multiplicative correction factors for the heat and
      mass transfer correlations for the liquid, heat and
      mass transfer correlations for the gas, and friction
      factor for the gas, respectively }

    Cond_Len:=2.000; { Condenser overall length (m) }
    PpmIn:=14.0;     { ppm of dissolved gas in liquid at entry }
    Super_In:=0.0;   { Superheat of the vapor at entry }
    {input calculations}
    C_S_Area:=1.0;   { flow superficial cross sectional area (m^2)}
    Yin[4]:=Gas_Load*C_S_Area;
    Yin[1]:=Yacob*Yin[4]*2470.0/(4.186*(T_Dew_In-Yin[8]));
    Yin[3]:=Yin[1]*PpmIn*1.0e-6;
    Yin[6]:=Yin[4]*Xinprc/100.0;
    Yin[2]:=0.0;
    Yin[10]:=0.0;
    Yin[11]:=0.0;
    Yin[5]:=T_Dew_In+Super_In;

    Afraction:=1.0;
    { effective area fraction of the packing }
    PackingCharacteristics;
    Saperv:=Afraction*Apgeom;
    { effective surface area per unit volume (1/m)}

END { Cocurrentinput };

PROCEDURE Co_Transfer_Coefficients;

    { This routine calculates the gas friction coefficient,
      the liquid heat and mass transfer coefficients, and
      the gas heat and mass transfer coefficients given
      local flow conditions and geometry. For
      the liquid, only turbulent flow is considered. }

VAR
    Chlen                               : Real;
    Diff,K_L                           : Real;
    GammaL,Delta,Lload,Reside           : Real;
    U_G                                 : Real;
BEGIN
    {
      -----
      liquid-Side coefficients
      -----
    }

    { Find liquid properties }
    WaterTransProp(Y_Est[8]);
    { Liquid Reynold's number }
    Lload:=Y_Est[1]/C_S_Area;
    GammaL:=Lload/Saperv;
    Rel:=4.0*GammaL/Muliq;
    { Turbulent flow coefficient }

```

```

Delta:=Exp(0.6*Ln(GammaL/(Rholiq*82.0*Sqrt(Sinalpha))));
{ Liquid film thickness for turbulent flow on an inclined plane,
  Manning Formula, p312 of John Haberman, Introduction to
  Fluid Mechanics, Prentice-Hall, 1980 }
U_L_Eff:=GammaL/(Rholiq*Delta);
Diff:=(Mulq/Rholiq)/Scliq;
K_L:=2.0*Sqrt(Diff*U_L_Eff/(Pi*Sprime));
{ Higbie's Penetration Theory }
Lmtc:=Rholiq*K_L; { liquid-side mass transfer coefficient }
{ Heat transfer coefficient is found using Chilton-Colburn analogy }
Lhtc:=Lmtc*Cpli*Exp((2.0/3.0)*Ln(Scliq/Prliq));
{
  -----
  Gas-Side transfer coefficients
  -----
}
{ Evaluations for Structured Packing flow characteristics
  are based on Bravo, Rocha, and Fair, Mass Transfer in
  Gauze Packings, Hydrocarbon Processing, January 1985,
  pp. 91-95. DB 7/28/86 }
{ Find gas Mixture properties }
Xmass:=Y_Est[6]/(Y_Est[4]+Y_Est[6]);
MixTransProp(Y_Est[5],Y_Est[7],Xmass);
{ Compute mass flux and dimensionless numbers }
RhoUb:=(Y_Est[4]+Y_Est[6])/C_S_Area;
U_G:=RhoUb/MixRho; U_G_Eff:=U_G/Sin(Theta*Pi/180);
{ Note Relative velocity is used here, according to Bravo }
Reg:=MixRho*(U_G_Eff-abs(U_L_Eff))*Pckdia/Mixmu;
{ for cocurrent flow }
{ If Relative velocity based Reynolds number goes below 5,
  then set flag for discontinuing calculations }
IF (Reg< 5.0) THEN
  BEGIN
    Setflag:=true;
    Xfinal:=X;
  END;
Nusselt_Gas:=0.0338*Exp(0.8*Ln(Reg))
               *Exp(0.333*Ln(Mixpr)); {Bravo}
{ Equivalent to Eqs. 2-29 and 2-31 in text }
Ghtc:=Nusselt_Gas*Mixk/Pckdia/1000.0;
{ Mass transfer coefficient is found using Chilton-Colburn analogy }
Gmtc:=Ghtc*Exp((2.0/3.0)*Ln(Mixpr/Mixsc))/MixCp;
{
  -----
  Gas friction coefficients
  -----
}
{ Note:-- Gas Reynolds Number Based on Side, per Bravo }
{ for friction evaluations, Correlations of Bravo is used }
{ Liquid Froude number corrections as in Bravo are not used here.}

```

```

Reside:=Reg*Side/Pckdia; { Side Reynolds Number}
Frcgas:=0.171+92.7*Pckdia/(Reg*Side);
    
```

```

END { Co_Transfer_Coefficients };
    
```

```

PROCEDURE CocurrentDerivatives;
    
```

```

{ This subroutine computes the first derivatives
  of the differential equations given the length
  and the values of the variables. An explanation
  of the variables is given above in the main routine. }
    
```

```

VAR
    
```

```

    all,a12,a21,a22,b1,b2           : Real;
    Molair,Molest                   : Real;
    Dmlsdx,Dmladx,Dppadx            : Real;
    Count                           : Integer;
    
```

```

BEGIN
    
```

```

    IF ((setflag=true) OR
        (Y_Est[9]<=(1.0+SatPressure(Y_Est[8])))) THEN
    
```

```

        BEGIN
            
```

```

            FOR Count:=1 TO 11 DO Yprime[Count]:=0.0;
            
```

```

            IF (Setflag=False) THEN
            
```

```

                BEGIN
                    
```

```

                    Xfinal:=x;
                    
```

```

                    setflag:=true;
                
```

```

            END;
        
```

```

    END Else
    
```

```

    BEGIN
        
```

```

        { Compute heat and mass transfer coefficients for use
          in the differential equations. Call Transfer
          Coefficients to initialize. }
    
```

```

        Co_Transfer_Coefficients;
    
```

```

        Tdew:=SatTemperature(Y_Est[9]);
    
```

```

        { CocurrentZeroin iteratively solves the Colburn-Hougen
          equation for the interface conditions and correct
          transfer coefficients. }
    
```

```

        CocurrentZeroin (Y_Est[8],Tdew,'inter',Tsurf);
    
```

```

        {find steam and water properties}
    
```

```

        Xmass:=Y_Est[6]/(Y_Est[6]+Y_Est[4]);
    
```

```

        MixTransProp(Y_Est[5],Y_Est[7],Xmass);
    
```

```

        WaterTransProp(Y_Est[8]);
    
```

```

        { Solve for overall heat and mass transfer coefficients
          using the interface temperature (Tsurf). }
    
```

```

        Ovhtc:=Lhtc*(Tsurf-Y_Est[8])/(Y_Est[5]-Y_Est[8]);
    
```

```

        Ovmtc:=Lmtc;
    
```

```

        { Compute first derivatives of all variables }
    
```

```

Yprime[1]:=SteamFlux*C_S_Area*Saperv;
Yprime[2]:=Lhtc*Saperv*C_S_Area*(Tsurf-Y_Est[8]);
Yprime[3]:=-Lmtc*C_S_Area*Saperv*
      (Y_Est[3]/Y_Est[1]-(Y_Est[7]-Y_Est[9])/
      (Henry(Y_Est[8]))*Molwti/Molwts);
Yprime[4]:=-Yprime[1];
Yprime[6]:=-Yprime[3];
{ Matrix solution needed for calculations of
  steam temperature and total pressure derivatives }
RhoUb:=(Y_Est[6]+Y_Est[4])/C_S_Area;
U_Bulk:=RhoUb/(Void*MixRho*Sln(Theta*Pi/180.0));
a11:=1.0+U_Bulk*U_Bulk/(1000.0*MixCp*(273.15+Y_Est[5]));
a22:=1.0-U_Bulk*U_Bulk/(8314.3/Mixmwts*(273.15+Y_Est[5]));
a12:=-U_Bulk*U_Bulk/(MixRho*1000.0*MixCp*8314.3/
      Mixmwts*(273.15+Y_Est[5]));
a21:=MixRho*U_Bulk*U_Bulk/(273.15+Y_Est[5]);
b1:=-Cht2*exp(-Czero)*Saperv*C_S_Area/(MixCp)/
      (Y_Est[4]+Y_Est[6])-U_Bulk*(Yprime[4]/C_S_Area)/
      (MixRho*MixCp*1000.0);
b2:=-U_Bulk*Yprime[4]/C_S_Area-0.5*MixRho*Sqr(U_Bulk-abs(U_L_Eff))*
      Apgeom*Frcgas*
      (Afraction*Ackf+1.0-Afraction);
{ Note Apgeom used here instead of Saperv, to account for
  friction associated with the ineffective mass transfer
  areas as well. }
Yprime[5]:=(a22*b1-a12*b2)/(a11*a22-a12*a21);
Yprime[7]:=(a11*b2-a21*b1)/(a11*a22-a12*a21);
{ Molar flow rates needed for calculating
  steam partial pressure derivative }
Molair:=Y_Est[6]/Molwti;
Molest:=Y_Est[4]/Molwts;
Dmladx:=Yprime[6]/Molwti;
Dmlsdx:=Yprime[4]/Molwts;
Dppadx:=Molair/(Molair+Molest)*Yprime[7]+
      Y_Est[7]*((Molair+Molest)*Dmladx-
      Molair*(Dmladx+Dmlsdx))/(Sqr(Molair+Molest));
Yprime[9]:=Yprime[7]-Dppadx;
Yprime[8]:=Yprime[2]/(Y_Est[1]*Cpliq);
Yprime[10]:=Yprime[8]/(Y_Est[5]-Y_Est[8]);
Yprime[11]:=0.0;

```

```

END {if};
{ save derivatives for printing }
Prime:=Yprime;

```

```
END { CocurrentDerivatives };
```

```

PROCEDURE CocurrentOutAdd(Nline,Nseg: Integer);
{ Additional cocurrent detailed output including
  dimensionless numbers and individual coefficients
  as a function of condenser length are generated here
  and recorded onto the file OutFile2.}

```

```

VAR
  Vout          : Vector;

```

BEGIN

```
{print label, header, and initial conditions on first call}
IF (Nline=0) THEN Writeln(OutFile2,Form6,Run_Lable);
IF (Nline=0) THEN Writeln(OutFile2,Cdate,' ',Ctime);
```

```
{re-solve for ackerman heat transfer Correlation}
Ackerh:=Czero/(1.0-exp(-Czero));
{load and print output matrix}
IF (Nline< 100) THEN
BEGIN
    Vout[1]:=X;
    Vout[2]:=Rel;
    Vout[3]:=Reg;
    Vout[4]:=PrLiq;
    Vout[5]:=Mixpr;
    Vout[6]:=ScLiq;
    Vout[7]:=Mixsc;
    Vout[8]:=Lhtc;
    Vout[9]:=Ghtc*1000.0;
    Vout[10]:=Lmtc*1000.0;
    Vout[11]:=Gmtc*1000.0;
    Vout[12]:=Ackerh;
    Vout[13]:=Ackf;
    Vout[14]:=SteamFlux*1000.0;
    Vout[15]:=Tdew;
    Vout[16]:=Prime[5];
    Vout[17]:=Nusselt Gas;
    Vout[18]:=Prime[9];
    Vout[19]:=Frcgas;
    FOR i:=1 TO 19 DO Write( OutFile2, Vout[i]:10,' ');
    Writeln(OutFile2);
```

END;

IF(Nline=100) THEN

BEGIN

```
    Writeln(OutFile2);
    FOR i:=1 TO 18 DO Write( OutFile2, 999.9:10,' ');
    Writeln(OutFile2);
    Writeln(OutFile2);
```

END;

END { CocurrentOutAdd} ;

PROCEDURE CocurrentOutput(Nline,Nseg: Integer);

```
{Output routine for cocurrent condenser model.
 Prints detailed results as a function of condenser
 length and a summary of actual and equilibrium
 outlet conditions on the file OutFile1. }
```

VAR

Vout	: Vector;
Tstago,Pstago,Superht	: Real;
Ploss,Poten	: Real;
Effweq,Effw	: Real;

```

        {print header, label, and inlet conditions
         for the first call}
BEGIN
    IF (Nline=0) THEN
        BEGIN
            Cdate:='' + date + ' ' ;
            Ctime:='' + time + ' ' ;
            WriteLn(OutFile1, Form6, Run_Lable);
            WriteLn(OutFile1, Cdate, ' ', Ctime);
            { Write inlet conditions }
            Vout[1]:=Xin;
            Vout[2]:=Yin[1]/C_S_Area;
            Vout[3]:=Yin[4]/C_S_Area;
            Vout[4]:=Yin[3]*1e6/(Yin[1]+Yin[3]);
            Vout[5]:=(Yin[6]*100.0)/(Yin[6]+Yin[4]);
            Vout[6]:=Yin[5];
            Vout[7]:=Tsurf;
            Vout[8]:=Yin[8];
            Vout[9]:=Super_In;
            Vout[10]:=Yin[7];
            Vout[11]:=Yin[9];
            Vout[12]:=SatPressure(Yin[5]);
            Vout[13]:=0.0;
            Vout[14]:=Yin[10];
            Vout[15]:=Yin[2]/C_S_Area;
            Vout[16]:=(1.0-Yin[4]/Yin[4])*100.0;
            Vout[17]:=Vel_In;
            Vout[18]:=0.0;
            Vout[19]:=0.0;
            FOR i:=1 TO 19 DO Write(OutFile1, Vout[i]:10, ' ');
            WriteLn(OutFile1);
            CocurrentOutAdd(Nline, Nseg);
        END ELSE
        IF (Nline< 100) THEN
            BEGIN
                {set output conditions}
                Tdew:=SatTemperature(Y[9]);
                {find stagnation temperature and pressure conditions}
                U_Bulk:=(Y[4]+Y[6])/C_S_Area/Mixrho;
                Gamma:=Mixcp/(Mixcp-8.3143/Mixmwt);
                A:=Sqrt(Gamma*8314.3/Mixmwt*(Y[5]+273.15));
                Mach:=U_Bulk/A;
                Tzbyt:=(1.0+(Gamma-1.0)*Sqr(Mach)/2.0);
                Pzbyp:=Exp(Gamma/(Gamma-1.0)*Ln(Tzbyt));
                Tstago:=Y[5]*Tzbyt;
                Pstago:=Y[7]*Pzbyp;
                Superht:=Y[5]-Tdew;
                {define a "pressure loss" Term which includes momentum}
                Ploss:=Yin[7]-Y[7]+(Mom_In-(Y[4]+Y[6])*U_Bulk/C_S_Area);
                {set output array and print intermediate results}

                Vout[1]:=X;
                Vout[2]:=Y[1]/C_S_Area;
            
```

```

Vout[3]:=Y[4]/C_S_Area;
Vout[4]:=Y[3]*1e6/(Y[1]+Y[3]);
Vout[5]:=(Y[6]*100.0)/(Y[6]+Y[4]);
Vout[6]:=Y[5];
Vout[7]:=Tsurf;
Vout[8]:=Y[8];
Vout[9]:=Superht;
Vout[10]:=Y[7];
Vout[11]:=Y[9];
Vout[12]:=SatPressure(Y[5]);
Vout[13]:=Ploss;
Vout[14]:=Y[10];
Vout[15]:=Y[2]/C_S_Area;
Vout[16]:=(1.0-Y[4]/Yin[4])*100.0;
Vout[17]:=U_Bulk;
Vout[18]:=Ovhtc;
Vout[19]:=Ovmtc*1000.0;
Pdrop:=Yin[7]-Y[7];
FOR i:=1 TO 19 DO Write(OutFile1, Vout[i]:11, ' ');
Writeln(OutFile1);
CocurrentOutAdd(Nline,Nseg);
END;
IF(Nline=100) THEN
BEGIN
  {**** Last two lines of output ****}
  Writeln(OutFile1);
  { Equilibrium Conditions }
  Vout[1]:=999.9;
  Vout[2]:=Yeq1bm[1]/C_S_Area;
  Vout[3]:=Yeq1bm[4]/C_S_Area;
  Vout[4]:=Yeq1bm[3]*1e6/(Yeq1bm[1]+Yeq1bm[3]);
  Vout[5]:=(Yeq1bm[6]*100.0)/(Yeq1bm[6]+Yeq1bm[4]);
  Vout[6]:=Yeq1bm[5];
  Vout[7]:=0.0;
  Vout[8]:=Yeq1bm[8];
  Vout[9]:=0.0;
  Vout[10]:=Yeq1bm[7];
  Vout[11]:=Yeq1bm[9];
  Vout[12]:=SatPressure(Yeq1bm[5]);
  Vout[13]:=0.0;
  Vout[14]:=Yeq1bm[10];
  Vout[15]:=Yeq1bm[2]/C_S_Area;
  Vout[16]:=(1.0-Yeq1bm[4]/Yin[4])*100.0;
  Vout[17]:=Vel_Eqlbm;
  Vout[18]:=999.9;
  Vout[19]:=999.9;
  FOR i:=1 TO 19 DO Write(OutFile1, Vout[i]:11, ' ');
  Writeln(OutFile1);

  CocurrentOutAdd(Nline,Nseg);
END;
END {CocurrentOutput };

```

```

PROCEDURE Runga(h,x0: Real; Y0:State);
    { Fourth-order Runge-Kutta integration scheme }
VAR
    k1,k2,k3,k4                : State;
BEGIN
    X_Est:=x0; Y_Est:=Y0;
    CocurrentDerivatives;
    IF (Iprint AND (x0=0.0)) THEN CocurrentOutput(0,40);
    FOR i:=1 TO Neqn DO
        BEGIN
            k1[i]:=h*Yprime[i];
            Y_Est[i]:=Y0[i]+k1[i]/2;
        END;
        X_Est:=X_Est+h/2;
        CocurrentDerivatives;
        FOR i:=1 TO Neqn DO
            BEGIN
                k2[i]:=h*Yprime[i];
                Y_Est[i]:=Y0[i]+k2[i]/2;
            END;
            CocurrentDerivatives;
            FOR i:=1 TO Neqn DO
                BEGIN
                    k3[i]:=h*Yprime[i];
                    Y_Est[i]:=Y0[i]+k3[i];
                END;
                X_Est:=X_Est+h/2;
                CocurrentDerivatives;
                FOR i:=1 TO Neqn DO
                    BEGIN
                        k4[i]:=h*Yprime[i];
                        Y[i]:=Y0[i]+(k1[i]+2*k2[i]+2*k3[i]+k4[i])/6;
                    END;
                X:=X0+h;
            END { Runga };

PROCEDURE Cocurrent_Main;
    { This Main procedure sets up inputs, then calls
      other calculation procedures, updates monitor
      display and then Ends calculations. It is repeated
      for every run case. }
VAR
    Ix                : Integer;
    Stmlfr            : Real;
    Mlfrar,Mlfrst     : Real;
BEGIN
    FOR Ix:=1 TO Nrun DO
        BEGIN
            FOR i:=1 TO 11 DO
                BEGIN
                    Y[i]:=0;
                    Yin[i]:=0;
                END;
            END;

```

```
X:=0;
Xin:=0;
{ Read the condenser initial values of most of the
  variables for the modeling differential equations
  by calling subroutine cinput.
  The differential equation variables are as follows:

Y[1]:=water flow rate (kg/s)
Y[2]:=condenser heat load (kW)
Y[3]:=dissolved gas flow rate (kg/s)
Y[4]:=steam flow rate (kg/s)
Y[5]:=steam temperature (C)
Y[6]:=inert gas mass flow rate (kg/s)
Y[7]:=condenser pressure (Pa)  ** calculated **
Y[8]:=water temperature (C)
Y[9]:=partial pressure of the steam (Pa)  ** calculated **
Y[10]:=ntu
Y[11]:=fog flow rate (kg/s) ** not used ** }

Cocurrentinput;
{ Solve for remaining initial values of
  integration variables }
Stmlfr:=(Yin[4]/Molwts/(Yin[4]/Molwts+Yin[6]/Molwti));
Yin[9]:=SatPressure(Yin[5]-Super_In);
Yin[7]:=Yin[9]/Stmlfr;
Tdew:=Yin[5]-Super_In;
{ save initial values of variables in an array
  Yin and length as Xin }
Y:=Yin;
X:=Xin;
{ Set initial heat, mass and friction
  coefficients to zero }
Lhtc:=0.0;  Lmtc:=0.0;  Ghtc:=0.0;  Gmtc:=0.0;
Frcgas:=0.0;  Frcliq:=0.0;
{ Find equilibrium conditions at the condenser
  outlet (infinite length or residence time).}

CocurrentEquilibrium;

{ Check for saturation of cold water with air
  at atmospheric pressure at the inlet
  using Henry's law, print a warning if
  supersaturated.}
Mlfrst:=101325.0/Henry(Y[5]);
Mlfrar:=Y[3]*Molwts/(Y[1]*Molwti);
IF (Mlfrar>Mlfrst) THEN Writeln(1st,Mlfrar,Mlfrst,
' specified inlet dissolved air Mole fraction',Mlfrar,
' saturation inlet dissolved air Mole fraction',Mlfrst,
'***** check inlet conditions --- supersaturated *****');
{ Set the integration Step size }
Step:=Cond_Len/Nseg;
Istep:=0;
Xend:=Xin;
Xfinal:=Cond_Len;
```

```
Setflag:=False;
REPEAT
  IF (Setflag) THEN Step:=Cond_Len-Xend;
  Xend:=Xend+Step;
  Runga(Step,X,Y);
  { Monitor print statements to check progress }
  Wateff:=(Y[8]-Yin[8])/(Yin[5]-Yin[8]);
  Cond_prc:=(Yin[4]-Y[4])*100.0/Yin[4];
  Pdrop:=Yin[7]-Y[7];
  Writeln(CON,Xend:6:3,Y[8]:6:2,Tsurf:6:2,Tdew:6:2,
    Cond_prc:6:2,Pdrop:7:2,
    U_G_Eff:6:2,U_L_Eff:6:2,
    Reg:6:1,MixSc:6:2,Nusselt_Gas:6:2,
    Y[6]:10:6);
  IF (abs(x-Cond_Len)< 0.005) THEN
    Writeln(1st,Run_Lable:20,Serial:5,Yin[5]:10:2,
      xfinal:10:2,Y[8]:10:2,
      Cond_prc:10:2,Pdrop:10:2,
      Tdew:10:2,Base:8:4,
      Saperv:10:2,Yacob:10:4);
  IF (abs(x-Cond_Len)< 0.005) THEN
    Writeln(OutFile3,Run_Lable:20,Serial:5,
      Yin[5]:11:4,xfinal:11:4,
      Y[8]:11:4,Cond_prc:11:4,
      Pdrop:11:4,Tdew:11:4,Base:8:4,
      Saperv:10:2,Yacob:10:4);
  Tdew:=SatTemperature(Y[9]);
  { Succesful integration, increment length
    and print intermediate results}
  Istep:=Istep+1;
  IF (Iprint) THEN CocurrentOutput(Istep,Nseg);
  { Final length reached, go on to next set of conditions}

UNTIL (Xend>=Cond_Len);

IF (Iprint) THEN CocurrentOutput(100,100);

END { Run-for-do loop };

END { Procedure Cocurrent_Main };

BEGIN

  FileSetUp;
  Machineaccuracy;
  Iprint:=False; { Printing to Files not opted }
  Write(1st,chr(27),chr(49));
  Cocurrent_Main;
  Close(OutFile1);
  Close(OutFile2);
  Close(OutFile3);

END.
```

```
PROGRAM Countercurrent_Condenser;
```

```
{ $U+ }      { User Interrupt enabled. }
```

```
{ This program contains routines which model a Countercurrent
direct contact condenser using structured packings for use in open
cycle ocean thermal energy conversion (OTEC). Details of the modeling
and the accompanying study can be found in this report (SERI/TR-252-3108).
This version is set up to run with the TURBO-Pascal compiler (version
3.0, Borland International Inc.) on an IBM or compatible personal
computer. }
```

```
In case of you may find errors or problems in using this code,
please contact the authors at SERI:
1617 Cole Boulevard
Golden, Colorado, 80401
Tel: (303)-231-1000
```

```
*****
Main Routine --CCcond-- version 871015, Revisions 10-15-87
*****
```

```
CONST
```

```
{ Physical Constants }
Molwts=18.015; Molwti=28.97;
G=9.81; Sigma=0.072;
{ Water saturation pressure curve-fit Constants }
p1=161.75743178; p2=18.477911547; p3=4026.97587317;
p4=234.73842369; p5=3.73834517667;
{ Water viscosity curve-fit Constants }
an1=241.4; an2=0.382809486; an3=0.2162830218;
{ integration and numerical error tolerance }
Tol=1e-12;
{ Mathematical Constant }
Pi=3.1415927;
Neqn=11 { Number of equations to be integrated };
Nseg=400 { Number of segments the condenser is divided into. };
```

```
TYPE
```

```
State      = ARRAY[1..11] of Real;
Lable      = String[20];
Vector     = ARRAY[1..20] of Real;
```

```
VAR
```

```
Istep                      : Integer;
Nrun, Serial               : Integer;
Cond_Len, Pckdia, C_S_Area, Saperv, Corliq, Corgas,
Corfrc, Theta, Void, Sinalpha : Real;
Run_Lable                  : String[15];
Xin, Velin, Pstgin, Tstgin, Super_In : Real;
X, X_Est, Tdew, Xend       : Real;
Kliq, Muliq, Cpliq, Prliq, Scliq, Rholiq, Diffaw : Real;
Lhtc, Lmtc, Ghtc, Gmtc, Frcgas, Frcliq, Rel, Reg : Real;
```

```

Tsurf,Ovhtc,Ovmtc,SteamFlux,Czero,Cht1,Cht2,Cht3,
Ackerh,Ackf           : Real;
Xeq,Veleq,Pstgeq,Tstgeq,Supreq      : Real;
Temp,Press,Volw,Vols,Enthw,Enths     : Real;
Y,Ytop,Ybot,Yeqlbm,Y_Est,Prime,Yprime : State;
Filein,Filot1,Filot2      : Lable;
Geometry                  : String[4];
Form6,Form7               : Char;
InFile,OutFile1,OutFile2,OutFile3    : Text;
TgasDB,Tsat,Tliq          : Real;
Ptotal,Satpr,Ppsteam      : Real;
Xmass,Ymole               : Real;
AirMu,AirK,AirCp          : Real;
StmMu,StmK,StmCp          : Real;
StmRho,StmDiff            : Real;
MixMu,MixK,MixCp,MixPr,MixSc,MixMwt,MixRho : Real;
Phil2,Phi2l              : Real;
MixEnth,Enthliq           : Real;
I,Iguess                  : Integer;
Epsilon,Toll,T,Tolzer,Tolerance      : Real;
Tot_In_Enth,Wat_In_Enth,Gas_In_Enth   : Real;
U_Bulk,Gamma,A,Mach        : Real;
Tzbyt,Pzbyp               : Real;
Vel_Eqlbm,Super_Eqlbm,X_Eqlbm         : Real;
Mom_In,Vel_In,K_E_In       : Real;
T_Stg_In,T_Dew_In,P_Stg_In          : Real;
T_Stg_Eq,P_Stg_Eq          : Real;
Mom_Out,K_E_Out            : Real;
Vel_Out,Gas_Out_Enth       : Real;
Yacob,PpmIn               : Real;
Gas_Load,Xinprc           : Real;
RhoUb,U_L_Eff,Nusselt_Gas          : Real;
Step,Afraction            : Real;
Base,Height,Side,Apgeom,Sprime       : Real;
Wateff,Cond_prc,Pdrop,Xfinal         : Real;
Convergence,Setflag,Iprint          : Boolean;

```

```
{ A TURBO-Pascal support file }
```

```
TYPE
```

```
  RegPack =
```

```
    RECORD { register pack Used in MSDos call }
```

```
      AX, BX, CX, DX, BP, SI, DI, DS, ES, Flags : Integer;
```

```
    END;
```

```
  TimeStr = String[8] ; DateStr = String[10] ;
```

```
VAR
```

```
  RecPack : RegPack;
```

```
  Ctime,Cdate : String[10];
```

```
FUNCTION Time: Timestr;
```

```
{ returns the current time in string format HH:MM:SS }
```

```
VAR
```

```
  Hour,Min,Sec,Frac : String[2];
```

```
BEGIN
```

```
  WITH RecPack DO
```

```
BEGIN AX := $2C00 ; MsDos(RecPack) ;
      AX := hi(CX); Str(AX,Hour);
      IF AX < 10 THEN Insert(' ',Hour,1);
      AX := lo(CX); Str(AX,Min );
      IF AX < 10 THEN Insert('0',Min ,1);
      AX := hi(DX); Str(AX,Sec );
      IF AX < 10 THEN Insert('0',Sec ,1);
      AX := lo(DX); Str(AX,Frac);
      IF AX < 10 THEN Insert('0',Frac,1);
      Time := Hour + ':' + Min + ':' + Sec;
      {+ '.' + Frac}
END;
END;

FUNCTION Date: DateStr;
{ returns the current date in string format : MM/DD/YYYY }
VAR
  Year : String[4] ; Month,Day : String[2] ;
BEGIN
  WITH RecPack DO
    BEGIN
      AX := $2A shl 8 ; MsDos(Recpack);
      AX := DX shr 8; Str(AX,Month);
      IF AX < 10 THEN Insert(' ',Month,1);
      AX := DX mod 256; Str(AX,Day);
      IF AX < 10 THEN Insert('0',Day ,1);
      Str (CX,Year);
      Date := Month + '/' + Day + '/' + Year;
    END;
  END;
END;

PROCEDURE MachineAccuracy;
{ Calculates the smallest discernable real number
  for the machine }
BEGIN
  Epsilon:=1.0;
  REPEAT
    Epsilon:=Epsilon/2.0;
    Tolerance:=1.0 + Epsilon;
  UNTIL (Tolerance<=1.0);
END;

FUNCTION InertMasstoMoleFraction(xm: Real): Real;
{ Converts inert mass fraction to mole fraction }
BEGIN
  InertMasstoMoleFraction:=xm/Molwti/(xm/Molwti+(1-xm)/Molwts);
END;

FUNCTION InertMoletomassFraction(ym1: Real): Real;
{ Converts inert mole fraction to mass fraction }
BEGIN
  InertMoletomassFraction:=ym1*Molwti/(ym1*Molwti+(1-ym1)*Molwts);
```

END;

FUNCTION SatTemperature(Satpr: Real): Real;
{ Returns saturation temperature (C) as a function of
saturation pressure (Pa) }

VAR

ak : real;

BEGIN

IF (Satpr>p5) THEN

BEGIN

ak:=(Satpr-p5)/p1;

SatTemperature:=p3/(p2-ln(ak))-p4;

END else

SatTemperature:=-270.15;

END { SatTemperature };

FUNCTION SatPressure(SatT: Real): Real;
{ Returns saturation pressure as a function of
saturation temperature (C) }

BEGIN

SatPressure:=p1*exp(p2-p3/(SatT+p4))+p5;

END { SatPressure };

FUNCTION Henry(Twater: Real): Real;
{ Returns Henry's Law constant for air solubility in
fresh water in (Pa/Mole Fraction) of Dissolved Air as a
function of Twater in Celcius. Curve fit from 0 to 40 C,
Taken from data in the Saline Water Conversion Engineering
Data Book, M.W. Kellogg Company, Office of Water Research
and Technology, PB-250 907, October 1975, p136. }

VAR

sol : real;

BEGIN

sol:=(2.3333 + Twater*(-0.05425579 + Twater*0.00623618))/100000.0;

Henry:=101325.0/sol;

END { Henry };

FUNCTION MixtureEnthalpy(TmixDB,IMF: Real): Real;
{ Returns mixture enthalpy (kJ/kg) as function of gas
mixture temperature (C), and inert mass fraction }

BEGIN

MixtureEnthalpy:=(1-IMF)*(2501.6+1.866*TmixDB)+
IMF*1.005*TmixDB;

END { MixtureEnthalpy };

FUNCTION LiquidEnthalpy(Tw: Real): Real;
{ Returns water enthalpy (kJ/kg) as a function of
water temperature (C) }

BEGIN

LiquidEnthalpy:=4.186*Tw;

END { LiquidEnthalpy };

PROCEDURE AirTransProp(Tair: Real);

{ Air Transport Properties as functions of temperature Tair (K)}

```

BEGIN
    AirK:=26.464e-4*exp(1.5*ln(Tair))/
        (Tair+245.4*exp((-12.0/Tair)*ln(10.0)));
    { Thermal Conductivity in (W/mK)}
    AirMu:=1.458e-6*exp(1.5*ln(Tair))/(Tair+110.4);
    { Dynamic Viscosity in (kg/ms) }
    AirCp:=1.005;
    { Specific Heat in (kJ/kg.K)}
END { AirTransProp};

PROCEDURE SteamTransProp(Tstm: Real);
{ Steam Transport Properties as functions of temperature (K)}
BEGIN
    StmK:=(1.82+0.006*(Tstm-273.15))/100;
    { Thermal Conductivity in (W/mK)}
    StmMu:=(8.02+0.04*(Tstm-273.15))*1.0e-6;
    { Dynamic Viscosity in (kg/ms) }
    StmCp:=1.854+0.000775*(Tstm-273.15);
    { Specific Heat in (kJ/kg.K)}
END { SteamTransProp};

PROCEDURE MixTransProp(TDB,Pt,IMF: Real);
{ Given    TDB = Dry-Bulb Steam Temperature in Celcius.
           Pt  = Total Mixture Pressure in Pascals.
           IMF = Inert Gas Mass Fraction.}

VAR
    Tabs,Gmolfr                               : Real;
BEGIN
    Tabs:=TDB+273.15;
    AirTransProp(Tabs);
    SteamTransProp(Tabs);
    { Calculate Mixture Properties, Wilke's Method
    { Section 9-5, p410, Reid et. al.,
      The properties of Gases and Liquids, McGraw Hill, 1977.}
    Gmolfr:=InertMasstoMoleFraction(IMF);
    StmDiff:=2.918*exp(1.75*ln(Tabs/313.0))/Pt;
    { Diffusivity in (m*m/s), p557, Reid et. al.,
      The properties of Gases and Liquids, McGraw Hill, 1977.}
    MixMwt:=1/(IMF/Molwti+(1.0-IMF)/Molwts);
    MixCp:=IMF*AirCp+(1.0-IMF)*StmCp;
    MixRho:=Pt*MixMwt/(8314.3*Tabs);
    Phi12:=sqr(1.0+exp(0.25*ln(Molwti/Molwts))*sqr(Stmmu/AirMu))
        /sqr(8.0+8.0*Molwts/Molwti);
    Phi21:=sqr(1.0+exp(0.25*ln(Molwts/Molwti))*sqr(AirMu/Stmmu))
        /sqr(8.0+8.0*Molwti/Molwts);
    MixMu:=(1.0-Gmolfr)*Stmmu/((1.0-Gmolfr)+Gmolfr*Phi12)+
        Gmolfr*AirMu/(Gmolfr+(1.0-Gmolfr)*Phi21);
    Phi12:=sqr(1.0+exp(0.25*ln(Molwti/Molwts))*sqr(StmK/AirK))
        /sqr(8.0+8.0*Molwts/Molwti);
    Phi21:=sqr(1.0+exp(0.25*ln(Molwts/Molwti))*sqr(AirK/StmK))
        /sqr(8.0+8.0*Molwti/Molwts);
    MixK:=(1.0-Gmolfr)*StmK/((1.0-Gmolfr)+Gmolfr*Phi12)+Gmolfr*AirK/
        (Gmolfr+(1.0-Gmolfr)*Phi21);
    MixPr:=1000.0*MixCp*MixMu/MixK;

```

```
MixSc:=MixMu/(MixRho*StmDiff);
END { MixTransProp };

PROCEDURE WaterTransProp(WaterTemp: Real);
{ as function of temperature, WaterTemp in Celcius }
VAR
    DelRho,en1,en2                : real;
BEGIN
    DelRho:=-0.69224607+WaterTemp*
    (-0.00175714+WaterTemp*0.00557143);
    IF (WaterTemp<11.85) THEN DelRho:=0.0;
    Rholiq:=1000.0-DelRho;
    { Specific Heat in (kJ/kg.K) }
    CpLiq:=(4217044.18+WaterTemp*
    (-3504.246+WaterTemp*(113.174+
    WaterTemp*(-1.309))))/1.0e6;
    { Dynamic Viscosity in (kg/m.s) }
    en1:=an2/((WaterTemp+273.15)/647.3-an3);
    en2:=exp(en1*ln(10.0));
    Muliq:=an1*en2*1.0e-7;
    { Thermal Conductivity of Fresh Water in (W/m.K) }
    Kliq:=0.569+0.001575*WaterTemp;
    { Prandtl Number }
    Prliq:=1000.0*CpLiq*Muliq/Kliq;
    { Schmidt Number }
    Scliq:=372.7*(sqr(muliq)/(watertemp+273.15))/(2.71e-9);
    { Derived from oxygen diffusivity in water,
      p576, Reid et. al.,
      The properties of Gases and Liquids, McGraw Hill, 1977.}
END { WaterTransProp };

PROCEDURE PackingCharacteristics;
{ Calculates packing characteristics given
  base,height,and angle of inclination Theta }
VAR
    Sheet,Contactloss            : Real;

{ all calculations in meters.}
BEGIN
    Base:=0.025;
    Height:=Base;
    Theta:=60.0;    { degrees }
    Side:=Sqrt(Sqr(Base/2) + Sqr(Height));
    Sprime:=Sqrt(Sqr(Base/(2*Cos(Theta*Pi/180.0))+Sqr(Height)));
    Sinalpha:=Base/(2*Sprime*Cos(Theta*Pi/180.0));
    Pckdia:=Base*Height*(1/(Base+2*Side) + 1/(2*Side));
    Sheet:=0.381/1000.0;
    Void:=1.0-4.0*Sheet/Pckdia;
    Contactloss:=0.0 { % };
    Apgeom:=(1.0-Contactloss/100.0)*4.0*Void/Pckdia;
END { PackingCharacteristics };

FUNCTION Colburn_Hougen(Tinterface: Real): Real;
{ Tinterface in Celcius }
```

```

VAR
    Stmlfr,Xbulk,Ybulk,Cfric                : Real;
    { Find steam properties at the interface temperature and
      Steam Mole fraction at the interface and bulk }
BEGIN
    Stmlfr:=SatPressure(Tinterface)/Y_Est[7];
    Xbulk:=Y_Est[4]/(Y_Est[4]+Y_Est[6]);
    Ybulk:=Xbulk/Molwts/(Xbulk/Molwts+(1.0-Xbulk)/Molwti);
    { Steam flux in kg/s/m^2 }
    IF (Stmlfr>1.0) THEN Stmlfr:=1.0-1.0e-12;
    IF (Ybulk>1.0) THEN Ybulk :=1.0-1.0e-12;
    SteamFlux:=-Gmtc*ln((1.0-Ybulk)/(1.0-Stmlfr));
    { Ackerman correction factors for high mass flux to heat and friction,
      Ref. Butterworth and Hewitt: Two-phase flow and heat transfer }
    Czero:=SteamFlux*StmCp/Ghtc;
    Ackerh:=Czero/(1.0-exp(-Czero));
    RhoUb:=(Y_Est[4]+Y_Est[6])/C_S_Area;
    Cfric:=2.0*SteamFlux/(RhoUb*Frcgas);
    IF (Cfric<1.0e-6) THEN Ackf:=Cfric/(1.0-exp(-1.0e-6))
        ELSE Ackf:=Cfric/(1.0-exp(-Cfric));
    { Liquid and Gas Side heat balance - via Colburn Hougen equation.
      IF interface temperature and coefficients are correct, the
        function value of Colburn-Hougen=ZERO }
    Cht1:=Lhtc*(Tinterface-Y_Est[8]);
    Cht2:=Ghtc*Ackerh*(Y_Est[5]-Tinterface);
    Enths:=MixtureEnthalpy(Tinterface,0);
    Enthw:=LiquidEnthalpy(Tinterface);
    Cht3:=(Enths-Enthw)*SteamFlux;

    Colburn_Hougen:=Cht1-Cht2-Cht3;

END { Colburn_Hougen};

PROCEDURE CountercurrentZeroIn (ax,bx: Real;Flag:Lable;VAR Tint: Real);
VAR
    a,b,c,d,e,fa,fb,fc                : Real;
    p,q,r,s,Xm                        : Real;
BEGIN
    IF (Flag='inter') THEN
        BEGIN
            a:=ax+1e-6;
            b:=bx-1e-6;
            fa:=Colburn_Hougen(a);
            fb:=Colburn_Hougen(b);
        END;
        c:=a;
        fc:=fa;
        d:=b-a;
        e:=d;
        { convergence test }
        Toll:=2.0*Epsilon*abs(b)+0.5*Tol;
        Xm:=0.5*(c-b);
        WHILE (abs(Xm)>Toll) AND
            (fb<>0.0) AND

```

```
(fb*(fc/abs(fc))< 0.0) DO
BEGIN
  IF (abs(fc)< abs(fb)) THEN
  BEGIN
    a:=b;
    b:=c;
    c:=a;
    fa:=fb;
    fb:=fc;
    fc:=fa;
  END;
  Xm:=0.5*(c-b);
  Toll:=2.0*Epsilon*abs(b)+0.5*Tol;
  IF (abs(e)< Toll) AND (abs(fa)<=abs(fb)) THEN
  BEGIN { bisection }
    d:=Xm;
    e:=d;
  END ELSE
  BEGIN
    { is quadratic interpolation possible }
    IF (a=c) THEN
    BEGIN
      { linear interpolation }
      s:=fb/fa;
      p:=2.0*Xm*s;
      q:=1.0-s;
    END ELSE
    BEGIN
      { inverse quadratic interpolation }
      q:=fa/fc;
      r:=fb/fc;
      s:=fb/fa;
      p:=s*(2.0*Xm*q*(q-r)-(b-a)*(r-1.0));
      q:=(q-1.0)*(r-1.0)*(s-1.0);
    END;
    { adjust signs }
    IF (p>0.0) THEN q:=-q;
    p:=abs(p);
    { is interpolation acceptable }
    IF ((2.0*p)< (3.0*Xm*q-abs(Toll*q))) AND
      (p< abs(0.5*e*q)) THEN
    BEGIN
      e:=d;
      d:=p/q;
    END ELSE
    BEGIN
      { bisection }
      d:=Xm;
      e:=d;
    END;
  END;
  { Complete Step }
  a:=b;
  fa:=fb;
```

```

    IF (abs(d)>Tol1) THEN b:=b+d;
    IF (abs(d)<=Tol1) THEN b:=b+Tol1*Xm/abs(Xm);
    fb:=Colburn Hougen(b);
    IF ((fb*(fc/abs(fc)))>0.0) THEN
    BEGIN
        c:=a;
        fc:=fa;
        d:=b-a;
        e:=d;
    END;
    { convergence test }
    Tol1:=2.0*Epsilon*abs(b)+0.5*Tol;
    Xm:=0.5*(c-b);
END { While };
Tint:=b;

END { CountercurrentZeroin };

PROCEDURE CCEquilibrium;
    { finds equilibrium outlet conditions (infinite length)
      for the Countercurrent condenser}
VAR
    Op_Flag,Zero_Flag           : Lable;
    T_Tol                       : Real;
    Two,Tso,Ppii,Xiwi,Yiwi,Ppio : Real;
    Xiwo,Yiwo,Sphwi,Sphwo,Pcout,Pcoutnew : Real;
    Xso,Yso,Desorbi,Mio,Xio,Yio : Real;
    Mwi,Mso,Msc,Mionew         : Real;

BEGIN
    {set temperature tolerance and
    operating conditions to Superheat}
    T_Tol:=1e-3;
    Op_Flag:='Super';
    { find steam and liquid properties
      at the inlet (assumed to be saturated)}
    Tdew:=SatTemperature(Ybot[9]);
    {check for Superheat or saturated conditions}
    IF ((Tdew-Ybot[5])>T_Tol) THEN
    BEGIN
        Writeln (OutFile1,' inlet conditions super saturated',
                  '***** calculations aborted *****');
    END ELSE
    BEGIN
        IF (abs((Tdew-Ybot[5]))< T_Tol) THEN
        BEGIN
            Op_Flag:='Satur';
            Tdew:=Ybot[5];
            Super_In:=0;
        END;
    END;
    {calculate inlet gas Mixture properties}
    Xmass:=Ybot[6]/(Ybot[6]+Ybot[4]);
    MixTransProp(Ybot[5],Ybot[7],Xmass);

```

```

{calculate inlet stagnation temperature
 and pressure using compressible gas equations}
Gamma:=Mixcp/(Mixcp-8.3143/Mixmw);
Vel_In:=(Ybot[4]+Ybot[6])/C_S_Area/Mixrho;
A:=Sqrt(Gamma*8314.3/Mixmw*(Ybot[5]+273.15));
Mach:=Vel_In/A;
Tzbyt:=(1.0+(Gamma-1.0)*Sqr(Mach)/2.0);
Pzbyp:=Exp((Gamma/(Gamma-1.0))*Ln(Tzbyt));
T_Stg_In:=(Ybot[5]+273.15)*Tzbyt-273.15;
P_Stg_In:=Ybot[7]*Pzbyp;
{inlet gas enthalpy}
Gas_In_Enth:=(Ybot[6]+Ybot[4])*MixtureEnthalpy(Ybot[5],Xmass);
{water inlet enthalpy, total inlet enthalpy,
 and inlet momentum flux}
Enthw:=LiquidEnthalpy(Ytop[8]);
Wat_In_Enth:=Ytop[1]*Enthw+Ytop[3]*AirCp*Ytop[8];
K_E_In:=(Ybot[6]+Ybot[4])*Sqr(Vel_In)/(2*1000.0);
Tot_In_Enth:=Wat_In_Enth+Gas_In_Enth+K_E_In;
Mom_In:=(Ybot[4]+Ybot[6])*Vel_In/C_S_Area;

{By definition for equilibrium water outlet temp=steam inlet temp;
 water outlet inert content corresponds to steam inlet inert content;
 steam outlet inert content corresponds to water inlet inert content;
 pressure loss is zero; water flow is minimum required;
 solve for both water and steam outlet properties and
 minimum water flow;}

Two:=Tdew; Tso:=Ytop[8];
Ppii:=Ybot[7]-Ybot[9];
Yiwo:=Ppii/Henry(Two);
Xiwo:=InertMoletoMassFraction(Yiwo);
Sphwo:=LiquidEnthalpy(Two)+Xiwo*AirCp*Two;
Mom_Out:=0.0;
REPEAT
    Pcout:=Ybot[7] + Mom_In - Mom_Out;
    Yso:=SatPressure(Tso)/Pcout;
    Yio:=1.0-Yso;
    Xio:=InertMoletoMassFraction(Yio);
    Xso:=1.0-Xio;
    Desorbi:=0.0;
    REPEAT
        Mio:=Ybot[6] + Desorbi;
        Xio:=1.0 - Xso;
        Mso:=Mio*Xso/Xio;
        Msc:=Ybot[4] - Mso;
        MixTransProp(Tso,Pcout,Xio);
        Vel_Out:=(Mso+Mio)/MixRho/C_S_Area;
        K_E_Out:=(Mso+Mio)*Sqr(Vel_Out)/2000.0;
        Mom_Out:=(Mso+Mio)*Vel_Out/C_S_Area;
        Gas_Out_Enth:=(Mso+Mio)*MixtureEnthalpy(Tso,Xio);
        { find top dissolved gas in water }
        Ppio:=Pcout*(1.0-Yso);
        Yiwi:=Ppio/Henry(Ytop[8]);
        Xiwi:=InertMoletoMassFraction(Yiwi);

```

```

        Sphwi:=LiquidEnthalpy(Ytop[8])+Xiwi*AirCp*Ytop[8];
        { find required waterflow and released gas }
        YEqlbm[2]:=(Gas_In_Enth - Gas_Out_Enth +
                    K_E_In - K_E_Out - Msc*Sphwo);
        Mwi:=YEqlbm[2]/(Sphwo - Sphwi);
        Desorbi:=Mwi*(Xiwi-Xiwo);
        { find new outlet gas flow and repeat until convergence }
        Mionew:=Ybot[6] + Desorbi;
        UNTIL (Abs((Mionew-Mio)/Mio)< 1.0e-5);
        { find new outlet pressure till convergence }
        Pcoutnew:=Ybot[7]+ Mom_In -Mom_Out;
        UNTIL (Abs((Pcoutnew-Pcout)/Pcout)< 1.0e-5);

        { Now save equilibrium values for later use }
        {stagnation equilibrium conditions
        from compressible gas equations}
        Gamma:=Mixcp/(Mixcp-8.3143/Mixmwt);
        A:=sqrt(Gamma*8214.3/Mixmwt*(Tso+273.15));
        Mach:=Vel_Out/A;
        Tzbyt:=(1.0+(Gamma-1.0)*Sqr(Mach)/2.0);
        Pzbyp:=Exp((Gamma/(Gamma-1.0))*Ln(Tzbyt));
        T_Stg_Eq:=(Tso+273.15)*Tzbyt-273.15;
        P_Stg_Eq:=Pcout*Pzbyp;
        {set array of equilibrium conditions}
        YEqlbm[1]:=Mwi+Msc;
        YEqlbm[3]:=Xiwo*(YEqlbm[1]);
        YEqlbm[4]:=Mso;
        YEqlbm[5]:=Tso;
        YEqlbm[6]:=Mio;
        YEqlbm[7]:=Pcout;
        YEqlbm[8]:=Two;
        YEqlbm[9]:=Pcout*Yso;
        YEqlbm[10]:=1e5;
        YEqlbm[11]:=0.0;
        Vel_Eqlbm:=Vel_Out;;
        Super_Eqlbm:=0.0;
        X_Eqlbm:=1e20;

    END { CCEquilibrium };

    PROCEDURE FileSetup;

    BEGIN
        { Interactive reading of input and output file names }
        Form6:=Char(012);
        Form7:=Char(012);
        { Writeln('Input File Name???
        - (EG. A:Cctml.Doc ', '-- 20 characters max)');
        ReadLn (Kbd,Filein);
        Writeln('First Output File Name??? - (EG. C:Tape6.Out)');
        ReadLn (Kbd,Filot1);
        Writeln('Second Output File Name??? - (EG. C:Tape7.Out)');
        ReadLn (Kbd,Filot2);}
        Assign (InFile, 'd:CCinput.par');
    
```

```
Assign (OutFile1,'d:CCTape6.out');
Assign (OutFile2,'d:CCTape7.out');
Assign (OutFile3,'d:CCTape8.out');
IF (Filot1='1st') THEN Form6:='1';
IF (Filot2='1st') THEN Form7:='1';
Reset (InFile);
Rewrite(OutFile1);
Rewrite(OutFile2);
Rewrite(OutFile3);
{ Read the number of condenser runs to be made
  from the first line of the input file }
Readln (Infile);
Readln (InFile,Nrun);
Afraction:=1.0;
PackingCharacteristics;
Saperv:=Afraction*Apgeom;

END { FileSetup };

PROCEDURE Countercurrentinput;
{ This procedure contains the input routines
  for the direct contact condenser routine
  Input routine for Countercurrent condenser reads from
  the file CCinput.par. }
VAR
  Verbage                                : String[80];
  Ipos                                   : Integer;
BEGIN
  {initialize condenser starting length to zero}
  Xin:=0.0;
  {read run label and Correction factors to Correlations
   Verbage is a dummy character variable which reads comment
   lines in the input file}
  Readln (InFile,Run_Lable,Serial,T_Dew_In,Ytop[8],
          Gas_Load,Yacob,Xinprc);
  Ipos:=Pos('-',Run_Lable);
  Delete(Run_Lable,1,Ipos-7);
  Ipos:=Pos('-',Run_Lable);
  Delete(Run_Lable,Ipos+3,15);
  Insert(' ',Run_Lable,1);
  Insert(' ',Run_Lable,11);
  Geometry:='Pack';

  Cond_Len:=2.000;
  PpmIn:=14.0; { Note: If PpmIn<PpmInmin for efficient operation
                  then PpmIn will be reset to PpmInmin }

  Super_In:=0.0;
  {input calculations}
  C_S_Area:=1.0;
  Ybot[4]:=Gas_Load*C_S_Area;
  Ytop[1]:=Yacob*Ybot[4]*2470.0/(4.186*(T_Dew_In-Ytop[8]));
```

```

Ytop[3]:=Ytop[1]*PpmIn*1.0e-6;
Ybot[6]:=Ybot[4]*Xinprc/100.0;
Ybot[2]:=0.0;
Ybot[10]:=0.0;
Ybot[11]:=0.0;
Ybot[5]:=T_Dew_In+Super_In;

END { Countercurrentinput };

PROCEDURE CC_Transfer_Coefficients;

{ This routine calculates the gas friction coefficient,
  the liquid heat and mass transfer coefficients, and
  the gas heat and mass transfer coefficients given local conditions.
  Both laminar and turbulent flow for the gas is considered.
  For the liquid only turbulent flow is incorporated. }

VAR
  Diff,K_L                               : Real;
  GammaL,Delta,Lload,Reside              : Real;
  U_G,U_G_Eff                           : Real;
BEGIN
  { -----
    liquid-Side coefficients
    ----- }
  { Find liquid properties }
  WaterTransProp(Y_Est[8]);
  { Liquid Reynolds number }
  Lload:=Y_Est[1]/C_S_Area;
  GammaL:=Lload/Saperv;
  Rel:=4.0*GammaL/Mulq;
  { Liquid film thickness }
  Delta:=Exp(0.6*Ln(GammaL/(Rholiq*82.0*Sqrt(Sinalpha))));
  { Turbulent flow over an inclined plane,
    Manning Formula, p312 of John Haberman }
  U_L_Eff:=GammaL/(Rholiq*Delta);
  Diff:=(Mulq/Rholiq)/Scliq;
  K_L:=2.0*Sqrt(Diff*U_L_Eff/(Pi*Sprime));
  { Liquid-side mass transfer coefficient }
  Lmtc:=Rholiq*K_L;
  { Heat transfer coefficient is found using Chilton-Colburn analogy }
  Lhtc:=Lmtc*Cpliq*Exp((2.0/3.0)*Ln(Scliq/Prliq));
  { -----
    Gas-Side transfer coefficients
    ----- }
  { Correlations from Bravo }
  { Find gas Mixture properties }
  Xmass:=Y_Est[6]/(Y_Est[4]+Y_Est[6]);
  MixTransProp(Y_Est[5],Y_Est[7],Xmass);
  { Compute mass flux and dimensionless numbers }
  RhoUb:=(Y_Est[4]+Y_Est[6])/C_S_Area;
  U_G:=RhoUb/MixRho; U_G_Eff:=U_G/Sin(Theta*Pi/180);

```

```

    { Note Relative velocity is used here, according to Bravo }
    Reg:=MixRho*(U_G_Eff+abs(U_L_Eff))*Pckdia/Mixmu;
    { Countercurrent flow }
    Nusselt_Gas:=0.0338*Exp(0.8*Ln(Reg))
                    *Exp(0.333*Ln(Mixpr)) { Bravo/Structured Packings};
    { Equivalent to Eqs. 2-29 and 2-31 in text }
    Ghtc:=Nusselt_Gas*Mixk/Pckdia/1000.0;
    Gmtc:=Ghtc*Exp((2.0/3.0)*Ln(Mixpr/Mixsc))/MixCp;
    {
        -----
        gas friction coefficients
        ----- }
    { Note:-- Gas Reynolds Number Based on Side, per Bravo }
    { for friction evaluations alone, Correlations of Bravo }
    { Liquid Froud number corrections as in bravo are not used.}
    Reside:=Reg*Side/Pckdia; { side Reynolds Number}
    Frcgas:=0.171+92.7/(Reside);

END { CC_Transfer_Coefficients };

PROCEDURE CountercurrentDerivatives;

    { This subroutine computes the first derivatives
      of the differential equations given the length
      and the values of the variables. An explanation
      of the variables is given above in the main routine. }

VAR
    a11,a12,a21,a22,b1,b2                : Real;
    Molair,Molest                         : Real;
    Dmlsdx,Dmladx,Dppadx                 : Real;
    Count                                 : Integer;

BEGIN
    IF ((Setflag=True) OR
        (Y_Est[9]<=(1.0+SatPressure(Y_Est[8])))) THEN
    BEGIN
        FOR Count:=1 TO 11 DO Yprime[Count]:=0.0;
        IF (Setflag=False) THEN
        BEGIN
            Xfinal:=x;
            Setflag:=True;
        END;
    END ELSE
    BEGIN

        { Compute heat and mass transfer coefficients for use
          in differential equations. Call Transfer Coefficients
          to initialize. }
    
```

```

CC Transfer_Coefficients;
{ Zeroin iteratively solves the Colburn-Hougen equation
  for interface conditions and correct transfer
  coefficients. }
Tdew:=SatTemperature(Y_Est[9]);
CountercurrentZeroin (Y_Est[8],Tdew,'inter',Tsurf);
{find steam and water properties}
Xmass:=Y_Est[6]/(Y_Est[6]+Y_Est[4]);
MixTransProp(Y_Est[5],Y_Est[7],Xmass);
WaterTransProp(Y_Est[8]);
{ Solve for overall heat and mass transfer
  coefficients using the interface temperature (Tsurf). }
Ovhtc:=Lhtc*(Tsurf-Y_Est[8])/(Y_Est[5]-Y_Est[8]);
Ovmtc:=Lmtc;
{ Compute first derivatives of the variables }
Yprime[1]:=-SteamFlux*C_S_Area*Saperv;
Yprime[2]:=Lhtc*Saperv*C_S_Area*(Tsurf-Y_Est[8]);
Yprime[3]:=Lmtc*C_S_Area*Saperv*(Y_Est[3]/Y_Est[1]-
  (Y_Est[7]-Y_Est[9])/
  (Henry(Y_Est[8]))*Molwti/Molwts);
Yprime[4]:=Yprime[1];
Yprime[6]:=Yprime[3];
{ Matrix solution is needed for calculating the
  steam temperature and total pressure derivatives }
RhoUb:=(Y_Est[6]+Y_Est[4])/C_S_Area;
U_Bulk:=RhoUb/(Void*MixRho*Sin(Theta*Pi/180.0));
a11:=1.0+U_Bulk*U_Bulk/(1000.0*MixCp*(273.15+Y_Est[5]));
a22:=1.0-U_Bulk*U_Bulk/(8314.3*Mixmwts*(273.15+Y_Est[5]));
a12:=-U_Bulk*U_Bulk/(MixRho*1000.0*MixCp*8314.3/
  Mixmwts*(273.15+Y_Est[5]));
a21:=MixRho*U_Bulk*U_Bulk/(273.15+Y_Est[5]);
b1:=-Cht2*exp(-Czero)*Saperv*C_S_Area/
  (MixCp)/(Y_Est[4]+Y_Est[6])
  -U_Bulk*(Yprime[4]/C_S_Area)/
  (MixRho*MixCp*1000.0);
b2:=-U_Bulk*Yprime[4]/C_S_Area-0.5*MixRho*
  Sqr(U_Bulk+abs(U_L_Eff))*
  Apeom*Frcgas*
  (Afraction*Ackf+(1.0-Afraction));
{ Note Apeom used here instead of Saperv to
  account for friction contribution from
  ineffective mass transfer area as well.}
Yprime[5]:=(a22*b1-a12*b2)/(a11*a22-a12*a21);
Yprime[7]:=(a11*b2-a21*b1)/(a11*a22-a12*a21);
{ Molar flow rates needed for steam partial pressure }
Molair:=Y_Est[6]/Molwti;
Molest:=Y_Est[4]/Molwts;
Dmladx:=Yprime[6]/Molwti;
Dmlsdx:=Yprime[4]/Molwts;
Dppadx:=Molair/(Molair+Molest)*Yprime[7]+
  Y_Est[7]*(((Molair+Molest)*Dmladx-
  Molair*(Dmladx+Dmlsdx))/(Sqr(Molair+Molest)));
Yprime[9]:=Yprime[7]-Dppadx;
Yprime[8]:=-Yprime[2]/(Y_Est[1]*Cpliq);

```

```
        Yprime[10]:=-Yprime[8]/(Y_Est[5]-Y_Est[8]);
        Yprime[11]:=0.0;
    END {if};
    { save derivatives for printing }
    Prime:=Yprime;

END { CountercurrentDerivatives };

PROCEDURE CountercurrentOutAdd(Nline,Nseg: Integer);
    { Additional Countercurrent detailed output including
      dimensionless numbers and individual coefficients
      as a function of condenser length are generated here
      and printed in file OutFile2. }

VAR
    Vout                                     : Vector;
BEGIN

    {print label, header, and initial conditions on first call}
    IF (Nline=0) THEN Writeln(OutFile2,Form6,Run_Lable);
    IF (Nline=0) THEN
        Writeln(OutFile2,Cdate,' ',Ctime,' Iteration ',Iguess);
        {re-solve for ackerman heat transfer Correlation}
        Ackerh:=Czero/(1.0-exp(-Czero));
        {load and print output matrix}
        IF (Nline< 100) THEN
            BEGIN
                Vout[1]:=X;
                Vout[2]:=Rel;
                Vout[3]:=Reg;
                Vout[4]:=Prliq;
                Vout[5]:=Mixpr;
                Vout[6]:=Scliq;
                Vout[7]:=Mixsc;
                Vout[8]:=Lhtc;
                Vout[9]:=Ghtc*1000.0;
                Vout[10]:=Lmtc*1000.0;
                Vout[11]:=Gmtc*1000.0;
                Vout[12]:=Ackerh;
                Vout[13]:=Ackf;
                Vout[14]:=SteamFlux*1000.0;
                Vout[15]:=Tdew;
                Vout[16]:=Prime[5];
                Vout[17]:=Prime[7];
                Vout[18]:=Nusselt_Gas;
                Vout[19]:=Frcgas;
                FOR i:=1 TO 19 DO Write(OutFile2,Vout[i]:10,' ');
                Writeln(OutFile2);
            END;
        IF(Nline=100) THEN
            BEGIN
                Writeln(OutFile2);
                FOR i:=1 TO 18 DO Write(OutFile2,999.9:10,' ');
                Writeln(OutFile2);
                Writeln(OutFile2);
            END;
        
```

```

        END;

    END { CountercurrentOutAdd} ;

    PROCEDURE CountercurrentOutput(Nline,Nseg: Integer);

        { Output routine for Countercurrent condenser model
          Prints detailed results as a function of condenser
          length and a summary with actual and equilibrium
          outlet conditions on the file OutFile1. }

    VAR
        Vout                                : Vector;
        Tstago,Pstago,Superht               : Real;
        Ploss,Poten                         : Real;
        Effweq,Effw                         : Real;
        {print header, label, and inlet conditions
         for the first call}

    BEGIN
        IF (Nline=0) THEN
            BEGIN
                Cdate:='' + date + '' ;
                Ctime:='' + time + '' ;
                Writeln(OutFile1,Form6,Run_Lable);
                Writeln(outfile1,Cdate,' ',Ctime,' Iteration ',Iguess);
                { write inlet conditions }
                Vout[1]:=Xin;
                Vout[2]:=Ybot[1]/C_S_Area;
                Vout[3]:=Ybot[4]/C_S_Area;
                Vout[4]:=Ybot[3]*1e6/(Ybot[1]+Ybot[3]);
                Vout[5]:=(Ybot[6]*100.0)/(Ybot[6]+Ybot[4]);
                Vout[6]:=Ybot[5];
                Vout[7]:=Tsurf;
                Vout[8]:=Ybot[8];
                Vout[9]:=Super_In;
                Vout[10]:=Ybot[7];
                Vout[11]:=Ybot[9];
                Vout[12]:=SatPressure(Ybot[5]);
                Vout[13]:=0.0;
                Vout[14]:=Ybot[10];
                Vout[15]:=Ybot[2]/C_S_Area;
                Vout[16]:=(1.0-Ybot[4]/Ybot[4])*100.0;
                Vout[17]:=Vel_In;
                Vout[18]:=0.0;
                Vout[19]:=0.0;
                FOR i:=1 TO 19 DO Write(OutFile1, Vout[i]:10,' ');
                Writeln(OutFile1);
                CountercurrentOutAdd(Nline,Nseg);
            END ELSE IF (Nline< 100) THEN
                BEGIN
                    {set output conditions}
                    Tdew:=SatTemperature(Y[9]);
                    {find stagnation temperature and pressure conditions}
                    U_Bulk:=(Y[4]+Y[6])/C_S_Area/Mixrho;
                END
            END
        END
    
```

```

Gamma:=Mixcp/(Mixcp-8.3143/Mixmwt);
A:=sqrt(Gamma*8314.3/Mixmwt*(Y[5]+273.15));
Mach:=U_Bulk/A;
Tzbyt:=(1.0+(Gamma-1.0)*Sqr(Mach)/2.0);
Pzbyp:=Exp(Gamma/(Gamma-1.0)*Ln(Tzbyt));
Tstago:=Y[5]*Tzbyt;
Pstago:=Y[7]*Pzbyp;
Superht:=Y[5]-Tdew;
{define a "pressure loss" Term which includes momentum}
Ploss:=Ybot[7]-Y[7]+(Mom_In-(Y[4]+Y[6])*U_Bulk/C_S_Area);
{set output array and print intermediate results}

Vout[1]:=X;
Vout[2]:=Y[1]/C_S_Area;
Vout[3]:=Y[4]/C_S_Area;
Vout[4]:=Y[3]*1e6/(Y[1]+Y[3]);
Vout[5]:=(Y[6]*100.0)/(Y[6]+Y[4]);
Vout[6]:=Y[5];
Vout[7]:=Tsurf;
Vout[8]:=Y[8];
Vout[9]:=Superht;
Vout[10]:=Y[7];
Vout[11]:=Y[9];
Vout[12]:=SatPressure(Y[5]);
Vout[13]:=Ploss;
Vout[14]:=Y[10];
Vout[15]:=Y[2]/C_S_Area;
Vout[16]:=(1.0-Y[4]/Ybot[4])*100.0;
Vout[17]:=U_Bulk;
Vout[18]:=Ovhtc;
Vout[19]:=Ovmtc*1000.0;
Pdrop:=Ybot[7]-Y[7];
FOR i:=1 TO 19 DO Write(OutFile1,Vout[i]:11,' ');
Writeln(OutFile1);
CountercurrentOutAdd(Nline,Nseg);
END;
IF(Nline=100) THEN
BEGIN
  {**** Last two lines of output ****}
  Writeln(OutFile1);
  { Equilibrium Conditions }
  Vout[1]:=999.9;
  Vout[2]:=Yeq1bm[1]/C_S_Area;
  Vout[3]:=Yeq1bm[4]/C_S_Area;
  Vout[4]:=Yeq1bm[3]*1e6/Yeq1bm[1]; {approx}
  Vout[5]:=(Yeq1bm[6]*100.0)/(Yeq1bm[6]+Yeq1bm[4]);
  Vout[6]:=Yeq1bm[5];
  Vout[7]:=0.0;
  Vout[8]:=Yeq1bm[8];
  Vout[9]:=0.0;
  Vout[10]:=Yeq1bm[7];
  Vout[11]:=Yeq1bm[9];
  Vout[12]:=SatPressure(Yeq1bm[5]);
  Vout[13]:=0.0;

```

```
Vout[14]:=Yeqlbm[10];
Vout[15]:=Yeqlbm[2]/C_S Area;
Vout[16]:=(1.0-Yeqlbm[4]/Ybot[4])*100.0;
Vout[17]:=Vel_Eqlbm;
Vout[18]:=999.9;
Vout[19]:=999.9;
FOR i:=1 TO 19 DO Write(OutFile1,Vout[i]:11,' ');
Writeln(OutFile1);

    CountercurrentOutAdd(Nline,Nseg);
END;

END {CountercurrentOutput };

PROCEDURE Runga(h,x0: Real;Y0:State);
{ Integration Routine }
VAR
    k1,k2,k3,k4                : State;
BEGIN
    X_Est:=x0;
    Y_Est:=Y0;
    CountercurrentDerivatives;
    IF ((x0=0.0) AND Convergence) THEN CountercurrentOutput(0,40);
    FOR i:=1 TO Neqn DO
        BEGIN
            k1[i]:=h*Yprime[i];
            Y_Est[i]:=Y0[i]+k1[i]/2;
        END;
        X_Est:=X_Est+h/2;
        CountercurrentDerivatives;
        FOR i:=1 TO Neqn DO
            BEGIN
                k2[i]:=h*Yprime[i];
                Y_Est[i]:=Y0[i]+k2[i]/2;
            END;
            CountercurrentDerivatives;
            FOR i:=1 TO Neqn DO
                BEGIN
                    k3[i]:=h*Yprime[i];
                    Y_Est[i]:=Y0[i]+k3[i];
                END;
                X_Est:=X_Est+h/2;
                CountercurrentDerivatives;
                FOR i:=1 TO Neqn DO
                    BEGIN
                        k4[i]:=h*Yprime[i];
                        Y[i]:=Y0[i]+(k1[i]+2*k2[i]+2*k3[i]+k4[i])/6;
                    END;
                    X:=X0+h;
                END { Runga };

PROCEDURE March;
VAR
```

```

        Increment      : Real;
        Stepflag       : Boolean;
BEGIN
    Y:=Ybot;
    X:=Xin;

    {set initial heat, mass and friction coefficients to zero}
    Lhtc:=0.0;  Lmtc:=0.0;  Ghtc:=0.0;  Gmtc:=0.0;
    Frcgas:=0.0;  Frcliq:=0.0;

    Istep:=0; Xend:=Xin; Xfinal:=Cond_Len;  Setflag:=False;
    Step:=Cond_len/Nseg;
    Stepflag:=False;

    Window(1,17,80,25);
    GotoXY(1,1);
    REPEAT
        Increment:=Step;
        Xend:=Xend+Increment;
        IF ((Xend>Cond_Len) OR ((Cond_Len-Xend)< 2.0*Step)
            OR (Setflag=True)) THEN
            BEGIN
                Xend:=Cond_Len;
                Increment:=Cond_Len-X;
            END;

        Runga(Increment,X,Y);

        Wateff:=(Y[8]-Ytop[8])/(Ybot[5]-Ytop[8]);
        Cond_prc:=(Ybot[4]-Y[4])*100.0/Ybot[4];
        Pdrop:=Ybot[7]-Y[7];
        Writeln(Iguess:2,Xend:6:3,Y[8]:6:2,Tsurf:6:2,
                Tdew:6:2,Wateff:8:4,
                Cond_prc:6:2,Pdrop:6:2,' ',
                Reg:7:1,' ',Y[4]:6:3,' ',
                Y[6]:8:6,' ',Y[3]:8:6);
        Tdew:=SatTemperature(Y[9]);
        { succesful integration, increment length
          and print intermediate results}
        Istep:=Istep+1;
        IF (Convergence AND Iprint) THEN
            CountercurrentOutput(Istep,Nseg);
        IF (convergence AND (x=Cond_Len)) THEN
            BEGIN
                Writeln(1st,Run_Lable:20,Serial:5,Iguess:3,
                        Ybot[5]:10:2,Xfinal:10:2,Y[8]:10:2,
                        Ybot[8]:10:2,Cond_prc:10:2,Pdrop:10:2,
                        Tdew:10:2,Gas_Load:6:2,Saperv:10:4);
                Writeln(OutFile3,Run_Lable:20,Serial:5,Iguess:3,
                        Ybot[5]:11:4,Xfinal:11:4,Y[8]:11:4,
                        Ybot[8]:11:4,Cond_prc:11:4,Pdrop:11:4,
                        Tdew:11:4,Gas_Load:6:2,Saperv:10:4);
                IF (Convergence AND Iprint) THEN
                    CountercurrentOutput(100,100);
            END;
        END;
    END;

```

```

        END;
        {final length reached, go on to next set of conditions}

        IF ((Stepflag=False) AND (Cond_prc>97.0)) THEN
        BEGIN
            Step:=Step/4.0;
            Stepflag:=True;
        END;

    UNTIL (Xend>=Cond_Len);

    Window(1,1,80,20);
    GotoXY(1,Iguess+2);
    Writeln(Con,Run_Lable:15,Iguess:4,Y[1]:8:2,
            Ybot[1]:8:2,Y[8]:8:2,Ybot[8]:8:2,
            Y[3]:12:8,Ybot[3]:12:8,' ',Convergence:1);

END { March };

PROCEDURE Iterate(VAR a,b,c,fa,fb,fc,new : Real; Tol: Real;
                  VAR Converged : Boolean);
    { note: tolerance set on fb for temperature only }
VAR
    d,e                : Real;
    p,q,r,s            : Real;
    Xm,Tol2             : Real;
BEGIN
    Converged:=False;
    d:=b-a;
    e:=d;
    { convergence test }
    Tol2:=2.0*Epsilon*abs(b);
    Xm:=0.5*(c-b);

    IF (abs(fb)< Tol) THEN Converged:=True;
    IF ((abs(Xm)>Tol2) AND
        (fb< >0.0) AND
        (fb*(fc/abs(fc))< 0.0)) THEN
    BEGIN
        IF (abs(fc)< abs(fb)) THEN
        BEGIN
            a:=b;
            b:=c;
            c:=a;
            fa:=fb;
            fb:=fc;
            fc:=fa;
        END;
        Xm:=0.5*(c-b);
        Tol2:=2.0*Epsilon*abs(b);
        IF (abs(e)< Tol2) AND (abs(fa)< =abs(fb)) THEN
        BEGIN { bisection }
            d:=Xm;
            e:=d;
    
```

```
END ELSE
BEGIN
  { is quadratic interpolation possible }
  IF (a=c) THEN
  BEGIN
    { linear interpolation }
    s:=fb/fa;
    p:=2.0*Xm*s;
    q:=1.0-s;
  END ELSE
  BEGIN
    { inverse quadratic interpolation }
    q:=fa/fc;
    r:=fb/fc;
    s:=fb/fa;
    p:=s*(2.0*Xm*q*(q-r)-(b-a)*(r-1.0));
    q:=(q-1.0)*(r-1.0)*(s-1.0);
  END;
  { adjust signs }
  IF (p>0.0) THEN q:=-q;
  p:=abs(p);
  { is interpolation acceptable }
  IF ((2.0*p)<(3.0*Xm*q-abs(Tol2*q))) AND
    (p<abs(0.5*e*q)) THEN
  BEGIN
    e:=d;
    d:=p/q;
  END ELSE
  BEGIN
    { bisection }
    d:=Xm;
    e:=d;
  END;
END;
END;
{ Complete Step }
IF (abs(d)>Tol2) THEN new:=b+d;
IF (abs(d)<=Tol2) THEN new:=b+Tol2*(Xm/abs(Xm));
a:=b;
fa:=fb;
IF (abs(fb)<=Tol) THEN Converged:=True;
END { IF };

END { Iterate };

PROCEDURE CountercurrentMain;
  {repeat the procedure from here on for every run}
VAR
  Ix,J                      : Integer;
  Stmlfr                   : Real;
  Ppiomax,Ytop3min         : Real;
  Xa,Xb,Xc,Fxa,Fxb,Fxc,Xnew : ARRAY [1..3] of Real;
  Ind                      : ARRAY [1..3] of Integer;
  Tolerance                : ARRAY [1..3] of Real;
  Stop                     : Boolean;
```

```

LABEL                                Quit;

BEGIN
  FOR Ix:=1 TO Nrun DO
    BEGIN
      FOR i:=1 TO 11 DO
        BEGIN
          Y[i]:=0;
          Ybot[i]:=0;
        END;
      X:=0;
      Xin:=0;
      {read the condenser initial values of most of the
        variables in the modeling differential equations
        by calling subroutine cinput. The variables are
        as follows:

      Y[1]:=water flow rate (kg/s)
      Y[2]:=condenser heat load (kW)
      Y[3]:=dissolved gas flow rate (kg/s)
      Y[4]:=steam flow rate (kg/s)
      Y[5]:=steam temperature (C)
      Y[6]:=inert gas mass flow rate (kg/s)
      Y[7]:=condenser pressure (Pa)  ** calculated **
      Y[8]:=water temperature (C)
      Y[9]:=partial pressure of the steam (Pa)  ** calculated **
      Y[10]:=ntu
      Y[11]:=fog flow rate (kg/s) ** not used **}

      Countercurrentinput;

      { Solve for remaining initial values of
        integration variables}
      Stmlfr:=(Ybot[4]/Molwts/(Ybot[4]/Molwts+Ybot[6]/Molwti));
      Ybot[9]:=SatPressure(Ybot[5]-Super_In);
      Ybot[7]:=Ybot[9]/Stmlfr;
      Tdew:=Ybot[5]-Super_In;

      { determine a minimum deaeration level practical for
        incoming water; below this we could be wasting energy }
      Ppiomax:=Ybot[7]-SatPressure(Ytop[8]);
      Ytop3min:=Ytop[1]*InertMoletoMassFraction
        (Ppiomax/Henry(Ytop[8]));
      IF (Ytop[3]< Ytop3min) THEN Ytop[3]:=Ytop3min;

      CCEquilibrium;

      {set the input parameters for the
        integration routine}
      Step:=Cond_Len/Nseg;
      Igues:=1;
      Convergence:=False;
      Stop:=False;
      Clrscr;
    END;
  END;

```

```
Window(1,1,80,20);
Writeln(con,'      Run Id      ','Iter',' WF-Top ',' WF-Bot ',
          ' Tw-Top ',' Tw-Bot ',
          ' Iw-Top ',' Iw-Bot ');
Writeln(con,Run_Lable:15,' -- ':4,Ytop[1]:8:2,'--des.--':8,
          Ytop[8]:8:2,'--des.--':8,Ytop[3]:12:8,
          ' desired. ':12);
{ outlet condition guessing game for Countercurrent operation }
{ first try }
Ind[1]:=1;  Tolerance[1]:=0.0;
Ind[2]:=3;  Tolerance[2]:=0.0;
Ind[3]:=8;  Tolerance[3]:=0.03; { on top water temperature }
{ convergence is determined when calculated water
  temperature on top matches the specified water
  inlet temperature within the specified tolerance
  limit. Only water temperature is used for testing
  convergence. Other tolerances for top water flow
  rate, Tolerance[1], and top water dissolved air
  content, Tolerance[2] are set to zero.}
Xa[1]:=Ytop[1]+1.00*Ybot[4];
{ first guess of bottom water flow rate }
Xa[2]:=Ytop[3];
{ first guess of bottom air flow rate dissolved in water }
Xa[3]:=Ytop[8]+Ybot[4]*1.00*2470.0/(4.186*Ytop[1]);
{ first guess of bottom water temperature }
IF (Xa[3]>=Tdew) THEN Xa[3]:=Tdew-0.1;
FOR J:=1 TO 3 DO Ybot[Ind[J]]:=Xa[J];
March;
FOR J:=1 TO 3 DO Fxa[J]:=Y[Ind[J]]-Ytop[Ind[J]];
{ second try }
Iguess:=2;
Xb[1]:=Ytop[1];
{ second guess of bottom water flow rate }
Xb[2]:=Ytop[3]-5.0*(Y[3]-Ybot[3]);
{ second guess of bottom air flow rate dissolved in water }
Xb[3]:=Ytop[8]+Ybot[4]*0.600*2470.0/(4.186*Xb[1]);
{ second guess of bottom water temperature }
{ the second guesses may be altered to narrow limits
  on bottom water flow rate, dissolved air content, and
  water temperatures suitably and aid in faster
  convergence on iterations.}
FOR J:=1 TO 3 DO Ybot[Ind[J]]:=Xb[J];
March;
FOR J:=1 TO 3 DO Fxb[J]:=Y[Ind[J]]-Ytop[Ind[J]];
{ Begin iterations to achieve convergence }
Xc:=Xa;  Fxc:=Fxa;  Xnew:=Xa;
WHILE ((NOT Convergence) AND (Iguess< 24)) DO
BEGIN
  Iguess:=Iguess+1;
  FOR J:=1 TO 3 DO
  BEGIN
    Iterate(Xa[J],Xb[J],Xc[J],Fxa[J],Fxb[J],Fxc[J],
            Xnew[J],Tolerance[J],Convergence);
  END {for};
```

```

        Xb:=Xnew;
        FOR J:=1 TO 3 DO Ybot[Ind[J]]:=Xb[J];
        Writeln('Ybot 1,3,8 ',Ybot[1]:6:2,
                Ybot[3]:12:8,Ybot[8]:10:4);
        Writeln(' Convergence ',convergence);
        March;
        FOR J:=1 TO 3 DO
        BEGIN
            Fxb[J]:=Y[Ind[J]]-Ytop[Ind[J]];
            IF (Fxb[J]*(Fxc[J]/abs(Fxc[J])) > 0.0) THEN
            BEGIN
                Xc[J]:=Xa[J];
                Fxc[J]:=Fxa[J];
            END { if };
        END {for}
    END { While };
    IF (NOT Convergence) THEN Writeln(OutFile3,Run_Lable:25,
                                     '" No Convergence, go to next run" ');
    IF (NOT Convergence) THEN Writeln(lst,Run_Lable:25,
                                     '" No Convergence, go to next run" ');
    END { Run-for-do loop };

Quit:

END { Procedure CountercurrentMain };

{ Beginning of Main Program }

BEGIN
    FileSetUp;
    Machineaccuracy;
    Iprint:=True;
    CountercurrentMain;
    Close(OutFile1);
    Close(OutFile2);
    Close(OutFile3);
    Close(Lst);

END { CCcond }.
    
```

Table F-1. Cross Reference of Computer Program Variables

Variable	Description	Units
a	lower limit of x in ZEROIN	---
Abs	absolute value	---
Ackerh	Ackermann correction factor for heat transfer	---
Ackf	Ackermann correction factor for friction	---
Afraction	fractional area effective in mass transfer	---
AirCp	specific heat of air	kJ/kg K
AirK	thermal conductivity of air	W/m K
AirMu	dynamic viscosity of air	kg/m s
Airtransprop	procedure for air transport property calculations	---
Ak	variable in SatTemperature Procedure	---
Apgeom	geometric transfer area per volume of the packing	1/m
Ax	register addressed in DATETIME functions	---
b	upper limit of x in ZEROIN	---
Base	base dimension of the packing	m
Bx	register addressed in DATETIME functions	---
c	intermediate value of x in ZEROIN	---
Cccond	program countercurrent condenser	---
Ccequilibrium	countercurrent equilibrium calculations procedure	---
Ccinput	countercurrent input procedure	---
Cdate	date in string format	---
Cfric	term for Ackermann friction correction	---
Char	character variable	---
Cht	terms in the Colburn-Hougen equation	kW/m ²
Clrscr	screen clear procedure	---
Cocond	program cocurrent condenser	---
Coinput	cocurrent condenser input procedure	---
Colburn-Hougen	value of the Colburn-Hougen equation	kW/m ²
Con	console screen monitor	---
Cond-Len	length of the condenser	m
Cond-Prc	percentage of condensed steam	%
Const	numerical constants	---
Contactloss	percent of lost area due to sheet contact	%
Cos	cosine of the angle	---
CountercurrentOutAdd	output procedure for the countercurrent condenser	---
CountercurrentOutput	output procedure for the countercurrent condenser	---
CpLiq	specific heat of the liquid	kJ/kg K
Ctime	time in string format	---
Cx	register addressed in DATETIME functions	---
Czero	non-dimensional steam flux	---
C-S-Area	condenser cross sectional area	m ²
d	domain of x in ZEROIN	---
Datestr	date in string format	---
Datetime	current date and time evaluation procedure	---
DelRho	water density correction term	kg/m ³

Table F-1. Cross Reference of Computer Program Variables (Continued)

Variable	Description	Units
Delta	liquid film thickness	m
Derivatives	derivative evaluation procedure	---
Di	register addressed in DATETIME functions	---
Diffaw	diffusivity of air in water	m ² /s
Dmladx	derivative of air molar flow	mole/s m
Dmlsdx	derivative of steam molar flow	mole/s m
Dppadx	derivative of the partial pressure of air	Pa/s
Ds	register addressed in DATETIME functions	---
Dx	register addressed in DATETIME functions	---
e	domain of x in ZEROIN	---
Effw	water effectiveness	---
Effweq	water effectiveness at equilibrium	---
En	water viscosity evaluation constants	---
Enthliq	enthalpy of the liquid	kJ/kg
Enths	enthalpy of the steam	kJ/kg
Enthw	enthalpy of water	kJ/kg
Epsilon	lowest discernable real number	---
Equil-Pressure-Balance	function for cocurrent equilibrium calculations	Pa
Es	register addressed in DATETIME functions	---
Exp	exponential function	---
Fa	value of f(x) at x=a in ZEROIN	---
Fb	value of f(x) at x=b in ZEROIN	---
Fc	value of f(x) at x=c in ZEROIN	---
Filesetup	set up procedure for input and output files	---
Frcgas	gas friction factor	---
Frcliq	liquid friction factor	---
Fxa	value of f(x) at x=a in ITERATE	---
Fxb	value of f(x) at x=b in ITERATE	---
Fxc	value of f(x) at x=c in ITERATE	---
G	gravitational acceleration	m ² /s
Gamma	ratio of specific heats for steam-air mixture	---
Gammal	liquid-film flow per unit length	kg/m s
Gas-In-Enth	enthalpy of the incoming steam-air mixture	kW
Gas-Load	steam-air mixture loading	kg/s m ²
Gas-Out-Enth	enthalpy of the outgoing steam-air mixture	kW
Ghtc	gas-side heat transfer coefficient	kW/m ² K
Gmolfr	inert gas	---
Gmtc	gas-side mass transfer coefficient	kg/m ² s
Gotoxy	a TURBO-pascal procedure	---
h	increment in x in integration procedure	m
Height	condenser packing height	m
Henry	procedure for estimating dissolved air in water	---
Hilimit	upper limit of steam to total water flow	---
I	integer counter	---
Iguess	integer counter for the number of guesses	---
Imf	inert gas mole fraction	---
Increment	step size for integration	m

Table F-1. Cross Reference of Computer Program Variables (Continued)

Variable	Description	Units
InertMasstoMoleFract	function to convert inert mass to mole fraction	---
InertMoletoMassFract	function to convert inert mole to mass fraction	---
Inert-Out-Eqlbm	inert gas flow at equilibrium	kg/s
Infile	input file	---
Insert	TURBO-pascal procedure	---
Ipos	integer variable	---
Iprint	boolean variable to set file outputs	---
Istep	integration step counter	---
Iter	iteration counter	---
Ix	run number counter	---
J	counter	---
K	counter	---
Kbd	key board designation	---
Kliq	thermal conductivity of liquid	W/m K
K-E-In	kinetic energy of the incoming steam-gas mixture	kW
K-E-Out	kinetic energy of the outgoing steam-gas mixture	kW
K-E-Term	kinetic energy term	kW
K-E-Term-New	kinetic energy term	kW
K-l	liquid-side mass transfer coefficient	m/s
Lable	run identification label	---
Lhtc	liquid-side heat transfer coefficient	kW/m ² K
LiquidEnthalpy	enthalpy of the liquid	kJ/kg
Lload	liquid loading	kg/m ² s
Lmtc	liquid-side mass transfer coefficient	kg/m ² s
Ln	natural logarithmic function	---
Lolimit	lower limit of steam to total water flow	---
Lst	line printer designation	---
Mach	Mach number	---
MachineAccuracy	function to calculate the machine accuracy	---
Mio	mass flow rate of outgoing inert gas	kg/s
Mionew	revised mass flow rate of outgoing inert gas	kg/s
MixCp	specific heat of the steam-air mixture	kJ/kg K
MixEnth	enthalpy of the steam-air mixture	kJ/kg
MixK	thermal conductivity of the steam-air mixture	W/m K
MixMu	dynamic viscosity of the steam-air mixture	kg/m s
MixMwt	molecular weight of the steam-air mixture	---
MixPr	Prandtl number of the steam-air mixture	---
MixRho	density of the steam-air mixture	kg/m ³
MixSc	Schmidt number of the steam-air mixture	---
MixTransProp	function to calculate transport properties of the steam-gas mixture	---
MixtureEnthalpy	enthalpy of the steam-air mixture	kJ/kg
Mlfrar	mole fraction of air	---

Table F-1. Cross Reference of Computer Program Variables (Continued)

Variable	Description	Units
Mlfrst	mole fraction of steam	---
Molair	molar air flow rate	mole/s
Molest	molar steam flow rate	mole/s
Molwti	molecular weight of the inert gas	---
Molwts	molecular weight of steam	---
Mom-In	momentum of the incoming steam-gas mixture	Pa
Mom-Out	momentum of the outgoing steam-gas mixture	Pa
Msc	mass flow of steam condensed	kg/s
Mso	mass flow of steam out	kg/s
MuLiq	dynamic viscosity of the liquid	kg/m s
Mwi	mass flow rate of incoming water	---
Neqn	number of equations to be integrated	---
Nline	counter for line printer	---
Nrun	number of runs to be processed	---
Nseg	number of segments the condenser is divided into	---
Ntu	number of transfer units	---
Nusselt-Gas	gas-side Nusselt number	---
Onecompflow	total component one (water+steam) flow rate	kg/s
Onefrac	fraction of steam outlet flow to total water flow	---
Op-Flag	indicator for inlet superheat or saturation	---
Outfile	output file designation	---
Ovhtc	overall heat transfer coefficient	kW/m ² K
Ovmtc	overall mass transfer coefficient	kg/m ² s
P	variable in ZEROIN	---
PackingCharacteristics	function to calculate packing geometric characteristics	---
Pckdia	equivalent packing diameter	m
Pcout	condenser outlet pressure	Pa
Pcoutnew	revised condenser outlet pressure	Pa
Pdrop	condenser static pressure loss	Pa
Phi	terms for gas mixture property evaluations	---
Pi	mathematical constant 3.141527...	---
Ploss	condenser total pressure loss	Pa
Poten	temperature driving potential	C
Pout	condenser outlet pressure	Pa
Pp	partial pressure	Pa
Ppii	partial pressure of incoming inert gas	Pa
Ppio	partial pressure of outgoing inert gas	Pa
Ppiomax	maximum partial pressure of outgoing inert gas	Pa
Ppmin	level of dissolved gas in incoming water	Pa
Ppminmin	minimum level of dissolved gas in incoming water	Pa
Ppsteam	partial pressure of steam	Pa
Pp-Inert	partial pressure of inert gas	Pa
Prime	derivative of the state variable	(varied)
Prliq	Prandtl number of the liquid	---
Pstago	stagnation pressure at outlet	Pa

Table F-1. Cross Reference of Computer Program Variables (Continued)

Variable	Description	Units
Pstgeq	stagnation pressure at outlet at equilibrium	Pa
Pstgin	stagnation pressure at inlet	Pa
Pt	static (total = sum of partials) pressure	Pa
Ptotal	static (total = sum of partials) pressure	Pa
Pzbyp	stagnation to static pressure ratio	---
P-Stg-Eq	stagnation pressure at outlet at equilibrium	Pa
P-Stg-In	stagnation pressure at inlet	Pa
q	variable in ZEROIN	---
r	variable in ZEROIN	---
Reg	gas Reynolds number	---
Rel	liquid Reynolds number	---
Reside	gas Reynolds number, based on side	---
Rholiq	liquid density	kg/m ³
Rhoub	gas mass flux	kg/m ² s
Run-Lable	run identification label	---
s	variable in ZEROIN	---
Saperv	effective surface area per volume of the packing	1/m
Satpr	steam saturation pressure	Pa
SatPressure	steam saturation pressure function	Pa
Satt	steam saturation temperature	C
SatTemperature	steam saturation temperature function	C
Satur	saturated inlet indicator	---
Scliq	liquid Schmidt number	---
Setflag	flag for discontinuing calculations	---
Sheet	packing sheet thickness	m
Side	packing side dimension	m
Sigma	water surface tension	N/m
Sin	sine function	---
Sinalpha	sine of liquid film plane angle w.r.to horizontal	---
Sol	air solubility in water	Pa
Sphwi	enthalpy of inlet water and dissolved air mixture	kJ
Sphwo	enthalpy of outlet water and dissolved air mixture	kJ
Sprime	liquid renewal distance	m
Sqr	square function	---
Sqrt	square-root function	---
State	variable type	---
Steamflux	interfacial steam flux	kg/m ² s
SteamTransProp	procedure for steam transport properties	---
Step	integration step size	m
Stepflag	flag for decreased step size	---
StmCp	specific heat of steam	kJ/kg K
StmDiff	diffusivity of steam in steam-gas mixture	m ² /s
StmK	thermal conductivity of steam	W/m K
Stmlfr	steam mole fraction	---
StmMu	dynamic viscosity of steam	kg/m s

Table F-1. Cross Reference of Computer Program Variables (Continued)

Variable	Description	Units
StmRho	steam density	kg/m ³
Stm-Out-Eqlbm	steam exhaust flow at equilibrium	kg/s
Super	superheated inlet indicator	---
SuperHeat	steam superheat	°C
Superht	steam superheat	°C
Super-Eqlbm	steam superheat at equilibrium (=0)	°C
Super-In	steam superheat at inlet	°C
SuprEq	steam superheat at equilibrium (=0)	°C
Tabs	absolute temperature	K
Tair	air temperature	°C
Tdb	dry-bulb temperature	°C
Tdew	dew point temperature	°C
Temp	temperature	°C
Term	terms in equilibrium calculations	kW
Tgasdb	gas dry-bulb temperature	°C
Theta	packing flow channel inclination from horizontal	(deg)
Time	time in string format	---
Timestr	time in string format	---
Tint	interface temperature	°C
Tinterface	interface temperature	°C
Tliq	liquid temperature	°C
Tmixdb	gas dry-bulb temperature	°C
Tol	convergence tolerance	---
Tolerance	convergence tolerance criteria	---
Tolzer	convergence tolerance in ZEROIN	---
Tot-In-Enth	total inlet enthalpy	kW
Tsat	saturation temperature	°C
Tso	steam outlet temperature	°C
Tstago	gas outlet stagnation temperature	°C
Tstgeq	gas outlet stagnation temperature at equilibrium	°C
Tstgin	gas inlet stagnation temperature	°C
Tstm	steam temperature	°C
Tsurf	interface temperature	°C
Tw	water temperature	°C
Twater	water temperature	°C
Two	water outlet temperature	°C
Twocompflow	total component two (air in water&steam) flow rate	kg/s
Twofrac	ratio of outlet inerts to total inert flow	---
Twofracnew	revised ratio of outlet inerts to total inert flow	---
Tzbyt	stagnation to static temperature ratio	---
T-Dew-In	inlet dew point temperature	°C
TsTago	gas outlet stagnation temperature	°C
T-Stg-Eq	stagnation temperature at equilibrium	°C
T-Stg-In	inlet stagnation temperature	°C
T-Tol	tolerance on temperature	°C

Table F-1. Cross Reference of Computer Program Variables (Continued)

Variable	Description	Units
U-bulk	effective velocity in condenser column	m/s
U-g	bulk gas superficial velocity in condenser column	m/s
U-g-eff	effective gas velocity in packing channel	m/s
U-L-eff	effective liquid film velocity	m/s
Veleg	gas outlet superficial velocity at equilibrium	m/s
Velin	gas inlet superficial velocity	m/s
Vel-Eqlbm	gas outlet superficial velocity at equilibrium	m/s
Vel-In	gas inlet superficial velocity	m/s
Vel-Out	gas outlet superficial velocity	m/s
Verbage	string variable to read in comments	---
Void	packing void fraction	---
Vols	steam specific volume	m ³ /kg
Volw	water specific volume	m ³ /kg
Vout	output variable array	(varied)
Wateff	water effectiveness	---
Waterflow	water flow rate	kg/s
Watertemp	water temperature	°C
Watertransprop	procedure for water transport properties	---
Wat-In-Enth	enthalpy of incoming water	kW
X	distance along main steam flow direction	m
Xa	countercurrent convergence variables	(varied)
Xb	countercurrent convergence variables	(varied)
Xbulk	bulk steam mass fraction	---
Xc	countercurrent convergence variables	(varied)
Xend	end distance at each integration step	m
Xeq	condenser length for equilibrium	m
Xfinal	distance at which calculations are terminated	m
Xin	inlet inert gas mass fraction	---
Xinprc	inlet inert gas mass fraction percent	%
Xio	outlet inert gas mass fraction	---
Xiwi	dissolved inert gas mass fraction	---
Xiwi	dissolved inert gas mass fraction at inlet	---
Xiwo	dissolved inert gas mass fraction at outlet	---
Xm	inert gas mass fraction	---
Xmass	inert gas mass fraction	---
Xnew	revised countercurrent convergence variables	(varied)
Xso	steam outlet mass fraction	---
X-Eqlbm	inert gas mass fraction at equilibrium	---
X-Est	revised condenser length	m
X-Out-Eqlbm	outlet inert gas mass fraction at equilibrium	---
Y	conditions at any point in the condenser	(varied)
Yacob	condenser Jakob number	---
Ybot	conditions at countercurrent condenser bottom	(varied)

Table F-1. Cross Reference of Computer Program Variables (Concluded)

Variable	Description	Units
Ybulk	bulk steam mole fraction	---
Yeqlbm	conditions at equilibrium at the condenser outlet	(varied)
Yin	conditions at the condenser inlet	(varied)
Yio	outlet inert gas mole fraction	---
Yiw	dissolved inert gas mole fraction	---
Yiwi	dissolved inert gas mole fraction at inlet	---
Yiwo	dissolved inert gas mole fraction at outlet	---
Yml	inert gas mole fraction	---
Ymole	inert gas mole fraction	---
Yprime	derivative of the state vector Y	(varied)
Yso	steam outlet mole fraction	---
Ysoeq	steam outlet mole fraction at equilibrium	---
Ytop	conditions at the top of countercurrent condenser	(varied)
Y-Est	estimated conditions at any point in the condenser	(varied)
Zeroin	procedure for finding zero of a function (labelled as CocurrentZeroin and CountercurrentZeroin)	---
Zero-Flag	flag to select zeroin options	---

APPENDIX G EQUILIBRIUM CALCULATIONS

G.1 Cocurrent Condenser

To evaluate a maximum possible performance of a cocurrent condenser, we performed equilibrium calculations that assume

- Steam and water exiting from the condenser are in equilibrium
- Dissolved inert gas level in the exiting coolant is in equilibrium at the partial pressure of the inert gases in the exiting steam-gas mixture
- Vapor pressure loss through the condenser is nonexistent; vapor kinetic energy is fully recovered.

With these assumptions, the calculation procedure is as follows.

The total flow rate of the water and steam, component 1, is denoted by

$$\dot{m}_1 = \dot{m}_{wi} + \dot{m}_{si} \quad (G-1)$$

and that of inert gas, component 2, is denoted by

$$\dot{m}_2 = \dot{m}_{i,s} + \dot{m}_{i,w} \quad (G-2)$$

The total energy of the incoming vapor and inert gas mixture is

$$E_{in} = \dot{m}_{wi}h_f(T_{wi}) + \dot{m}_{si}h_g(T_{si}) + K_{in} \\ + \dot{m}_{i,w} C_{pi}T_{wi} + \dot{m}_{i,s}C_{pi}T_{si} \quad (G-3)$$

where K_{in} is the contribution caused by the kinetic energy of the mixture as

$$K_{in} = (\dot{m}_{si} + \dot{m}_{i,s}) \frac{u_{bulk}^2}{2} \quad (G-4)$$

The incoming vapor momentum is calculated as

$$M_{in} = (\dot{m}_{si} + \dot{m}_{i,s})u_{bulk} \quad (G-5)$$

Assuming that the water and steam exist at the equilibrium temperature T_{eq} , three unknowns, namely T_{eq} , the equilibrium temperature, \dot{m}_{so} , the outlet steam flow rate, and $\dot{m}_{i,so}$, the inert gas flow in the exiting vapor mixture, need to be defined to fully quantify the exit conditions.

These unknowns can be evaluated (in an iterative fashion) using the following equations.

Energy balance:

$$\text{Energy in} = \text{Energy out} \quad (G-6)$$

Momentum balance:

$$P_{in} + M_{in} = P_{out} + M_{out} , \quad (G-7)$$

and Dalton's law of partial pressure of component yields

$$y_{so} = \frac{\dot{m}_{so}/M_s}{\dot{m}_{so}/M_s + \dot{m}_{iso}/M_i} = \frac{PP_{so}}{P_{out}} . \quad (G-8)$$

We denote the outlet steam flow rate as

$$\dot{m}_{so} = \dot{m}_1 f_1 \quad (G-9)$$

and

$$\dot{m}_{iwo} = \dot{m}_2 f_2 , \quad (G-10)$$

where

$$0 < f_1 < 1 \text{ and } 0 < f_2 < 1 .$$

Under equilibrium, we note that for condensation and desorption, f_1 and f_2 approach zero.

The outgoing energy of the water-steam-gas mixture is expressed as

$$\begin{aligned} E_{out} = & \dot{m}_{wo} h_f(T_{eq}) + \dot{m}_{so} h_g(T_{eq}) \\ & + \dot{m}_{i,wo} C_{pi} T_{eq} + \dot{m}_{iso} C_{pi} T_{eq} \\ & + K_{out} , \end{aligned} \quad (G-11)$$

where

$$\begin{aligned} K_{out} = & \text{kinetic energy of the exiting gas mixture} \\ = & (\dot{m}_{so} + \dot{m}_{iso}) \frac{u_{bulk}^2}{2} . \end{aligned} \quad (G-12)$$

Energy out can be rewritten as

$$\begin{aligned} E_{out} = & \dot{m}_1 h_f(T_{eq}) + \dot{m}_1 f_1 h_{fg}(T_{eq}) \\ & + \dot{m}_2 C_{pi} T_{eq} + K_{out} . \end{aligned} \quad (G-13)$$

A momentum balance across the condenser yields

$$P_{out} = P_{in} + M_{in} - M_{out} , \quad (G-14)$$

where

$$M_{out} = (\dot{m}_{so} + \dot{m}_{iso})u_{bulk} \quad (G-15)$$

Equations G-8, G-13, and G-15 are solved simultaneously in an iterative manner to arrive at f_1 , f_2 , and T_{eq} in the neighborhood of f_1 and $f_2 = 0$.

At this point, we observe that an ideal cocurrent condenser may perform worse than an actual condenser because we assumed 100% of equilibrium gas liberation in the ideal case as opposed to less than 20% liberation in an actual case.

G.2 Countercurrent Condenser

To evaluate the maximum performance of an ideal countercurrent condenser, we calculated the equilibrium assuming

- Water exiting the condenser is in equilibrium with the steam entering from the bottom
- Dissolved inert gas in the exiting water is also in equilibrium with the partial pressure of inerts in the entering steam
- The steam and inert gas mixture exiting from the top of the condenser is in equilibrium with the incoming water
- The incoming water is predeaerated to an extent corresponding to its equilibrium level with the steam and inert gas mixture at the top.

Countercurrent equilibrium calculations differ from cocurrent calculations since steam and water enter the condenser at different ends. Based on a given set of steam and inert gas mixture inlet conditions and a specified inlet water temperature, we calculate a minimum water flow to attain equilibrium at both ends of the condenser. The dissolved inert gas level in the water is adjusted to satisfy equilibrium concentrations. Steam pressure at the exit is adjusted to account for momentum recoveries. The calculations proceed as follows.

Exit momentum of vapor is initially assumed to be zero

$$M_{out} = 0 \quad (G-16)$$

then the outlet static pressure is evaluated using

$$P_{out} = P_{in} + M_{in} - M_{out} \quad (G-17)$$

Exit vapor is in equilibrium at a saturation temperature equal to the water inlet temperature T_{wi} , i.e.,

$$T_{so} = T_{wi} \quad (G-18)$$

Assuming the desorbed gas from the coolant is initially zero, $\dot{m}_{id} = 0$, we evaluate the exit steam mole fraction

$$y_{so} = \frac{PP_{so}(T_{so})}{P_{out}} . \quad (G-19)$$

The inert gas mass flow rate is

$$\dot{m}_{io} = \dot{m}_{ii} + \dot{m}_{id} . \quad (G-20)$$

The partial pressure of inert gases at the exit now defines an equilibrium for the dissolved gas level in the incoming water as

$$y_{iwi} = \frac{PP_{io}}{He(T_{wi})} . \quad (G-21)$$

The dissolved gas level in the exiting water for equilibrium is given by

$$y_{iwo} = \frac{PP_{ii}}{He(T_{si})} . \quad (G-22)$$

Equations G-21 and G-22 allow us to evaluate the inert gas desorbed per unit of water mass flow rate.

The energy balance on the inlet and outlet steam and inert gas mixture and the specified water temperature rise allows us to evaluate the equilibrium water flow rate. Pressures are reevaluated using the momentum balance. Calculations are repeated until we obtain the convergence on desorbed inert gas and condenser exit pressures.

APPENDIX H WATER, STEAM, AND AIR PROPERTIES

H.1 Water (Coolant)

The present version of the computer code uses freshwater properties with a molecular weight of 18.015. Other properties are fitted to curves as functions of temperature in degrees Celsius from data in Kellogg (1975) as follows:

Density (kg/m^3):

$$\rho = 1000.0 - (-0.6922 - 0.001757T + 0.005571T^2) \quad (\text{H-1})$$

for $T > 11.85^\circ\text{C}$; otherwise $\rho = 1000.0$. The temperature T is in degrees Celsius.

Specific heat ($\text{kJ/kg } ^\circ\text{C}$):

$$C_p = (4217044 - 3504.25T + 113.17T^2 - 1.309T^3)/10^6 . \quad (\text{H-2})$$

Viscosity (kg/m s):

$$\mu = (2.414 \times 10^{-5})10^a , \quad (\text{H-3})$$

where

$$a = \left[\frac{0.38 \ 281}{(T + 273.15)/647.3 - 0.2163} \right] .$$

Thermal conductivity ($\text{W/m } ^\circ\text{C}$):

$$k = 0.569 + 0.001575T . \quad (\text{H-4})$$

Schmidt number (air diffusing in water):

$$Sc = \frac{372.7\mu^2}{2.71 \times 10^{-9} (T + 273.15)} \quad (\text{H-5})$$

(Reid, Prausnitz, and Sherwood 1987).

These fitted curves are applicable from 2° to 40°C and are coded in the computer program (procedure Watertransprop).

Equilibrium inert gas concentration is determined by Henry's Law. The Henry's Law constant H_e is a function of temperature and determined from a fitted curve of solubility (Sol) in moles air per mole water at atmospheric pressure as follows (Kellogg 1975):

$$Sol = (2.333 - 0.054256T + 0.006236T^2)/10^5 \quad (\text{H-6})$$

$$H_e = P_{atm}/S_{ol} , \quad (H-7)$$

where P_{atm} is atmospheric pressure (101,325 Pa).

H.2 Saturated Steam Properties

Saturated steam properties, including temperature, pressure, specific volume of liquid and gas, and the enthalpy of liquid and vapor, are fitted with simple equations. The saturation temperature and pressure curves are fitted to a modified Antoine equation (Smith and Van Ness 1975) with data from properties of water and steam in SI units (Schmidt 1969) between 0° and 40°C. The curves have the following form:

$$P_{sat} = P_1 \exp \left(P_2 - \frac{P_3}{T_{sat} + P_4} \right) + P_5 \quad (H-8)$$

and

$$T_{sat} = \frac{P_3}{\{P_2 - \ln [(P_{sat} - P_5)]\} - P_4} , \quad (H-9)$$

where

$$\begin{aligned} P_{sat} &= \text{saturation pressure (Pa)} \\ T_{sat} &= \text{saturation temperature (°C)} \\ P_1 &= \text{constant} = 161.7574 \\ P_2 &= \text{constant} = 18.4779 \\ P_3 &= \text{constant} = 4026.9759 \\ P_4 &= \text{constant} = 234.7384 \\ P_5 &= \text{constant} = 3.7383. \end{aligned}$$

The specific volume of the saturated water is assumed to be constant at 0.001 m³/kg. The specific volume of the saturated gas is found using the ideal gas law.

The enthalpy of the saturated water is based on an average constant specific heat:

$$h_L = C_{pL} T_{sat} , \quad (H-10)$$

where

$$\begin{aligned} h_L &= \text{enthalpy of water (kJ/kg)} \\ C_{pL} &= \text{specific heat of water} = 4.186 \text{ (kJ/kg °C)}. \end{aligned}$$

The enthalpy of the saturated steam is found similarly as

$$h_G = h_{Go} + C_{pG} T_{sat} , \quad (H-11)$$

where

$$\begin{aligned} h_G &= \text{enthalpy of steam (kJ/kg)} \\ h_{Go} &= \text{enthalpy of steam at 0°C} = 2501.6 \text{ (kJ/kg)} \\ C_{pG} &= \text{specific heat of steam} = 1.860 \text{ (kJ/kg °C)}. \end{aligned}$$

Approximate expressions for steam transport properties valued in the range of 0° to 40°C were used as follows:

Thermal conductivity (W/m K):

$$k = (1.82 + 0.006T) \times 10^{-2} \quad (\text{H-12})$$

Viscosity (kg/m s):

$$\mu = (8.02 + 0.04T) \times 10^{-6} \quad (\text{H-13})$$

Specific heat(kJ/kg K):

$$C_p = 1.854 + 0.00775T, \quad (\text{H-14})$$

where T is in degrees Celsius (Schmidt 1969).

H.3 Air Properties

Air thermal conductivity k (W/m K):

$$k = \frac{(264.64 \times 10^{-3})T^{1.5}}{T + 245.4 \times 10^{-12}/T} \quad (\text{H-15})$$

with T in kelvins.

Air viscosity μ (kg/m s):

$$\mu = \frac{(1.458 \times 10^{-6})T^{1.5}}{T + 110.4} \quad (\text{H-16})$$

with T in kelvins and a constant air specific heat C_p (kJ/kg K) used as

$$C_p = 1.005. \quad (\text{H-17})$$

Air molecular weight used is 28.97 (Bolz and Tuve 1976).

For air-water vapor mixtures, mutual diffusivity was calculated as

Molecular diffusivity (m^2/s):

$$D_{12} = \frac{2.918(T/313)^{1.75}}{p}, \quad (\text{H-18})$$

where T is in kelvins, and p is the mixture pressure in Pascals.

H.4 Gas Mixture Properties

The gas mixture properties are calculated using the properties of the pure components, at the proper temperature and pressure, and the standard mixture rules.

If X_1 and X_2 stand for the mass fractions of steam and gas in the mixture, then the mixture properties are written as

Specific heat:

$$C_p = X_1 C_{p,1} + (1 - X_1) C_{p,2} \quad (H-19)$$

Mole fraction:

$$y_1 = \frac{1}{1 + (1/X_1 - 1)(M_1/M_2)} \quad (H-20)$$

Density (kg/m^3):

$$\rho = \frac{p(X_1 M_1 + X_2 M_2)}{8314.3T} \quad (H-21)$$

Factor:

$$\phi_{ij} = [1 + (M_j/M_i)^{1/4}(\mu_i/\mu_j)^{1/2}]^2(8 + 8M_i/M_j)^{1/2} \quad (H-22)$$

Viscosity:

$$\mu = \frac{y_1 \mu_1}{y_1 + y_2 \phi_{12}} + \frac{y_2 \mu_2}{y_2 + y_1 \phi_{21}} \quad (H-23)$$

Thermal conductivity:

$$k = \frac{y_1 k_1}{y_1 + y_2 \phi_{12}} + \frac{y_2 k_2}{y_2 + y_1 \phi_{21}} \quad (H-24)$$

Prandtl number:

$$Pr = C_p \mu / k \quad (H-25)$$

Schmidt number:

$$Sc = \mu / \rho D_{12} , \quad (H-26)$$

where

T = temperature (K)

M = molecular weight

Subscript 1 = water vapor

Subscript 2 = air.

H.5 References

Bolz, R. E., and G. L. Tuve, eds., 1976, Handbook of Tables for Applied Engineering Science, 2nd ed., Cleveland, OH: CRC Press.

M. W. Kellogg Company, 1975 (Oct.), Saline Water Conversion Engineering Data Book, NTIS No. PB 250 907, Washington, DC: Office of Water Research and Technology.

Reid, R. C., J. M. Prausnitz, and T. K. Sherwood, 1987, The Properties of Gases and Liquids, 4th ed., New York: McGraw Hill.

Schmidt, E., 1969, Properties of Water and Steam in SI-Units, New York: Springer-Verlag.

Smith, J. M., and H. C. Van Ness, 1975, Introduction to Chemical Engineering Thermodynamics, 3rd ed., New York: McGraw-Hill.

SELECTED DISTRIBUTION LIST

Applied Physics Laboratory
Johns Hopkins Road
Laurel, MD 20707
Professor William Avery

Argonne National Laboratory
9700 South Cass Avenue
Argonne, IL 60439
Anthony Thomas
C. B. Panchal
T. Rabas

Center for Energy and Environmental
Research
Caparra Heights Station
San Juan, PR 00935
Juan Bonnet

Creare, Inc.
P.O. Box 71
Hanover, NH 03755
Bharatan Patel

Dartmouth College
Thayer School of Engineering
Hanover, NH 03755
Professor Graham B. Wallis

DOE/Hawaii
Pacific Area Support Office
300 Ala Moana Blvd.
P.O. Box 50168
Honolulu, HI 96850
John Shupe

Electric Power Research Institute
Coal Combustion Systems Division
3412 Hillview Avenue
Palo Alto, CA 94303
John A. Bartz

Hawaii Natural Energy Institute
University of Hawaii - Monoa
2540 Dole Street
Holmes 246
Honolulu, HI 96822
Patrick Takahaski

HTRI
1000 South Fremont Avenue
Alhambra, CA 91802
Dr. J. Taborek
Technical Director

Koch Engineering Company
161 East 42nd Street, 31st Floor
New York, NY 10017
Neil Yeoman
Director, Technology Development

Meridian Corporation
4300 King Street
Alexandria, VA 22302
D. Kerner

Natural Energy Laboratory of Hawaii
P.O. Box 1749
Kailua-Kona, HI 96740
Thomas H. Daniel

Naval Postgraduate School
Department of Mechanical Engineering
Monterey, CA 93940
Professor Paul J. Marto, Chairman

Northwestern University
Chemical Engineering Department
Evanston, IL 60201
Professor George Bankoff

Oklahoma State University
College of Engineering
Stillwater, OK 74074
Professor Kenneth J. Bell

Pacific International Center for
High Technology Research
Honolulu, HI 96814
Fujio Matsuda
Keith Matsunaga
Luis Vega

R & D Associates
P.O. Box 9695
4640 Admiralty Way
Marina del Rey, CA 90295
Stuart Ridgway

Richardson School of Law
Ocean Engineering
Law of Sea Institute
University of Hawaii
Honolulu, HI 96822
Professor John P. Craven

Science Applications, Inc.
2615 Pacific Coast Highway
#300
Hermosa Beach, CA 90254
A. T. Wassel

The Munters Corporation
P.O. Box 6428
Ft. Myers, FL 33911
E. A. Winkler

The Pennsylvania State University
Department of Mechanical Engineering
208 Mechanical Engineering Building
University Park, PA 16802
Professor Ralph L. Webb

U.S. Department of Energy
Route CE-351; Room 5E-098
1000 Independence Avenue S.W.
Washington, DC 20585
Carmine Castellano
Lloyd Lewis
Leonard Rogers

University of California -
Los Angeles
School of Engineering
5532 Boelter Hills
Los Angeles, CA 90024
Professor A. Mills

University of Hawaii
J.K.K. Look Laboratory
811 Olomehani Street
Honolulu, HI 96813
Professor Hans-Jurgen Krock

University of Hawaii at Manoa
Mechanical Engineering Department
Holmes Hall 302
2540 Dole Street
Honolulu, HI 96822
Professor Ping Cheng

University of Pennsylvania
Mechanical Engineering Department
3451 Walnut St.
Philadelphia, PA 19104
Professor Noam Lior

University of Texas
Department of Chemical Engineering
Austin, TX 78712
Professor J. L. Bravo
Professor James Fair

Document Control Page	1. SERI Report No. SERI/TR-252-3108	2. NTIS Accession No.	3. Recipient's Accession No.
4. Title and Subtitle Direct-Contact Condensers for Open-Cycle OTEC Applications Model Validation with Fresh Water Experiments for Structured Packings.		5. Publication Date October 1988	
7. Author(s) D. Bharathan, B. K. Parsons, and J. A. Althof		8. Performing Organization Rept. No.	
9. Performing Organization Name and Address Solar Energy Research Institute A Division of Midwest Research Institute 1617 Cole Boulevard Golden, CO 80401-3393		10. Project/Task/Work Unit No. OE 713101	
		11. Contract (C) or Grant (G) No. (C) DE-AC02-83CH10093 (G)	
12. Sponsoring Organization Name and Address Solar Energy Research Institute A Division of Midwest Research Institute 1617 Cole Boulevard Golden, CO 80401-3393		13. Type of Report & Period Covered Technical Report	
15. Supplementary Notes		14.	
16. Abstract (Limit: 200 words) The objective of the reported work was to develop analytical methods for evaluating the design and performance of advanced, high-performance heat exchangers for use in open-cycle ocean thermal energy conversion (OC-OTEC) systems. This report describes the progress made on validating a one-dimensional, steady-state analytical computer model of direct-contact condenser using structured packings based on extensive sets of fresh water experiments. The condenser model represents the state of the art in direct-contact heat exchange for condensation for OC-OTEC applications. This is expected to provide a basis for optimizing OC-OTEC plant configurations. Using the model, we examined two condenser geometries, a cocurrent and a countercurrent configuration. This report provides detailed validation results for important condenser parameters for cocurrent and countercurrent flows. Based on the comparisons and uncertainty overlap between the experimental data and predictions, the model is shown to predict critical condenser performance parameters with an uncertainty acceptable for general engineering design and performance evaluations.			
17. Document Analysis a. Descriptors Condensers; Ocean Thermal Energy Conversion; OTEC; Direct Contact Heat Exchangers; Packings; Fresh Water; Seawater; Desalination; Numerical Solution b. Identifiers/Open-Ended Terms Direct Contact Condensers; Cocurrent Condensers; Countercurrent Condensers; Structured Packings c. UC Categories 262			
18. Availability Statement National Technical Information Service U.S. Department of Commerce 5285 Port Royal Road Springfield, Virginia 22161		19. No. of Pages 272	
		20. Price A12	